

For Reference

NOT TO BE TAKEN FROM THIS ROOM

Ex libris
UNIVERSITATIS
ALBERTAENSIS





Digitized by the Internet Archive
in 2024 with funding from
University of Alberta Library

<https://archive.org/details/Yap1977>

THE UNIVERSITY OF ALBERTA

RELEASE FORM

NAME OF AUTHOR.....Nonita T. Yap.....
TITLE OF THESIS.....Chemistry and Stereochemistry of.....
.....Some Methyl(trifluoromethyl)phosphoranes.....
.....and Related Compounds.....
DEGREE FOR WHICH THESIS WAS PRESENTED.....Ph.D.....
YEAR THIS DEGREE GRANTED.....1977.....

Permission is hereby granted to THE UNIVERSITY
OF ALBERTA LIBRARY to reproduce single copies of this
thesis and to lend or sell such copies for private,
scholarly or scientific research purposes only.

The author reserves other publication rights,
and neither the thesis nor extensive extracts from
it may be printed or otherwise reproduced without
the author's written permission.

THE UNIVERSITY OF ALBERTA

CHEMISTRY AND STEREOCHEMISTRY OF SOME METHYL(TRIFLUORO-
METHYL)PHOSPHORANES AND RELATED COMPOUNDS

by



NONITA T. YAP

A THESIS

SUBMITTED TO THE FACULTY OF GRADUATE STUDIES AND
RESEARCH IN PARTIAL FULFILMENT OF THE REQUIREMENTS
FOR THE DEGREE OF DOCTOR OF PHILOSOPHY

DEPARTMENT OF CHEMISTRY

EDMONTON, ALBERTA

SPRING, 1977

THE UNIVERSITY OF ALBERTA
FACULTY OF GRADUATE STUDIES AND RESEARCH

The undersigned certify that they have read,
and recommend to the Faculty of Graduate Studies
and Research, for acceptance, a thesis entitled
CHEMISTRY AND STEREOCHEMISTRY OF SOME METHYL(TRI-
FLUOROMETHYL)PHOSPHORANES AND RELATED COMPOUNDS
submitted by Nonita T. Yap in partial fulfilment of the
requirements for the degree of Doctor of Philosophy
in Chemistry.

sa mahal kong papa

獻
給
敬
愛
的
爸
爸

ABSTRACT

$\text{CH}_3(\text{CF}_3)\text{PCl}_3$ (I) was prepared primarily from mono-methylation of CF_3PCl_4 using tetramethyllead. Subsequent fluorination of (I) with SbF_3 yielded $\text{CH}_3(\text{CF}_3)\text{PF}_3$ (II) which when reacted with $(\text{CH}_3)_3\text{SiSCH}_3$ or $(\text{CH}_3)_2\text{NH}$ gave $\text{CH}_3(\text{CF}_3)\text{PF}_2(\text{SCH}_3)$ (III) or $\text{CH}_3(\text{CF}_3)\text{PF}_2\text{N}(\text{CH}_3)_2$ (IV), respectively.

$(\text{CF}_3)_2\text{PF}_2\text{N}(\text{CH}_3)_2$ (V) was prepared from the reaction of $(\text{CF}_3)_2\text{PCl}_2\text{N}(\text{CH}_3)_2$ (VI) and SbF_3 . $(\text{CF}_3)_2\text{PF}(\text{OCH}_3)\text{N}(\text{CH}_3)_2$ (VII), which was detected only in trace amounts from the reaction between (V) and $(\text{CH}_3)_3\text{SiOCH}_3$ at elevated temperatures for several days, was obtained with relative ease from $(\text{CF}_3)_2\text{PFClN}(\text{CH}_3)_2$ (VIII) and $(\text{CH}_3)_3\text{SiOCH}_3$. Compound (VIII) was synthesized from $(\text{CF}_3)_2\text{PFCl}_2$ and $(\text{CH}_3)_3\text{SiN}(\text{CH}_3)_2$.

The reaction (or lack thereof) of (I), (II), (IV), (V), (VI) and (VIII) with either $(\text{CH}_3)_3\text{SiOCH}_3$ or $(\text{CH}_3)_3\text{SiSCH}_3$ demonstrated the contrasting chemical behavior of chloro- and fluorophosphoranes, the most striking example being the preferred synthetic route for (VII).

The ^1H and ^{19}F nmr spectra of (I), (IV), (V) and (VIII) were invariant with temperature and the magnitude of the $^2\text{J}_{\text{P-F}}$ values evaluated from the spectra suggested equatorial positions for the CF_3 group(s) and axial positions for the directly-bound halogens; assuming a trigonal bipyramidal (TBP) framework throughout. The ^1H , ^{19}F and ^{31}P nmr spectra of (II), (III) and (VII) were temperature-dependent. The low-temperature limiting spectra indicated two different P-F

environments, i.e., axial and equatorial, for the three fluorines in (II), two different axial P-F environments for the two fluorines in (III), and two different environments, namely axial and equatorial, for the two CF_3 groups in (VIII). These temperature-dependent spectral changes were interpreted as arising from a slowing down of a ligand positional exchange process, or in the case of (III), of SCH_3 rotation about the P-S bond. The latter averaging process was also evident in the temperature-dependent nmr spectra of $\text{F}_4\text{P}(\text{SCH}_3)$ (IX), $\text{CF}_3\text{PF}_3(\text{SCH}_3)$ (X) and $(\text{CF}_3)_2\text{PF}_2(\text{SCH}_3)$ (XI). Computer-simulation of the $^{31}\text{P} \sim \{^1\text{H}\}$ nmr spectra of (II), (III), (VII), (IX), (X), (XI) as well as those of $(\text{CF}_3)_3\text{PF}(\text{SCH}_3)$ (XII) at particular temperatures with specific rate constants gave reasonably good fit with experimental spectra. The ΔG^\ddagger values evaluated from the calculated spectra could be correlated with the "apicophilicity" of the substituents other than fluorine in each compound where a "pseudorotation" type of ligand permutation process was postulated. In contrast the ΔG^\ddagger value for SCH_3 rotation about the P-S bond in compounds where this process seemed to be the most reasonable source of the temperature dependency of the spectra, was fairly constant, ranging from 10.0 to 11.0 kcal/mole.

ACKNOWLEDGMENTS

Women's liberation notwithstanding, this author acknowledges her great debt of gratitude foremost to five men:

First, to her dear father who granted a daughter's wish for higher education although he did not, still does not, and perhaps never will, understand the why of it.

Second, to Dr. R. G. Cavell, who was supervisor, mentor, and confidante rolled into one.

Third, to Dr. J. A. Gibson, whose stimulating discussions on nmr spectroscopy helped her see the challenge and the excitement in this particular aspect of her work.

Fourth, to Dr. Kwat I. The, without whose help and patience, this author feels she would not have seen the first of her compounds, nor the last.

And fifth, to dear Alexi, who helped make everything worthwhile.

Finally, this author acknowledges the help of the technicians, secretaries, and other non-academic staff in the chemistry department who must remain nameless because of sheer number . Their warmth, their friendliness and their smiles certainly helped make this foreign student feel welcome in a strange land.

TABLE OF CONTENTS

<u>CHAPTER</u>		<u>PAGE</u>
I	INTRODUCTION	1
II	MATERIALS, APPARATUS AND TECHNIQUES	6
	High Vacuum System and Techniques	6
	Reaction Conditions	7
	Materials	7
	Instrumental Techniques	8
III	SYNTHESIS AND REACTIONS OF SOME	
	METHYL (TRIFLUOROMETHYL) PHOSPHORANES	10
	Experimental	10
	Preparation of Methyl(trifluoro-	
	methyl)trichlorophosphorane	10
	Reactions of $\text{CH}_3(\text{CF}_3)\text{PCl}_3$	11
	Preparation of Methyl(trifluoro-	
	methyl)trifluorophosphorane	14
	Reactions of $\text{CH}_3(\text{CF}_3)\text{PF}_3$	16
	Reactions of $\text{CH}_3(\text{CF}_3)\text{PF}_2\text{N}(\text{CH}_3)_2$	19
	Reactions of $\text{CH}_3(\text{CF}_3)\text{PF}_2(\text{SCH}_3)$	20
	Synthesis of $\text{CH}_3(\text{CF}_3)\text{PF}_2(\text{SCD}_3)$	21
	Results and Discussion	31
	Synthesis, Characterization and	
	Reactions of $\text{CH}_3(\text{CF}_3)\text{PX}_2\text{Y}$	31
	Mass Spectra	45
	Infrared Spectra	48
	Conclusions	50

<u>CHAPTER</u>		<u>PAGE</u>
IV	SYNTHESIS AND REACTIONS OF SOME AMINOBIS- (TRIFLUOROMETHYL)FLUOROPHOSPHORANES	52
	Experimental	53
	Synthesis of $(\text{CF}_3)_2\text{PF}_2\text{N}(\text{CH}_3)_2$	53
	Reactions of $(\text{CF}_3)_2\text{PF}_2\text{N}(\text{CH}_3)_2$	54
	Reactions of $(\text{CF}_3)_2\text{PCl}_2\text{N}(\text{CH}_3)_2$	56
	Synthesis of $(\text{CF}_3)_2\text{PFCln}(\text{CH}_3)_2$	57
	Reactions of $(\text{CF}_3)_2\text{PFCln}(\text{CH}_3)_2$	58
	Reactions of $(\text{CF}_3)_2\text{PF}(\text{OCH}_3)\text{N}(\text{CH}_3)_2$	60
	Results and Discussion	60
	Synthesis and Reactions	60
	Mass Spectra	79
	Infrared Spectra	80
	Conclusions	81
V	NMR DATA AND STRUCTURAL INFERENCES ON PENTA- COORDINATE PHOSPHORUS COMPOUNDS	83
	Theory of ^{31}P and ^{19}F Nuclear Magnetic Resonance Spectroscopy	83
	Pentacoordinate Phosphorus Compounds: Stereochemical Studies and Bonding Theories	87
	Stereochemical Studies	87
	Theory of Bonding of Pentacoordinate Phosphorus	89
	Nmr Spectral Results	94
	Methyl(trifluoromethyl)trifluoro- phosphorane	94

<u>CHAPTER</u>		<u>PAGE</u>
	Methyl(trifluoromethyl)trichloro-	
	phosphorane	108
	Methyl(trifluoromethyl)dimethyl-	
	aminodifluorophosphorane	108
	Methyl(trifluoromethyl)difluoro-	
	(methylthio)phosphorane	122
	Bis(trifluoromethyl)dimethylamino-	
	(methoxy)fluorophosphorane	126
	Bis(trifluoromethyl)dimethylamino-	
	difluorophosphorane	139
	Bis(trifluoromethyl)dimethylamino-	
	chlorofluorophosphorane	151
	Conclusions	161
VI	THE EXCHANGE BARRIER OF $\text{CH}_3(\text{CF}_3)\text{PF}_3$ FROM	
	DYNAMIC NMR SPECTROSCOPY	163
	Introduction	163
	Stereochemical Non-rigidity in Phosphorus	163
	High Resolution NMR Bandshape Analysis	169
	Results	171
	Discussion	178
	Conclusions	189
VII	EXCHANGE PROCESSES IN SOME METHYLTHIO-	
	PHOSPHORANES REVEALED BY VARIABLE-TEMPERATURE	
	DYNAMIC NMR SPECTROSCOPY	190
	Introduction	190
	Experimental	190

<u>CHAPTER</u>		<u>PAGE</u>
	Results and Discussion of Dynamic Nmr Spectra	193
	Tetrafluoro(methylthio)phosphorane	193
	Methyl(trifluoromethyl)difluoro-(methylthio)phosphorane	210
	Trifluoromethyltrifluoro(methylthio)-phosphorane	216
	Bis(trifluoromethyl)difluoro(methylthio)phosphorane	227
	Tris(trifluoromethyl)fluoro(methylthio)phosphorane	235
	Energy Barriers	239
	Conclusions	248
VIII	PROPERTIES OF SOME TETRACOORDINATE PHOSPHINE OXIDES AND SULFIDES	249
	Introduction	249
	Characterization of Methyl(trifluoromethyl)phosphine Oxides and Sulfides	251
	Discussion of Results	260
	Hydrolytic Reactions	260
	Infrared Spectra	260
	Mass Spectra	261
	Nmr Spectra	261
	Conclusions	283
IX	SUMMARY AND CONCLUSIONS	284

<u>CHAPTER</u>	<u>PAGE</u>
REFERENCES	288
APPENDIX	297

LIST OF TABLES

<u>TABLE</u>	<u>Description</u>	<u>PAGE</u>
1	Infrared Spectra of Methyl(trifluoromethyl)-trihalophosphorane	22
2	Infrared Spectra of Methyl(trifluoromethyl)-difluorophosphoranes	23
3	NMR Data for Methyl(trifluoromethyl)halophosphoranes	24
4	Mass Spectral Data for Methyl(trifluoromethyl)halogenophosphoranes	26
5	Mass Measurement Data for Methyl(trifluoromethyl)halophosphoranes	46
6	Infrared Spectral Data for $(\text{CF}_3)_2\text{PFXN}(\text{CH}_3)_2$	61
7	NMR Data for Aminobis(trifluoromethyl)-fluorophosphoranes	62
8	Mass Spectral Data for $(\text{CF}_3)_2\text{PF}_2\text{N}(\text{CH}_3)_2$, $(\text{CF}_3)_2\text{PFClN}(\text{CH}_3)_2$ and $(\text{CF}_3)_2\text{PF}(\text{OCH}_3)\text{N}(\text{CH}_3)_2$	64
9	Mass Measurement Data for Aminobis(trifluoromethyl)fluorophosphoranes	70
10	Activation Parameters for "Pseudorotation" in Some Phosphoranes	172
11	NMR Data for Methylthiofluorophosphoranes	194
12	Free Energy of Activation for Exchange in Some Phosphoranes	240
13	Activation Parameters of Some Trifluoromethylphosphoranes	241

<u>TABLE</u>	<u>Description</u>	<u>PAGE</u>
14	Infrared Spectra of Tetracoordinate Phosphorus Compounds	253
15	NMR Data for Methyl(trifluoromethyl)-phosphine Oxides	254
16	Mass Spectral Data for $\text{CH}_3(\text{CF}_3)\text{P}(\text{O})\text{F}$, $\text{CH}_3(\text{CF}_3)\text{P}(\text{O})\text{OCH}_3$ and $\text{CH}_3(\text{CF}_3)\text{P}(\text{S})\text{Cl}$	255
17	Mass Measurement Data for Tetracoordinated Phosphorus Compounds	259

APPENDIX

<u>TABLE</u>		
1	K Matrix for Axial-Equatorial F Exchange in $\text{CH}_3(\text{CF}_3)\text{PF}_3$	298
2	K Matrix for Axial-Equatorial F Exchange in F_4PSCH_3	299
3	Different K Matrices Investigated for Axial-Equatorial F Exchange in F_4PSCH_3	300
4	K Matrix for $\text{CH}_3(\text{CF}_3)\text{PF}_2(\text{SCH}_3)$	303
5	K Matrix for F Exchange in $\text{CF}_3\text{PF}_3(\text{SCH}_3)$	304
6	K Matrix for Axial-Equatorial CF_3 Exchange in $(\text{CF}_3)_3\text{PF}(\text{SCH}_3)$	306
7	NMR Parameters of Miscellaneous Compound/Ions Encountered in this Investigation	308

LIST OF FIGURES

<u>CHAPTER</u>	<u>Figure</u>	<u>Description</u>	<u>PAGE</u>
III	1.	Proposed Pathway for CH_3Cl Elimination	37
	2	Proposed Pathway for $(\text{CH}_3)_2\text{O}$ Elimination	38
	3	^{19}F Nmr Spectra of $\text{CH}_3(\text{CF}_3)\text{PF}_4^-$	43
	4	Proposed Structure of $\text{CH}_3(\text{CF}_3)\text{PF}_4^{--}$	44
V	1	1,3,2-dioxaphosphanes with Square Pyramidal Ground State Geometry	87
	2	Rundle's Bonding Scheme for Pentacoordinate Phosphorus Compounds	92
	3	^1H Nmr spectrum of $\text{CH}_3(\text{CF}_3)\text{PF}_3$	96
	4	Temperature-Dependent ^{19}F Nmr Spectra of $\text{CH}_3(\text{CF}_3)\text{PF}_3$	98
	5	$^{31}\text{P} \sim \{^1\text{H}\}$ Limiting Nmr Spectra of $\text{CH}_3(\text{CF}_3)\text{PF}_3$	100
	6	Possible Structures of $\text{CH}_3(\text{CF}_3)\text{PX}_3$	102
	7	^1H Nmr Spectra of $\text{CH}_3(\text{CF}_3)\text{PCl}_3$	105
	8	$^{31}\text{P} \sim \{^1\text{H}\}$ Nmr Spectrum of $\text{CH}_3(\text{CF}_3)\text{-}$ PCl_3	107
	9	^1H (60 MHz) Nmr Spectra of $\text{CH}_3(\text{CF}_3)\text{PF}_2\text{N}(\text{CH}_3)_2$	110
	10	^{19}F Nmr Spectra of $\text{CH}_3(\text{CF}_3)\text{PF}_2\text{N}(\text{CH}_3)_2$	113
	11	$^{31}\text{P} \sim \{^1\text{H}\}$ Nmr Spectra of $\text{CH}_3(\text{CF}_3)\text{-}$ $\text{PF}_2\text{N}(\text{CH}_3)_2$	115

<u>CHAPTER</u>	<u>Figure</u>	<u>Description</u>	<u>PAGE</u>
V	12	Possible Structures of $\text{CH}_3(\text{CF}_3)\text{PF}_2\text{N}(\text{CH}_3)_2$	122
	13	^1H nmr Spectra of $\text{CH}_3(\text{CF}_3)\text{PF}_2(\text{SCH}_3)$ and $\text{CH}_3(\text{CF}_3)\text{PF}_2(\text{SCD}_3)$	117
	14	Temperature-Dependent ^{19}F nmr Spectra (P-F region) of $\text{CH}_3(\text{CF}_3)-$ $\text{PF}_2(\text{SCH}_3)$	119
	15	^{31}P Limiting nmr Spectra of $\text{CH}_3(\text{CF}_3)\text{PF}_2(\text{SCH}_3)$	121
	16	Possible Structures of $\text{CH}_3(\text{CF}_3)-$ $\text{PF}_2(\text{SCH}_3)$	125
	17	Proposed Ground State Structure of $\text{CH}_3(\text{CF}_3)\text{PF}_2(\text{SCH}_3)$	126
	18	^1H nmr Spectrum of $(\text{CF}_3)_2\text{PF}(\text{OCH}_3)-$ $\text{N}(\text{CH}_3)_2$	128
	19	Temperature-Dependent ^{19}F nmr Spectra of $(\text{CF}_3)_2\text{PF}(\text{OCH}_3)\text{N}(\text{CH}_3)_2$	130
	20	Proposed Ground State Structure of $(\text{CF}_3)_2\text{PF}(\text{OCH}_3)\text{N}(\text{CH}_3)_2$	132
	21	High-Temperature ^{19}F nmr Spectra of $(\text{CF}_3)_2\text{PF}(\text{OCH}_3)\text{N}(\text{CH}_3)_2$	136
	22	$^{31}\text{P} \sim \{^1\text{H}\}$ nmr Spectra of $(\text{CF}_3)_2-$ $\text{PF}(\text{OCH}_3)\text{N}(\text{CH}_3)_2$	138
	23	^1H (60 and 100 MHz) nmr Spectra of $(\text{CF}_3)_2\text{PF}_2\text{N}(\text{CH}_3)_2$	141

<u>CHAPTER</u>	<u>Figure</u>	<u>Description</u>	<u>PAGE</u>
V	24A	Experimental ^{19}F (56.4 MHz) nmr Spectrum of $(\text{CF}_3)_2\text{PF}_2\text{N}(\text{CH}_3)_2$	143
	24B	Experimental ^{19}F (94.1 MHz) nmr Spectrum of $(\text{CF}_3)_2\text{PF}_2\text{N}(\text{CH}_3)_2$	145
	24C	Calculated ^{19}F (56.4 MHz) nmr Spectra of $(\text{CF}_3)_2\text{PF}_2\text{N}(\text{CH}_3)_2$ for two possible sign combinations of $^1J_{\text{PF}}$ and $^2J_{\text{PF}}$	147
	25	^{31}P nmr Spectra of $(\text{CF}_3)_2\text{PF}_2\text{N}(\text{CH}_3)_2$	149
	26	Possible Structures of $(\text{CF}_3)_2\text{PF}_2^-$ $\text{N}(\text{CH}_3)_2$	150
	27	^1H nmr Spectrum of $(\text{CF}_3)_2\text{PFClN}(\text{CH}_3)_2$	153
	28	^{19}F nmr Spectra of $(\text{CF}_3)_2\text{PFClN}(\text{CH}_3)_2$	155
	29	$^{31}\text{P} \sim \{^1\text{H}\}$ nmr Spectrum of $(\text{CF}_3)_2\text{PFClN}(\text{CH}_3)_2$	157
	30	Possible Structures for $(\text{CF}_3)_2^-$ $\text{PFClN}(\text{CH}_3)_2$	158
VI	1	BPR Mechanism for Exchange in PX_5	165
	2	TR Mechanism for Exchange in PX_5	167
	3	Equivalence of TR and BPR Processes	168
	4	Observed and Calculated $^{31}\text{P} \sim \{^1\text{H}\}$ nmr Spectra of $\text{CH}_3(\text{CF}_3)\text{PF}_3$ at Various Temperatures	175
	5	Intermolecular Exchange Simulation of Low-Temperature Limiting $^{31}\text{P} \sim \{^1\text{H}\}$ nmr Spectrum of $\text{CH}_3(\text{CF}_3)\text{PF}_3$	180

<u>CHAPTER</u>	<u>Figure</u>	<u>Description</u>	<u>PAGE</u>
VI	6	BPR Pathway for Exchange in $\text{CH}_3(\text{CF}_3)\text{PF}_3$	183
	7	TR Pathway for Exchange in $\text{CH}_3(\text{CF}_3)\text{PF}_3$	185
VII	1A	Temperature-Dependent ^{19}F nmr Spectra of F_4PSCH_3	197
	1B	Expansion of ^{19}F half-spectra of F_4PSCH_3	199
	2	Proposed Ground State Structure of F_4PSCH_3	201
	3	Mechanism for Ligand Exchange in the Model Compound X_4PSR	203
	4	$^{31}\text{P} \sim \{^1\text{H}\}$ Limiting nmr Spectra of F_4PSCH_3	205
	5	Observed and Calculated $^{31}\text{P} \sim \{^1\text{H}\}$ nmr Spectra of F_4PSCH_3 at Various Temperatures	207
	6	Simulation of ^{31}P nmr Spectra of F_4PSCH_3 using Various Exchange Matrices	209
	7	Observed and Calculated $^{31}\text{P} \sim \{^1\text{H}\}$ nmr Spectra of $\text{CH}_3(\text{CF}_3)\text{PF}_2(\text{SCH}_3)$ at Various Temperatures	212
	8	Possible Mechanisms for Exchange in $\text{CH}_3(\text{CF}_3)\text{PF}_2(\text{SCH}_3)$	214

<u>CHAPTER</u>	<u>Figure</u>	<u>Description</u>	<u>PAGE</u>
VII	9	Temperature-Dependent ^{19}F nmr Spectra of $\text{CF}_3\text{PF}_3(\text{SCH}_3)$	218
	10	Proposed Ground State Structure of $\text{CF}_3\text{PF}_3(\text{SCH}_3)$	221
	11	$^{31}\text{P} \sim \{^1\text{H}\}$ Limiting nmr Spectra of $\text{CF}_3\text{PF}_3(\text{SCH}_3)$	223
	12	Observed and Calculated $^{31}\text{P} \sim \{^1\text{H}\}$ nmr Spectra of $\text{CF}_3\text{PF}_3(\text{SCH}_3)$ at Various Temperatures	225
	13	$^{31}\text{P} \sim \{^1\text{H}\}$ Limiting nmr Spectra of $(\text{CF}_3)_2\text{PF}_2(\text{SCH}_3)$	229
	14	Proposed Ground State Structure of $(\text{CF}_3)_2\text{PF}_2(\text{SCH}_3)$	230
	15	Temperature-Dependent $^{31}\text{P} \sim \{^1\text{H}\}$ nmr Spectra of $(\text{CF}_3)_2\text{PF}_2(\text{SCH}_3)$	232
	16	$^{31}\text{P} \sim \{^1\text{H}\}$ nmr Spectrum of $(\text{CF}_3)_3\text{PF}(\text{SCH}_3)$ at 273°K	234
	17	Proposed Ground State Structure of $(\text{CF}_3)_3\text{PF}(\text{SCH}_3)$	235
	18	Observed and Calculated $^{31}\text{P} \sim \{^1\text{H}\}$ nmr Spectra of $(\text{CF}_3)_3\text{PF}(\text{SCH}_3)$	238
	19	Arrhenius Plot for Intramolecular Exchange for Some Phosphoranes	244

<u>CHAPTER</u>	<u>Figure</u>	<u>Description</u>	<u>PAGE</u>
VIII	1	^1H nmr Spectrum of $\text{CH}_3(\text{CF}_3)\text{P}(\text{O})\text{Cl}$	263
	2	^{19}F nmr Spectrum of $\text{CH}_3(\text{CH}_3)\text{P}(\text{O})\text{Cl}$	265
	3	^{31}P nmr Spectrum of $\text{CH}_3(\text{CF}_3)\text{P}(\text{O})\text{Cl}$	267
	4	^1H nmr Spectrum of $\text{CH}_3(\text{CF}_3)\text{P}(\text{O})\text{F}$	269
	5	^{31}P nmr Spectrum of $\text{CH}_3(\text{CF}_3)\text{P}(\text{O})\text{F}$	271
	6	^1H nmr Spectrum of $\text{CH}_3(\text{CF}_3)\text{P}(\text{O})\text{OCH}_3$	275
	7	^{19}F nmr Spectrum of $\text{CH}_3(\text{CF}_3)\text{P}(\text{O})\text{OCH}_3$	277
	8	^{31}P nmr Spectrum of $\text{CH}_3(\text{CF}_3)\text{P}(\text{O})\text{OCH}_3$	279
	9	^{19}F nmr Spectrum of $\text{CH}_3(\text{CF}_3)\text{P}(\text{S})\text{Cl}$	281

CHAPTER ONE

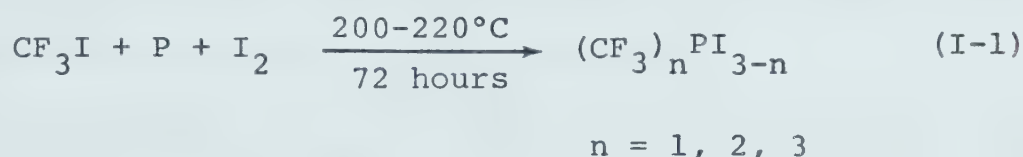
INTRODUCTION

Although the simplest phosphorus(V) halides OPF_3 , PF_5 , SPF_3 , OPCl_3 and PCl_5 were known prior to 1900 the chemistry of these pentavalent phosphorus compounds received scant attention until about 1930 when interest in the derivatives of these simple compounds was stimulated by the discovery of the biological activity of certain organophosphorus compounds.¹ Sustained interest in this field over the last thirty years is attested to by the voluminous literature extant, including much industrial patent literature on anticholinesterases (i.e., nerve gases) and phosphorus-based insecticides.

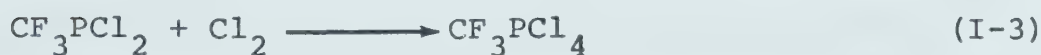
Current interest in synthetic and structural studies of five-coordinate phosphorus compounds arises largely from observed molecular fluxionality of PF_5 first observed by nmr in 1953.² Considerable development in this area has occurred in the last twenty years as a result of improved synthetic procedures and handling techniques. These studies have provided numerous examples of fluxional five-coordinate compounds related to or derived from PF_5 . In addition to the interesting problems of molecular dynamics, these five-coordinate compounds provide a challenge to modern valence theory.

In 1953 a new branch of phosphorus-fluorine chemistry was opened up by the discovery by Bennett,

Emeleus, and Haszeldine³ of a direct and easy route to the synthesis of perfluoromethyliodophosphines. The elevated-temperature reaction of CF_3I and elemental phosphorus in the presence of I_2 yields a mixture of the trifluoromethyliodophosphines:

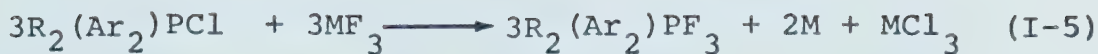


All other trifluoromethyl derivatives of phosphorus are prepared from these three phosphines. For instance, reaction of an iodophosphine with HgCl_2 yields the chlorophosphine which in turn can be readily converted into a halophosphorane by simple oxidative halogenation with molecular halogens such as Cl_2 .

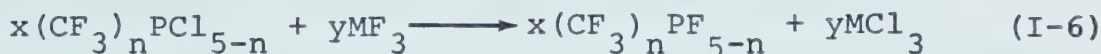


Schmutzler⁴ developed a novel and facile synthetic approach to fluorophosphoranes utilizing oxidative fluorination reactions of variously substituted chlorophosphines with either AsF_3 or SbF_3 . The choice of fluorinating agent depends on the volatility of the desired phosphorane. The stoichiometry of this redox reaction is given by the equations:





Halophosphines containing strongly electronegative perfluoroalkyl substituents do not suffer such oxidative fluorination.⁵ However, AsF₃ and SbF₃ can readily convert previously oxidized compounds such as the chlorophosphoranes into their fluoro analogs:



The ready availability of Group V fluorinating agents coupled with the relatively mild conditions required provide a generally convenient route to a large variety of fluorophosphoranes which can be further studied.

Our present interest in pentavalent pentacoordinate phosphorus compounds has been focused on two principal goals. We wish to extend our knowledge of the chemistry of five-coordinate phosphorus which, in spite of much recent activity, is still relatively untouched. For example, the simplest pentaalkyl phosphorane, (CH₃)₅P, is presently unknown even though a variety of more complex phosphoranes with polycyclic substituents such as homocubane⁶ and adamantane⁶ have been prepared. A second area of interest is the stereochemistry of the pentacoordinate compounds, a subject which has excited much theoretical and experimental interest especially over the last five years.⁷⁻¹⁴

The two common pentacoordinate structures, the trigonal bipyramid and the square pyramid, are unique among structures associated with simple coordination numbers in that they provide two distinguishable bond types within the molecular framework. Structural studies done on the various simple and mixed halogeno-phosphoranes as well as the various substituted trifluoromethylphosphoranes employing varied physical methods have suggested that the trigonal bipyramid is the ground state geometry of these simple phosphoranes. Notable among such studies are the electron diffraction work by Bartell and co-workers¹⁵⁻¹⁷ on PX_5 ($X = F, Cl$) and $(CH_3)_3PF_2$, the vibrational studies by Holmes and co-workers on the PCl_nF_{5-n} series of compounds¹⁸⁻²¹ as well as those of Griffiths on the series²²⁻²⁵ $(CF_3)_nPX_{5-n}$ ($X = F, Cl, n = 1, 2$), the nuclear magnetic resonance studies by Schmutzler^{7,8} and his colleagues on the various substituted fluorophosphoranes and the more recent work by Cavell²⁶⁻²⁸ *et. al.* on the trifluoromethylphosphorane series. Almost all of this work has been directed toward the establishment of the ground state geometry for these simple phosphoranes, and while recent studies have centered on the factors influencing the positional lability and site preference of the ligands, these factors are not yet clearly defined.

The five-coordinate compounds studied in this work can be divided into two main classes, those containing two trifluoromethyl groups, and those containing one methyl and one trifluoromethyl group.

The synthesis and chemical behavior of each of the phosphoranes of the type $\text{CH}_3(\text{CF}_3)\text{PXYZ}$ ($\text{X} = \text{F}, \text{Cl}$; $\text{Y} = \text{F}, \text{Cl}$; $\text{Z} = \text{F}, \text{Cl}, \text{N}(\text{CH}_3)_2, \text{SCH}_3, \text{OCH}_3$) are described in Chapter III. A similar development of the series $(\text{CF}_3)_2\text{PXYZ}$ ($\text{X} = \text{F}$; $\text{Y} = \text{F}, \text{Cl}, \text{OCH}_3$, and $\text{Z} = \text{N}(\text{CH}_3)_2$) is described in Chapter IV. Nuclear magnetic resonance data and resultant structural inferences for these pentacoordinate phosphorus compounds are presented in Chapter V.

Energy barriers to the ligand averaging processes observed in $\text{CH}_3(\text{CF}_3)\text{PF}_3$ and $\text{CH}_3(\text{CF}_3)\text{PF}_2(\text{SCH}_3)$ were calculated and the results are presented in Chapter VI. Similar investigations were carried out on a series of thiophosphoranes $(\text{CF}_3)_n\text{PF}_{4-n}(\text{SCH}_3)$ where $n = 0, 1, 2, 3$, and the results are given in Chapter VII.

A group of pentavalent four-coordinate phosphorus compounds was obtained during the course of this work. Their synthesis, characterization, and spectroscopic data are given in Chapter VIII. Observations on the chemistry and stereochemistry of the various compounds investigated herein are summarized and conclusions proposed in Chapter IX.

CHAPTER TWO

MATERIALS, APPARATUS AND TECHNIQUES

This chapter describes the materials, apparatus and techniques used in the course of this investigation. Special techniques or apparatus will be described in greater detail where applicable.

High Vacuum System and Techniques

Due to the sensitivity of most of the starting materials and products of the reactions to either air or moisture or both, all manipulations of volatile compounds were carried out using standard vacuum techniques in a system constructed from Pyrex glass including vacuum stopcocks lubricated with Apiezon "L" grease. A pressure of less than 10 microns of mercury was attained by incorporating a mercury diffusion pump into the vacuum system. This diffusion pump is separated from the main vacuum system by a cold trap held at -196°C with a liquid nitrogen bath and is backed by a rotary oil pump. Separation of volatile compounds was effected by passing the mixture through a series of U-traps cooled by slush baths at different temperatures.²⁹ This procedure is referred to in the text as vacuum fractionation. Purification of compounds was generally achieved by means of repeated vacuum fractionations using slush baths at close temperature intervals.

Nonvolatile materials which remained in the reaction vessels were handled in a dry box under an atmosphere of argon or nitrogen. Aqueous solutions were handled in open air since they had been found by experience to be invariably air stable.^{26a,b}

Reaction Conditions

Most of the reactions were carried out in Pyrex tubes of 10, 25, or 75 cc volume. Those expected to generate high pressure (> 2 atm) were performed in thick-walled Carius tubes of approximately 50 cc volume. Reaction temperatures are quoted in appropriate sections. In general iodotrifluoromethylphosphines were synthesized in a 500-cc stainless steel reactor fitted with a large heatable valve. This reactor was heated to 200-220°C for 48 hrs in a large silicone oil bath. Occasionally these same compounds were prepared in 75 ml Carius tubes heated to 200-220°C for similar periods in a tube oven.

Materials

Compounds which were not commercially available were prepared by literature methods modified as described in appropriate sections. Reagent grade chemicals were subjected to simple fractionation to remove gross impurities prior to reaction.

Instrumental Techniques

Infrared spectra of gases were obtained using a 9 cm gas cell with KBr or CsBr windows. All spectra were recorded with a Perkin-Elmer 457 spectrometer.

Mass spectra were obtained on an AEI MS-9 spectrometer, operating at an ionizing voltage of 70 eV. Samples were introduced as gases using a heated inlet system.

Routine purity checks and preliminary studies of temperature-dependent nmr spectra were done with a Varian A60 or A56/60 spectrometer. Higher resolution spectra and temperature dependence studies were executed using a Varian HA 100 instrument, equipped with a variable temperature controller (Bruker) which was capable of maintaining temperatures as low as -150°C . The precision of the temperature values quoted is $\pm 1^{\circ}$, established by calibration of the temperature controller and no detectable gradients were present in the sample tube.⁸⁵ Proton spectra were obtained at 100 MHz and ^{19}F spectra at 94.1 MHz on this instrument. Phosphorus-31 nmr spectra were obtained at 34.6 MHz on a Bruker HFX-90 spectrometer in Fourier transform mode. Either 5,000 or 10,000 Hz sweep widths were collected in 8K or 16K data points on the Nicolet 1085 computer incorporated into the system. The temperature controller on this instrument

has the same characteristics as those described above.

Volatile samples for nmr were prepared under vacuum in 5 mm diameter tubes and consisted of approximately 25% of the compound by volume in CFCl_3 or CF_2Cl_2 or in some cases a mixture of both solvents, plus a very small amount of tetramethylsilane for the internal reference for ^1H spectra. The fluorinated solvent also served to provide the heteronuclear reference and lock for the Bruker HFX-90 instrument. In some cases CD_2Cl_2 or CD_3CN solvents were used to provide heteronuclear lock and reference signals.

Nmr spectra of solid compounds were obtained as solutions in either water or acetonitrile. The former systems were prepared in air and the latter samples were prepared in a dry box under a nitrogen or argon atmosphere.

Chemical shifts given in this thesis are measured relative to tetramethylsilane for proton, CFCl_3 for fluorine. Phosphorus chemical shifts are quoted relative to neat P_4O_6 but were actually measured relative to the heteronuclear lock signal and converted to the appropriate chemical shift values by adding to this measured value the resonance frequency of P_4O_6 relative to the machine zero obtained with the particular heteronuclear lock. Unless stated otherwise all nmr parameters were obtained from spectra obtained with the Varian HA-100 or Bruker HFX-90 instruments.

CHAPTER THREE

SYNTHESIS AND REACTIONS OF SOME METHYL(TRIFLUOROMETHYL)PHOSPHORANES

Methylation of tetrahalogenophosphoranes CF_3PX_4 ($\text{X} = \text{F}, \text{Cl}$) with reagents such as tetramethyltin³⁰ or tetramethyllead³¹ gave the methyl(trifluoromethyl)phosphoranes $\text{CH}_3(\text{CF}_3)\text{PX}_3$. The preparation of a series of derivatives of this system was undertaken to provide possible insight into the effects of electronic factors on the chemistry of phosphoranes.

Experimental

A. Preparation of Methyl(trifluoromethyl)trichlorophosphorane.

Methyl(trifluoromethyl)trichlorophosphorane, $\text{CH}_3(\text{CF}_3)\text{-PCl}_3$, was prepared either by the careful chlorination of $\text{CH}_3(\text{CF}_3)\text{PCl}$, prepared according to the method established by Burg,^{32a} or alternatively by methylation of CF_3PCl_4 with $(\text{CH}_3)_4\text{Pb}$.³¹ Although the latter route required a reaction period of several days, repeated vacuum fractionation and was a relatively low-yield reaction, it was the preferred route because CF_3PCl_4 is easily prepared and $(\text{CH}_3)_4\text{Pb}$ is commercially available. On the other hand, preparation of $\text{CH}_3(\text{CF}_3)\text{PCl}$ is tedious and requires the initial preparation of $(\text{CH}_3)_3\text{P}$. Most of the $\text{CH}_3(\text{CF}_3)\text{PCl}_3$ used in this study was therefore prepared by the second method as outlined below.

In a typical reaction CF_3PCl_4 (5.736 g, 23.89 mmol) was condensed onto $(\text{CH}_3)_4\text{Pb}$ (~ 9 g, 70% solution in toluene) in a 75 cc reaction tube; this was sealed under vacuum and agitated for several days at room temperature. The reaction was taken to be complete when precipitation of $(\text{CH}_3)_3\text{PbCl}$, an insoluble white solid, ceased. The desired product, $\text{CH}_3(\text{CF}_3)\text{PCl}_3$, (1.500 g, 6.82 mmol) was separated from the toluene solvent under vacuum and collected at -78°C . Infrared data for $\text{CH}_3(\text{CF}_3)\text{PCl}_3$ are given in Table 1, nmr data in Table 3 and mass spectral data in Tables 4 and 5.

B. Reactions of $\text{CH}_3(\text{CF}_3)\text{PCl}_3$

(i) Alkaline hydrolysis

Treatment of $\text{CH}_3(\text{CF}_3)\text{PCl}_3$ (0.130 g, 0.591 mmol) with about 0.5 ml degassed saturated NaOH solution for several days gave CF_3H (0.040 g, 0.580 mmol). The nmr spectra of the nonvolatile products in the hydrolysate showed the presence of $\text{CH}_3\text{PO}_3^{=}$ ions.^{33,34}

(ii) Neutral hydrolysis

Hydrolysis of $\text{CH}_3(\text{CF}_3)\text{PCl}_3$ (0.105 g, 0.476 mmol) with neutral water yielded no CF_3H and the nmr spectra of the hydrolysate showed the presence of $\text{CH}_3(\text{CF}_3)\text{PO}_2^-$ ions.³⁴

(iii) Reaction with $(\text{CH}_3)_3\text{SiOCH}_3$

The main phosphorus-containing product of the reaction between $\text{CH}_3(\text{CF}_3)\text{PCl}_3$ and $(\text{CH}_3)_3\text{SiOCH}_3$ varied depending on

the stoichiometry of the reactants. A 1:3 mole ratio of $\text{CH}_3(\text{CF}_3)\text{PCl}_3$ to $(\text{CH}_3)_3\text{SiOCH}_3$ yielded $\text{CH}_3(\text{CF}_3)\text{P}(\text{O})\text{OCH}_3$ whereas a 1:1 mole ratio yielded mainly $\text{CH}_3(\text{CF}_3)\text{P}(\text{O})\text{Cl}$.

In a typical reaction, $\text{CH}_3(\text{CF}_3)\text{PCl}_3$ (0.408 g, 1.83 mmoles) was condensed onto $(\text{CH}_3)_3\text{SiOCH}_3$ (0.659 g, 6.33 mmoles) in a 5 mm diameter nmr tube, sealed under vacuum, and gradually brought to room temperature. The ^1H nmr spectrum obtained after 24 hours showed that the reaction was far from complete. The mixture was then agitated for about 6 days and vacuum fractionated. $\text{CH}_3(\text{CF}_3)\text{P}(\text{O})\text{OCH}_3$ (0.261 g, 1.61 mmoles) was collected at -45°C trap. Infrared spectroscopy of the -84°C fraction showed it to be a mixture of $(\text{CH}_3)_3\text{SiCl}$ and unreacted $(\text{CH}_3)_3\text{SiOCH}_3$ (combined mass, 0.658 g). CH_3Cl and very small amounts of $(\text{CH}_3)_3\text{SiCl}$ and $(\text{CH}_3)_3\text{SiOCH}_3$ were trapped at -196°C (combined mass = 0.095 g). Traces of an unidentified compound was found in the -63°C trap.

In a reaction with 1:1 mole ratio $\text{CH}_3(\text{CF}_3)\text{PCl}_3$ (0.541 g, 2.46 mmoles) was condensed onto $(\text{CH}_3)_3\text{SiOCH}_3$ (0.258 g, 2.45 mmoles) in a 5 mm diameter nmr tube. The tube was sealed under vacuum and agitated for several days at room temperature after which the contents were vacuum fractionated. $\text{CH}_3(\text{CF}_3)\text{P}(\text{O})\text{Cl}$ was collected at -45°C together with trace of unreacted $\text{CH}_3(\text{CF}_3)\text{PCl}_3$ and a small amount of $\text{CH}_3(\text{CF}_3)\text{P}(\text{O})\text{OCH}_3$. From the total mass of the -45°C fraction

(0.383 g) and the relative proportions of $\text{CH}_3(\text{CF}_3)\text{P}(\text{O})\text{Cl}$ to $\text{CH}_3(\text{CF}_3)\text{P}(\text{O})\text{OCH}_3$ (26:1 by nmr) the quantities of $\text{CH}_3(\text{CF}_3)\text{P}(\text{O})\text{Cl}$ (2.22 mmoles) and $\text{CH}_3(\text{CF}_3)\text{P}(\text{O})\text{OCH}_3$ (0.09 mmole) were estimated. Other products of the reaction as identified by infrared spectroscopy were $(\text{CH}_3)_3\text{SiCl}$ (0.259 g, 2.40 mmoles) which was trapped at -96°C , unreacted $(\text{CH}_3)_3\text{SiOCH}_3$ trapped at -116°C together with more $(\text{CH}_3)_3\text{SiCl}$ (total mass, 0.008 g). A trace of this same mixture and CH_3Cl (total mass, 0.111 g approx. 2.2 mmoles) was collected at -196°C .

Nmr data for $\text{CH}_3(\text{CF}_3)\text{P}(\text{O})\text{OCH}_3$ and $\text{CH}_3(\text{CF}_3)\text{P}(\text{O})\text{Cl}$ are given in Table 15, ir data in Table 14, and mass spectral data for $\text{CH}_3(\text{CF}_3)\text{P}(\text{O})\text{OCH}_3$ in Tables 16 and 17 of Chapter VIII.

(iv) Reaction with $(\text{CH}_3)_3\text{SiSCH}_3$

$\text{CH}_3(\text{CF}_3)\text{PCl}_3$ (0.324 g, 1.47 mmoles) was condensed onto $(\text{CH}_3)_3\text{SiSCH}_3$ (0.208 g, 1.73 mmoles) in a 10 cc reaction tube. The reaction tube was sealed under vacuum and agitated at room temperature for six days. An inseparable mixture of $\text{CH}_3(\text{CF}_3)\text{P}(\text{S})\text{Cl}$ and CH_3SSCH_3 was collected at -78°C . From the total mass of this fraction (0.758 g) and the relative proportions (by nmr), the individual quantities of $\text{CH}_3(\text{CF}_3)\text{P}(\text{S})\text{Cl}$ (0.86 mmole) and CH_3SSCH_3 (0.11 mmole) were estimated. Fluorine-19 nmr spectra of the -45°C fraction showed it to consist of $\text{CH}_3(\text{CF}_3)\text{PCl}_3$ and $\text{CH}_3(\text{CF}_3)\text{PCl}^{32\text{b}}$ in approximately equal amounts plus two unidentified phosphorus-fluorine containing compounds ($\phi_{\text{F}} = 72.2$ ppm, $^2J_{\text{P-F}} = 77$ Hz

(CF_3PCl_2 ? ^{32}C); $\phi_{\text{F}} = 75.1$ ppm, $^2J_{\text{P-F}} = 92$ Hz) (combined mass = 0.052 g). A mixture of $(\text{CH}_3)_3\text{SiCl}$ and unreacted $(\text{CH}_3)_3\text{SiSCH}_3$ (combined mass = 0.194 g) was identified in the -96°C fraction by infrared spectroscopy. The -196°C fraction was similarly shown to consist of CH_3Cl (~9 mmoles) and small amounts of $(\text{CH}_3)_3\text{SiCl}$ and $(\text{CH}_3)_3\text{SiSCH}_3$ (total mass, 0.044 g)

(v) Reaction with $(\text{CH}_3)_3\text{SiN}(\text{CH}_3)_2$

$\text{CH}_3(\text{CF}_3)\text{PCl}_3$ (0.114 g, 0.518 mmole) was condensed onto $(\text{CH}_3)_3\text{SiN}(\text{CH}_3)_2$ (0.108 g, 0.923 mmole) in a 10 cc reaction tube and sealed under vacuum. The reaction tube was brought up to room temperature, agitated overnight and the volatile products vacuum fractionated. Infrared spectroscopy of the volatile fraction showed it to consist of a mixture of $(\text{CH}_3)_3\text{SiCl}$ and unreacted $(\text{CH}_3)_3\text{SiN}(\text{CH}_3)_2$ (total mass, 0.105 g). Among the identifiable phosphorus-containing products were $\text{CH}_3(\text{CF}_3)\text{PCl}[\text{N}(\text{CH}_3)_2]_2$ and $\text{CH}_3(\text{CF}_3)\text{PCl}_2\text{N}(\text{CH}_3)_2$ with the former in greater amount. An unidentified white non-fluorine containing solid was also formed.

C. Preparation of Methyl(trifluoromethyl)trifluorophosphorane.

Methyl(trifluoromethyl)trifluorophosphorane, $\text{CH}_3(\text{CF}_3)\text{-PF}_3$, was prepared either by fluorination of $\text{CH}_3(\text{CF}_3)\text{PCl}_3$ using SbF_3 , or by stoichiometric methylation of CF_3PF_4 with $(\text{CH}_3)_4\text{Sn}$.³⁰

A typical fluorination reaction consisted of condensing $\text{CH}_3(\text{CF}_3)\text{PCl}_3$ (0.749 g, 3.40 mmoles) into a reaction tube containing sublimed SbF_3 (1.26 g, 7.07 mmoles); this tube was sealed under vacuum and then agitated for about three days at room temperature. The volatile products were vacuum fractionated to give a nearly quantitative yield of $\text{CH}_3(\text{CF}_3)\text{PF}_3$ which was collected at -96°C .

A typical methylation reaction consisted in co-condensing CF_3PF_4 (0.811 g, 4.61 mmoles) and $(\text{CH}_3)_4\text{Sn}$ (0.570 g, 3.19 mmoles) in a 25 cc reaction tube which was then sealed under vacuum. After agitation at room temperature for about three days the reaction tube was opened under vacuum and the volatile components transferred into a fresh reaction tube. Approximately 20 mole % (0.8 mmole) additional CF_3PF_4 was added to the reaction vessel before it was re-sealed under vacuum and agitated at room temperature once again. This procedure was repeated two or three times until the fraction at -96°C , which contains the bulk of the product $\text{CH}_3(\text{CF}_3)\text{PF}_3$, showed no trace of $(\text{CH}_3)_4\text{Sn}$. The yield of $\text{CH}_3(\text{CF}_3)\text{PF}_3$ in this synthetic route varies according to the scale of the reaction, ranging from 17% obtained with an initial charge of 10 mmoles of CF_3PF_4 up to 78% with an initial charge of half this amount. The principal advantage of this procedure is that it provides pure $\text{CH}_3(\text{CF}_3)\text{PF}_3$ which is otherwise very difficult to separate from $(\text{CH}_3)_4\text{Sn}$ by

fractionation techniques.³⁰

Infrared spectral data are given in Table 1, mass spectral data in Tables 4 and 5 and nmr data in Table 3.

D. Reactions of $\text{CH}_3(\text{CF}_3)\text{PF}_3$.

(i) Alkaline hydrolysis

Treatment of $\text{CH}_3(\text{CF}_3)\text{PF}_3$ (0.143 g, 0.834 mmole) with 0.5 ml degassed 10% aqueous NaOH solution under vacuum gave no CF_3H even after three days agitation at room temperature. The nmr and ir spectra of the fractions showed the product of hydrolysis to be mainly $\text{CH}_3(\text{CF}_3)\text{PO}_2^-$ ions. The presence of HF_2^- ions³⁵ was also indicated by a broad peak ($\phi_{\text{F}} = 150.5$ ppm) in the ^{19}F nmr spectrum.

Use of saturated NaOH solution under similar conditions gave CF_3H in the volatile fraction and CH_3PO_3^- and F^- ($\phi_{\text{F}} = 121.0$ ppm) ions³⁵ in the aqueous solution.

(ii) Neutral hydrolysis

Treatment of $\text{CH}_3(\text{CF}_3)\text{PF}_3$ with degassed water yielded $\text{CH}_3(\text{CF}_3)\text{PO}_2^-$ ions as indicated by the nmr spectra. A sharp peak at $\phi_{\text{F}} = 128.0$ ppm in the ^{19}F nmr spectrum is assigned to F^- ions.³⁵

(iii) With $(\text{CH}_3)_3\text{SiOCH}_3$

$\text{CH}_3(\text{CF}_3)\text{PF}_3$ (0.112 g, 0.651 mmole) was condensed onto $(\text{CH}_3)_3\text{SiOCH}_3$ (0.051 g, 0.490 mmole) in a 10 cc reaction tube and sealed under vacuum. The sealed tube

was gradually warmed up to room temperature and vacuum fractionated after about ten minutes of reaction. Infrared and nmr spectra of the different fractions showed the products of the reaction to be $\text{CH}_3(\text{CF}_3)\text{P}(\text{OCH}_3)\text{F}_2$, trapped with small amounts of $\text{CH}_3(\text{CF}_3)\text{P}(\text{O})\text{OCH}_3$ and $\text{CH}_3(\text{CF}_3)\text{P}(\text{O})\text{F}$ at -63°C (total mass, 0.086 g). $(\text{CH}_3)_3\text{SiF}$ was collected at -116°C , together with unreacted $\text{CH}_3(\text{CF}_3)\text{PF}_3$ and $(\text{CH}_3)_2\text{O}$ (total mass, 0.079 g).

Reaction of a *ca.* 1:2 molar ratio of $\text{CH}_3(\text{CF}_3)\text{PF}_3$ (0.186 g, 1.08 mmoles) to $(\text{CH}_3)_3\text{SiOCH}_3$ (0.188 g, 1.81 mmoles) was attempted under the same experimental conditions, this time in a 5 mm diameter nmr tube. The nmr spectra of the system after 10 minutes showed that a reaction had commenced but had not proceeded to completion. The products, as identified through the nmr spectrum, were $\text{CH}_3(\text{CF}_3)\text{P}(\text{OCH}_3)\text{F}_2$, a trace of $\text{CH}_3(\text{CF}_3)\text{P}(\text{O})\text{OCH}_3$, and $(\text{CH}_3)_3\text{SiF}$.

A 1:3 molar ratio of $\text{CH}_3(\text{CF}_3)\text{PF}_3$ (0.181 g, 1.06 mmoles) to $(\text{CH}_3)_3\text{SiOCH}_3$ (0.329 g, 3.16 mmoles) was likewise combined in an nmr tube and found to yield products identical to those in the 1:1 and 1:2 mole ratio in essentially similar proportions.

(iv) With $(\text{CH}_3)_2\text{NH}$

A gas phase reaction between $\text{CH}_3(\text{CF}_3)\text{PF}_3$ (0.367 g, 2.13 mmoles) and $(\text{CH}_3)_2\text{NH}$ (0.148 g, 3.29 mmoles) was

carried out with the amine added in small portions at 0°C, in a reactor described elsewhere.³⁶ This temperature was maintained for about 30 minutes after which the products were vacuum fractionated. The monosubstitution product, $\text{CH}_3(\text{CF}_3)\text{PF}_2\text{N}(\text{CH}_3)_2$, was collected at -23°C (0.206 g, 1.05 mmoles). Excess $(\text{CH}_3)_2\text{NH}$ (0.045 g, 1.00 mmole) was trapped at -196°C. The solid residue left in the reaction vessel was found to consist of $(\text{CH}_3)_2\text{NH}_2^+$ and $\text{CH}_3(\text{CF}_3)\text{PF}_4^-$ ions according to ^1H and ^{19}F nmr spectra.

Infrared spectral data for $\text{CH}_3(\text{CF}_3)\text{PF}_2\text{N}(\text{CH}_3)_2$ are given in Table 2, nmr data in Table 3, and mass spectral data in Tables 4 and 5.

(v) With $(\text{CH}_3)_3\text{SiSCH}_3$

$\text{CH}_3(\text{CF}_3)\text{PF}_3$ (0.275 g, 1.60 mmoles) was reacted with $(\text{CH}_3)_3\text{SiSCH}_3$ (0.147 g, 1.23 mmoles) at room temperature. After agitation for 2 days the system was vacuum fractionated. The bulk of the desired product, $\text{CH}_3(\text{CF}_3)\text{PF}_2(\text{SCH}_3)$, was trapped at -45°C with a small amount passing through to the -63°C trap, giving in total a 100% yield (0.248 g, 1.24 mmoles) of the desired methylthiophosphorane. The volatile fractions consisted of $(\text{CH}_3)_3\text{SiF}$ and excess $\text{CH}_3(\text{CF}_3)\text{PF}_3$ (total mass, 0.179 g).

Infrared spectral data for $\text{CH}_3(\text{CF}_3)\text{PF}_2(\text{SCH}_3)$ are given in Table 2, nmr data in Table 3, and mass spectral data in Tables 4 and 5.

E. Reactions of $\text{CH}_3(\text{CF}_3)\text{PF}_2\text{N}(\text{CH}_3)_2$.

(i) Alkaline hydrolysis

$\text{CH}_3(\text{CF}_3)\text{PF}_2\text{N}(\text{CH}_3)_2$ (0.105 g, 0.532 mmole) was agitated with 0.5 ml degassed 10% NaOH solution for several days at room temperature. Nmr spectra of the hydrolysate indicated the presence of $\text{N}(\text{CH}_3)_2\text{H}_2^+$ and $\text{CH}_3(\text{CF}_3)\text{PO}_2^-$ ions.³⁴ A sharp peak at $\phi_{\text{F}} = 120.4$ ppm in the ^{19}F nmr spectrum was attributed to F^- ion.³⁵

Use of saturated NaOH solution resulted in the quantitative liberation of CF_3H and $(\text{CH}_3)_2\text{NH}$. Nmr spectroscopy of the aqueous solution showed the presence of CH_3PO_3^- ions.^{33,34}

(ii) Neutral hydrolysis

Treatment of $\text{CH}_3(\text{CF}_3)\text{PF}_2\text{N}(\text{CH}_3)_2$ with H_2O gave $\text{CH}_3(\text{CF}_3)\text{PO}_2^-$ and HF_2^- ($\phi_{\text{F}} = 149.8$ ppm) ions.

(iii) With $(\text{CH}_3)_3\text{SiOCH}_3$

No reaction was observed between $\text{CH}_3(\text{CF}_3)\text{PF}_2\text{N}(\text{CH}_3)_2$ (0.235 g, 1.194 mmole) and $(\text{CH}_3)_3\text{SiOCH}_3$ (0.150 g, 1.44 mmole) at room temperature even after several days. The reaction tube was then heated to 96°C and kept at this temperature for nearly five days during which time some white solid formed on the walls of the tube. The volatile products were removed and fractionated under vacuum. Nmr showed the contents to be mainly the starting materials and a small amount of $(\text{CH}_3)_3\text{SiF}$. The quantity of white solid was insufficient for characterization.

F. Reactions of $\text{CH}_3(\text{CF}_3)\text{PF}_2(\text{SCH}_3)$.

(i) Alkaline hydrolysis

$\text{CH}_3(\text{CF}_3)\text{PF}_2(\text{SCH}_3)$ (0.100 g, 0.5 mmole) was agitated with 0.5 ml of degassed 10% NaOH solution for several days after which the contents were fractionated under vacuum. CH_3SH (0.0213 g, 0.444 mmole) was collected at -116°C while the hydrolysate contained $\text{CH}_3(\text{CF}_3)\text{PO}_2^-$ ions.³⁴ Two peaks ($\phi_{\text{F}} = 120.9$ ppm; $\phi_{\text{F}} = 148.8$ ppm) in the ^{19}F spectrum were attributed³⁵ to F^- and HF_2^- ions. Use of saturated NaOH resulted in quantitative yield of CF_3H leaving F^- , CH_3PO_3^- ion,³³⁻³⁵ and CH_3S^- ($\tau = 7.90$) in the hydrolysate.

(ii) Neutral hydrolysis

The hydrolysis of $\text{CH}_3(\text{CF}_3)\text{PF}_2(\text{SCH}_3)$ (0.120 g, 0.601 mmole) in neutral medium yielded $\text{CH}_3(\text{CF}_3)\text{PO}_2^-$ in the hydrolysate and CH_3SH (0.022 g, 0.462 mmole) in the volatile fraction. Peaks assigned to F^- ($\phi_{\text{F}} = 121.0$ ppm) and HF_2^- ($\phi_{\text{F}} = 150.0$ ppm) ions were observed in the ^{19}F spectrum of the hydrolysate.

G. Synthesis of $(\text{CH}_3)_3\text{SiSCD}_3$

$(\text{CH}_3)_3\text{SiSCD}_3$ was prepared by reacting $(\text{CH}_3)_3\text{SiN}(\text{CH}_3)_2$ (1.330 g, 11.4 mmoles) with CD_3SH (0.647 g, 12.7 mmoles) for three days at room temperature. The yield of the deuterated silylthioether was 75.6% based on the initial amount of $(\text{CH}_3)_3\text{SiN}(\text{CH}_3)_2$ used.

H. Synthesis of $\text{CH}_3(\text{CF}_3)\text{PF}_2(\text{SCD}_3)$.

$\text{CH}_3(\text{CF}_3)\text{PF}_3$ (0.140 g, 0.813 mmole) was condensed upon $(\text{CH}_3)_3\text{SiSCD}_3$ (0.087 g, 0.706 mmole) and the reaction vessel was agitated for 2 hours at 0°C . This gave a 98% yield (0.1392 g, 0.685 mmole) of the deuteriothio-methylated phosphorane based on $(\text{CH}_3)_3\text{SiSCD}_3$ consumed.

TABLE 1
Infrared Spectra of Methyl(trifluoromethyl)-
trihalophosphoranes^a

$\text{CH}_3(\text{CF}_3)\text{PF}_3$	$\text{CH}_3(\text{CF}_3)\text{PCl}_3$	Assignment ^b
-	1380 s	} $\sigma_{\text{as}}\text{CH}_3$
1325 w	1325 w	
1216 s	1245 m	} ν_{CF_3}
1153 s	1190 s	
961 s	-	} $\nu_{\text{P-F}}$
873 m	-	
828 s	-	
733 m	740 m	$\sigma_{\text{as}}\text{CF}_3(?)$
-	580 m	$\nu_{\text{as}}\text{P-Cl}$
-	540 m	$\nu_{\text{sym}}\text{P-Cl}$
512 m	-	} $\nu_{\text{P-CF}_3}$
466 w	488 m	

^a Gas phase spectra, all values in cm^{-1} . s = strong, m = medium, w = weak, ν = stretching, σ = deformation, sym = symmetric, as = antisymmetric, ? = very tentative.

^b These assignments are tentative and based mainly on available data for related compounds. See for instance, ref. 41, 103.

TABLE 2

Infrared Spectra of Methyl(trifluoromethyl)-
difluorophosphoranes^a

$\text{CH}_3(\text{CF}_3)\text{PF}_2\text{N}(\text{CH}_3)_2$	$\text{CH}_3(\text{CF}_3)\text{PF}_2(\text{SCH}_3)$	Assignment ^b
-	2976 m	} $\nu_{\text{C-H}}$
2952 m	2951 m	
2882 m	2911 vw	
2834 m	2841 vw	
-	2771 w	
-	1436 w	} $\sigma_{\text{as}} \text{CH}_3$
1319 m	1316 w	
1299 m	1266 s	$\sigma_{\text{sym}} \text{CH}_3(?)$
1212 s	1214 s	} $\nu_{\text{P-CH}_3}, \nu_{\text{CF}_3}$
1186 s	1196 s	
1136 s	1147 s	
1067 w	1076 vw	
1022 s	1027 vw	
-	971 m	} $\nu_{\text{P-NC}_2}$
897 s	891 s	
-	859 s	
809 s	799 s	} $\sigma_{\text{as}} \text{CF}_3(?)$
771 s	769 s	
-	712m	} $\sigma_{\text{sym}} \text{CF}_3(?)$
666 s	643 m	
601 m	607 m	
511 m	583 s	} $\nu_{\text{P-CF}_3}$
473 m	471 s	
436 w	-	

^a Gas phase spectra, all values in cm^{-1} . s = strong, m = medium, w = weak, ν = stretching, σ = deformation, sym = symmetric, as = antisymmetric, ? = highly tentative.

^b These assignments are tentative, and based mainly on available data on related compounds. See for instance, ref. 41, 103.

TABLE 3

NMR Data for Methyl(trifluoromethyl)halophosphoranes

Compound	Temp	τ^a	ϕ_F^b	$\phi_{CF_3}^b$	$\delta_{CF_3}^c$	$1J_{PF}$ Hz	$2J_{PF}$ Hz	$3J_{PH}$ Hz	$3J_{FH}$ Hz	$4J_{FH}$ Hz	$5J_{FH}$ Hz	$2J_{FF}$ Hz	$3J_{FF}$ Hz
$CH_3(CF_3)PCl_3$	30°	6.96	-	74.5	154.9	-	112	12.4	-	0.7 ^p	-	-	-
$CH_3(CF_3)PF_3$	0°	8.30	46.2	69.6	124.2	955 _l	156	~18	-	9.0	-	-	13.2
	-100°		25.9 ^h 86.5 ⁱ			919 _l 1023 ^m						~48 ^r	-
$CH_3(CF_3)P(OCH_3)F_2$	0°	8.56 ^d 6.51 ^e	31.5	70.0	136.0	830	156	18.3	15.1	12.1	~1.1	-	18.6
$CH_3(CF_3)P(OCH_3)_2F$	0°	8.48 ^s 6.46 ^t	46.7	76.4	149.3	812	66.5	~15	13.8	q	1.9	-	8.4
$CH_3(CF_3)PF_2N(CH_3)_2$	30°	8.80 ^d 7.60 ^f	38.2	70.5	157.4	850	141	19.1	10.5	13.5	2.5	-	17.0
$CH_3(CF_3)PF_2(SCH_3)$	30°	8.06 ^d 7.81 ^g	20.4	69.8	127.2	804	148	18.0	20.0	12.2	1.7	-	15.0
	-90°		18.0 ^j 26.4 ^k			728 ⁿ 860 ^o						50	

^a τ ppm relative to internal tetramethylsilane, $\tau = 10.0$ ^b ϕ ppm relative to internal (solvent) CCl_3F standard with positive values indicating resonance to high field of standard^c ppm vs. P_4O_6 as external standard (capillary), positive values indicating resonance to high field of standard.

TABLE 3 FOOTNOTES (continued)

d	CH ₃ on P, a doublet of triplets	^s CH ₃ on P, a doublet of doublets
e	OCH ₃ group, a doublet of triplets	^t OCH ₃ group, a doublet of doublets
f	N(CH ₃) ₂ group, a doublet of triplets	
g	SCH ₃ group	
h	F axial	
i	F equatorial	
j	Axial F	
k	Axial F'	
l	¹ J _{P-Faxial} , evaluated from low-temperature ³¹ P limiting spectrum	
m	¹ J _{P-F} equatorial, evaluated from low-temperature ³¹ P limiting spectrum	
n	¹ J _{P-Fax}	
o	¹ J _{P-F'ax}	
p	From expansion of ¹ H nmr spectrum, a quartet of 1:3:3:1 intensity ratio	
q	not resolved	
r	² J _{Fax-F'eq} , from equatorial F region of low-temperature ¹⁹ F limiting nmr spectrum, a doublet of very broad triplets.	

TABLE 4

Mass Spectral Data for Methyl(trifluoromethyl)halogenophosphoranes

m/e	Intensity ^a			Assignment ^b
	$\text{CH}_3(\text{CF}_3)\text{PF}_3$	$\text{CH}_3(\text{CF}_3)\text{PCl}_3$	$\text{CH}_3(\text{CF}_3)\text{PF}_2\text{N}(\text{CH}_3)_2$	
205		1.51		CF_3PCl_3
185				$\text{CF}_3\text{PF}_2(\text{SCH}_3)$
182			2.26	$\text{CF}_3\text{PF}_2\text{N}(\text{CH}_3)_2$
181				$\text{CH}_3(\text{CF}_3)\text{PF}(\text{SCH}_3)$
178			1.30	$\text{CH}_3(\text{CF}_3)\text{PFN}(\text{CH}_3)_2$
171		1.51		$\text{CH}_2(\text{CF}_3)\text{PCl}_2$
169		4.31		CF_3PCl_2
158	2.15			$\text{CF}_3\text{PF}_3\text{H}$
157	6.70			CF_3PF_3
154	0.31			$\text{C}_2\text{H}_4\text{F}_5\text{P}$
153	6.42		0.41	$\text{CH}_3\text{CF}_3\text{PF}_2$
152	2.51	4.10	7.41	$\text{CH}_2\text{CF}_3\text{PF}_2$
151		0.54		CH_3PCl_3
150		0.65		CH_2PCl_3
137		1.08		$\text{PCl}_3, \text{CCl}_3\text{F}$
135		1.73	2.11	$\text{CFCl}_2\text{P}, \text{CH}_3\text{F}_3\text{PS}$

TABLE 4 (continued)

134	0.41			CHF ₄ NP
132	1.71			C ₂ HFP
131			4.87	CH ₃ PF ₂ (SCH ₃)
129	0.75			C ₃ H ₁₀ F ₂ NP
128	3.36			C ₃ H ₄ F ₂ NP
123		0.75		H ₂ FCF ₂ P
121		2.80		CH ₂ F ₄ P, PCl ₂ F
119		8.63		CF ₄ P, CHCl ₃
117		1.19		CH ₃ PCl ₂
116			0.54	PF ₂ (SCH ₃)
113				(CH ₃) ₂ NPF ₂
112	0.55			C ₂ H ₅ F ₂ NP
109	1.65			H ₂ F ₄ P
108	0.41			HF ₄ P
107	7.41			F ₄ P
106				C ₃ H ₆ FNP
105	0.48			C ₃ H ₅ FNP
104				CH ₃ PF ₃ H, PF ₂ Cl
103	8.23		17.20	CH ₃ PF ₃ , HCl ₂ P
102	0.62		0.65	CH ₂ PF ₃
101	2.47			CHF ₃ P
100				CF ₃ , C ₂ F ₄ , CH ₃ PFCl

TABLE 4 (continued)

99	1.83				CH ₂ FC1P
98				1.78	CH ₂ F ₂ P
97	4.31				CHF ₂ P
94			1.10		(CH ₃) ₂ NPF, C ₂ H ₇ PS
93				0.73	C ₂ H ₆ PS
89		0.33		0.65	HPF ₃
88		4.46			PF ₃
86			0.41		HFC1P
85		0.45			SiF ₃ , FC1P
84		1.95	0.89	2.60	CH ₃ PF ₂
83		2.23	0.41	0.63	CH ₂ PF ₂
82		0.84			CHF ₂ P
81		2.23		3.25	CF ₂ P
79				0.57	CH ₄ PS
78			0.48	0.57	CH ₂ FNP, CH ₃ PS
77			0.48	6.49	CH ₂ FNP, CH ₂ PS
75			0.48		CHFNP
74			1.03		CFNP
73			8.23		C ₂ H ₄ NP
70		1.39			HF ₂ P
69		10.60	2.81	10.06	CF ₃ , PF ₂
66			0.41		H ₂ FNP
65		3.07	1.10	3.49	CH ₃ FP

TABLE 4 (continued)

64	1.95					CH ₂ FP	0.54	
63	1.39					CHFP	1.27	
62	0.84					CFP		
61								
58				0.48		C ₂ H ₆ P	0.66	
57				1.03		C ₂ H ₃ P		
56				0.34		C ₂ H ₂ P		
55				0.34		C ₂ HP		
53				0.34		C ₂ P		
51	0.84					H ₂ FP		
50	4.74		3.34			HFP		
49				0.55		FP, CH ₃ Cl	1.15	
48						CH ₆ P	1.15	
47	0.84					CH ₅ P	1.30	
46				0.69		SiF, CH ₃ S	6.65	
45	1.67			0.55		C ₂ H ₈ N, CH ₂ S	4.87	
44	1.39			6.04		C ₂ H ₇ N, CHS, CH ₂ P	6.98	
43	0.28			8.23		C ₂ H ₆ N, CS, CHP	1.15	
42				2.95		CP, C ₂ H ₅ N		
41				5.49		C ₂ H ₄ N		
40	1.12			1.17		C ₂ H ₃ N		
35	4.46			0.82		H ₂ F ₂	2.92	
						H ₂ P		

TABLE 4 (continued)

33	4.46				H ₂ P
32	8.37		4.94	4.87	HP, CFH, CH ₃ NH
31	3.63	3.34	3.57	0.65	CF, P
30			3.57		C ₂ H ₆

^a Intensity is expressed as % total ionization based on the sum of the intensities of ions with m/e greater than 30.

^b Assignments of some ions are given in terms of the structural formula for ease of recognition only.

Results and Discussion

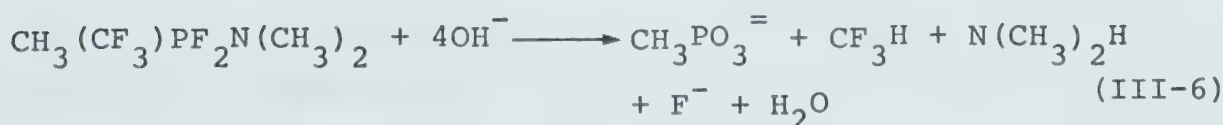
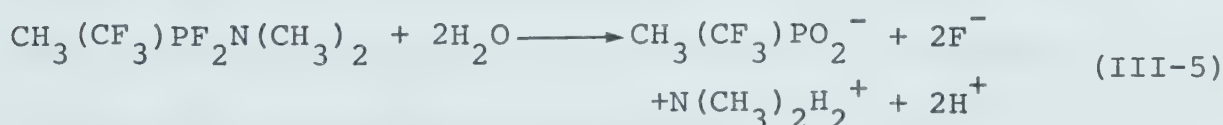
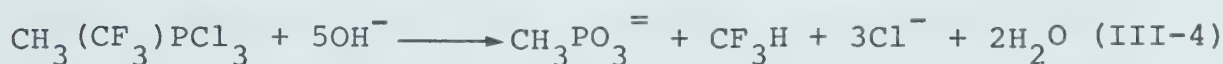
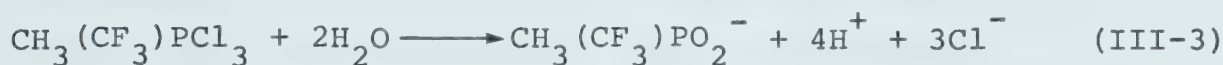
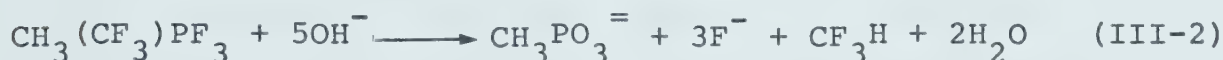
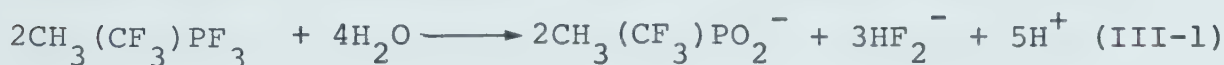
A. Synthesis, Characterization and Reactions of $\text{CH}_3(\text{CF}_3)_3\text{PX}_2\text{Y}$.

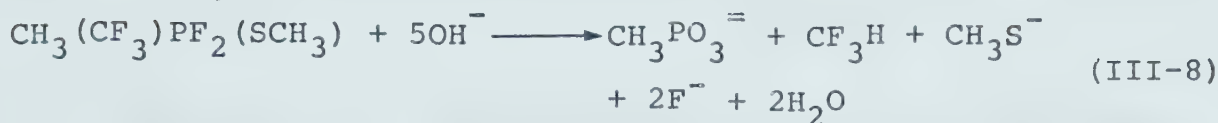
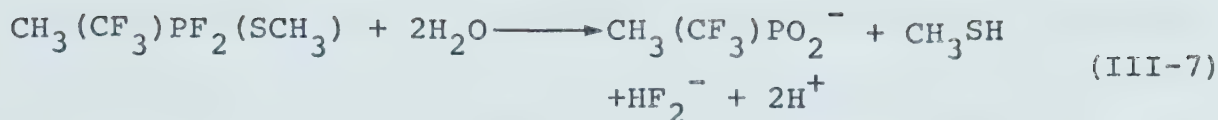
Previous studies on the basic hydrolysis of $(\text{CF}_3)_n\text{PX}_{5-n}$ ($\text{X} = \text{F}, \text{Cl}; n = 1, 2, 3$) series of compounds have indicated that basic hydrolysis generally cleaves all but one $\text{P}-\text{CF}_3$ linkage, leaving CF_3PO_3^- ions in the aqueous solution.^{3,34} Investigations on $(\text{CF}_3)_3\text{P}(\text{NR}_2)_2$ and $(\text{CF}_3)_3\text{PFNR}_2$ systems^{26a,b} indicated that these trifluoromethylhalo-phosphoranes behaved similarly. Under similar conditions of strongly basic hydrolysis the halogenophosphoranes $\text{CH}_3(\text{CF}_3)_3\text{PX}$ ($\text{X} = \text{F}, \text{Cl}$) suffered cleavage of all but one CF_3 group to leave $\text{CF}_3(\text{CH}_3)\text{PO}_2^-$ ions in solution.^{28a} Thus the present methyl(trifluoromethyl)phosphorane series might have been expected to exhibit parallel behavior to the non-methylated trifluoromethylphosphoranes.

Recently however, unusual hydrolytic behavior has been observed in the $(\text{CH}_3)_n\text{P}(\text{CF}_3)_{5-n}$ ($n = 2, 3$) and $\text{CH}_3(\text{CF}_3)_3\text{PY}$ series of compounds (where $\text{Y} = \text{OCH}_3, \text{N}(\text{CH}_3)_2$ or SCH_3) in which all of the $\text{P}-\text{CF}_3$ groups were cleaved under conditions of strongly basic hydrolysis to be liberated as CF_3H leaving CH_3PO_3^- ions in the aqueous solution.³⁴ Use of 10% NaOH solution in some cases gave no CF_3H , and $\text{CH}_3(\text{CF}_3)\text{PO}_2^-$ ions remained in solution. Thus the cleavage of CF_3 groups in these methyl(trifluoromethyl)phosphorane systems is complex and heavily

dependent on the strength of the medium and the nature of the compound. We have found that complete cleavage of CF_3 groups occurs for $\text{CH}_3(\text{CF}_3)\text{PX}_3$ ($\text{X} = \text{F}, \text{Cl}$) and $\text{CH}_3(\text{CF}_3)\text{-PF}_2\text{Y}$ ($\text{Y} = \text{N}(\text{CH}_3)_2, \text{SCH}_3$) systems in parallel with the observations^{28a} of complete cleavage of CF_3 for the systems $\text{CH}_3(\text{CF}_3)_3\text{PY}$ ($\text{Y} = \text{OCH}_3, \text{N}(\text{CH}_3)_2$ or SCH_3). This behavior clearly indicates that the $\text{CH}_3(\text{CF}_3)\text{PO}_2^-$ ion is not as resistant to basic hydrolysis as CF_3PO_3^- and that the rate of hydrolysis is affected by the species present in the hydrolysate.

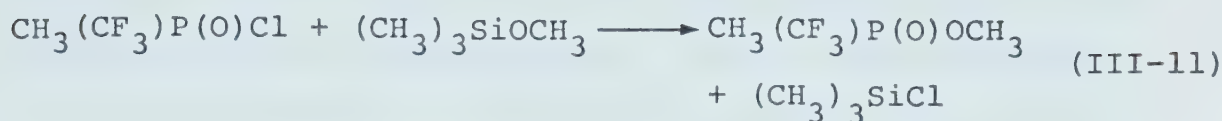
Equations III-1 to 8 express the hydrolytic behavior of the various methyl(trifluoromethyl)halophosphoranes and their derivatives.





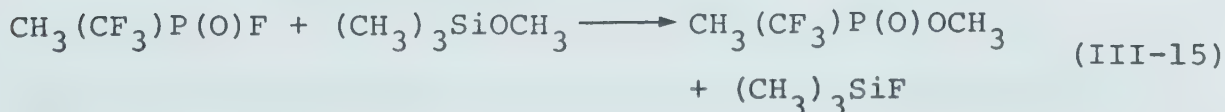
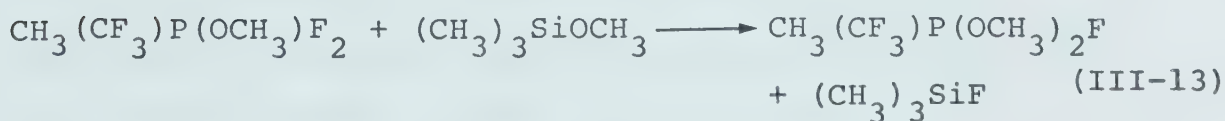
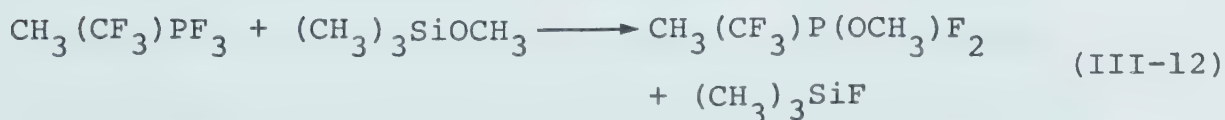
Both $\text{CH}_3(\text{CF}_3)\text{PCl}_3$ and $\text{CH}_3\text{CF}_3\text{PF}_3$ react with $(\text{CH}_3)_3\text{SiOCH}_3$, even at 0°C , with the chlorophosphorane reacting much more slowly than the fluorophosphorane. Furthermore, the mole ratio of the reactants influenced only the proportion, not the nature of the products. With $\text{CH}_3(\text{CF}_3)\text{PCl}_3$, the products obtained were $\text{CH}_3(\text{CF}_3)\text{P}(\text{O})\text{Cl}$, $\text{CH}_3(\text{CF}_3)\text{P}(\text{O})\text{OCH}_3$, $(\text{CH}_3)_3\text{SiCl}$, and CH_3Cl . Equimolar proportions of the reagents led to a greater proportion of $\text{CH}_3(\text{CF}_3)\text{P}(\text{O})\text{Cl}$ whereas an excess of silylether gave $\text{CH}_3(\text{CF}_3)\text{P}(\text{O})\text{OCH}_3$ as the major product. This may be rationalized as the result of a sequential substitution process (eqs III-9 to III-11) involving perhaps $\text{CH}_3(\text{CF}_3)\text{P}(\text{OCH}_3)\text{Cl}_2$ as a fast reacting or unstable intermediate which has not been isolated or identified. For this reason this compound is enclosed in [] brackets. We note that the analogous difluoride (*vide infra*) is easily obtained suggesting that the dichloride is a reasonable intermediate.



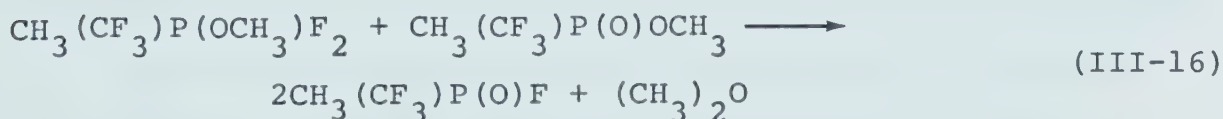


Equation III-11 would explain the greater proportion of $\text{CH}_3(\text{CF}_3)\text{P}(\text{O})\text{OCH}_3$ relative to $\text{CH}_3(\text{CF}_3)\text{P}(\text{O})\text{Cl}$ when $(\text{CH}_3)_3\text{SiOCH}_3$ was in excess over $\text{CH}_3(\text{CF}_3)\text{PCl}_3$. This reaction (eq III-11) occurs only to a very minor extent when the reactants are in a 1:1 mole ratio.

In contrast, $\text{CH}_3(\text{CF}_3)\text{PF}_3$ reacted with $(\text{CH}_3)_3\text{SiOCH}_3$ to form $(\text{CH}_3)_2\text{O}$, $(\text{CH}_3)_3\text{SiF}$, and varying proportions of $\text{CH}_3(\text{CF}_3)\text{P}(\text{OCH}_3)\text{F}_2$, $\text{CH}_3(\text{CF}_3)\text{P}(\text{O})\text{OCH}_3$, $\text{CH}_3(\text{CF}_3)\text{P}(\text{OCH}_3)_2\text{F}$, and $\text{CH}_3(\text{CF}_3)\text{P}(\text{O})\text{F}$ depending on the length of the reaction period. The following sequence of reactions represented by equations III-12 to III-15 may account for these observations.



One can further speculate on the mechanism of the reaction between $\text{CH}_3(\text{CF}_3)\text{PF}_3$ and $(\text{CH}_3)_3\text{SiOCH}_3$ by considering the following observations. First, the proportion of $\text{CH}_3(\text{CF}_3)\text{P}(\text{O})\text{OCH}_3$ in the reacting mixture observed at arbitrary time intervals was always greater than that of $\text{CH}_3(\text{CF}_3)\text{P}(\text{O})\text{F}$, suggesting therefore that the process in eq III-15, is faster than that of eq III-14. Second, we noted that if the product mixture of $\text{CH}_3(\text{CF}_3)\text{P}(\text{OCH}_3)\text{F}_2$, $\text{CH}_3(\text{CH}_3)\text{P}(\text{OCH}_3)_2\text{F}$, $\text{CH}_3(\text{CF}_3)\text{P}(\text{O})\text{OCH}_3$, and $\text{CH}_3(\text{CF}_3)\text{P}(\text{O})\text{F}$ was allowed to stand at room temperature for several weeks, the proportion of $\text{CH}_3(\text{CF}_3)\text{P}(\text{O})\text{F}$ in the sample increased with a concomitant decrease in the amounts of $\text{CH}_3(\text{CF}_3)\text{P}(\text{OCH}_3)\text{F}_2$ and $\text{CH}_3(\text{CF}_3)\text{P}(\text{O})\text{OCH}_3$ and the eventual disappearance of $\text{CH}_3(\text{CF}_3)\text{P}(\text{OCH}_3)_2\text{F}$. In addition dimethyl ether was produced. An isolated relatively pure sample of $\text{CH}_3(\text{CF}_3)\text{P}(\text{OCH}_3)\text{F}_2$ remained unchanged after several weeks at room temperature indicating that the above transformations arise from secondary reaction between the various products and not from inherent instability of $\text{CH}_3(\text{CF}_3)\text{P}(\text{OCH}_3)\text{F}_2$. These observations can be explained by assuming that the following reaction (eq III-16) occurred in addition to eq III-14.



Thus two possible routes to the formation of $(\text{CH}_3)_2\text{O}$ can

be proposed but to date neither of the processes described by eqs III-14 or III-16 have been verified by independent experiments. It is notable that the formation of methyl fluoride, analogous to eq III-10, proposed as a reaction step for the chlorophosphoranes, does not appear to be an accessible route for the decomposition of $\text{CH}_3(\text{CF}_3)\text{P}(\text{OCH}_3)\text{F}_2$.

It is not clear why $\text{CH}_3(\text{CF}_3)\text{PF}_3$ and $\text{CH}_3(\text{CF}_3)\text{PCl}_3$ behave so differently but it is reasonable to suppose, since $(\text{CH}_3)_3\text{SiF}$ and $(\text{CH}_3)_3\text{SiCl}$ were formed in appropriate amounts, that the initial metathetical replacement of a halogen by the OCH_3 substituent is common to both systems and that the observed differences arise from the secondary reactions suffered by the products. Thus the unique formation of $(\text{CH}_3)_2\text{O}$ from the former and CH_3Cl from the latter are the notable differences which require explanation as well as the fact that the trifluorophosphorane produced both the mono- and bis(methoxy)-substituted phosphoranes, $\text{CH}_3(\text{CF}_3)\text{P}(\text{OCH}_3)\text{F}_2$ and $\text{CH}_3(\text{CF}_3)\text{P}(\text{OCH}_3)_2\text{F}$, the latter being the most likely source of $(\text{CH}_3)_2\text{O}$ (eq III-14), although other routes (eq III-16) are possible, while the chlorophosphorane produced no detectable amount of methoxy-substituted chlorophosphoranes.

One possible reason for the differences in stability and reactivity and the initially formed products may be in the character of the substituents involved, Cl,

OCH_3 and F. An internal intramolecular rearrangement can be proposed (Fig III-1) for the elimination of CH_3Cl from the initially formed postulated intermediate, $\text{CH}_3(\text{CF}_3)\text{PCl}_2\text{OCH}_3$ (eq III-10).



Fig III-1

This process (an internal nucleophilic substitution reaction)⁶⁹ is likely to be much more feasible for the chlorophosphoranes because Cl is a much better leaving group than either F or OCH_3 .⁶⁹ Equivalent bimolecular processes involving the postulated intermediate with itself or $\text{CH}_3(\text{CF}_3)\text{PCl}_3$ can easily be written.

In contrast fluorophosphoranes are less likely to suffer such internal displacement reactions because F is a poorer leaving group than Cl.⁶⁹ This difference can explain why $\text{CH}_3(\text{CF}_3)\text{P}(\text{OCH}_3)\text{F}_2$ was apparently much more stable and was indeed readily isolated from the reaction system. The stability of $\text{CH}_3(\text{CF}_3)\text{P}(\text{OCH}_3)\text{F}_2$ leads to subsequent substitution by $(\text{CH}_3)_3\text{SiOCH}_3$ with the resultant formation of $\text{CH}_3(\text{CF}_3)\text{P}(\text{OCH}_3)_2\text{F}$. This species appears to decompose to $\text{CH}_3(\text{CF}_3)\text{P}(\text{O})\text{F}$ and $(\text{CH}_3)_2\text{O}$ and the process can be depicted as an internal nucleophilic substitution

reaction (Fig III-2) of $\text{CH}_3(\text{CF}_3)\text{P}(\text{OCH}_3)_2\text{F}$, now involving OCH_3 which is a better leaving group than F, leading to the observed products given by eq III-14.

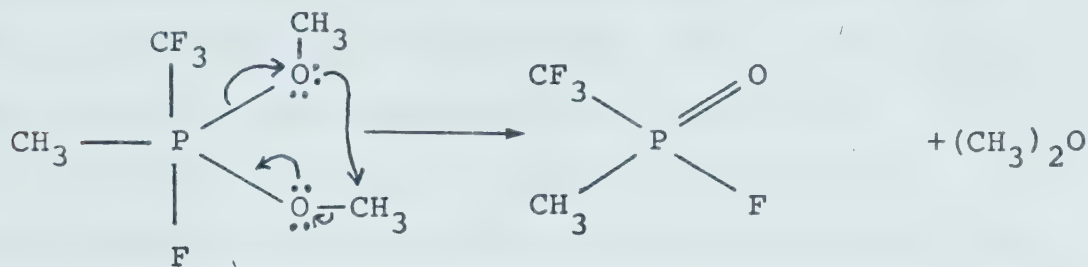
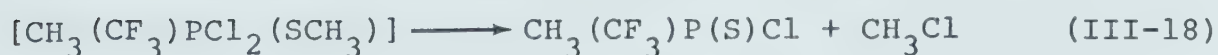


Fig III-2

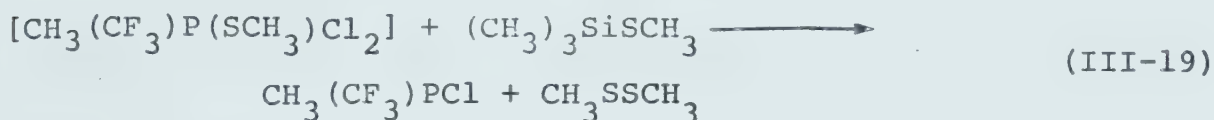
As before equivalent bimolecular processes can be written to yield the same overall products.

The effect of different leaving group character of substituents is to therefore greatly alter the overall chemistry of the two systems. In the absence of more detailed information, further speculation is unwise. However, it is clear that there is much interesting substitutional chemistry of pentavalent pentacoordinate phosphorus to be done. In the present case additional investigations of the reactions described above are needed to establish where possible the validity of equations III-9 to III-16. Likewise, establishing the particular origin of the CH_3 groups in the CH_3Cl and $(\text{CH}_3)_2\text{O}$ products by means of isotopic labelling (for example, preparing OCD_3 phosphoranes and following their reactions) would likely prove rewarding.

The reaction of $\text{CH}_3(\text{CF}_3)\text{PF}_3$ with $(\text{CH}_3)_3\text{SiSCH}_3$ was analogous to its reaction with $(\text{CH}_3)_3\text{SiOCH}_3$ except that only the monosubstituted thiophosphorane, $\text{CH}_3(\text{CF}_3)\text{PF}_2\text{-(SCH}_3)$, was formed and in excellent yield. This compound was stable at room temperature for a period of several months. In sharp contrast, the trichlorophosphorane yielded the thiophosphorylchloride, $\text{CH}_3(\text{CF}_3)\text{-P(S)Cl}$, and CH_3Cl , rather than the analogous thiophosphorane, $\text{CH}_3(\text{CF}_3)\text{PCl}_2(\text{SCH}_3)$, a behavior reminiscent of the reaction of $\text{CH}_3(\text{CF}_3)\text{PCl}_3$ with $(\text{CH}_3)_3\text{SiOCH}_3$, although the products are somewhat different. Again it seems reasonable to suggest that the dichlorothiophosphorane, $\text{CH}_3(\text{CF}_3)\text{PCl}_2(\text{SCH}_3)$, is first formed by means of the expected metathetical substitution (eq III-17 analogous to eq III-9) but this compound is unstable and decomposes in the same way as that suggested for the oxy analog (eq III-10), perhaps involving a process similar to that postulated for $\text{CH}_3(\text{CF}_3)\text{PCl}_2(\text{OCH}_3)$ depicted in Figure III-1. Thus the behavior of the system is expressed by eqs III-17 and III-18.



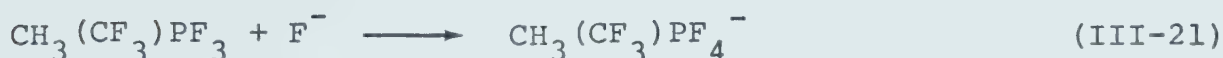
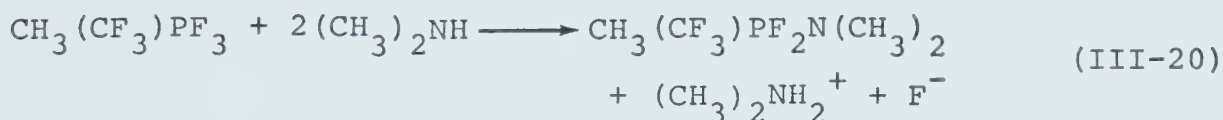
The presence of $\text{CH}_3(\text{CF}_3)\text{PCl}$ and CH_3SSCH_3 indicate that another decomposition route involving oxidation and reduction processes (eq III-19) exists for the postulated intermediate $\text{CH}_3(\text{CF}_3)\text{P}(\text{SCH}_3)\text{Cl}_2$, in addition to methyl chloride elimination (eq III-18). The detection among the products of $\text{CH}_3(\text{CF}_3)\text{PCl}$ and other unidentified phosphorus-fluorine compounds whose nmr parameters indicate a trivalent state for phosphorus suggest that a mutual redox reaction involving the phosphorane and another mole of $(\text{CH}_3)_3\text{SiSCH}_3$ (eq III-19) can occur.



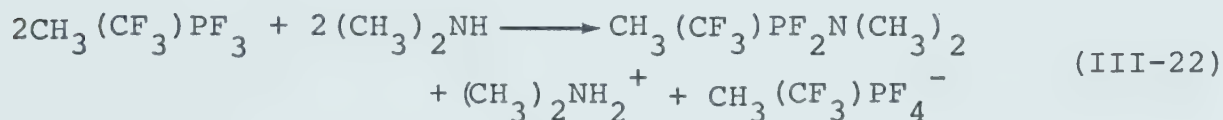
This process is important in this system because CH_3S is more readily oxidized than CH_3O .

While the reaction of $(\text{CH}_3)_2\text{NH}$ with $(\text{CF}_3)_n\text{PCl}_{5-n}$ ($n = 2, 3$) resulted in a mixture of both $(\text{CF}_3)_3\text{PClN}(\text{CH}_3)_2$ and $(\text{CF}_3)_3\text{P}[\text{N}(\text{CH}_3)_2]$ from $(\text{CF}_3)_3\text{PCl}_2$ or $(\text{CF}_3)_2\text{PCl}_2\text{N}(\text{CH}_3)_2$ and $\text{CF}_3\text{P}[\text{N}(\text{CH}_3)_2]_3^+$ from $(\text{CF}_3)_2\text{PCl}_3$,^{26a} its reaction with $\text{CH}_3(\text{CF}_3)\text{PF}_3$ yielded only the monosubstituted product, $\text{CH}_3(\text{CF}_3)\text{PF}_2\text{N}(\text{CH}_3)_2$, together with hexacoordinate species $\text{CH}_3(\text{CF}_3)\text{PF}_4^-$ which was identified principally by means of its ^{19}F nmr spectrum (Fig. III-3). These differences in the extent of amine substitution may have arisen from the greater lability of the P-Cl bond relative to the P-F bond.

The formation of the hexacoordinate anionic species $\text{CH}_3(\text{CF}_3)\text{PF}_4^-$ is not surprising since the trifluorophosphorane $\text{CH}_3(\text{CF}_3)\text{PF}_3$ should be a rather strong Lewis acid considering the high electronegativity of both the CF_3 and the fluorine substituents. Hence the phosphorane readily abstracts a fluoride ion according to the following equations:



and the overall reaction is:



in agreement with the observed 1:1 stoichiometry of the reaction.

The ^{19}F nmr spectrum of $\text{CH}_3(\text{CF}_3)\text{PF}_4^-$ (Fig III-3) consists of two resonance regions, one is a doublet of quintets with a 1:4:6:4:1 intensity ratio, the other, a doublet of multiplets, the line intensity ratio of which was difficult to assess because of the breadth of the lines. This multiplet structure within each portion of the major doublet was interpreted as arising from a partially overlapping quartet of quartets due to

Figure III-3 Observed ^{19}F (84.6 MHz) nmr spectrum of the $\text{CH}_3(\text{CF}_3)\text{PF}_4^-$ ion at 306°K, obtained from a solution in CD_3CN . The frequency scale gives chemical shift values in Hz relative to external CFCl_3 (cap.).

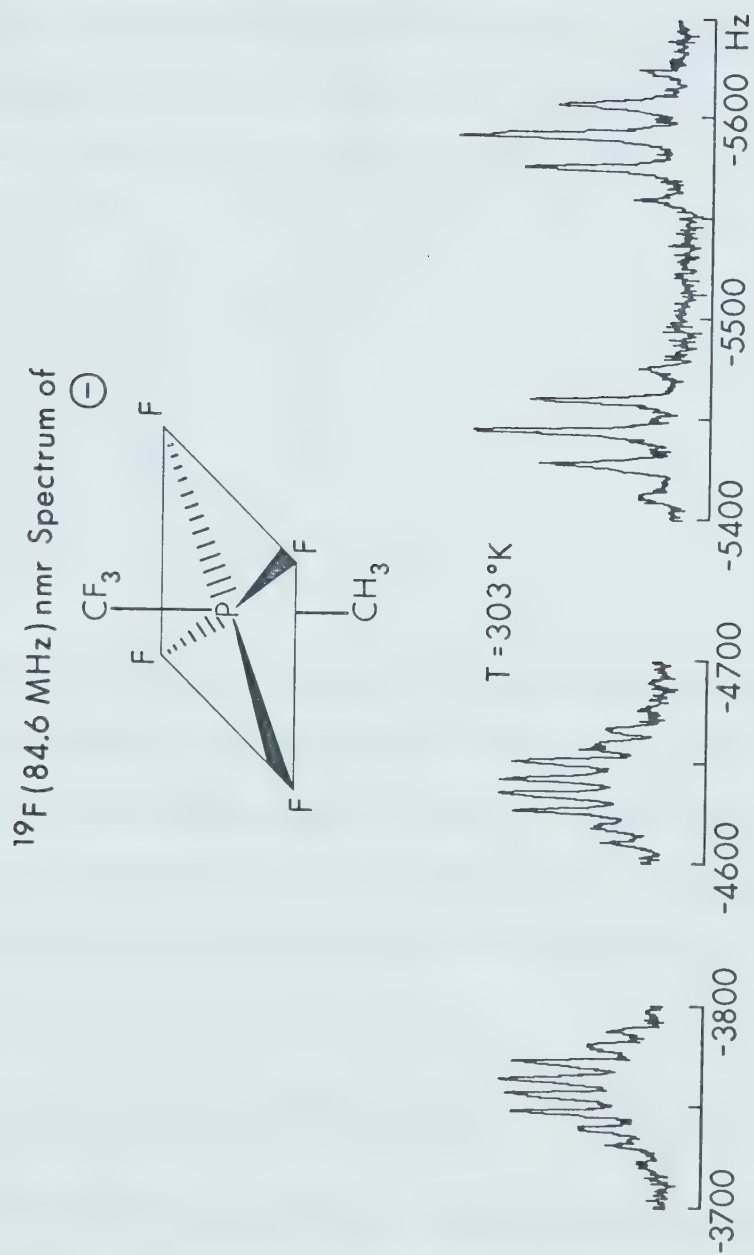


Figure III-3

coupling of the observed directly-bound fluorines with the CF_3 and CH_3 groups. The doublet of quintets upfield of the first signal was assigned to the CF_3 group which is coupled with the four directly-bound fluorine atoms. The ionic structure compatible with this interpretation is the octahedral structure with the CH_3 and CF_3 groups possessing a mutual *trans* relationship (Fig III-4).

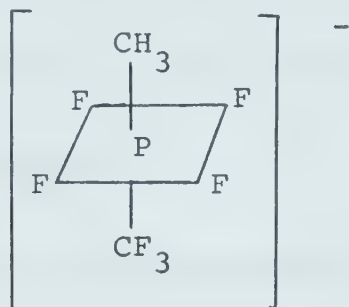


Figure III-4

The aminophosphorane $\text{CH}_3(\text{CF}_3)\text{PF}_2\text{N}(\text{CH}_3)_2$, is stable to disproportionation in contrast to the related aminofluorophosphoranes, $\text{C}_6\text{H}_5\text{PF}_3\text{N}(\text{CH}_3)_2$ and $\text{CH}_3\text{PF}_3\text{N}(\text{CH}_3)_2$, which after three weeks at room temperature rearranged to the isomeric salts according to the following equation:³⁸



$\text{CH}_3(\text{CF}_3)\text{PF}_2\text{N}(\text{CH}_3)_2$ remained unchanged even after being heated to 90°C for several days. Similar stability was observed for $(\text{CF}_3)_2\text{PF}_2\text{N}(\text{CH}_3)_2$ (chapter IV). The observation that the diethylamino(phenyl)phosphorane, $\text{C}_6\text{H}_5\text{PF}_3\text{N}(\text{C}_2\text{H}_5)_2$,

was unchanged even after six months at room temperature has led to the conclusion that special conditions are required for this isomerization to occur.³⁸

The resistance of $\text{CH}_3(\text{CF}_3)\text{PF}_2\text{N}(\text{CH}_3)_2$ to P-F bond cleavage is further demonstrated by its lack of reactivity with $(\text{CH}_3)_3\text{SiOCH}_3$ even at elevated temperatures. These observations are in complete agreement with those reported on attempted disubstitution of other trifluorophosphoranes with either -SR or -NR₂ groups.³⁹

B. Mass Spectra.

The trihalophosphoranes $\text{CH}_3(\text{CF}_3)\text{PF}_3$ and $\text{CH}_3(\text{CF}_3)\text{PCl}_3$ did not exhibit any parent ion peak in their mass spectra, in keeping with the usual behavior of phosphoranes.⁴⁰ The relative abundance of the accurately measured mass fragments suggests that cleavage of P-CH₃ is nearly as easy as cleavage of P-CF₃, for example, $\text{CH}_3\text{PCl}_3^+$ (0.54%) and $\text{CF}_3\text{PCl}_3^+$ (1.51%) were formed in reasonably equivalent abundance from $\text{CH}_3(\text{CF}_3)\text{PCl}_3$ (Tables 4 and 5).

The dimethylaminodifluorophosphorane on the other hand showed a peak due to the parent ion (calculated m/e, 197.0393; measured m/e, 197.0398). A few other aminophosphoranes have similarly shown appreciable parent ion intensities.⁴⁰

The methylthiophosphorane $\text{CH}_3(\text{CF}_3)\text{PF}_2(\text{SCH}_3)$, did not show a parent ion peak in its mass spectrum.

TABLE 5

Mass Measurement Data for Methyl(trifluoromethyl)-
halophosphoranes

Compound	Ion ^a	m/e	
		Calculated	Measured
$\text{CH}_3(\text{CF}_3)\text{PF}_3$	CF_3PF_3^+	156.9642	156.9647
	$\text{CH}_3(\text{CF}_3)\text{PF}_2^+$	152.9893	152.9898
	CH_3PF_3^+	102.9925	102.9922
	CH_2PF_3^+	101.9846	101.9846
$\text{CH}_3(\text{CF}_3)\text{PCl}_3$	$\text{CF}_3\text{PCl}_3^+$	204.8757	204.8761
	$\text{CH}_3\text{PCl}_3^+$	150.9039	150.9034
	CF_3^+	68.9952	68.9952
	CH_3Cl^+	49.9923	49.9924
$\text{CH}_3(\text{CF}_3)\text{PF}_2\text{N}(\text{CH}_3)_2$	$\text{CH}_3(\text{CF}_3)\text{PF}_2\text{N}(\text{CH}_3)_2^+$	197.0393	197.0398
	$\text{CH}_3\text{PF}_2\text{N}(\text{CH}_3)_2^+$	182.0158	182.0155
	$\text{CH}_3(\text{CF}_3)\text{PFN}(\text{CH}_3)_2^+$	178.0409	178.0406
	$\text{CH}_3(\text{CF}_3)\text{PF}_2^+$	153.9893	153.9890
	$\text{CH}_3\text{PF}_2\text{N}(\text{CH}_3)_2^+$	128.0441	128.0444
	$\text{CH}_3\text{PF}_2\text{NCH}_2^+$	112.0128	112.0124
$\text{CH}_3(\text{CF}_3)\text{PF}_2(\text{SCH}_3)$	$\text{CH}_2(\text{CF}_3)\text{PF}_2(\text{SCH}_3)^+$	198.9770	198.9764
	$\text{CF}_3\text{PF}_2(\text{SCH}_3)^+$	184.9613	184.9608
	$\text{CH}_3(\text{CF}_3)\text{PF}(\text{SCH}_3)^+$	180.9864	180.9870
	$\text{CH}_3(\text{CF}_3)\text{P}(\text{SCH}_3)^+$	161.9880	161.9876

continued.....

TABLE 5 (continued)

$\text{CH}_3(\text{CF}_3)\text{PF}_2^+$	152.9893	152.9898
$\text{CH}_3\text{PF}_2(\text{SCH}_3)^+$	130.9896	130.9892
CH_3PF_3^+	102.9925	102.9922

^a A reasonable structural formula rather than the molecular formula is given for each fragment ion merely for convenience of recognition.

Nevertheless, accurate mass measurement of some of the higher mass fragments indicate that these fragments must arise from the loss of CH_3 , or CF_3 , or SCH_3 , or directly-bound fluorine from the appropriate parent molecule. Their distribution may be correlated with the relative ease of the possible bond cleavages.

C. Infrared Spectra.

The infrared spectra of the halophosphoranes described in this chapter are supportive rather than conclusive evidence of their molecular ground state structures, primarily because the number of atoms in the molecule, and the low molecular symmetry, provide a complicated system which in the present study has only been qualitatively analyzed by comparison with characteristic group assignments given elsewhere.⁴¹ The spectral bands observed do support the presence of certain structural units in these compounds.⁴¹ The four compounds $\text{CH}_3(\text{CF}_3)\text{PCl}_3$, $\text{CH}_3(\text{CF}_3)\text{PF}_3$, $\text{CH}_3(\text{CF}_3)\text{PF}_2\text{N}(\text{CH}_3)_2$ and $\text{CH}_3(\text{CF}_3)\text{PF}_2(\text{SCH}_3)$ all absorb in the 1300 cm^{-1} region, indicative of a P-CH_3 bond,¹⁰¹ and in the regions between $1100\text{-}1200\text{ cm}^{-1}$ and $400\text{-}520\text{ cm}^{-1}$, which are characteristic of P-CF_3 absorption. In addition, $\text{CH}_3(\text{CF}_3)\text{PF}_3$ shows peaks between $820\text{-}980\text{ cm}^{-1}$ which are indicative of P-F vibrations and similarly the trichlorophosphorane shows peaks between $540\text{-}740\text{ cm}^{-1}$, the characteristic absorption for a P-Cl bond in R_2PCl_3

compounds. ⁴¹

In the case of $\text{CH}_3(\text{CF}_3)\text{PF}_2\text{N}(\text{CH}_3)_2$ the absorption frequency of the P-NC_2 unit ($\sim 1000 \text{ cm}^{-1}$) is difficult to identify since it occurs close to the absorption frequency region of the P-CF_3 grouping.

Limited data on, and inherent weakness of, P-S-C vibrations make assignment of group frequencies arising from this structural feature in the infrared spectra of $\text{CH}_3(\text{CF}_3)\text{PF}_2(\text{SCH}_3)$ less certain but the region at about 700 cm^{-1} has been assigned to the vibration frequency of P-S-CH_3 ⁴¹ grouping and $\text{CH}_3(\text{CF}_3)\text{PF}_2(\text{SCH}_3)$ shows bands in this region in agreement with expectation.

Conclusions

The trihalophosphoranes $\text{CH}_3(\text{CF}_3)\text{PCl}_3$ and $\text{CH}_3(\text{CF}_3)\text{PF}_3$ react very differently with $(\text{CH}_3)_3\text{SiOCH}_3$, $(\text{CH}_3)_3\text{SiN}(\text{CH}_3)_2$, and $(\text{CH}_3)_3\text{SiSCH}_3$. The reactions can be rationalized by considering that the initial metathetical substitution reaction of $(\text{CH}_3)_3\text{SiOCH}_3$ and $(\text{CH}_3)_3\text{SiSCH}_3$ with the halophosphoranes is followed by decompositions and subsequent reactions with starting materials which can be qualitatively understood in terms of the relative leaving group characters of the substituents on phosphorus. The formation of CH_3Cl from the reactions of $\text{CH}_3(\text{CF}_3)\text{PCl}_3$ with $(\text{CH}_3)_3\text{SiOCH}_3$ or $(\text{CH}_3)_3\text{SiSCH}_3$ suggests that both reactions follow similar pathways. In addition, the detection of approximately equal amounts of $\text{CH}_3(\text{CF}_3)\text{PCl}_2$ and CH_3SSCH_3 among the products of the reaction of $\text{CH}_3(\text{CF}_3)\text{PCl}_3$ with $(\text{CH}_3)_3\text{SiSCH}_3$ indicate a redox reaction (eq III-19) as an additional decomposition route for the postulated dichloro-intermediate, $\text{CH}_3(\text{CF}_3)\text{P}(\text{SCH}_3)\text{Cl}_2$.

In contrast, the poorer leaving group character of OCH_3 and F leads to higher stability of $\text{CH}_3(\text{CF}_3)\text{P}(\text{OCH}_3)\text{F}_2$ and the formation of the disubstituted product, $\text{CH}_3(\text{CF}_3)\text{P}(\text{OCH}_3)_2\text{F}$ becomes feasible. The formation of $(\text{CH}_3)_2\text{O}$ can be rationalized as a decomposition of the latter by a similar internal rearrangement (or equivalent) involving OCH_3 as the most nucleophilic site in the molecule.

The aminosilane reacted in a straightforward fashion with $\text{CH}_3(\text{CF}_3)\text{PCl}_3$. The only unusual feature was the formation of a diaminochlorophosphorane, $\text{CH}_3(\text{CF}_3)\text{-PCl}[\text{N}(\text{CH}_3)_2]_2$ in contrast to the monosubstitution limit observed for $(\text{CF}_3)_3\text{PCl}_2$.³⁷ In general many more stable compounds were isolated from the $\text{CH}_3(\text{CF}_3)\text{PF}_3$ system, indicating the greater stability of the fluorides compared to the chlorides.

The mass spectral behavior of the four methyl(tri-fluoromethyl)phosphoranes, $\text{CH}_3(\text{CF}_3)\text{PCl}_3$, $\text{CH}_3(\text{CF}_3)\text{PF}_3$, $\text{CH}_3(\text{CF}_3)\text{PF}_2\text{N}(\text{CH}_3)_2$, and $\text{CH}_3(\text{CF}_3)\text{PF}_2(\text{SCH}_3)$ is similar and reflects relative stabilities of the parent ions. With the exception of $\text{CH}_3(\text{CF}_3)\text{PF}_2\text{N}(\text{CH}_3)_2$, none showed a parent ion peak.

The base hydrolysis of the methyl(trifluoromethyl)-phosphoranes is rather interesting in that use of 10% NaOH solution cleaved only the P-X, P-N and P-S bonds leaving $\text{CH}_3(\text{CF}_3)\text{PO}_2^-$ ions in solution. More concentrated NaOH solutions cleaved the P- CF_3 bond as well to give CH_3PO_3^- ions. Thus the $\text{CH}_3(\text{CF}_3)\text{PO}_2^-$ ions is stable to mild alkaline conditions but not to very strong alkaline conditions.

CHAPTER FOUR

SYNTHESIS AND REACTIONS OF SOME AMINOBIS (TRIFLUOROMETHYL) FLUORO- PHOSPHORANES

Acyclic halogenophosphoranes containing the trifluoromethyl group in the series CF_3PX_4 , $(\text{CF}_3)_2\text{PX}_3$, and $(\text{CF}_3)_3\text{PX}_2$ where X = F, Cl or Br,^{7,22-24,42} have been investigated by various spectroscopic techniques. Detailed nmr studies of various related trifluoromethylphosphoranes containing substituents such as F, Cl, $\text{OSi}(\text{CH}_3)_3$, OCH_3 , SCH_3 , $\text{N}(\text{CH}_3)_2$ by Cavell and co-workers^{26-28,42} have indicated that each of the halogens, regardless of its electronegativity, appears to preferentially occupy the axial position in the trigonal bipyramidal framework. The axial preference rule of Muetterties *et. al.*⁷ which stated that the groups of highest electronegativity preferentially occupy the axial positions must therefore be slightly modified. A small amount of additional data bearing on this problem is provided by the present study.

In this chapter the synthesis and chemical behaviour of the phosphoranes $(\text{CF}_3)_2\text{PF}(\text{X})\text{N}(\text{CH}_3)_2$ (X = F, Cl, OCH_3) are described. In general the desired compounds were prepared directly from either $(\text{CF}_3)_2\text{PFCl}_2$ ⁴³ or $(\text{CF}_3)_2\text{PCl}_2\text{-N}(\text{CH}_3)_2$ ^{26a} both of which were synthesized according to published methods.

Experimental

A. Synthesis of $(\text{CF}_3)_2\text{PF}_2\text{N}(\text{CH}_3)_2$.

Bis(trifluoromethyl)dimethylaminodifluorophosphorane, $(\text{CF}_3)_2\text{PF}_2\text{N}(\text{CH}_3)_2$, was first synthesized by Sawin,³⁰ by means of the reaction of bis(trifluoromethyl)tri-fluorophosphorane with N,N-dimethylaminotrimethylsilane, $(\text{CH}_3)_3\text{SiN}(\text{CH}_3)_2$. This approach gave a very low (16%) yield of $(\text{CF}_3)_2\text{PF}_2\text{N}(\text{CH}_3)_2$, and the product could not be properly purified. A better method which gave a nearly quantitative yield of pure $(\text{CF}_3)_2\text{PF}_2\text{N}(\text{CH}_3)_2$ was the fluorination of the corresponding dichlorophosphorane prepared as reported by Cavell and Poulin.^{26a}

In a typical reaction, $(\text{CF}_3)_2\text{PCl}_2\text{N}(\text{CH}_3)_2$ (1.53 g, 5.40 mmoles) was condensed into a reaction tube containing sublimed SbF_3 . The tube was sealed under vacuum, and agitated for several days at room temperature, after which the volatile products were fractionated under vacuum. Pure $(\text{CF}_3)_2\text{PF}_2\text{N}(\text{CH}_3)_2$ was collected in the -78°C trap (1.25 g, 5.00 mmoles, 93% yield). The compound was identified by its spectroscopic properties (ir, Table 6; nmr, Table 7; mass spectra, Tables 8 and 9) which corresponded well with the data obtained by Sawin.³⁰

B. Reactions of $(\text{CF}_3)_2\text{PF}_2\text{N}(\text{CH}_3)_2$

(i) Alkaline hydrolysis

Treatment of $(\text{CF}_3)_2\text{PF}_2\text{N}(\text{CH}_3)_2$ (0.404 g, 1.61 mmol) with about 0.5 ml of degassed 10% aqueous NaOH solution yielded CF_3H and $(\text{CH}_3)_2\text{NH}$ (total mass = 0.143 g) as volatile products. ^{19}F and ^1H nmr spectra of the nonvolatile materials left in solution indicated the presence of F^- , $\text{CF}_3\text{PO}_3^{4-}$ and $(\text{CH}_3)_2\text{NH}_2^+$ ions.

(ii) Neutral hydrolysis

Treatment of $(\text{CF}_3)_2\text{PF}_2\text{N}(\text{CH}_3)_2$ with water (0.130 g, 0.520 mmol) gave no CF_3H . Instead $(\text{CF}_3)_2\text{PO}_2^-$ and $(\text{CH}_3)_2\text{NH}_2^+$ ions remained in the hydrolysate as indicated by ^1H and ^{19}F nmr spectra. Single nmr peaks corresponding to those of F^- ($\phi_{\text{F}} = 120.9$ ppm) and HF_2^- ($\phi_{\text{F}} = 150.0$ ppm) ions were also indicated in the ^{19}F nmr spectrum.

(iii) Reaction with $(\text{CH}_3)_3\text{SiOCH}_3$

$(\text{CF}_3)_2\text{PF}_2\text{N}(\text{CH}_3)_2$ (0.275 g, 1.10 mmol) was condensed onto $(\text{CH}_3)_3\text{SiOCH}_3$ (0.133 g, 1.28 mmol) in a reaction tube. No reaction occurred either at room temperature or upon heating the mixture to 50°C for several days. Heating the mixture to 96°C for four days resulted in the formation of transparent

crystals on the walls of the reaction tube. The volatile contents of the tube were vacuum fractionated leaving behind an involatile solid which was identified, by means of the ^1H and ^{19}F nmr spectra of a solution of this solid in CD_3CN , as a salt mixture containing $(\text{CH}_3)_4\text{N}^+$, $(\text{CF}_3)_2\text{PO}_2^-$, and $(\text{CF}_3)_2\text{PF}_4^-$ ⁴⁵ ions (total mass = 0.116 g) plus an unidentified fluorine-containing compound (very broad quartet $\phi_{\text{F}} = 67.7$ ppm, $J = 12$ Hz). The volatile fraction (total mass = 0.293 g) contained $(\text{CH}_3)_3\text{SiF}$, $(\text{CF}_3)_2\text{PF}(\text{OCH}_3)\text{N}(\text{CH}_3)_2$, $(\text{CF}_3)_2\text{P}(\text{O})\text{N}(\text{CH}_3)_2$ and unreacted $(\text{CF}_3)_2\text{PF}_2\text{N}(\text{CH}_3)_2$ and $(\text{CH}_3)_3\text{SiOCH}_3$. Since the only novel product of this reaction, $(\text{CF}_3)_2\text{PF}(\text{OCH}_3)\text{N}(\text{CH}_3)_2$, was obtained in better yield from $(\text{CF}_3)_2\text{PF}(\text{Cl})\text{N}(\text{CH}_3)_2$ (*vide infra*) no further investigation of this system was undertaken.

(iv) Reaction with $(\text{CH}_3)_2\text{NH}$

$(\text{CF}_3)_2\text{PF}_2\text{N}(\text{CH}_3)_2$ (0.362 g, 1.44 mmol) was condensed onto $(\text{CH}_3)_2\text{NH}$ (0.037 g, 0.827 mmol). Since no visible reaction occurred during one week at room temperature the reaction vessel was heated to 96°C for five days, which resulted in the formation of some white solid which was deposited on the walls of the tube. The volatile contents of the reaction vessel were fractionated in vacuum yielding in the -45°C fraction, the bulk of the product, $\text{CF}_3\text{PF}_2[\text{N}(\text{CH}_3)_2]_2$ ^{26b}

with a trace amount of $(\text{CF}_3)_2\text{P}(\text{O})\text{N}(\text{CH}_3)_2$, some unreacted $(\text{CF}_3)_2\text{PF}_2\text{N}(\text{CH}_3)_2$, and an unidentified fluorine-containing compound (a broad doublet, $\phi_{\text{F}} = 58$ ppm, $J_{\text{P-F}} \approx 80$ Hz) (total mass = 0.031 g). More unreacted $(\text{CF}_3)_2\text{PF}_2\text{N}(\text{CH}_3)_2$ (0.275 g, 1.10 mmol) was trapped at -78°C . The -196°C fraction consisted of unreacted $(\text{CH}_3)_2\text{NH}$ and a small amount of CF_3H (total mass = 0.040 g). The nmr spectra of a solution in CD_3CN of the white nonvolatile solid indicated that the solid was principally a salt containing the ions $\text{CF}_3\text{P}[\text{N}(\text{CH}_3)_2]_3^+$ ^{26a}, $(\text{CF}_3)_2\text{PF}_4^-$ ⁴⁵ (approx. mass, 0.044 g) and an unidentified phosphorus-containing compound (a doublet, $\tau_{\text{H}} = 7.58$ J_{P-H} = 10.8 Hz).

C. Reactions of $(\text{CF}_3)_2\text{PCl}_2\text{N}(\text{CH}_3)_2$.

(i) Reaction with $(\text{CH}_3)_3\text{SiOCH}_3$

Bis(trifluoromethyl)dimethylaminodichlorophosphorane^{26a} (0.221 g, 0.777 mmol) was condensed into a 10 cc reaction tube with $(\text{CH}_3)_3\text{SiOCH}_3$ (0.157 g, 1.50 mmol) which was then sealed under vacuum and agitated at room temperature for five days. The products were identified by ^1H , ^{19}F and ^{31}P nmr and ir spectroscopy as $(\text{CF}_3)_2\text{P}(\text{O})[\text{N}(\text{CH}_3)_2]$ (0.157 g, 0.684 mmol), and CH_3Cl (0.0314 g, 0.628 mmol). Some $(\text{CH}_3)_2\text{O}$ in an approximate 1:1 molar ratio with CH_3Cl plus traces of $(\text{CF}_3)_2\text{P}(\text{O})\text{OCH}_3$ (Appendix Table 7) and an unidentified fluoro-

phosphorus compound ($\phi_F = 71.5$ ppm, $J_{P-F} = 121$ Hz) were also detected. A mixture of $(CH_3)_3SiCl$ and unreacted $(CF_3)_2PCl_2N(CH_3)_2$ and $(CH_3)_3SiOCH_3$ (total mass = 0.182 g) was trapped at $-96^\circ C$.

D. Synthesis of $(CF_3)_2PF(Cl)N(CH_3)_2$.

Bis(trifluoromethyl)dimethylaminochlorofluorophosphorane, $(CF_3)_2PF(Cl)N(CH_3)_2$, was synthesized by condensing $(CF_3)_2PFCl_2$ (0.499 g, 1.930 mmoles) with $(CH_3)_3SiN(CH_3)_2$ (0.224 g, 1.910 mmoles) in a 10 cc reaction tube which was sealed under vacuum and allowed to gradually warm up to room temperature. After agitation for 24 hours the volatile contents of the tube were vacuum fractionated yielding, as the bulk of the product, the desired compound, $(CF_3)_2PF(Cl)N(CH_3)_2$, which was collected in the $-23^\circ C$ trap (0.304 g, 1.14 mmole) along with small quantities of $(CF_3)_2PCl_2N(CH_3)_2$ and $(CF_3)_2PCl_3$. Other products of the reaction were $(CF_3)_2PF_2N(CH_3)_2$, $(CF_3)_2PN(CH_3)_2$, $(CF_3)_2PCl$ and $(CH_3)_3SiCl$ (obtained as an unseparated mixture, combined mass, 0.315 g). The nmr spectra of a solution of the white involatile solid which remained in the reaction tube (approx. mass, 0.118 g) indicated the presence of $(CH_3)_2NH_2^+$, two unidentified phosphorus-containing compounds (or ions) ($\phi_F = 67.0$ ppm, $^2J_{P-F} = 190$ Hz, $^2J_{F-F} = 14.5$ Hz; $\phi_F = 70.4$ ppm,

$^2J_{\text{P-F}} = 176 \text{ Hz}$, $^2J_{\text{F-F}} = 14.5 \text{ Hz}$), and at least one other phosphorus-containing compound which gave a doublet of very broad peaks in the proton spectrum.

The infrared spectral data for $(\text{CF}_3)_2\text{PF}(\text{Cl})\text{N}(\text{CH}_3)_2$ are given in Table 6, nmr data in Table 7, and mass spectral data in Tables 8 and 9.

E. Reactions of $(\text{CF}_3)_2\text{PF}(\text{Cl})\text{N}(\text{CH}_3)_2$.

(i) Alkaline hydrolysis

Treatment of $(\text{CF}_3)_2\text{PF}(\text{Cl})\text{N}(\text{CH}_3)_2$ (0.063 g, 0.234 mmole) with about 0.5 ml of degassed saturated aqueous NaOH solution for several days gave, as the only volatile product, CF_3H (0.017 g, 0.235 mmole). Fluorine-19 and ^1H nmr spectra of the hydrolysate showed the presence of CF_3PO_3^- , F^- , and $(\text{CH}_3)_2\text{NH}_2^+$ ions.

(ii) Neutral hydrolysis

Treatment of $(\text{CF}_3)_2\text{PF}(\text{Cl})\text{N}(\text{CH}_3)_2$ (0.130 g, 0.480 mmole) with water gave no volatile product. The hydrolysate, according to ^1H and ^{19}F nmr spectroscopy, contained $(\text{CH}_3)_2\text{NH}_2^+$, $(\text{CF}_3)_2\text{PO}_2^-$, and probably F^- ($\phi_{\text{F}} = 129.2 \text{ ppm}$) ions.

(iii) Reaction with SbF_3

$(\text{CF}_3)_2\text{PF}(\text{Cl})\text{N}(\text{CH}_3)_2$ (0.190 g, 0.690 mmole) was condensed into a reaction tube containing freshly sublimed

SbF_3 . A 70% yield of $(\text{CF}_3)_2\text{PF}_2\text{N}(\text{CH}_3)_2$ (0.119 g, 0.48 mmole) was obtained. The compound was identified by means of its ir and nmr spectra.

(iv) Reaction with $(\text{CH}_3)_3\text{SiOCH}_3$

$(\text{CF}_3)_2\text{PF}(\text{Cl})\text{N}(\text{CH}_3)_2$ (0.368 g, 1.38 mmole) was condensed onto $(\text{CH}_3)_3\text{SiOCH}_3$ (0.259 g, 2.49 mmole) in a 10 cc reaction tube and agitated for one week at room temperature. The volatile products were vacuum fractionated and yielded, as the bulk of the product, the desired compound, $(\text{CF}_3)_2\text{PF}(\text{OCH}_3)\text{N}(\text{CH}_3)_2$, which was trapped at -16°C together with small amounts of $(\text{CF}_3)_2\text{P}(\text{O})\text{N}(\text{CH}_3)_2$ and two unidentified compounds ($\phi_{\text{F}} = 73.4$ ppm, $^2J_{\text{P-F}} = 110$ Hz; $\phi_{\text{F}} = 73.2$ ppm, $^2J_{\text{P-F}} = 64.0$ Hz) (total mass = 0.186 g). More $(\text{CF}_3)_2\text{PF}(\text{OCH}_3)\text{N}(\text{CH}_3)_2$ was collected at -45°C together with some unreacted $(\text{CF}_3)_2\text{PF}(\text{Cl})\text{N}(\text{CH}_3)_2$, some $(\text{CF}_3)_2\text{P}(\text{O})\text{N}(\text{CH}_3)_2$ plus a trace of another unidentified compound ($\tau_{\text{H}} = 6.27$, $J_{\text{P-H}} = 14.7$ Hz) (total mass = 0.0107 g) which showed no ^{19}F signal. The fraction collected at -96°C (0.311 g) consisted of unreacted $(\text{CH}_3)_3\text{SiOCH}_3$ and $(\text{CH}_3)_3\text{SiCl}$. More of this mixture was trapped at -196°C with CH_3Cl and a trace of $(\text{CH}_3)_3\text{SiF}$ (total mass = 0.019 g).

The ir spectral data for $(\text{CF}_3)_2\text{PF}(\text{OCH}_3)\text{N}(\text{CH}_3)_2$ are given in Table 6, nmr data in Table 7, and mass spectral data in Tables 8 and 9.

F. Reactions of $(\text{CF}_3)_2\text{PF}(\text{OCH}_3)\text{N}(\text{CH}_3)_2$

(i) Alkaline hydrolysis

$(\text{CF}_3)_2\text{PF}(\text{OCH}_3)\text{N}(\text{CH}_3)_2$ (0.107 g, 0.410 mmole) was treated for several days with about 0.5 ml saturated NaOH solution. Nmr spectroscopy showed the volatile products to be a mixture of CF_3H , $(\text{CH}_3)_2\text{NH}$, and CH_3OH in approximately 3:1:1 molar ratio (combined mass = 0.043 g). The remaining aqueous solution contained CH_3OH and the ions $(\text{CH}_3)_2\text{NH}_2^+$, CF_3PO_3^- , F^- , and a trace of $(\text{CF}_3)_2\text{PO}_2^-$ according to the ^1H and ^{19}F nmr spectra.

(ii) Neutral hydrolysis

Treatment of $(\text{CF}_3)_2\text{PF}(\text{OCH}_3)\text{N}(\text{CH}_3)_2$ (0.113 g, 0.431 mmole) with water yielded $(\text{CH}_3)_2\text{NH}$ (0.016 g, 0.356 mmole) as the only volatile product, with CH_3OH and the $(\text{CH}_3)_2\text{NH}_2^+$, and $(\text{CF}_3)_2\text{PO}_2^-$ ions remaining in the aqueous solution according to ^1H and ^{19}F nmr spectra obtained on this solution. Single peaks corresponding to F^- ($\phi_{\text{F}} = 129.4$ ppm) and HF_2^- ($\phi_{\text{F}} = 150.0$ ppm) were also evident in the ^{19}F nmr spectrum of the aqueous solution.

Results and Discussion

A. Synthesis and Reactions.

Dimethylaminobis(trifluoromethyl)difluorophosphorane, $(\text{CF}_3)_2\text{PF}_2\text{N}(\text{CH}_3)_2$, reacted with $(\text{CH}_3)_3\text{SiOCH}_3$ and $(\text{CH}_3)_2\text{NH}$

TABLE 6

Infrared Spectral Data for $(\text{CF}_3)_2\text{PFXN}(\text{CH}_3)_2^a$

X = F	X = Cl	X = OCH ₃	Assignment ^b
2951 w	3470 w	3014 vw	} $\nu_{\text{C-H}}$
2922 w	2960 m	2966 m	
2883 w	2880 w	2924 vw	
2831 w	2840 w	-	
-	-	-	
1471 w	1475 w	1466 w	} $\sigma_{\text{as}}\text{CH}_3$
1381 w	1460 w	-	
-	1410 w	-	
1311 m	1290 w	1296 w	} $\sigma_{\text{sym}}\text{CH}_3$
1211 w	1200 m	1284 s	
1161 s	1180 s	1186 s	} ν_{PNC_2}
-	-	1171 s	
1066 s	1155 s	1136 s	} $\nu_{\text{C-F'}}$ $\nu_{\text{POC}}(\text{X}=\text{OCH}_3)$ (?)
1026 s	1060 vw	1111 m	
	1005 m	1076 m	
		1014 m	
837 s	890 m	896 w	} $\nu_{\text{P-F'}}$ $\nu_{\text{P-N'}}$ $\sigma_{\text{as}}\text{CF}_3(?)$
780 m	850 vw	846 m	
731 m	825 vw	811 m	
-	800 vw	769 w	
-	765 m	766 w	
-	730 s	745 m	
-	712 m	696 s	
611 s	610 m	684 m	} $\sigma_{\text{sym}}\text{CF}_3(?)$
537 vw	540 w	616 w	
-	-	583 w	
494 w	-	501 w	} $\nu_{\text{P-CF}_3}$
420 w	-	-	

^a Gas phase spectra and all values in cm^{-1} . s = strong, m = medium, w = weak

^b These assignments are tentative and based mainly on available data on related compounds, as in ref. 41, 103. ν = stretching, σ = deformation, sym = symmetric, as = antisymmetric, ? = a highly tentative assignment.

TABLE 7

NMR Data for Aminobis(trifluoromethyl)fluorophosphoranes

Compound	Temp	τ^a	ϕ_F^b	$\phi_{CH_3}^b$	σ_{31P}^c	$1J_{PF}$ Hz	$2J_{PF}$ Hz	$2J_{PH}$ Hz	$3J_{PH}$ Hz	$3J_{FH}$ Hz	$4J_{FH}$ Hz	$5J_{FH}$ Hz	$3J_{FF}$ Hz	$4J_{FF}$ Hz
$(CF_3)_2PF_2N(CH_3)_2$	30°	7.20	59.4	68.8	170.5	902	157	-	10.4	-	2.2	-	-	-
$(CF_3)_2PFCIN(CH_3)_2$	30°	7.25	44.7	65.1	163.9	883	161	-	12.3	-	2.5	n	18.8	-
$(CF_3)_2PF(OCH_3)N(CH_3)_2$	-10°	7.10 ^d	52.1	62.1 ^f	184.5	816	~62 ^f	-	10.7 ^h	-	2.9 ^j	~0.6 ^l	n	n
		6.28 ^e		65.3 ^g			~130 ^g		14.5 ⁱ		1.9 ^k	~0.5 ^m		

^a τ relative to internal tetramethylsilane, $\tau = 10.0$ (in ppm)^b ϕ relative to internal (solvent) CCl_3F standard with positive values indicating resonance to high field of standard, (in ppm).^c ppm vs. P_4O_6 as external standard (capillary), positive values indicating resonance to high field of standard.^d $N(CH_3)_2$ region, a doublet of poorly resolved doublets^e OCH_3 region, a doublet of poorly resolved doublets^f axial CF_3 , a very broad doublet^g equatorial CF_3 , a broad doublet of "quintets"^h $J_{P-N(CH_3)_2}$

TABLE 7 FOOTNOTES (continued)

- i J_{P-OCH_3}
- j $J_{FPN(CH_3)_2}$, from expansion of $N(CH_3)_2$ resonance peaks into a doublet of doublets of septets
- k $J_{FP(OCH_3)}$, from expansion of OCH_3 resonance peaks into a doublet of doublet of septets
- l $J_{F_3CPN(CH_3)_2}$, from expansion of $N(CH_3)_2$ resonance peaks.
- m $J_{F_3CP(OCH_3)}$, from expansion of OCH_3 resonance peaks.
- n not resolved

TABLE 8

Mass Spectral Data for $(\text{CF}_3)_2\text{PF}_2\text{N}(\text{CH}_3)_2$, $(\text{CF}_3)_2\text{PFCIN}(\text{CH}_3)_2$,
and $(\text{CF}_3)_2\text{PF}(\text{OCH}_3)\text{N}(\text{CH}_3)_2$

m/e	Intensity ^a	Assignment ^b
	$(\text{CF}_3)_2\text{PFCIN}(\text{CH}_3)_2$	$(\text{CF}_3)_2\text{PF}(\text{OCH}_3)\text{N}(\text{CH}_3)_2$
265	3.41	$(\text{CF}_3)_2\text{PFCINCH}_2\text{CH}_2$
244		$(\text{CF}_3)_2\text{P}(\text{OCH}_3)\text{N}(\text{CH}_3)_2$
236	0.51	$\text{C}_3\text{HF}_7\text{ClP}$
235		$\text{C}_4\text{H}_9\text{F}_7\text{NP}$
233		$\text{C}_4\text{H}_8\text{F}_7\text{NP}$
232	0.41	$(\text{CF}_3)_2\text{PFN}(\text{CH}_3)_2$
230	5.97	$(\text{CF}_3)_2\text{PFN}(\text{CH}_3)_2$
229		$(\text{CF}_3)_2\text{PFN}(\text{CH}_3)_2$
228		$\text{C}_4\text{H}_3\text{F}_7\text{NP}$
226		$\text{C}_4\text{HF}_7\text{NP}$
223	1.36	$\text{C}_4\text{H}_3\text{F}_6\text{NOP}$
218	1.02	$(\text{CF}_3)_2\text{PFCl}$
		$\text{C}_3\text{H}_4\text{F}_7\text{NP}$
		1.47

TABLE 8 (continued)

217		0.68	$\text{CF}_3\text{PF}_2\text{ClN}(\text{CH}_3)_2$
216		1.36	$\text{C}_3\text{H}_5\text{F}_5\text{ClNP}$
215		2.73	$\text{C}_3\text{H}_2\text{F}_7\text{NP}$
214			$\text{C}_3\text{H}_4\text{F}_6\text{NOP}$
207	1.63	1.22	$(\text{CF}_3)_2\text{PF}_2$
206		2.09	CF_7NOP
204		0.19	$(\text{CF}_3)_2\text{PCl}$
200		0.68	$\text{C}_3\text{H}_2\text{F}_7\text{P}$
198		2.05	$\text{CF}_3\text{PClN}(\text{CH}_3)_2$
195		5.46	$\text{C}_3\text{H}_4\text{F}_5\text{NOP}$
194		0.46	$\text{CF}_3\text{PF}(\text{OCH}_3)[\text{N}(\text{CH}_3)_2]$
185		8.80	$\text{C}_4\text{HF}_4\text{NOP}$
183		0.91	$\text{C}_2\text{F}_6\text{NP}$
182	0.72	4.35	$\text{CF}_3\text{PF}_2[\text{N}(\text{CH}_3)_2]$
180	18.10	7.85	$\text{C}_3\text{H}_7\text{F}_4\text{NOP}$
178		2.08	$\text{C}_3\text{H}_5\text{F}_4\text{NOP}$
176		0.36	$\text{C}_3\text{H}_3\text{F}_4\text{NOP}$
		0.25	

TABLE 8 (continued)

174						C ₃ H _F NOP 4	0.64		
173				1.71		CH ₂ FNP 6			
168						C ₂ H ₇ FNOP 4	0.78		
166						C ₂ H ₅ FNOP 4	0.70		
162			1.72	1.19		C ₃ H ₅ FNP 4			
160						C ₃ H ₆ FNP 3	6.58		
157				2.05		CH ₅ FNP 5	0.86		
150			7.24			CH ₃ CH ₃ NPF 3			
148			1.45	3.07		C ₂ H ₃ FNP 4			
147						C ₃ F ₅ O	3.49		
144						C ₄ H ₆ FN 4	5.18		
133				0.72		C ₂ H ₂ F ₄ P			
132			22.62	9.56		(CH ₃) ₂ NPF 3	3.30		
130						C ₅ H ₆ FNP	1.30		
128						C ₅ H ₄ FNP	1.04		
124						CHF ₅ O	0.62		
119			1.09			CF ₄ P	0.46		

TABLE 8 (continued)

81	1.08	3.41	0.74	C_4H_3NO
80			0.63	C_4H_2NO
79			0.33	CH_3FNP
78			2.09	CH_2FNP, C_4NO
77				C_5H_3N, C_2H_4FNO
76			0.21	C_5H_2N, C_2H_3FNO
73			0.21	C_2FNO, H_4F_2P
69	14.47	11.43	2.95	CF_3, PF_2
67			0.28	CH_6FNO
66			0.18	CH_5FNO
65			0.47	CH_4FNO
60	0.63	4.78	3.43	C_2H_3FN, C_2HFO, CH_3NP
59			0.45	C_3H_9N
58			1.69	$C_3H_8N, CHNP$
52	0.63			H_2FP, CH_2F_2
51		1.19	0.37	CHF_2, HFP
50	0.63	1.02		CF_2, PF

TABLE 8 (continued)

44	0.81	C_2H_6N
43	3.62	C_2F
42	13.57	C_2H_4N
41	0.99	C_2H_3N
40	0.54	C_2H_2N
33	0.51	H_2P
32	8.53	CHF, CH_4N, HP
31	0.72	CF, P
30	0.54	C_2H_6

a Intensity is expressed as % total ionization based on the sum of the intensities of ions with m/e greater than 30, except for $(CF_3)_2PF(OCU_3)[N(CH_3)_2]$ where the data are limited to ions with m/e greater than 50.

b Assignments of some ions are given in terms of the structural formula for ease of recognition only.

TABLE 9

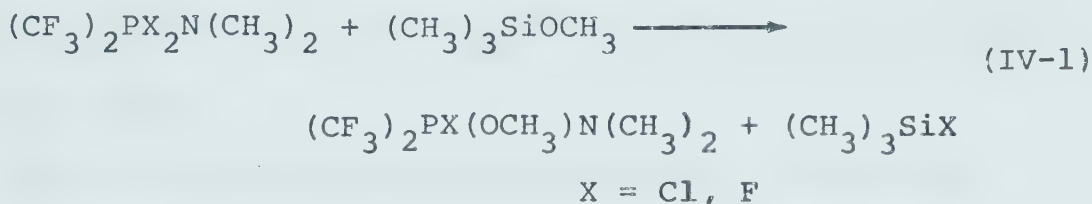
Mass Measurement Data for Aminobis(trifluoromethyl)-
fluorophosphoranes

Compound	Ion ^a	m/e	
		Calculated	Measured
$(\text{CF}_3)_2\text{PF}_2\text{N}(\text{CH}_3)_2$	$(\text{CF}_3)_2\text{PF}_2\text{N}(\text{CH}_3)_2^+$	251.0110	251.0104
	$(\text{CF}_3)_2\text{PFN}(\text{CH}_3)_2^+$	232.0126	232.0134
	$(\text{CF}_3)_2\text{PF}_2^+$	206.9610	206.9605
	$\text{CF}_3\text{PF}_2\text{N}(\text{CH}_3)_2^+$	182.0158	182.0162
	$\text{CH}_2\text{CH}_3\text{NPF}_4^+$	150.0096	150.0093
	$(\text{CH}_3)_2\text{NPF}_3^+$	132.0190	132.0194
$(\text{CF}_3)_2\text{PF}(\text{Cl})\text{N}(\text{CH}_3)_2$	$(\text{CF}_3)_2\text{PF}(\text{Cl})\text{N}(\text{CH}_3)_2^+$	264.9658	264.9658
	$(\text{CF}_3)_2\text{PClN}(\text{CH}_3)_2^+$	247.9831	247.9839
	$(\text{CF}_3)_2\text{PFN}(\text{CH}_3)_2^+$	232.0126	232.0125
	$(\text{CF}_3)_2\text{PFCl}^+$	222.9315	232.9323
	$\text{CF}_3\text{PF}_2(\text{Cl})\text{N}(\text{CH}_3)_2^+$	216.9847	216.9843
	$(\text{CF}_3)_2\text{PCl}^+$	203.9331	203.9324
	$\text{CF}_3\text{PF}(\text{Cl})\text{N}(\text{CH}_3)_2^+$	197.9863	197.9860
$(\text{CF}_3)_2\text{PF}(\text{OCH}_3)\text{N}(\text{CH}_3)_2$	$(\text{CF}_3)_2\text{P}(\text{OCH}_3)\text{N}(\text{CH}_3)_2^+$	244.0326	244.0292
	$(\text{CF}_3)_2\text{P}(\text{O})\text{N}(\text{CH}_3)_2^+$	229.0091	229.0078
	$\text{CF}_3\text{PF}(\text{OCH}_3)\text{N}(\text{CH}_3)_2^+$	194.0358	194.0347
	$\text{CF}_3\text{P}(\text{O})\text{N}(\text{CH}_3)_2^+$	160.0139	160.0120
	$\text{F}_2\text{P}(\text{OCH}_3)\text{N}(\text{CH}_3)_2^+$	144.0390	144.0387
	$\text{FP}(\text{O})\text{N}(\text{CH}_3)_2^+$	110.0139	110.0176
	PF_2^+	68.9706	68.9708

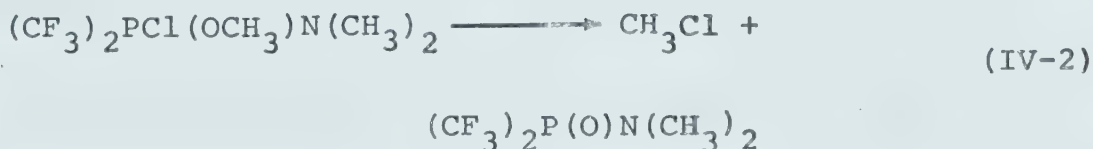
Footnote for Table 9

- ^a A reasonable structural formula rather than the molecular formula is given for each fragment ion merely for convenience of recognition.

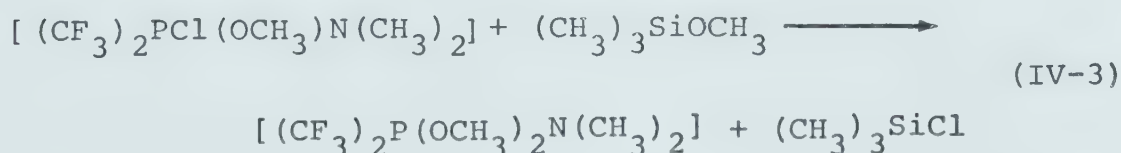
only at elevated temperatures and even then prolonged reaction periods were required to effect a reaction. This reactivity contrasts sharply with that of the dichlorophosphorane $(\text{CF}_3)_2\text{PCl}_2\text{N}(\text{CH}_3)_2$, which reacted with either $(\text{CH}_3)_3\text{SiOCH}_3$ or $(\text{CH}_3)_2\text{NH}$.^{26a} Both dihalogenophosphoranes however, appeared to initially react with metathetical substitution of one halogen with a methoxy group.



The methoxy-substituted chlorophosphorane $(\text{CF}_3)_2\text{PCl}(\text{OCH}_3)\text{N}(\text{CH}_3)_2$, was not detected probably because the CH_3Cl elimination reaction,

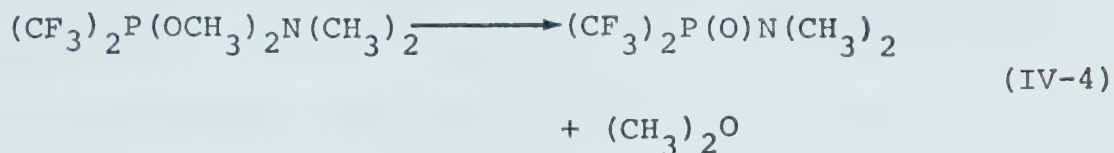


and/or the substitution of a second methoxy group:



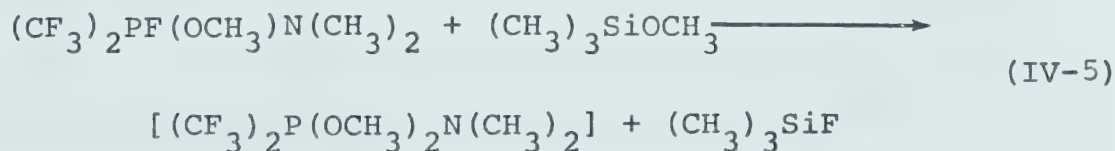
occurred too readily. The formation of apparently equal amounts of CH_3Cl and $(\text{CH}_3)_2\text{O}$, the latter presumably from

the decomposition of the bis(methoxy)phosphorane,



suggested that the second methoxy substitution reaction (eq IV-3) was competitive with the elimination of CH_3Cl (eq IV-2). The absence of detectable amounts of $(\text{CF}_3)_2\text{P}(\text{OCH}_3)_2\text{N}(\text{CH}_3)_2$ in the products would seem to indicate that elimination (eq IV-4) of $(\text{CH}_3)_2\text{O}$ was likewise very facile.

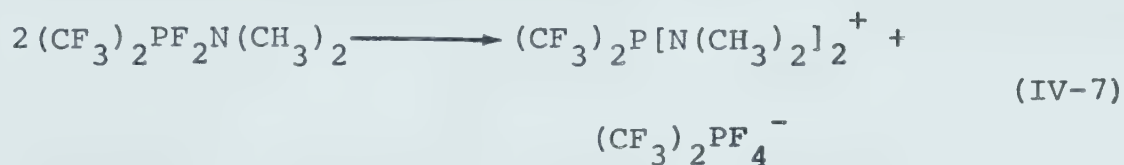
That the disubstitution reaction with $(\text{CH}_3)_3\text{SiOCH}_3$ occurred with the difluorophosphorane as well was evidenced by the presence of $(\text{CF}_3)_2\text{PO}_2^-$ and $(\text{CH}_3)_4\text{N}^+$ ions in the solid products of these reactions. These ions may be accounted for by the following sequence of equations:



Reaction IV-6 might reasonably involve the formation of trimethylamine as an intermediate. Abstraction of an

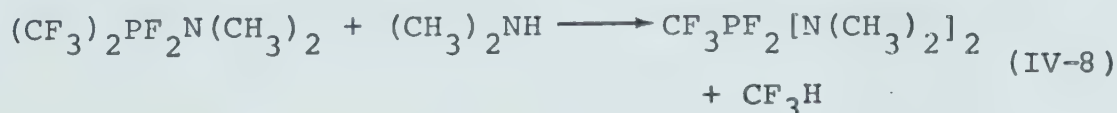
alkyl group by $(\text{CH}_3)_3\text{N}$ from esters or thioesters of bis(trifluoromethyl)phosphine oxides has been demonstrated elsewhere.⁴⁶

The formation of the hexacoordinate phosphorus anion $(\text{CF}_3)_2\text{PF}_4^-$ in the reaction of $(\text{CF}_3)_2\text{PF}_2\text{N}(\text{CH}_3)_2$ and $(\text{CH}_3)_3\text{SiOCH}_3$ is most likely accounted for by a disproportionation reaction of $(\text{CF}_3)_2\text{PF}_2\text{N}(\text{CH}_3)_2$ rather than from reactions with the silyl ether (eq IV-7).

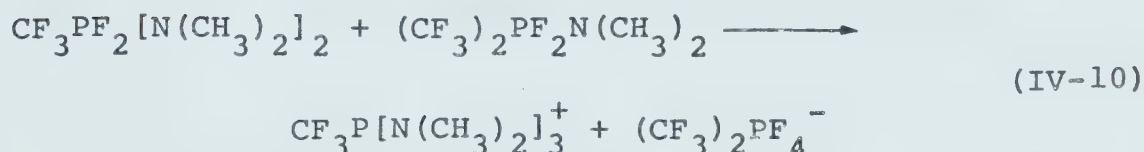
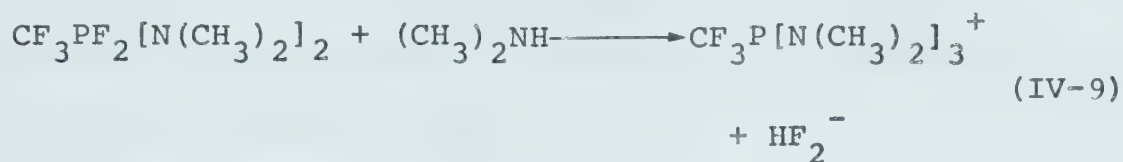


The former reaction appears reasonable even though definite identification of a cation such as $(\text{CF}_3)_2\text{P}[\text{N}(\text{CH}_3)_2]_2^+$ was not obtained and the complexity of the solid products discouraged further investigation. This interpretation is supported by the detection of this same anion in the reaction of $(\text{CF}_3)_2\text{PF}_2\text{N}(\text{CH}_3)_2$ and $(\text{CH}_3)_2\text{NH}$. A disproportionation reaction similar to IV-7 has been reported to occur with $\text{C}_6\text{H}_5\text{PF}_3\text{N}(\text{CH}_3)_2$.³⁸

The reaction of $(\text{CF}_3)_2\text{PF}_2\text{N}(\text{CH}_3)_2$ with $(\text{CH}_3)_2\text{NH}$ paralleled those reported for related halogenophosphoranes containing at least two trifluoromethyl groups.^{26a} The principal reaction was the replacement of a CF_3 group by $\text{N}(\text{CH}_3)_2$.



As before, the $(\text{CF}_3)_2\text{PF}_4^-$ ion in the system presumably arises from the disproportionation of $(\text{CF}_3)_2\text{PF}_2^- \text{N}(\text{CH}_3)_2$. The phosphonium ion $\text{CF}_3\text{P}[\text{N}(\text{CH}_3)_2]_3^+$ was also identified among the products, and was formed most likely from a reaction between $\text{CF}_3\text{PF}_2[\text{N}(\text{CH}_3)_2]_2$ and $(\text{CH}_3)_2\text{NH}$ (eq IV-9), although a fluoride ion transfer reaction could also occur (eq IV-10).

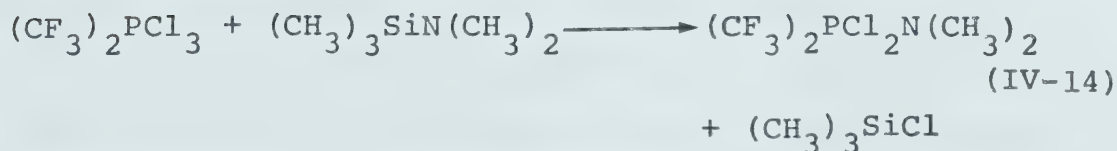
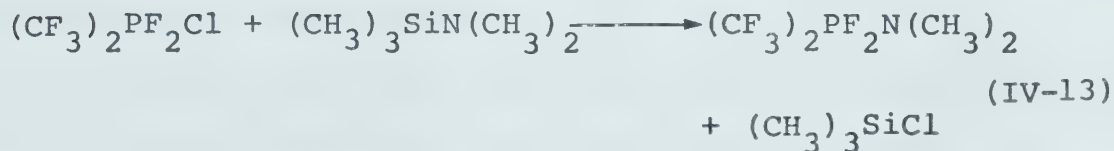
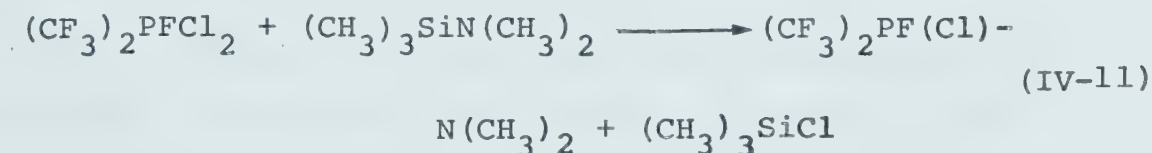


Previous studies⁴⁷ have indicated that the $\text{CF}_3-\text{P}[\text{N}(\text{CH}_3)_2]_3^+$ ion is very stable, and readily detected because of its resistance to hydrolysis.

The observed yield of CF_3H in the reaction described by eq IV-8 was not equal to that of $\text{CF}_3\text{PF}_2[\text{N}(\text{CH}_3)_2]_2$. The reaction is undoubtedly not straightforward, some rearrangement and salt formation occurred as well as the principal substitution. This system was not extensively evaluated because the reaction was not complete under the conditions employed and the relatively severe reaction conditions which would be required to ensure completion could also induce CF_2 elimination and produce

a further complex series of products.⁴⁷

Among the identifiable side products in the synthesis of $(\text{CF}_3)_2\text{PF}(\text{Cl})\text{N}(\text{CH}_3)_2$ from the aminosilane, $(\text{CH}_3)_3\text{SiN}(\text{CH}_3)_2$, and $(\text{CF}_3)_2\text{PFCl}_2$ were $(\text{CH}_3)_3\text{SiCl}$, $(\text{CF}_3)_2\text{PN}(\text{CH}_3)_2$, $(\text{CF}_3)_2\text{PF}_2\text{N}(\text{CH}_3)_2$, $(\text{CF}_3)_2\text{PCl}_2\text{N}(\text{CH}_3)_2$, $(\text{CF}_3)_2\text{PCl}$ and $(\text{CH}_3)_2\text{NH}_2^+$ ions. The initial metathetical substitution reaction (eq IV-11) was probably accompanied by substitution reaction of rearrangement products of the starting material (eq IV-12) leading to the difluoro- and dichlorophosphorane (eqs IV-13,14).

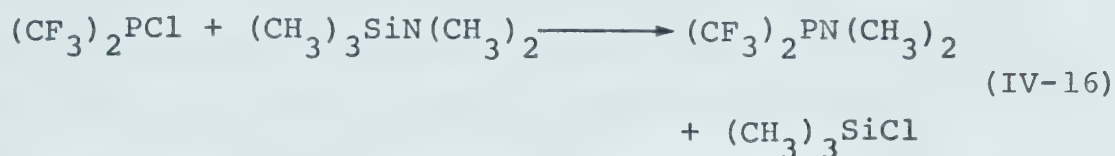


Complications arise because of the known tendency of $(\text{CF}_3)_2\text{PFCl}_2$ to rearrange (eq IV-12).⁴³ The presence of significant amounts of $(\text{CF}_3)_2\text{PN}(\text{CH}_3)_2$ and $(\text{CF}_3)_2\text{PCl}$ is rather difficult to rationalize since no oxidized

products were detected in the system. One possible mechanism that can account for these products is a disproportionation reaction of $(\text{CF}_3)_2\text{PCl}_3$ similar to that reported for the bromo analog.⁴⁸



followed by substitution of the phosphine:

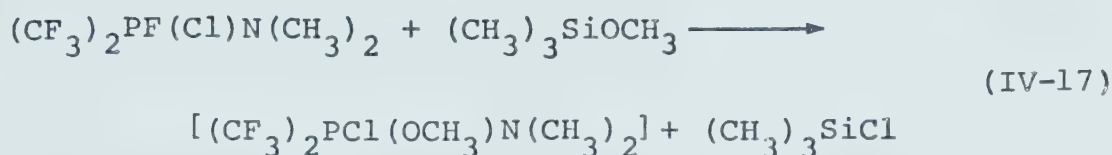


These reactions are consistent with the observation of a greater quantity of $(\text{CF}_3)_2\text{PN}(\text{CH}_3)_2$ than $(\text{CF}_3)_2\text{PCl}$. However, since CF_3Cl was not detected in the nmr spectrum of the products, this reaction pathway can only be considered as speculative.

The formation of $\text{N}(\text{CH}_3)_2\text{H}_2^+$ ions cannot be explained either unless one considers the possibility of traces of moisture being present in the reaction tube.

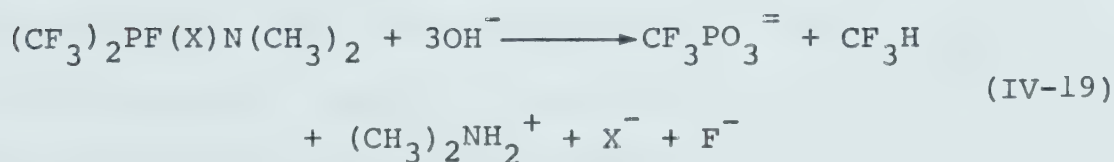
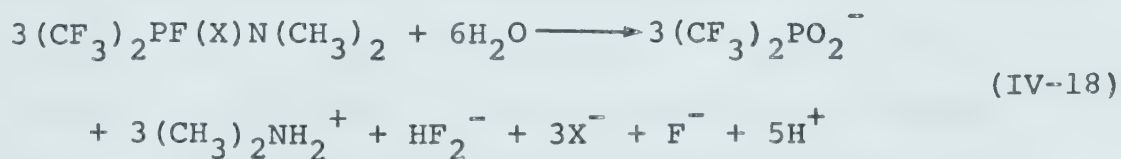
The observation that $(\text{CF}_3)_2\text{PF}(\text{OCH}_3)\text{N}(\text{CH}_3)_2$, and not $(\text{CF}_3)_2\text{PCl}(\text{OCH}_3)\text{N}(\text{CH}_3)_2$, is formed as the principal product in the reaction between $(\text{CF}_3)_2\text{PF}(\text{Cl})\text{N}(\text{CH}_3)_2$ and $(\text{CH}_3)_3\text{SiOCH}_3$ demonstrated once again the greater lability of the P-Cl relative to the P-F bond. However, the presence of small amounts of $(\text{CF}_3)_2\text{P}(\text{O})\text{N}(\text{CH}_3)_2$, $(\text{CH}_3)_3\text{SiF}$ and CH_3Cl suggested that substitution of the fluorine

ligand with the methoxy group (eq IV-14) also occurred,

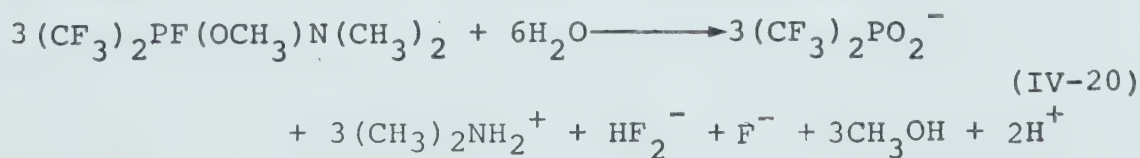


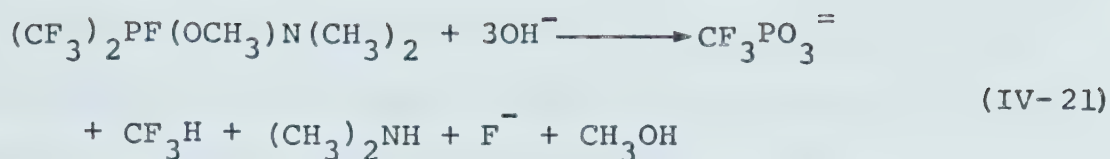
albeit at a much slower rate than the substitution of the chloride, and was followed by the fast elimination of CH_3Cl (eq IV-2). The formation of unidentifiable phosphorus-fluorine compounds clearly indicates that the reactions are not as simple as described in the above equations, and that complex processes occur in addition to these simple substitution-elimination reactions.

The hydrolytic reactions of the dimethylaminobis-(trifluoromethyl)fluorophosphoranes can be summarized in the following equations:



where X is chlorine or fluorine, and





This behavior is in accord with previous work on trifluoromethylphosphoranes, wherein the CF_3 groups are not removed by neutral hydrolysis and the product of alkaline hydrolysis is the ion $\text{CF}_3\text{PO}_3^{=}$ with $(n-1)$ moles of CF_3H , where n is the number of CF_3 groups.^{3,44} These reactions are often used for analytical characterization of these compounds.

B. Mass Spectra.

Of the three bis(trifluoromethyl)halophosphoranes reported in this chapter, only $(\text{CF}_3)_2\text{PF}_2\text{N}(\text{CH}_3)_2$ showed a peak due to the parent ion (calculated: m/e 251.0110, measured: m/e 251.0119) with an abundance of 1.2% relative to the most intense peak which appears to arise from the loss of one CF_3 group. The detection of the parent ion peak in the mass spectra of this phosphorane is unusual although not without precedence,⁴⁰ since such peaks are generally absent in the mass spectra of pentacoordinated phosphorus compounds.

Although the parent ion peaks were not observed in the mass spectra of $(\text{CF}_3)_2\text{PF}(\text{Cl})\text{N}(\text{CH}_3)_2$ and $(\text{CF}_3)_2\text{PF}(\text{OCH}_3)\text{N}(\text{CH}_3)_2$, accurate mass measurements of

the larger mass fragments (Table 9) strongly suggest that these fragments arise from the indicated molecular composition through loss of CF_3 or $\text{N}(\text{CH}_3)_2$ from $(\text{CF}_3)_2\text{PF}(\text{Cl})\text{N}(\text{CH}_3)_2$, or CF_3 , OCH_3 , or $\text{N}(\text{CH}_3)_2$ from $(\text{CF}_3)_2\text{PF}(\text{OCH}_3)\text{N}(\text{CH}_3)_2$.

The intensity distribution of the ions in the mass spectra of all the three compounds suggest that the major fragmentation processes involve cleavage of P-C, P-O, and P-N rather than P-F bonds.

C. Infrared Spectra.

The complexity and low symmetry of these phosphoranes preclude definitive assignments of their infrared bands. However, the infrared spectra definitely support the presence of certain structural units in the compounds (e.g., C-O-P band at 1076 cm^{-1} in the case of $(\text{CF}_3)_2\text{PF}(\text{OCH}_3)\text{N}(\text{CH}_3)_2$). Extensive mixing of vibrational modes especially in the region from $700\text{--}780\text{ cm}^{-1}$ (i.e., where bands due to CF_3 deformation, P-F and P-N stretches are expected) renders spectral band assignments uncertain.

Conclusions

The reactions of $(\text{CF}_3)_2\text{PF}_2\text{N}(\text{CH}_3)_2$, $(\text{CF}_3)_2\text{PCl}_2\text{N}(\text{CH}_3)_2$ and $(\text{CF}_3)_2\text{PFClN}(\text{CH}_3)_2$ with $(\text{CH}_3)_3\text{SiOCH}_3$ sharply demonstrate the greater lability of the P-Cl bond relative to P-F bond. The reaction of the difluorophosphorane took place only at elevated temperatures and prolonged reaction period, and was incomplete even under these relatively vigorous conditions, whereas the reaction of chlorophosphoranes was complete within 24 hours at room temperature. Further, the mono(methoxy)fluorophosphorane $(\text{CF}_3)_2\text{PF}(\text{OCH}_3)\text{N}(\text{CH}_3)_2$ was isolable and stable up to about 70°C . In contrast, the only evidence for $(\text{CF}_3)_2\text{PCl}(\text{OCH}_3)\text{N}(\text{CH}_3)_2$ were the decomposition products $(\text{CF}_3)_2\text{P}(\text{O})\text{N}(\text{CH}_3)_2$ and CH_3Cl , which most likely arise from the cleavage of P-Cl and O-C bonds in $(\text{CF}_3)_2\text{PCl}(\text{OCH}_3)\text{N}(\text{CH}_3)_2$.

The hydrolytic behavior of the three bis(trifluoromethyl)phosphoranes is consonant with that of trifluoromethylphosphoranes previously investigated, in that basic hydrolysis cleaves all but one P- CF_3 bond and neutral hydrolysis does not cleave any.

Likewise, the mass spectral behavior of these three bis(trifluoromethyl)phosphoranes is typical of pentacoordinate phosphorus compounds, except for $(\text{CF}_3)_2\text{PF}_2\text{N}(\text{CH}_3)_2$, which gave a parent ion.

The stability of $(\text{CF}_3)_2\text{PF}_2\text{N}(\text{CH}_3)_2$ was demonstrated by the rather vigorous conditions required for it to undergo any reaction, exemplified by the reaction with $(\text{CH}_3)_3\text{SiOCH}_3$, or its rearrangement to the tetrahedral and hexacoordinated ions, both of which processes occurred only at elevated temperatures after prolonged periods of time.

CHAPTER FIVE

NMR DATA AND STRUCTURAL INFERENCES ON

PENTACOORDINATE PHOSPHORUS COMPOUNDS

Interpretation of ^{31}P and ^{19}F Nuclear Magnetic Resonance Spectroscopy.

In contrast to ^1H nmr theory, the theory of the origin of chemical shifts and spin-spin couplings for both ^{31}P and ^{19}F nuclei is less well developed because of the greater complexity of the electronic configuration of these nuclei.⁴⁹⁻⁵⁶

To a first approximation, ^{31}P chemical shifts are independent of the overall charge of the molecule,^{2,58} but are strongly dependent on the number and kind of atoms directly attached to the phosphorus nucleus. Triply-coordinated phosphorus compounds are in general less shielded than the more highly coordinated phosphorus compounds. In addition, the range of chemical shift values encompassed by the former is much larger than that of the latter. It is further notable that indirect spin-spin coupling involving phosphorus does not generally decrease monotonically with increasing internuclear distance, and many cases are known in which the addition of an additional bridging atom between the coupled nuclei does not greatly alter the magnitude of the observed coupling constant.

Gutowsky and McCall⁵⁰ attributed the lower shielding of triply-coordinated phosphorus to the fact that this

system possesses fewer valence electrons than the more highly coordinated derivatives. The wide range of triply-coordinated phosphorus chemical shifts (~500 ppm) was ascribed by van Wazer and Letcher⁵⁸ to the greater variation of bond hybridization and bond angles possible within this coordination; for example, they associated this variation to the range of hybridization types exhibited by trivalent phosphorus from nearly "pure" p^3 in PH_3 to sp^3 in PF_3 .⁵²

Tetracoordinated phosphorus shows a range of chemical shifts which is less than half that observed for phosphines.⁵⁸ Attempts have been made to explain the observed shielding in terms of bond angles, electronegativity, and π -bonding contributions, but adequate interrelationships have not yet been established.

Penta- and hexacoordinate phosphorus compounds show an even smaller range of chemical shifts. This is in accord with the association of the chemical shift range with variations in bond hybridization and bond angles, because such variations would be minimal in the more highly coordinated phosphorus compounds.

Interpretation of the wide range of ^{19}F chemical shifts and indirect spin-spin coupling constants in ^{19}F spectra are based on the suggestion that the electron spin-orbital and orbital-orbital interaction involved in the coupling interaction become more effective in atoms

with occupied p- or d-orbitals.⁵⁶ Calculations by Pople⁵² of the F-F and F-H coupling constants indicated that electron-orbital interaction, although appreciable, is not the dominant factor, and that ^{19}F nuclear spin couplings are not controlled solely by the Fermi contact term.

A rather unusual feature of ^{19}F spin-spin coupling is the magnitude of the long-range coupling constants. Many long-range F-F coupling constants have been reported to be greater than the short-range coupling interaction. An example is provided by $(\text{CF}_3)_2\text{NCF}_2\text{CF}_3$ where the CF_2 fluorines have a smaller coupling constant with the fluorines of the adjacent CF_3 group ($J < 1$ Hz) than with the fluorines of the more remote $(\text{CF}_3)_2\text{N}$ group ($J = 16$ Hz).⁵⁵ Likewise, long-range F-H coupling has been reported between nuclei separated by five or six saturated bonds.⁵⁶

These observations have led to the suggestion that ^{19}F nuclear coupling interaction proceeds *via* a through-space mechanism.⁵³ However, the work of Evans⁵⁹ on substituted fluoroethanes showed that such a simple correlation between coupling behavior and internuclear distance would not exist if the different relative signs of various ^{19}F coupling constants were taken into account.

The interpretation of ^{19}F chemical shift variation is likewise in an imperfect state but some progress has

been made in simple molecules. A theoretical analysis by Saika and Slichter⁵¹ of atomic contributions to observed ^{19}F magnetic resonance of F_2 and HF predicted chemical shifts in good qualitative agreement with observed data. The principal origin of ^{19}F chemical shifts was attributed to the variation in the second order paramagnetic term in Ramsay's equation⁶⁰ for nuclear shielding (eq V-1),

$$\sigma_A = \sigma_{AA}^{\text{dia}} + \sigma_{AA}^{\text{para}} + \underbrace{\sum_{B \neq A} \sigma_{AB}} + \sigma_A^{\text{deloc}} \quad (\text{V-1})$$

where σ_{AA}^{dia} is a term arising from induced diamagnetic currents on atom A and whose magnitude depends on the electron density around nucleus A, $\sigma_{AA}^{\text{para}}$ is the contribution of induced paramagnetic current on A and is a consequence of the mixing of ground and excited states by the applied magnetic field, and σ_{AB} and σ_A^{deloc} are contributions arising from local induced currents of all atoms other than A and the magnitude of the terms depend on the nature of these atoms and their distance from A.

Pople⁶¹ has shown that $\sigma_{AA}^{\text{para}}$ is equal to zero if the electrons on A are in S states. In other words, the magnitude of the effect of the paramagnetic term on ^{19}F chemical shifts is dependent on the degree of covalency of the bond. Additional support has been provided by more recent investigations.^{49,54-56} Variations in ^{19}F chemical shifts therefore, are generally thought to

reflect variations in the paramagnetic rather than the Lamb diamagnetic term.

Pentacoordinate Phosphorus Compounds: Stereochemical Studies and Bonding Theories.

A. Stereochemical Studies.

Two common pentacoordinate structures can be visualized: the trigonal bipyramid and the square pyramid. Most of the pentacoordinate phosphorus compounds investigated to date by X-ray and electron diffraction studies have been assigned a trigonal bipyramidal ground state geometry.^{13,15-17} Vibrational studies of simple molecules have supported the trigonal bipyramidal framework.¹⁸⁻²⁵ The only phosphoranes for which a square pyramidal structure has been established are the 1,3,2-dioxaphosphoranes⁶² (Fig. V-1) both of which involve

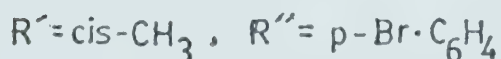
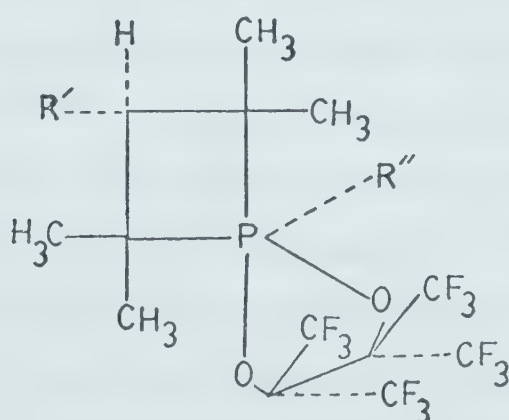


Figure V-1

bidentate chelating ligands.

In 1963 Muetterties *et. al.*⁷ proposed an "electronegativity rule" governing positional site preferences in trigonal bipyramidal phosphoranes. Stated simply, the "electronegativity rule" postulates that axial positions in a trigonal bipyramid are preferentially occupied by the ligands with greatest electronegativity. Exceptional behavior was attributed to steric strain.⁷ In the past five years however, it has become clear that trifluoromethylhalogenophosphoranes of the type $(\text{CF}_3)_{5-m-n} \text{PX}_m \text{Y}_n$ ($\text{X} = \text{F}, \text{Cl}$; $\text{Y} = -\text{OSi}(\text{CH}_3)_3, -\text{OCH}_3, -\text{SCH}_3, -\text{N}(\text{CH}_3)_2$) do not obey this simple rule. The CF_3 group appears to exhibit a lower apicophilicity than expected from its electronegativity value which is intermediate between that of F and Cl.²⁶⁻²⁸ Especially clear examples of this anomaly were provided by variable-temperature nmr spectroscopic studies of those compounds where both Cl and CF_3 were present as directly-bound ligands to phosphorus.^{26a,27,28a} In these compounds chlorine, with an electronegativity of 3.16, appeared to possess a stronger preference for the axial position than the trifluoromethyl group with an electronegativity of 3.46.²⁷ It was proposed²⁷ that the Hammett-Taft parameter σ_{I} may provide a better gauge for apicophilicity than electronegativity.

Analysis of the spectroscopic data further indicated that $^2J_{P-F}$ was a more reliable^{26a} indicator of the stereochemical position of the CF_3 in these phosphoranes (which were assumed to have a consistent trigonal bipyramidal ground state geometry) than chemical shift values used previously.⁴ Apical $^2J_{P-F}$ values are generally smaller (<100 Hz) than equatorial $^2J_{P-F}$ (>100 Hz) values. It must be recognized, however, that $^2J_{P-F}$ values will be determined by the total electronic nature of the molecule, and hence the absolute values cannot be reliably used as the indicator of substituent location; indeed only relative values within a molecule can be reliably used. Recently, in this laboratory, it has been shown that $^1J_{P-C}$ of CF_3 phosphoranes correlates with $^2J_{P-F}$ values,⁶³ enhancing the basis for the use of $^2J_{P-F}$ values as stereochemical indicators.

B. Theory of Bonding of Pentacoordinate Phosphorus.

The literature is replete with applications of modern bonding theories to pentacoordinate phosphorus compounds, covering the whole spectrum of approaches from *ab initio* molecular orbital theory⁶⁴⁻⁶⁷ to a rationale based on pure electrostatics.^{9a,b} Several *ab initio* molecular orbital calculations of varying sophistication have been reported recently,⁶⁴⁻⁶⁷ employing small to medium size basis sets of Gaussian functions. The main points

discussed are (1): the role and importance of phosphorus d-orbital participation in the bonding, (2) quantitative difference in bonding between axial and equatorial bonds, and (3) the contribution of p_{π} - d_{π} interactions to the bonding.

Any bonding theory of trigonal bipyramidal phosphoranes must account for the following experimental observations:

- (1) non-equivalence of the axial and equatorial positions and the ramifications of this non-equivalence and
- (2) the stereochemical preferences of the different substituents in the trigonal bipyramidal framework.

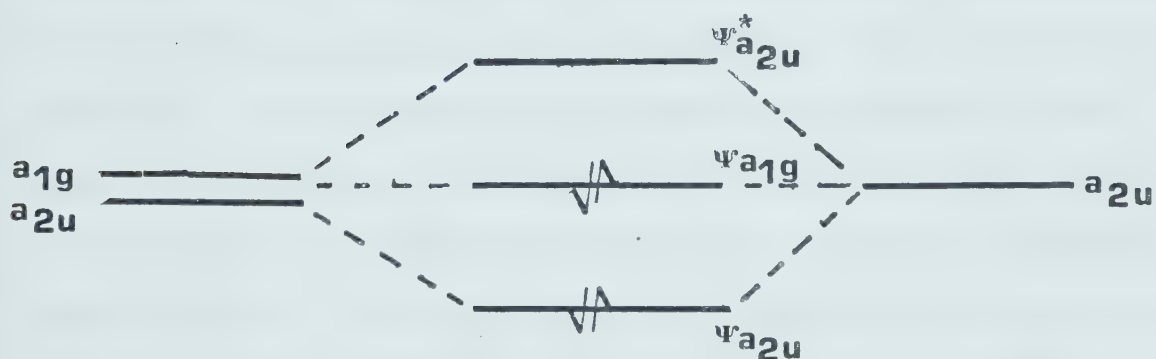
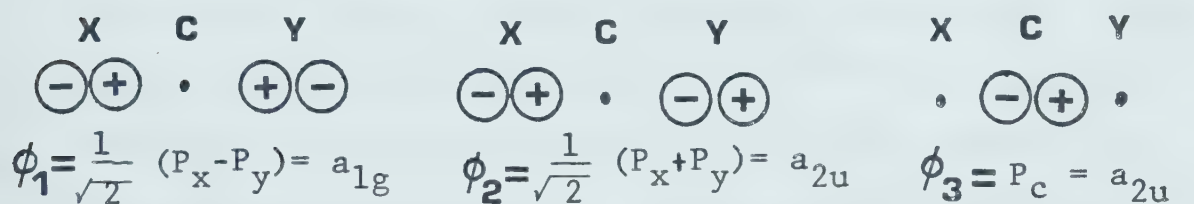
Muetterties, Mahler, and Schmutzler⁷ suggested that their "electronegativity rule" arises from the greater s-orbital character which is contained in the equatorial phosphorus hybrid orbitals. This in turn leads to greater overlap with the more electropositive ligands which therefore preferentially occupy the equatorial plane. The most electronegative substituents then occupy the axial positions as a result of stronger preferences of electropositive substituents for the equatorial sites. Extensive rationalization of much chemical behavior at an empirical, qualitative level has been achieved by Bent⁶⁸ using the concept that s-orbital character of an atom concentrates towards the electropositive substituents.

Holmes¹⁸ analyzed the ¹⁹F chemical shifts of a series of chlorofluorophosphoranes $\text{PF}_n\text{Cl}_{5-n}$ and suggested that

$d\pi-p\pi$ bonding provided the critical factor in the bonding and stereochemistry of these compounds. Subsequent investigations based on orbital overlap population analysis have since shown Holmes' conclusions to be in error.^{12,70} The VSEPR theory originated by Sidgwick and Powell and popularized by Gillespie and Nyholm,^{9a,b} rationalizes the principal features of the bonding in trigonal bipyramidal structures by attributing the difference in bond lengths in PX_5 compounds solely to electrostatic repulsion of bonding electron pairs in the valence shell of these compounds. The inequivalence of axial and equatorial bonds is therefore a consequence of molecular symmetry, with the electrostatic imbalance leading to the lengthening of the axial bonds. To explain the seemingly greater apicophilicity of electronegative ligands, it is necessary to assume that, in a bond to a more electronegative substituent the bonding electron density is held closer to the ligand, whereas in a bond to an electropositive substituent this electron density concentrates close to the central atom. Hence, as the electronegativity of the ligand increases, the amount of repulsive interaction between the bonding orbital and neighboring orbitals decreases. Optimization of this reduction in interelectronic repulsion is achieved by placing the more electronegative ligand in the axial position where electron pair interaction is inherently greater because of the smaller

bond angle (90°) with its three nearest neighbors.

Rundle⁷¹ described the axial X-P-X bonding framework in terms of a linear three-center molecular orbital picture utilizing one orbital on each of the three atoms involved. The linear combination gives one bonding, one non-bonding, and one anti-bonding molecular orbital. The symmetry combinations for a set of three $P\sigma$ orbitals, one from each atom, are shown in Fig. V-2 in which the terminal atoms are labelled X and Y, and the central atom, C.



$$\psi_{a_{1g}} = \phi_1$$

$$\psi_{a_{2u}} = N(\phi_2 - \lambda \phi_3)$$

$$\psi^*_{a_{2u}} = N(\phi_2 + \lambda' \phi_3)$$

Figure V-2

Of the four electrons available for bonding, two are placed in a bonding orbital and two in a non-bonding orbital for a bond order of one in the X-C-Y unit. The non-bonding orbital is essentially terminal atom in character, therefore a greater electron density resides in the terminal atoms. Hence the greater apical positional preference of electronegative ligands.

Several groups have calculated the energy profiles of the intramolecular rearrangement of PH_5 ,^{64,65} which, although instructive, may be inadequate to explain properly the behavior of more complex molecules such as PF_5 . Two recent *ab initio* calculations on PF_5 ^{66,67} and related molecules considered also the permutational interchange process in these molecules. Using a small basis set, van Wazer, *et. al.*⁶⁷ obtained consistently higher orbital energies (less stable) than those obtained by Strich and Veillard,⁶⁶ who used a medium size basis set including d orbitals. Both sides were in essential agreement with each other on the following points: (1) axial bonds are weaker than the equatorial bonds with or without d-orbital participation, (2) equatorial $\text{p}\pi\text{-d}\pi$ bonding is more efficient than axial $\text{p}\pi\text{-d}\pi$ bonding, (3) phosphorus equatorial orbitals in a trigonal bipyramidal geometry have more s character than the axial orbitals, (4) equatorial substituents with a lone-pair will adopt a preferential orientation in which the maximum lone-pair electron

density lies in the equatorial plane.

According to Strich and Veillard,⁶⁶ d-orbital participation is important in the bonding of pentacoordinate phosphorus. They state that "although d functions on the phosphorus atom may be omitted for a qualitative description of the bonding, they do play a significant role in the bonding as shown by the population analysis." Semi-empirical calculations, in contrast, have categorically discounted the importance of the d-orbital participation in the bonding of pentacoordinate phosphorus.^{70,72}

Nmr Spectral Results

A. Methyl(trifluoromethyl)trifluorophosphorane.

The normal temperature (+31°) ^1H spectrum of $\text{CH}_3(\text{CF}_3)\text{PF}_3$ (Fig. V-3) consists of 6 lines with the apparent intensity ratio of 1:3:4:4:3:1. This multiplet structure is due to the partial overlapping of two sets of quartets, illustrated by the stick diagram also shown in Fig. V-3. The parameters are given in Table 3. The major doublet splitting is due to coupling with the phosphorus and the quartet fine structure is due to coupling with three magnetically equivalent, directly-bound fluorines. The apparent magnetic equivalence of the three directly-bound fluorines is also suggested by the presence of only two resonance regions in the ^{19}F nmr spectrum at 31°C (Fig V-4): one, a doublet of

Figure V-3 Observed ^1H (60.0 MHz) nmr spectrum of $\text{CH}_3(\text{CF}_3)\text{PF}_3$ at 304°K, obtained from a 50:50 solution in $\text{CFCl}_3:\text{CF}_2\text{Cl}_2$ with about 5% TMS. The frequency scale gives chemical shift values in Hz relative to internal TMS. The stick diagram traces the splitting pattern as a doublet of quartets arising from coupling with phosphorus and with three equivalent directly-bound fluorines.

^1H (60.0 MHz) Spectrum of

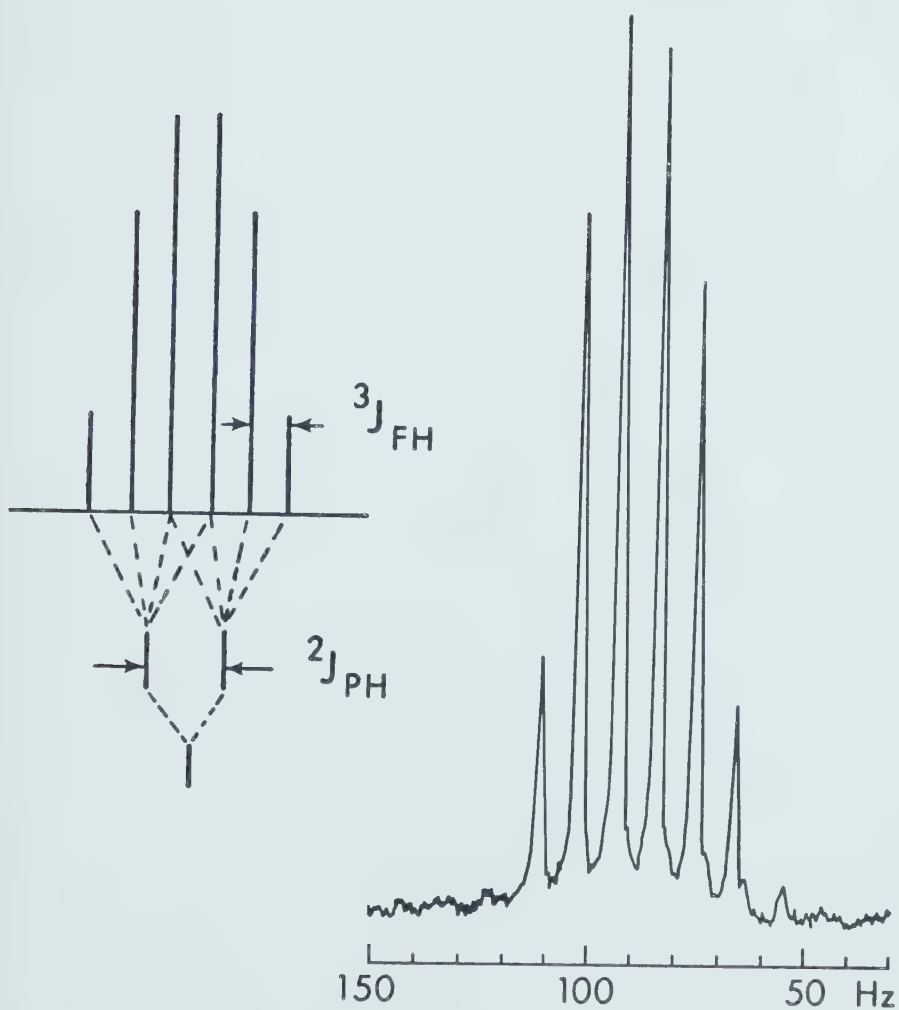
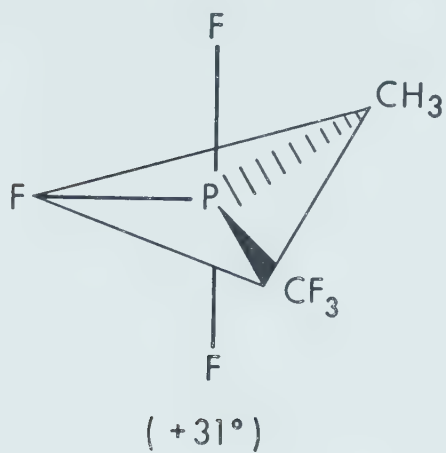


Figure V-3

Figure V-4

Observed ^{19}F (94.1 MHz) nmr spectra of $\text{CH}_3(\text{CF}_3)\text{PF}_3$ at various temperatures from the fast-exchange to the slow-exchange limit, obtained from a solution in approximately 50:50 $\text{CFCl}_3:\text{CF}_2\text{Cl}_2$ containing about 5% TMS. The frequency scale gives chemical shift values in Hz relative to CFCl_3 .

^{19}F (94.1 MHz) nmr Spectra of

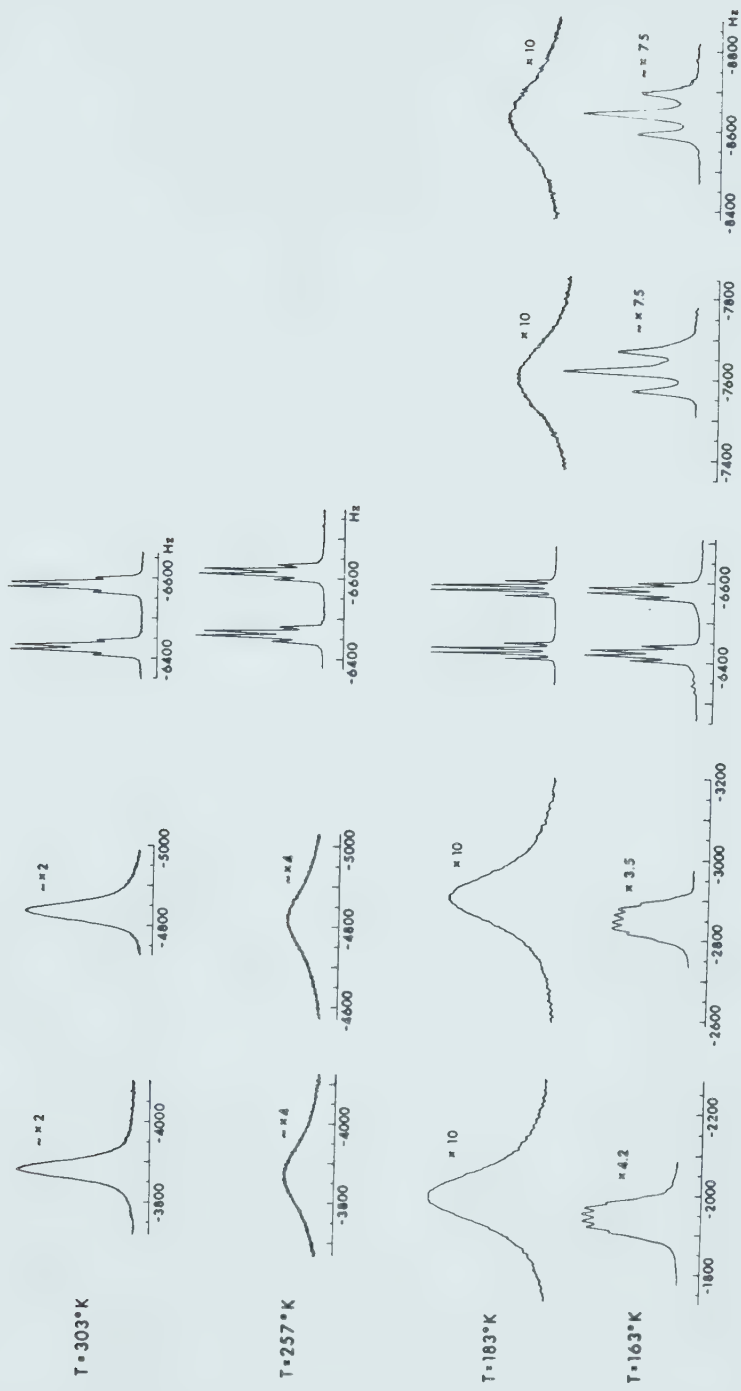
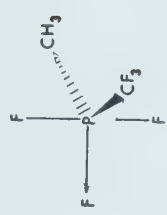
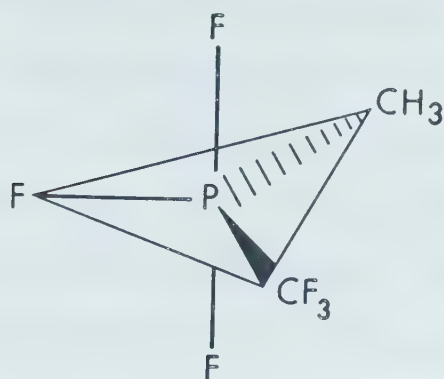


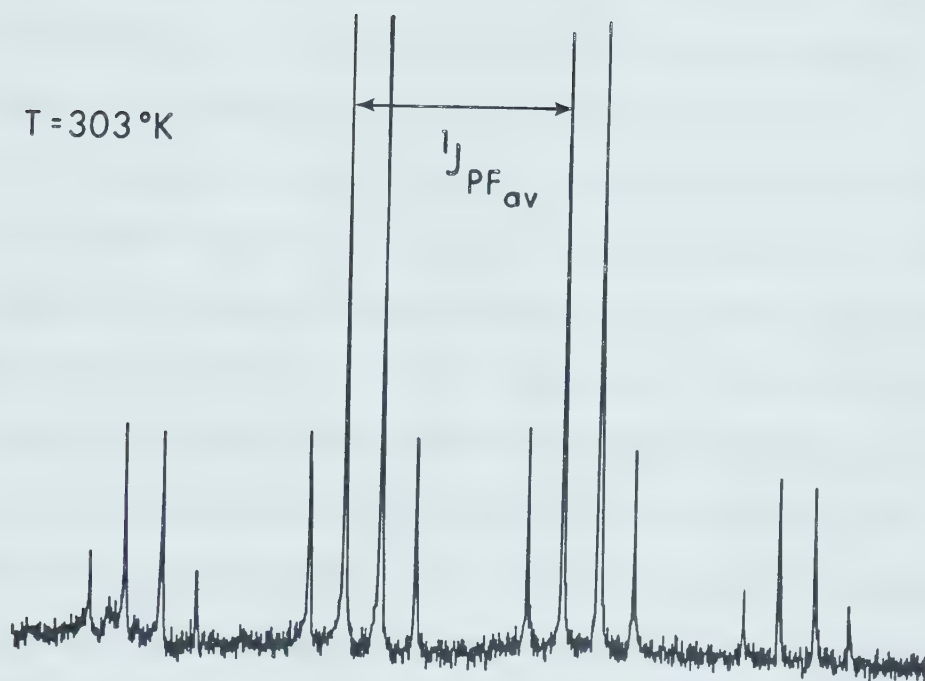
Figure V-4

Figure V-5 Observed $^{31}\text{P} \sim \{^1\text{H}\}$ (36.4 MHz) nmr spectra of $\text{CH}_3(\text{CF}_3)\text{PF}_3$ at the fast- and slow-exchange limits, obtained from an approximate 50:50 solution in $\text{CFCl}_3:\text{CF}_2\text{Cl}_2$ containing about 5% TMS. The frequency scale, which gives chemical shift values relative to P_4O_6 , was measured relative to the ^{19}F (CFCl_3) heteronuclear lock, and converted to appropriate values for the ^{31}P standard.

Limiting ^{31}P (36.4 MHz) $\sim \{^1\text{H}\}$ nmr Spectra of



$T = 303^\circ\text{K}$



$T = 153^\circ\text{K}$

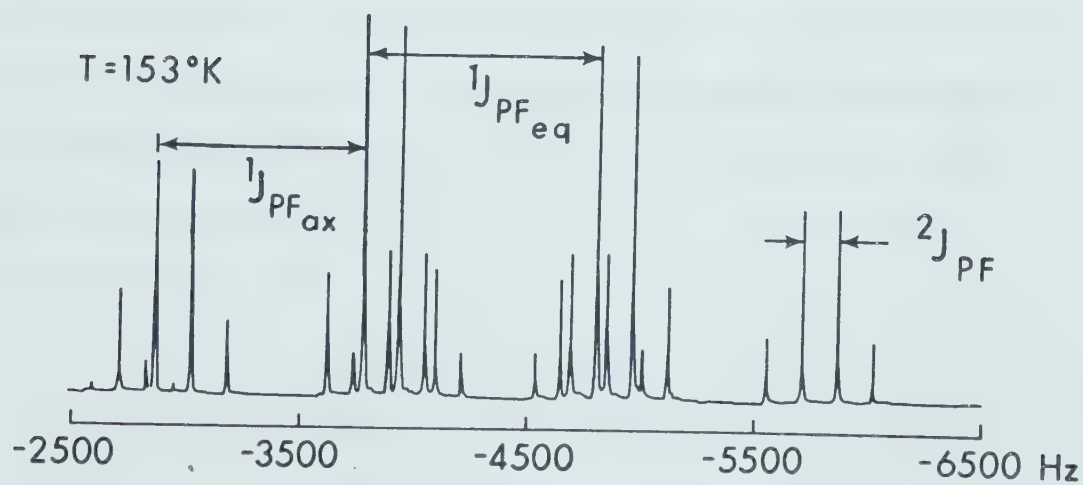


Figure V-5

relatively broad quartets, is the CF_3 region. The major doublet is due to coupling with phosphorus and the quartet splitting is due to additional coupling of the CF_3 signal with the three equivalent directly-bound fluorines. At a much lower field is the P-F region which consists of two very broad peaks. The P-F fluorine coupling with the CF_3 fluorines is not resolved.

The ^{31}P nmr spectrum (Fig V-5) of $\text{CH}_3(\text{CF}_3)\text{PF}_3$ provides more information on the structure of this compound. The normal temperature, proton-decoupled spectrum is a quartet of quartets; the primary quartet is due to coupling with the three equivalent directly-bound fluorines and the secondary quartet fine structure of each line is due to further coupling with the CF_3 fluorines. Upon cooling the sample to 153°K, the spectrum is transformed into a twenty-four-line spectrum consisting of a doublet of triplets of quartets (Fig V-5). Clearly, the directly-bound fluorine environments have become non-equivalent and three possible structures, the two trigonal bipyramidal structures (A) or (B) allowing free rotation of the CH_3 and CF_3 groups, or the square pyramidal structure (C or the equivalent cis analog) can account for the observed spectrum.

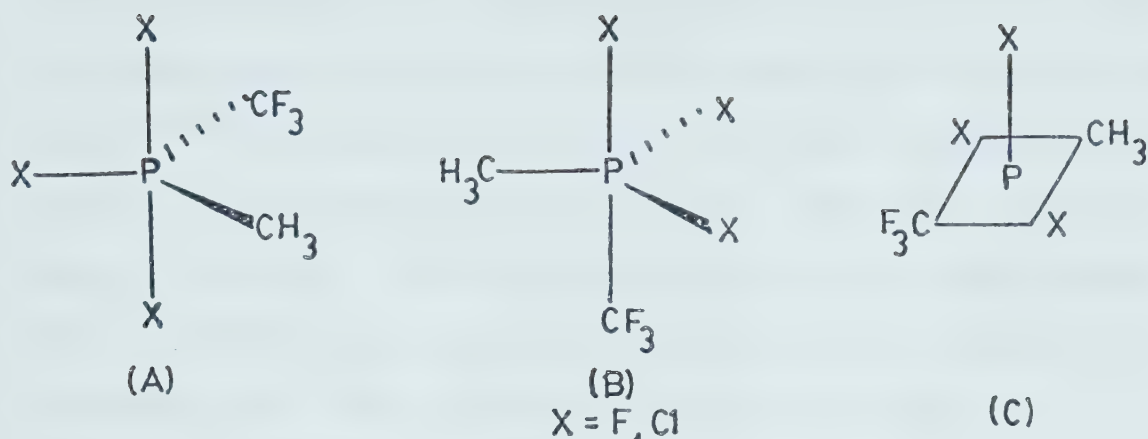


Figure V-6

In view of the preponderance of evidence supporting the trigonal bipyramid as the ground state geometry for the simple phosphoranes, the trigonal bipyramidal alternatives (A) and (B) seem to be the most reasonable structures and it is necessary to choose between only these two alternatives.

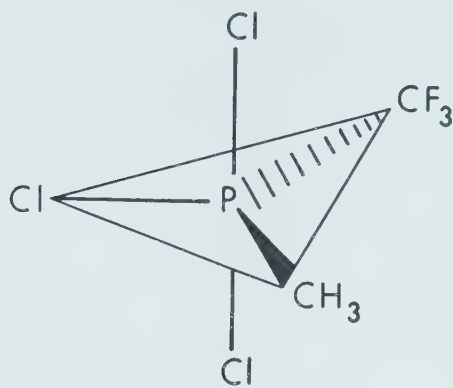
The pattern and magnitudes of the splitting in the low temperature ^{31}P limiting spectrum of $\text{CH}_3(\text{CF}_3)\text{PF}_3$ are clearly indicative of two distinct P-F environments. The main doublet ($^1J_{\text{PF}} = 1023 \text{ Hz}$) arises from coupling of one such directly-bound fluorine to phosphorus, and the triplet structure on each doublet component is due to coupling ($^1J_{\text{PF}} = 919 \text{ Hz}$) of the two remaining magnetically equivalent fluorines directly attached to phosphorus.

The magnitude of the two $^1J_{PF}$ coupling constants strongly suggests that the unique fluorine with the larger coupling constant occupies the equatorial site, and the pair of fluorine atoms with the smaller coupling constant occupy the axial sites.²⁶⁻²⁸ The magnitude of $^2J_{P-F}$ (156 Hz) is consistent with equatorial placement of the CF_3 group. The data therefore support structure (A) in Fig V-6 as the most likely ground state structure for $CH_3(CF_3)PF_3$. It should be noted that structure (A) is the structure predicted by the "electronegativity rule."⁷

The apparent magnetic equivalence of the three directly-bound fluorines indicated by the normal probe temperature 1H , ^{19}F , and ^{31}P nmr spectra arises from a ligand rearrangement process which is a very common phenomenon in pentacoordinate phosphorus compounds.^{10,11} This interpretation is supported by the fact that the single $^1J_{P-F}$ value evaluated from the room temperature ^{19}F and ^{31}P spectra ($^1J_{P-F} = 955$ Hz) is in good agreement with the weighted average ($^1J_{PF_{avg}} = 954$ Hz) of the two unique values obtained from the low temperature ^{31}P limiting spectrum. The weighted average value of the two different low temperature ^{19}F chemical shifts, 46.1 ppm, is also in agreement with the observed average chemical shift of the directly-bound fluorines (46.2 ppm) obtained at normal probe temperatures.

Figure V-7 Observed ^1H (100.1 MHz) nmr spectrum of $\text{CH}_3(\text{CF}_3)\text{PCl}_3$ at 273°K, obtained from a solution in CFCl_3 containing about 5% TMS reference. The frequency scale gives chemical shift values in Hz measured relative to internal TMS.

^1H (100.1 MHz) Spectrum of



(0°C)

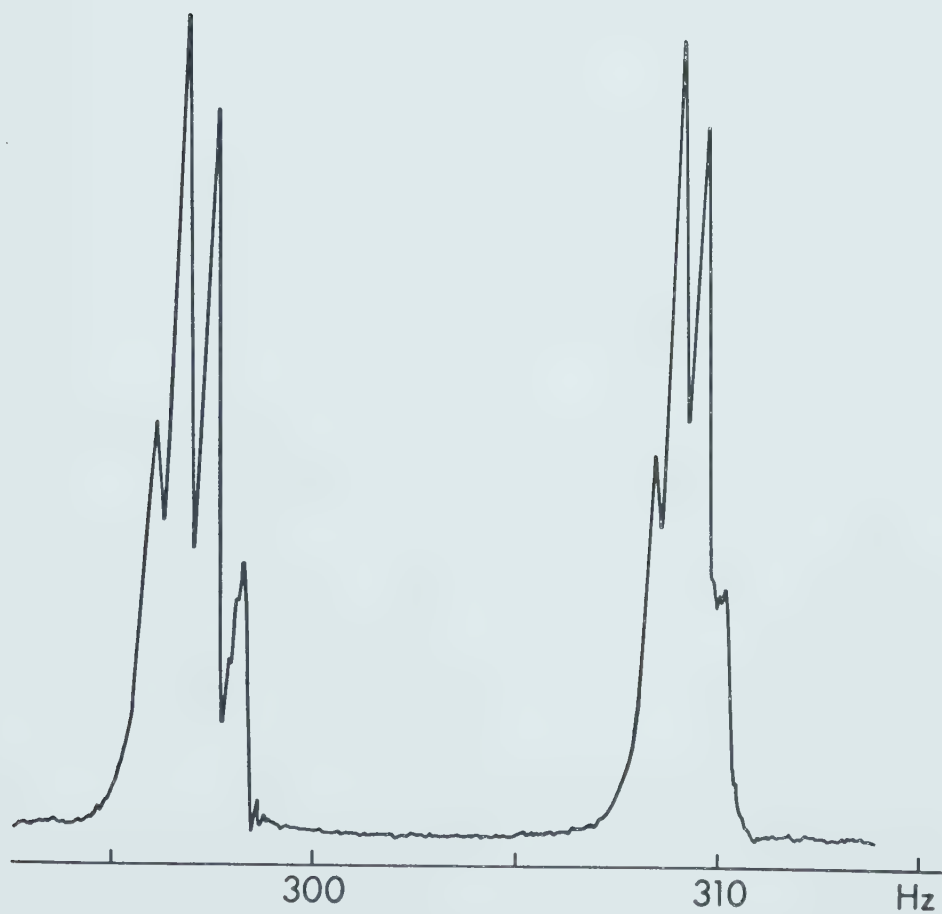
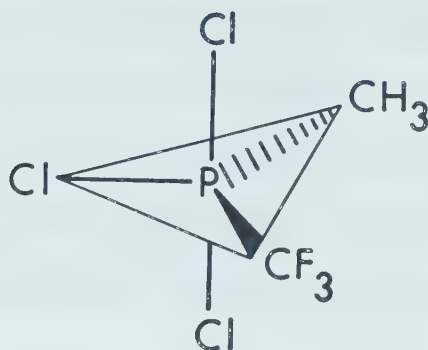


Figure V-7

Figure V-8 Observed $^{31}\text{P} \sim \{^1\text{H}\}$ (36.4 MHz) nmr spectrum of $\text{CH}_3(\text{CF}_3)\text{PCl}_3$ at 304°K obtained from a solution in CFCl_3 containing about 5% TMS. The frequency scale, which gives chemical values relative to P_4O_6 , was measured relative to the ^{19}F (CFCl_3) heteronuclear lock and converted to appropriate values of the ^{31}P reference compound.

$^{31}\text{P} \sim \{^1\text{H}\}$ (36.4 MHz) nmr Spectrum of



(+ 31°)

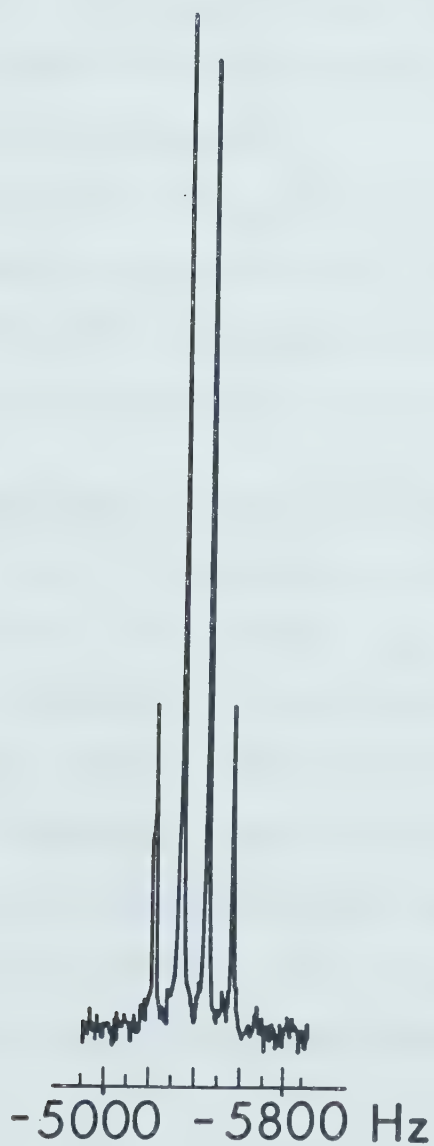


Figure V-8

B. Methyl(trifluoromethyl)trichlorophosphorane.

The ^1H , ^{19}F , and ^{31}P nmr spectra of $\text{CH}_3(\text{CF}_3)\text{PCl}_3$ are characteristic of a first-order A_3MX_3 system. The ^1H nmr at 60 MHz (Fig V-7) is a broad doublet which exhibits a quartet fine structure of 1:3:3:1 intensity ratio upon expansion of each component. The ^{19}F nmr spectrum shows a similar pattern. The parameters are given in Table 3.

The proton-decoupled ^{31}P nmr spectrum consists of four lines of 1:3:3:1 intensity ratio (Fig V-8). Each component of the quartet is split further into a quartet in the proton-coupled spectrum.

The magnitude of the $^2\text{J}_{\text{P-F}}$ value (157 Hz) is compatible²⁶⁻²⁸ with an equatorial CF_3 location, hence structure (A) in Fig V-6 is considered to be the most likely ground state structure of $\text{CH}_3(\text{CF}_3)\text{PCl}_3$.

C. Methyl(trifluoromethyl)dimethylaminodifluorophosphorane.

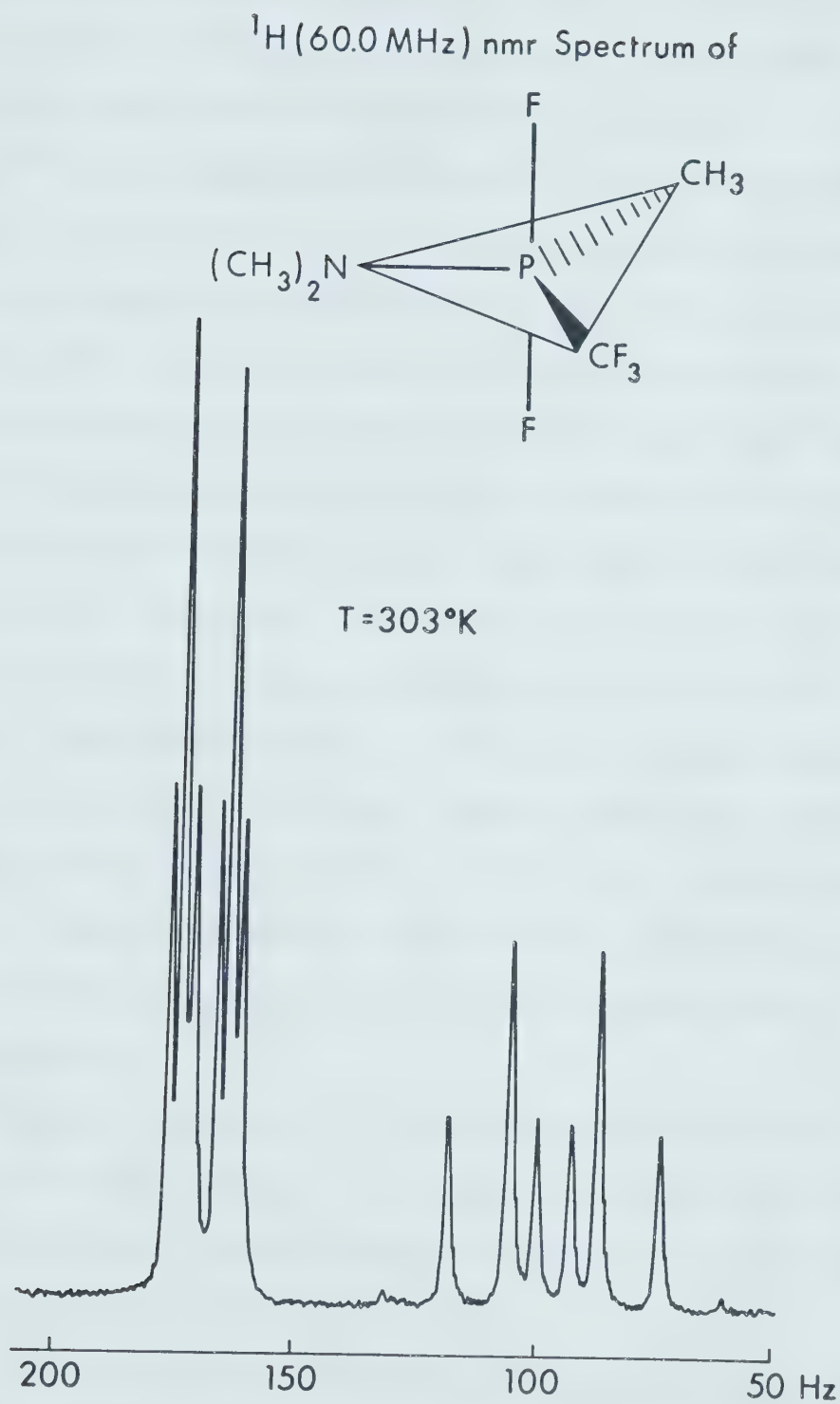
The ^1H , ^{19}F , and ^{31}P nmr spectra of $\text{CH}_3(\text{CF}_3)\text{PF}_2\text{N}(\text{CH}_3)_2$ can be interpreted on a first-order basis. The ^1H nmr spectrum (Fig V-9) consists of two sets of doublets of triplets. The lower field resonance is twice as intense as the high field resonance, thus it is reasonably assigned to dimethylamino protons, and the high field resonance to the directly-bound CH_3 protons. The primary doublet in each region is due to coupling with phosphorus and the

...the ... of ...
...the ... of ...
...the ... of ...
...the ... of ...
...the ... of ...



...the ... of ...
...the ... of ...
...the ... of ...
...the ... of ...
...the ... of ...

Figure V-9 Experimental ^1H (100.1 MHz) nmr spectrum of $\text{CH}_3(\text{CF}_3)\text{PF}_2\text{N}(\text{CH}_3)_2$ at 303°K, obtained from a solution in CFCl_3 containing about 5% TMS reference. The frequency scale gives chemical shift values in Hz measured relative to internal TMS.

Figure V-9

triplet structure is due to coupling with the two fluorine atoms directly-bound to phosphorus. Mutual coupling of the two sets of protons is not observed, nor is the coupling of the protons with the CF_3 fluorines.

The ^{19}F nmr spectrum (Fig V-10) shows two resonance regions, one at a high field arising from the CF_3 group, and one at a much lower field due to the directly-bound fluorine atoms. The CF_3 region consists of a doublet of triplets and remains essentially unchanged with temperature. The doublet splitting is due to phosphorus coupling and the triplet structure due to coupling with the two directly-bound fluorines. The P-F region is a doublet of septets of septets. The main doublet is due to P-F coupling, the primary septet is due to coupling with the CH_3 protons and CF_3 fluorines, and the secondary septet structure arises from coupling with the six dimethylamino protons. This assignment is supported by the magnitude of the relevant coupling constants evaluated from the ^1H nmr spectrum.

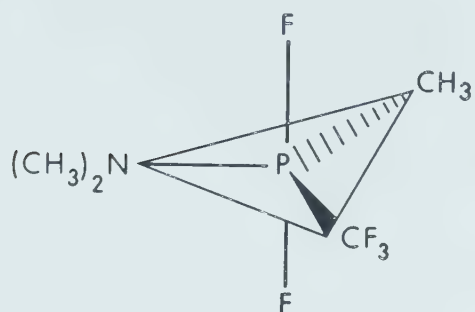
The proton-decoupled ^{31}P nmr spectrum (Fig V-11) consists of twelve lines, the primary triplet due to coupling with the two directly-bound fluorines and the quartet fine structure due to P- CF_3 coupling.

All these spectral patterns are consistent with any one of the following trigonal bipyramidal structures (Fig V-12) assuming that any axial-equatorial permutations



Figure V-10 Observed ^{19}F (94.1 MHz) nmr spectrum of $\text{CH}_3(\text{CF}_3)\text{PF}_2\text{N}(\text{CH}_3)_2$ at 303°K obtained from a solution in CFCl_3 containing about 5% TMS. The frequency peak gives chemical shift values in Hz relative to internal CFCl_3 .

^{19}F (94.1 MHz) nmr Spectrum of



$T = 303^\circ\text{K}$

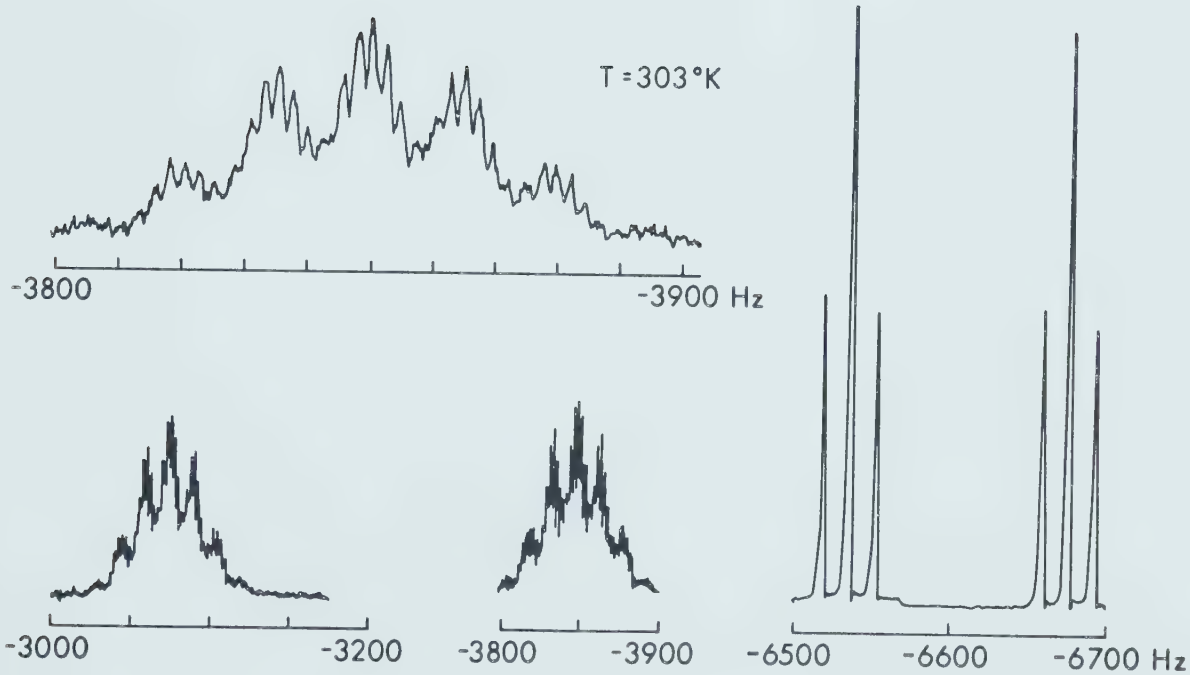
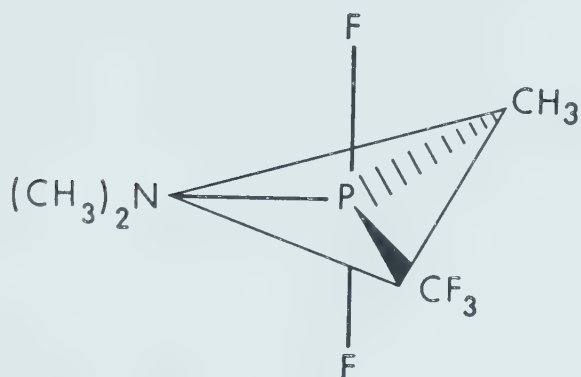


Figure V-10



Figure V-11 Observed $^{31}\text{P} \sim \{^1\text{H}\}$ (36.4 MHz) nmr spectrum of $\text{CH}_3(\text{CF}_3)\text{PF}_2\text{N}(\text{CH}_3)_2$ at 303°K obtained from a solution in CFCl_3 containing about 5% TMS. The frequency scale which gives chemical shift values relative to P_4O_6 was measured relative to the ^{19}F (CFCl_3) heteronuclear lock and converted to appropriate values of the ^{31}P reference compound.

^{31}P (36.4 MHz) $\sim \{^1\text{H}\}$ nmr Spectrum of



$T = 303^\circ\text{K}$

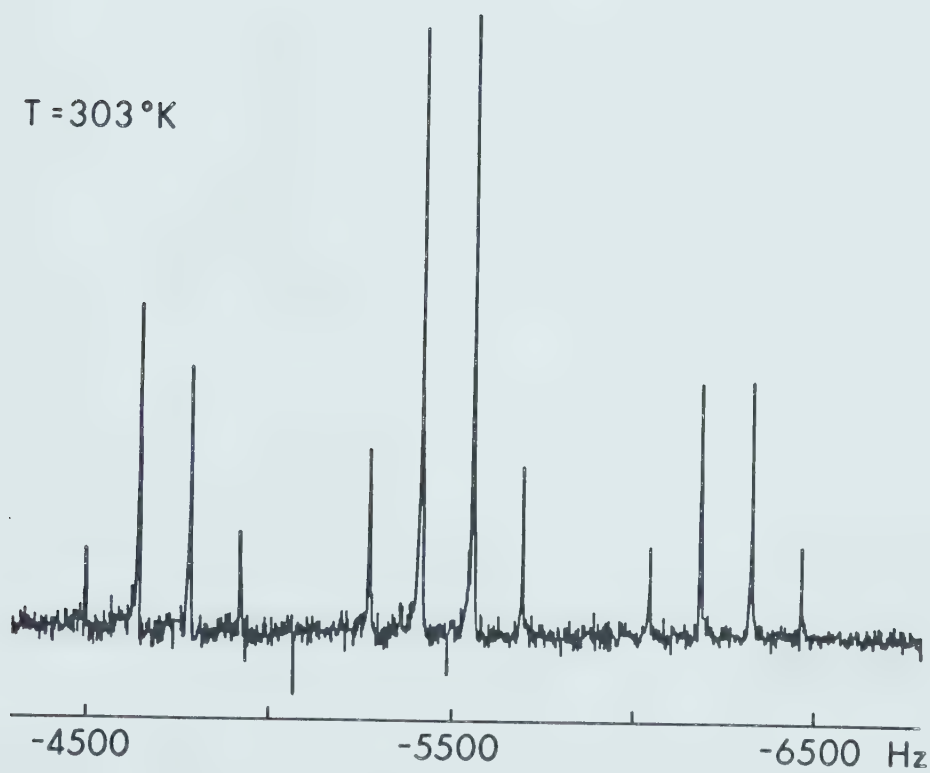
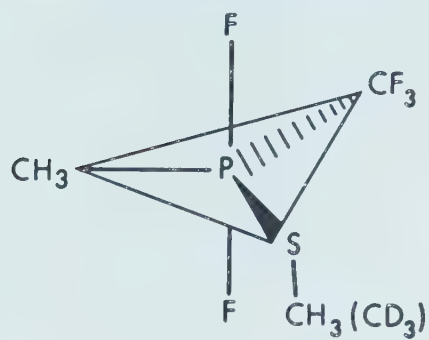


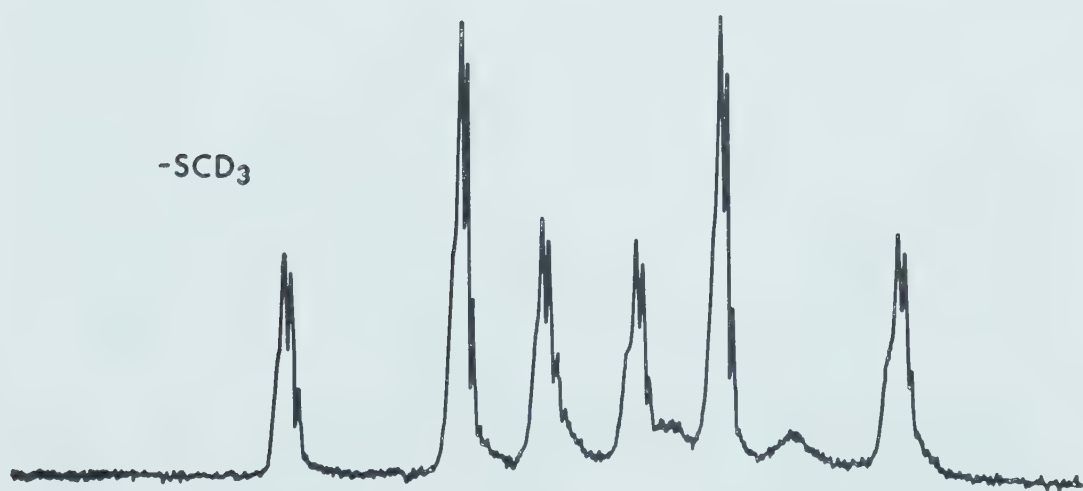
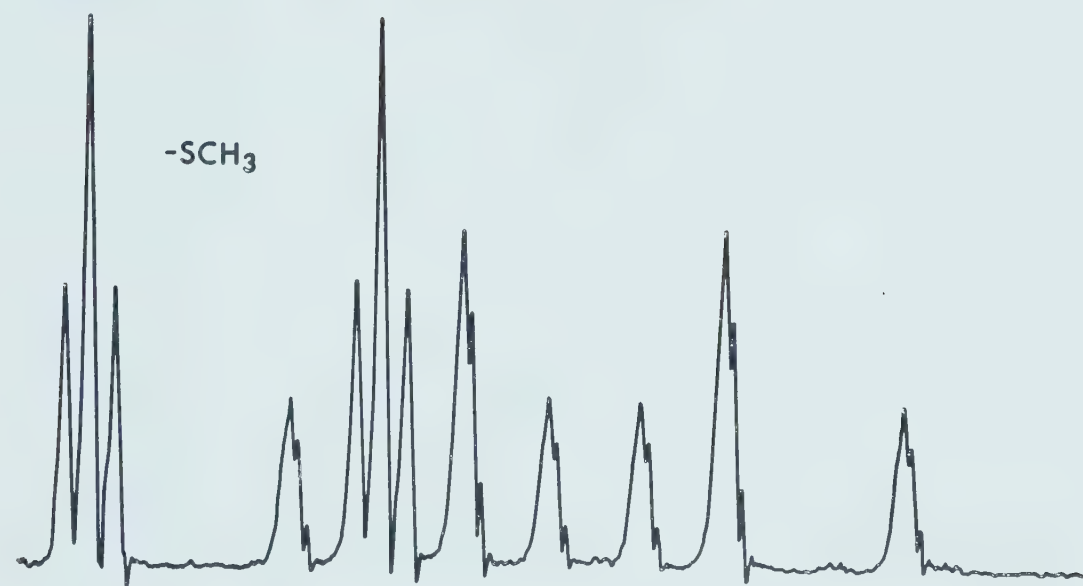
Figure V-11

Figure V-13 Comparison of the experimental ^1H (100.1 MHz) nmr spectra of $\text{CH}_3(\text{CF}_3)\text{PF}_2(\text{SCH}_3)$ and $\text{CH}_3(\text{CF}_3)\text{PF}_2(\text{SCD}_3)$ at 304°K. The spectrum of $\text{CH}_3(\text{CF}_3)\text{PF}_2(\text{SCH}_3)$ was obtained from an approximate 50:50 solution in CFCl_3 and CF_2Cl_2 containing about 5% TMS while that of $\text{CH}_3(\text{CF}_3)\text{PF}_2(\text{SCD}_3)$ was obtained from a solution in CFCl_3 and TMS. The doublet of triplets subspectrum arising from SCH_3 is absent in the deuterated compound. The frequency scale in Hz was measured relative to internal TMS in both cases.

^1H (100.1 MHz) Spectra of



$T = 304^\circ\text{K}$



220

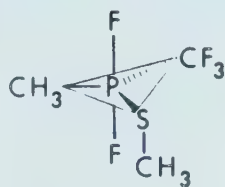
200

180

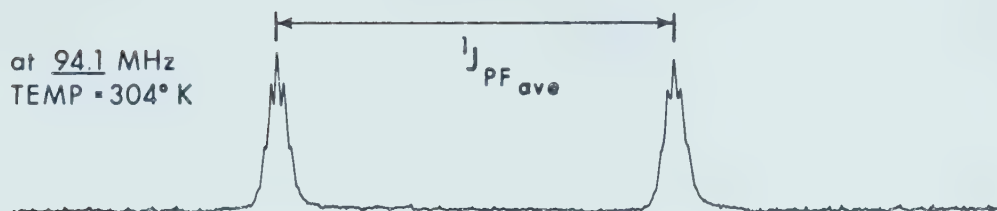
160 Hz

Figure V-13

Figure V-14 Experimental ^{19}F nmr spectra of $\text{CH}_3(\text{CF}_3)\text{PF}_2^-$ (SCH_3) (P-F region only) at various temperatures between the fast- and slow-exchange limits obtained from a solution in approximately 50:50 $\text{CFCl}_3:\text{CF}_2\text{Cl}_2$ containing about 5% TMS. The frequency scale gives the chemical shift values in Hz relative to internal CFCl_3 .

^{19}F SPECTRA (PE PORTION) OF

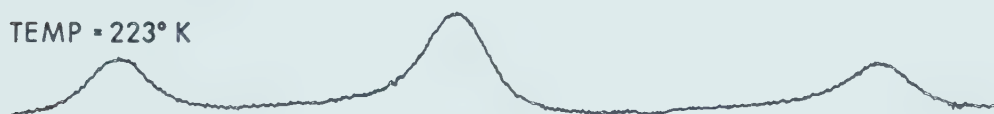
at 94.1 MHz
TEMP = 304° K



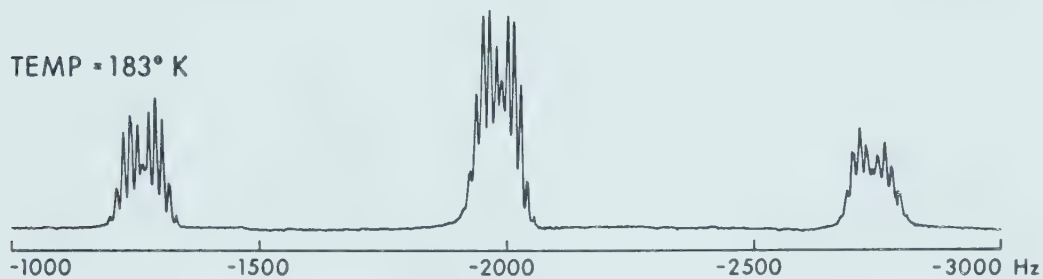
TEMP = 253° K



TEMP = 223° K



TEMP = 183° K



at 84.6 MHz - $\{^1\text{H}\}$
TEMP = 183° K

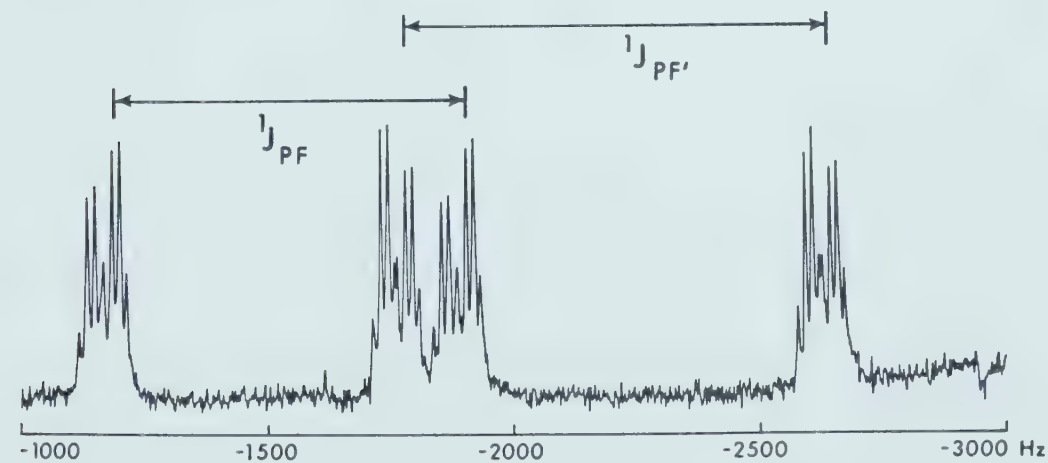
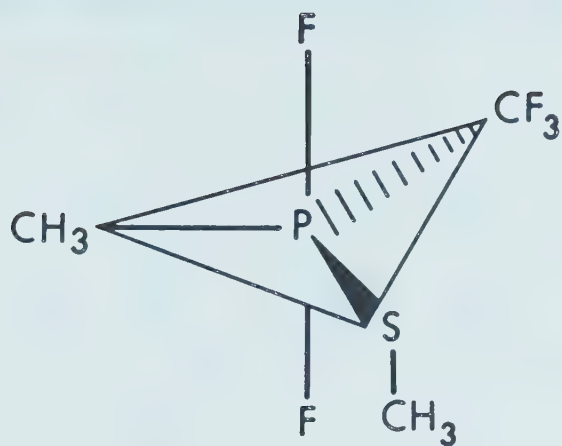


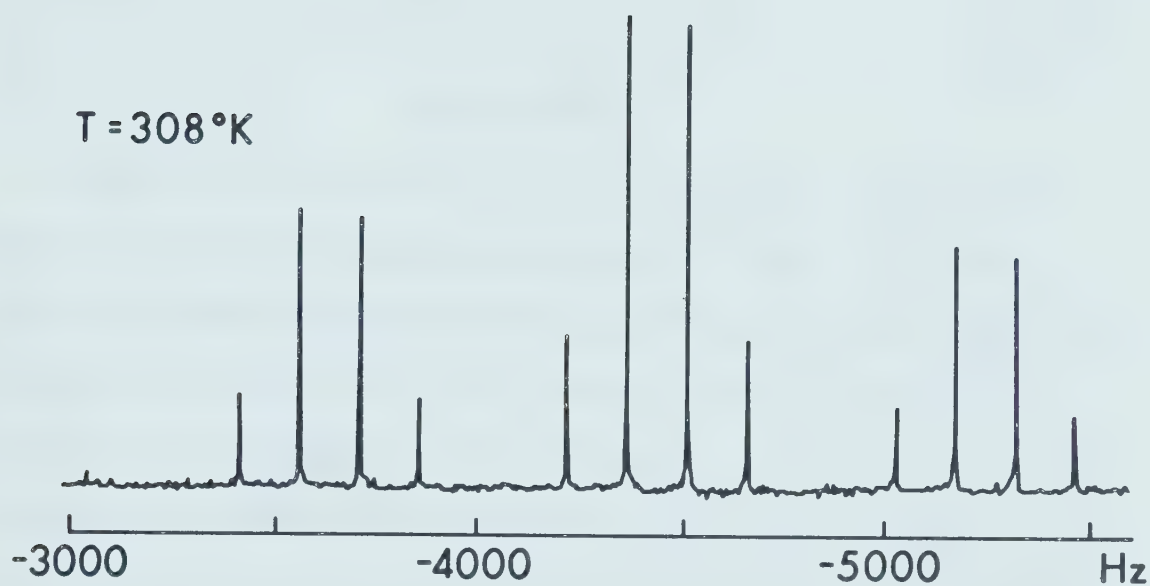
Figure V-14



Figure V-15 Observed $^{31}\text{P} \sim \{^1\text{H}\}$ (36.4 MHz) nmr spectra of $\text{CH}_3(\text{CF}_3)\text{PF}_2(\text{SCH}_3)$ at the fast- and slow-exchange temperature limits obtained from a solution in approximately 50:50 $\text{CFCl}_3:\text{CF}_2\text{Cl}_2$ containing about 5% TMS. The frequency scale which gives chemical shift values relative to P_4O_6 was measured relative to the ^{19}F (CFCl_3) heteronuclear lock and converted to appropriate values of the ^{31}P reference compound.



T = 308°K



T = 170°K

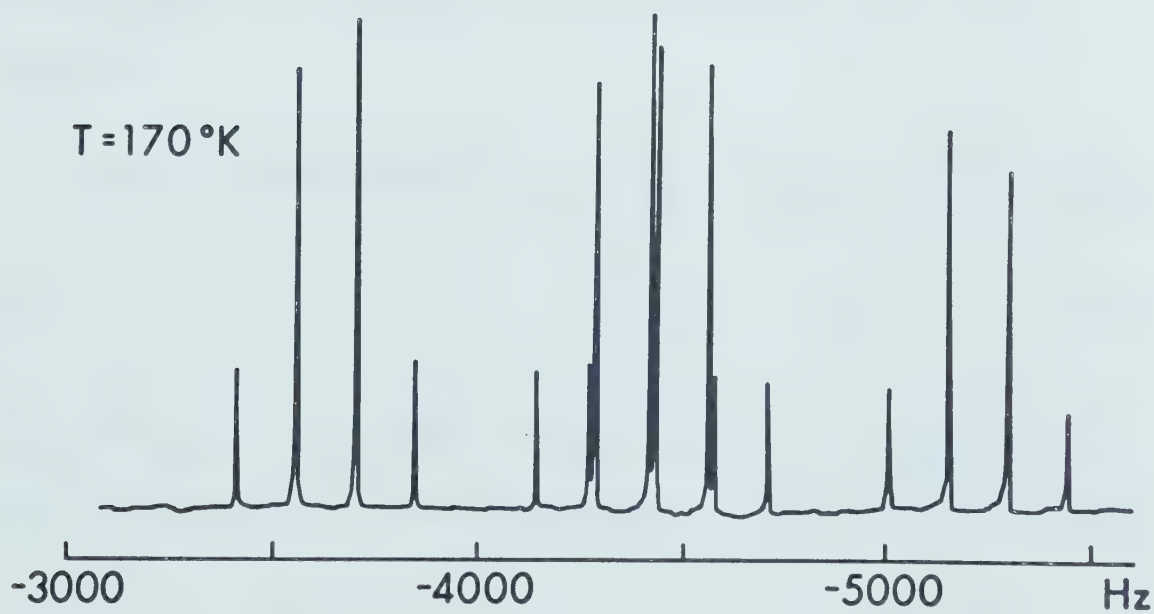


Figure V-15

would be resolved within the temperature range examined.

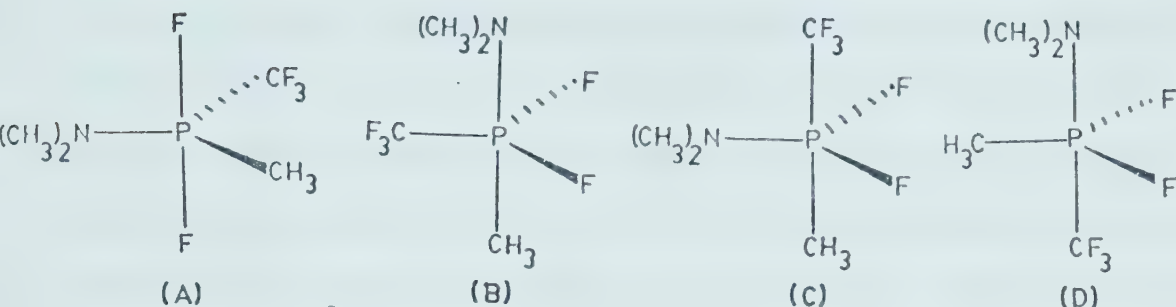


Figure V-12

The numerical values of $^1J_{P-F}$ (850 Hz) and $^2J_{P-F}$ (157 Hz) observed strongly suggest²⁶⁻²⁸ that the two directly-bound fluorines occupy equivalent axial positions and that the single CF_3 group occupies the equatorial position indicating that structure (A) in Fig V-12 is the ground state geometry for $CH_3(CF_3)PF_2N(CH_3)_2$. This is also in agreement with the "electronegativity rule"⁷ which predicts that the fluorine atoms would occupy the axial positions.

D. Methyl(trifluoromethyl)difluoro(methylthio)phosphorane

The normal temperature (+31°C) 1H , ^{19}F , and ^{31}P nmr spectra of $CH_3(CF_3)PF_2(SCH_3)$ are shown in Figs. V-13 to 15. The 1H nmr spectral pattern is similar to that of $CH_3-CF_3PF_2N(CH_3)_2$, except that the two resonance regions exhibit equal intensities because each arises from one methyl group.

The high field resonance peaks are assigned to the protons of the CH_3 group attached to phosphorus and the downfield peaks to the SCH_3 protons because the deuterated compound $\text{CH}_3(\text{CF}_3)\text{PF}_2\text{SCD}_3$ exhibits only the high field resonance (Fig V-13). This assignment is consistent with the relative electronegativities of the atoms to which the CH_3 groups are attached, the highest field resonance signal arising from the CH_3 group attached to the atom of lower electronegativity (P), thus it is the most highly shielded CH_3 group.⁵⁶

The ^{19}F nmr spectrum at normal temperatures (304°K) shows two resonance regions corresponding to the CF_3 (high field) and the P-F (low field) groups in the molecule. The CF_3 region is a relatively sharp doublet of triplets showing good resolution of the coupling to phosphorus as well as to the two directly-bound fluorine atoms. The P-F region at 304°K (Fig V-14) consists of a doublet with apparent septet splitting on each doublet component arising from partially resolved coupling with the CF_3 fluorines and the CH_3 protons. The P-F region proved to be temperature-dependent. At 253°K , the septet fine structure is lost and the two peaks shift upfield with the peak separation increased by 18 Hz. At 223°K , a new broad peak emerges at a lower field (~ 1240 Hz). The limiting spectrum, obtained at 183°K , shows three distinct sets of multiplets with an apparent intensity ratio of 1:2:1. The interpretation of this low-temperature ^{19}F nmr spectrum was aided by the proton-decoupled ^{19}F

spectrum of the P-F region at the same temperature but at a lower spectrometer frequency which showed a much simplified spectrum consisting of two sets of equal intensity doublets, indicative of two distinct P-F resonances. Thus the two directly-bound fluorine atoms have become magnetically non-equivalent at the lower temperature. At this low temperature, each component of both doublets is further split into a doublet of quartets with a 1:3:3:1 intensity ratio. This secondary doublet splitting is due to coupling between the two fluorine atoms directly-bound to phosphorus, and the quartet fine structure is due to the coupling of these fluorine atoms with the CF_3 group. The relevant parameters are given in Table 3 (Chapter III).

The normal temperature proton-decoupled ^{31}P nmr spectrum (Fig V-15) consists of a triplet of quartets, indicating resolved coupling with the two magnetically equivalent directly-bound fluorine atoms and the three CF_3 fluorines. At 180°K, a sixteen line spectrum results, consisting of a doublet of doublets of quartets with two nearly overlapping central quartets. The principal doublets are due to phosphorus coupling separately with each of the non-equivalent directly-bound fluorine atoms. The quartet fine structure on each line arises from coupling of phosphorus with the CF_3 group. The 308°K nmr spectra of $\text{CH}_3(\text{CF}_3)\text{PF}_2(\text{SCH}_3)$ are consistent with any one of the following trigonal bipyramidal structures:

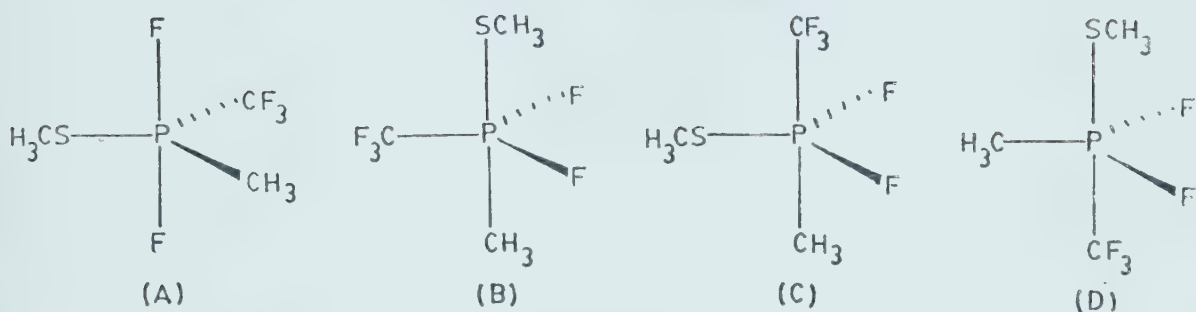


Figure V-16

Comparison with other systems and consideration of the electronegativity rule would suggest structure (A) (Fig V-16) as the most reasonable alternative for the ground state structure of this molecule. The loss of equivalence of the fluorine environments clearly shown in the variable-temperature proton-decoupled ^{19}F and ^{31}P nmr spectra is most likely due to cessation of free rotation about the P-S bond analogous to the behavior of tetrafluoroalkyl- and arylthiophosphoranes.³⁹ Theoretical studies^{66,67,70} suggest that the most likely ground state conformation is the structure in which the methyl group lies in the axial plane placing lone pair (or $p\pi$) electron density in the equatorial plane (Fig V-17).

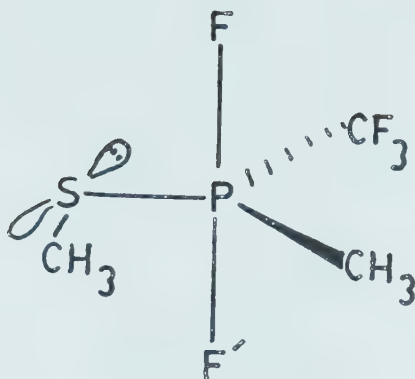


Figure V-17

Whether the fluorine which shows coupling with the SCH_3 protons is *trans* or *cis* to the SCH_3 group cannot be decided on the basis of available information, and more extensive and comprehensive investigations are required on this and similar compounds to resolve this problem.

E. Bis(trifluoromethyl)dimethylamino(methoxy)fluorophosphorane

The ^1H nmr spectrum of $(\text{CF}_3)_2\text{PF}(\text{OCH}_3)\text{N}(\text{CH}_3)_2$ at normal temperatures shows two resonance regions of 1:2 relative intensity ratio corresponding to the resonance of the three methoxy group protons and the six dimethylamino protons respectively. Each region consists of a

Observed ^1H (100.1 MHz) nmr spectrum of $(\text{CF}_3)_2\text{PF}(\text{OCH}_3)\text{N}(\text{CH}_3)_2$ at 303°K and obtained from a solution in approximately 50:50 $\text{CFCl}_3:\text{CF}_2\text{Cl}_2$ with about 5% TMS. The frequency scale gives chemical shift values in Hz relative to internal TMS.

Figure V-18

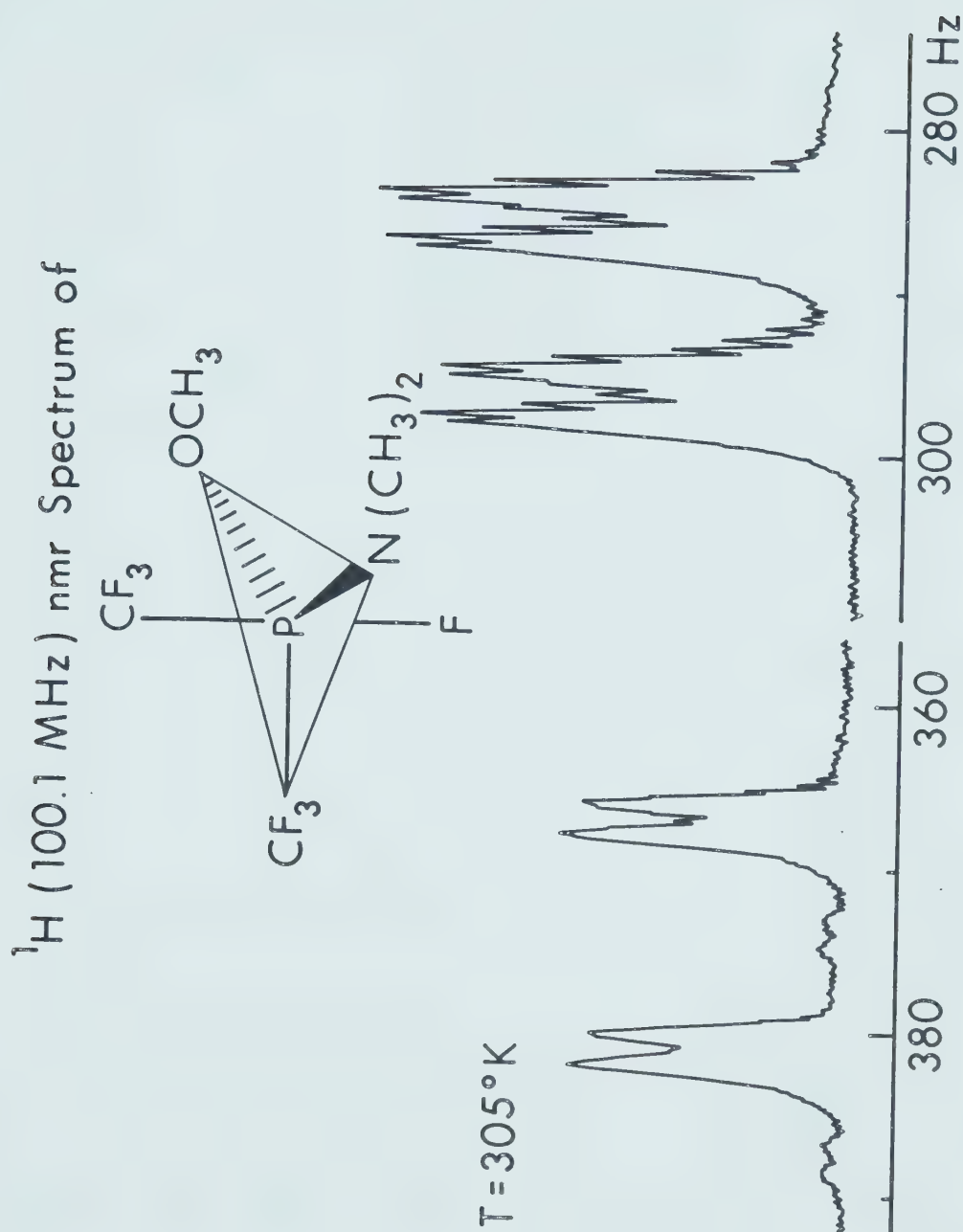


Figure V-18

Figure V-19 Experimental ^{19}F (94.1 MHz) nmr spectra of $(\text{CF}_3)_2\text{PF}(\text{OCH}_3)\text{N}(\text{CH}_3)_2$ at various temperatures, obtained from a solution in approximately 50:50 $\text{CFCl}_3:\text{CF}_2\text{Cl}_2$ with about 5% TMS. The frequency scale gives chemical shift values in Hz relative to internal CFCl_3 .

^{19}F (94.1 MHz) nmr Spectra of

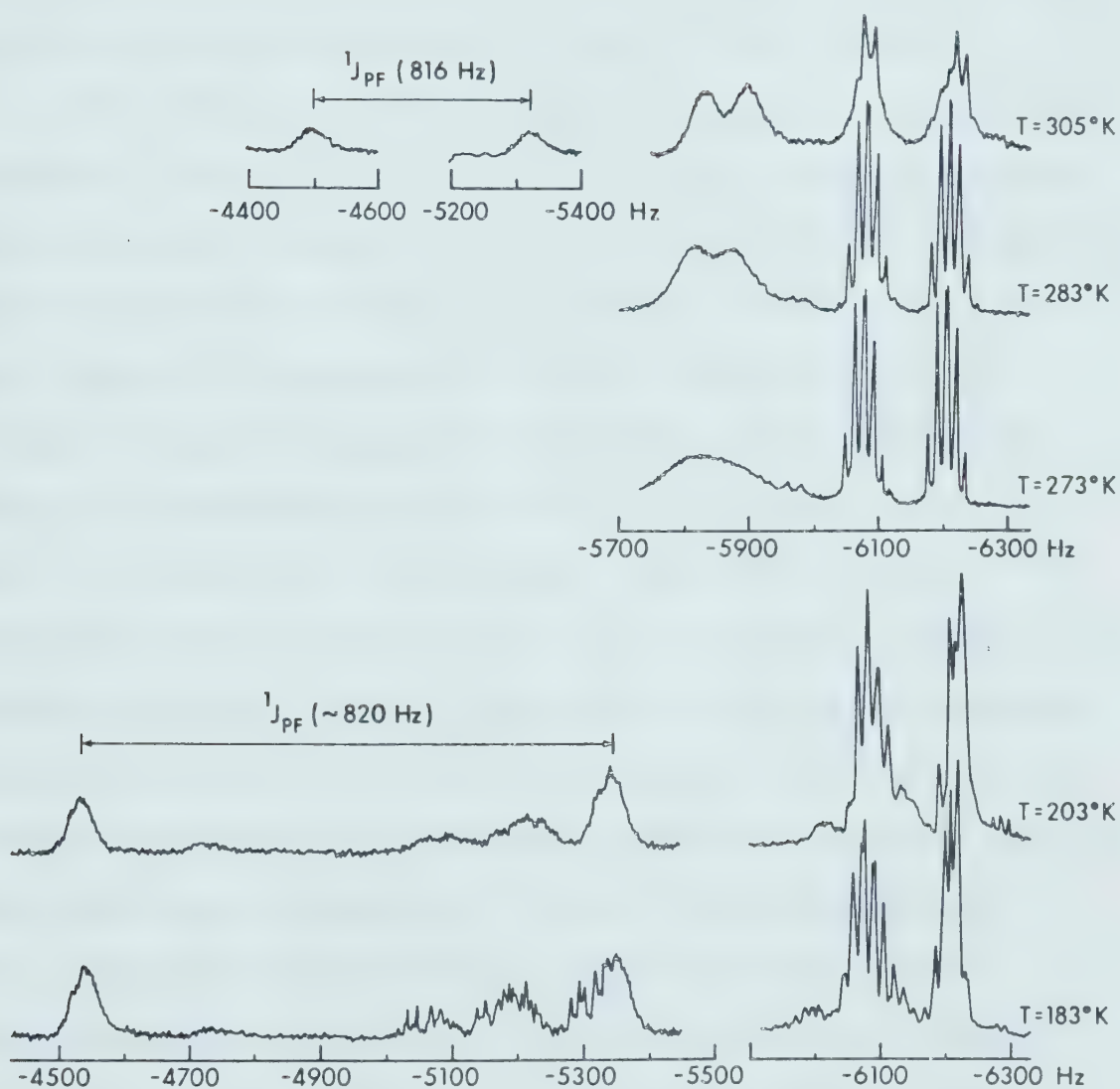
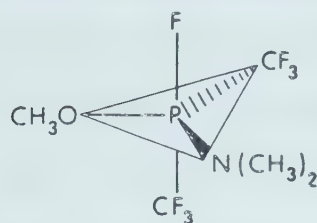


Figure V-19

relatively broad doublet of doublets indicating that the proton signals are coupled with phosphorus and with the single fluorine directly attached to phosphorus. Upon expansion of each doublet component, the dimethylamino proton signals (at higher field) show the coupling with the six fluorines in the two CF_3 groups with moderately good resolution (Fig V-18). The coupling of the methoxy protons with the CF_3 groups is not as well resolved.

The ^{19}F nmr spectrum shows three distinct resonance regions at 305°K (Fig V-19). The lowest field resonance consists of two widely separated ($J \sim 816$ Hz) broad peaks, and is assigned to the directly-bound fluorine atom on the basis of the magnitude of the chemical shift and coupling constant values. The middle field resonance region is similarly a broad doublet but with a much smaller separation ($J = 62$ Hz). The highest field resonance region consists of a pair of broad doublets apparently split into 5 lines each. The major separation of this doublet ($J = 130$ Hz) is greater than that of the middle field set but is still considerably smaller than for the first set of doublets. These latter two regions are assigned to the axial and equatorial CF_3 groups respectively, in agreement with the trends established previously. The ground state structure therefore is:

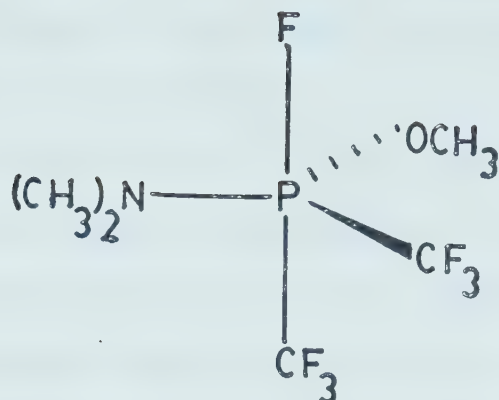


Figure V-20

This structure is in agreement with the simple electronegativity (and apicophilicity) predictions since the most electronegative substituent F is placed in an axial position while the $-OCH_3$ and $-N(CH_3)_2$ groups occupy equatorial positions. The CF_3 groups, more electronegative than the $-OCH_3$ or $-N(CH_3)_2$ but less electronegative than F are forced to occupy the two dissimilar remaining sites and hence are non-equivalent. The structure is supported by the splitting patterns, by the magnitude of $^1J_{P-F}$ (816 Hz) which is in the correct range for axial fluorine on phosphorus and by the $^2J_{P-F}$ values of the CF_3 groups. The smaller $^2J_{P-F}$ value ($J = 62$ Hz, $\phi_{CF_3} = 62.1$ ppm) is associated with the axial CF_3 group while the larger of the two values ($J = 130$ Hz, $\phi_{CF_3} = 65.3$ ppm)

is associated with the equatorial CF_3 group. The resolution of the two different CF_3 environments at 305°K implies that the barrier to positional exchange of these two CF_3 groups is relatively high.

The best resolution of the apparent quintet fine structure appearing in the highest field resonance peaks (equatorial CF_3 doublet) was obtained at 283°K , and a septet structure became apparent, but at the same time the axial CF_3 doublet became even broader. At 273°K more drastic changes appeared in the spectrum. The axial CF_3 resonance doublet is almost completely collapsed and the doublet of septets due to equatorial CF_3 resonance shows some asymmetry. At 163°K a number of complex asymmetric multiplets appear between the P-F doublet and the original high field doublet of multiplets (equatorial CF_3), with the latter becoming even more asymmetric both in height and splitting pattern. Such complex spectral patterns appear similar to those observed in the low temperature ^{19}F spectra of a number of phosphoranes containing CF_3 and $\text{N}(\text{CH}_3)_2$ ^{26a,b} or $\text{OSi}(\text{CH}_3)_3$ groups.⁷³ These changes, which appear to affect the axial CF_3 signals more than the equatorial CF_3 signals, have been interpreted as arising from the cessation of conformational averaging processes either of the OCH_3 or $\text{N}(\text{CH}_3)_2$ group or both, thus locking the axial CF_3 group and destroying the magnetic equivalence of the fluorine atoms

of the axial CF_3 group. The spectrum is too complex and too poorly resolved to assign completely at this time.

Heating the sample also alters the appearance of the ^{19}F nmr spectrum. At 333°K the two distinct CF_3 resonance peaks start to broaden with concomitant loss of the fine structure of the equatorial CF_3 region. At 343°K one observes only four broad humps in these two resonance regions (Fig V-21).

Much higher temperatures were not explored because of the likely thermal instability of the compound, which, in keeping with similar trifluoromethylphosphoranes, would probably suffer ready elimination of CF_2 .⁷⁴ The observed behavior of the nmr spectrum at elevated temperatures is strongly suggestive of the onset of magnetic equivalence of the CF_3 groups presumably due to a process similar to that observed in analogous compounds.²⁷

The proton-decoupled ^{31}P nmr spectrum of $(\text{CF}_3)_2\text{-PF}(\text{OCH}_3)\text{N}(\text{CH}_3)_2$ is readily assigned as a first order AMX_3Y_3 pattern with some overlapping of lines. The basic pattern arises from a major doublet, each line of which is further split into a quartet by the equatorial CF_3 group and each line is then further split into a quartet with accidental overlapping of some lines. The stick diagram in Fig V-22 traces the origin of the spectral splittings.

Figure V-21 Experimental and calculated ^{19}F (94.1 MHz) nmr spectra of $(\text{CF}_3)_2\text{PF}(\text{OCH}_3)-\text{N}(\text{CH}_3)_2$ at particular temperatures and with appropriate rates of exchange of magnetization. The experimental spectra were obtained from a solution in C_6F_6 and the calculated spectra were obtained using a K matrix constructed for an intramolecular axial-equatorial CF_3 exchange mechanism. The chemical shift values in Hz are given relative to external CFCl_3 . Lines marked (*) arise from an impurity in the sample.

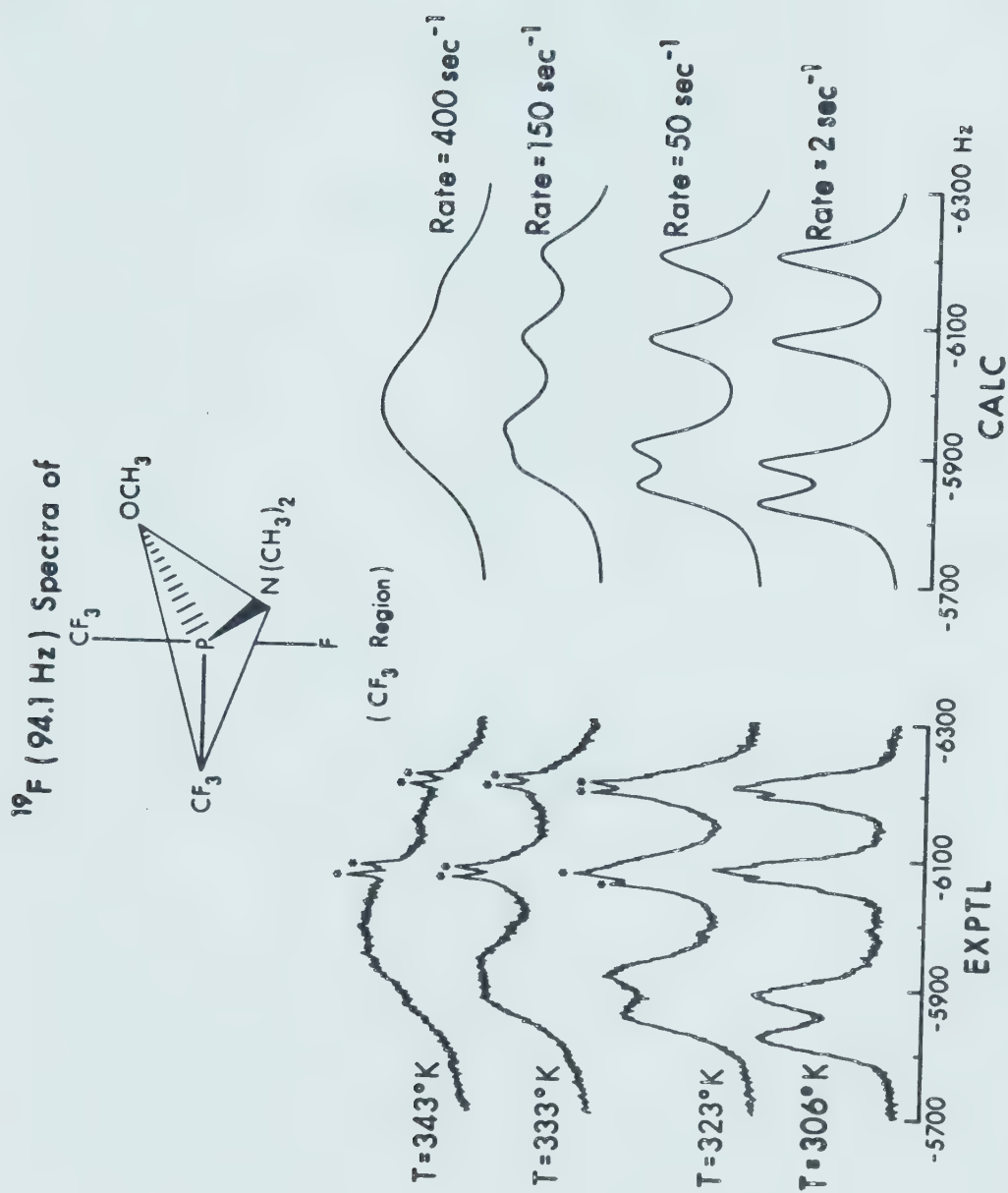
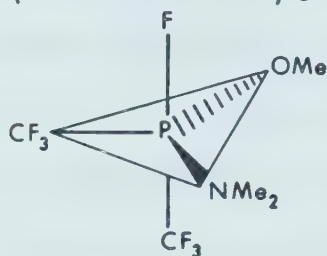


Figure V-21

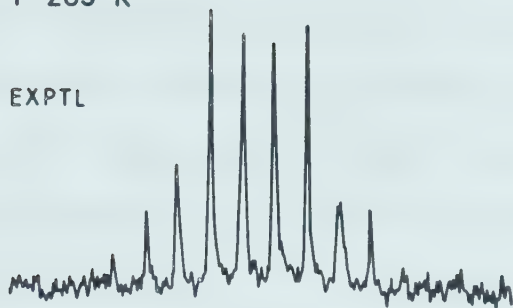
Figure V-22 Experimental and calculated $^{31}\text{P} \sim \{^1\text{H}\}$ (36.4 MHz) nmr half-spectra of $(\text{CF}_3)_2\text{PF}(\text{OCH}_3)\text{N}(\text{CH}_3)_2$ near the high-temperature exchange limit. The experimental spectrum was obtained from a solution in CFCl_3 with about 5% TMS. The frequency scale which gives chemical shift values in Hz relative to P_4O_6 was measured relative to CFCl_3 as a heteronuclear lock. The stick diagram traces the origin of a pattern of a quartet of quartets of quartets arising from phosphorus coupling with two non-equivalent CF_3 groups and one CH_3 group. The central pair of lines, which should be the strongest lines in the spectrum, are not the tallest lines because the system is beginning to show the effects of a reduced rate of exchange at this temperature.

^{31}P nmr (36.4 MHz) $\sim \{^1\text{H}\}$ Half-Spectrum
(Low Field Portion) of

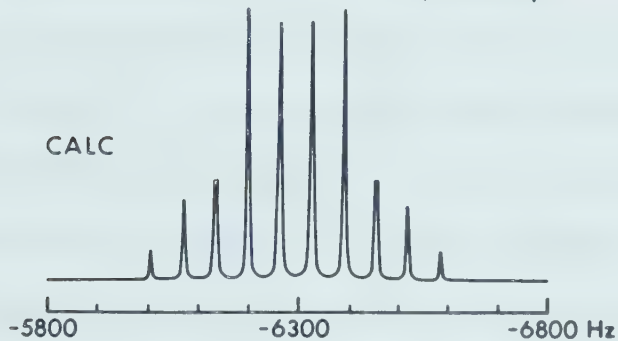


$T = 283^\circ\text{K}$

EXPTL



CALC



First Order
Stick Diagram

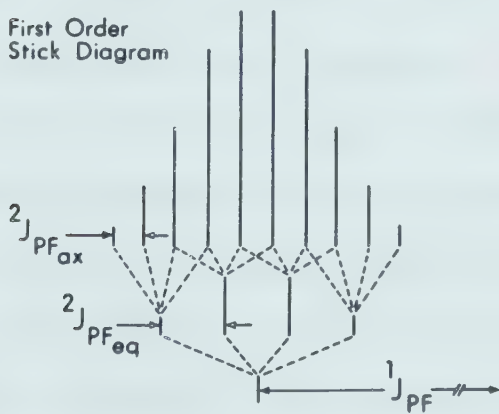


Figure V-22

F. Bis(trifluoromethyl)dimethylaminodifluorophosphorane.

The ^1H and ^{19}F nmr spectra of $(\text{CF}_3)_2\text{PF}_2\text{N}(\text{CH}_3)_2$ obtained at 60 and 56.4 MHz, respectively, depart strikingly from a first-order splitting pattern (Fig V-23,24A). Simulation of the spectra by means of the computer program NUMARIT⁹⁰, using the parameters derived from the high frequency spectrum, confirmed this interpretation. The ^1H spectrum gave reasonable agreement with experiment and the ^{19}F spectrum gave excellent agreement with experiment only when $^1J_{\text{PF}}$ and $^2J_{\text{PF}}$ were assigned opposite signs, confirming the general relationship of these coupling constants¹⁰⁰ (Fig V-24C).

At higher operating frequency, 100 and 94.1 MHz, respectively for ^1H and ^{19}F , the second-order effects disappeared (Fig 23,24B) reducing the splitting pattern to that of a simple first-order spectrum. Under these conditions the ^1H spectrum consists of a doublet of triplets due to proton coupling with phosphorus and further coupling with the two directly-bound fluorines. The ^{19}F nmr spectrum shows two resonance regions with the multiplicity and intensities consistent with the presence of two magnetically equivalent directly-bound fluorines and two CF_3 groups (Fig V-23). The CF_3 region (Fig 24B) is a doublet of 1:2:1 triplets while the P-F region is a doublet of septets of septets. The primary septet structure of each P-F component arises from the coupling of the

Figure V-23 Observed ^1H nmr spectra of $(\text{CF}_3)_2\text{PF}_2\text{N}(\text{CH}_3)_2$ at 303°K and obtained from a solution in CFCl_3 with about 5% TMS at both 60.0 MHz and 100.1 MHz spectrometer frequencies. The second-order effect evident in the 60.0 MHz spectrum disappears in the 100.1 MHz spectrum. Chemical shift values are given in Hz, relative to internal TMS.

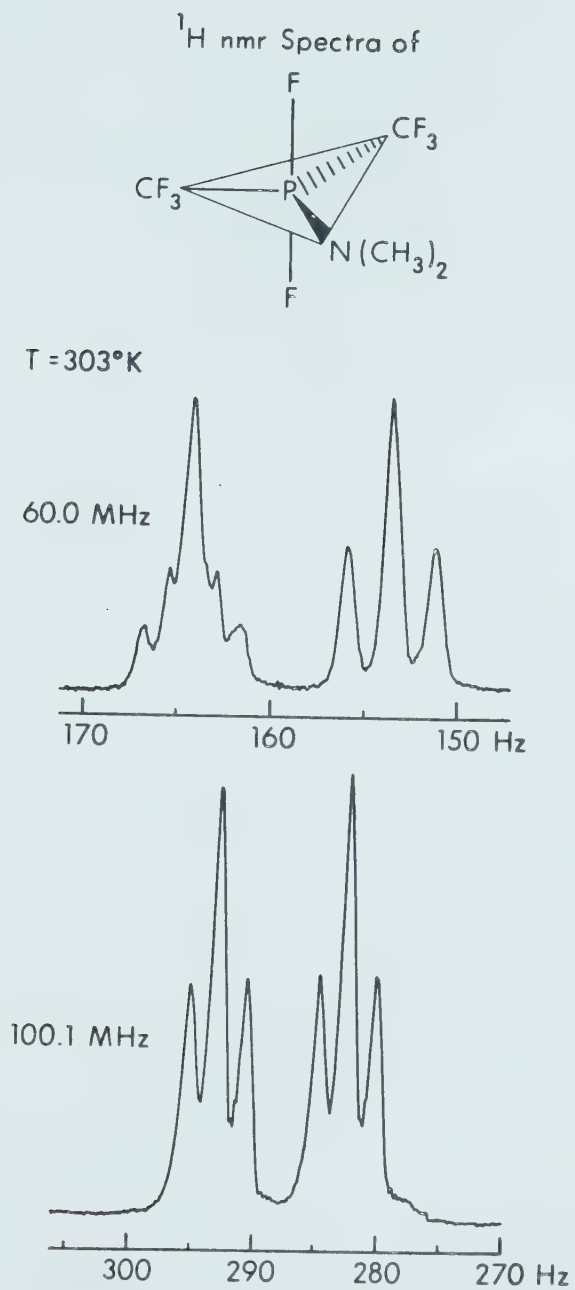


Figure V-23

Figure V-24A Observed ^{19}F (56.4 MHz) nmr spectra of $(\text{CF}_3)_2\text{PF}_2\text{N}(\text{CH}_3)_2$ obtained on a solution in CFCl_3 . The scale gives chemical shift values in Hz relative to external CFCl_3 . The expansions are shown with arbitrary vertical scale. The singlet at -3850 Hz has an integrated relative intensity of 3.9 units relative to 3.0 units for the triplet centered at -3975 Hz.

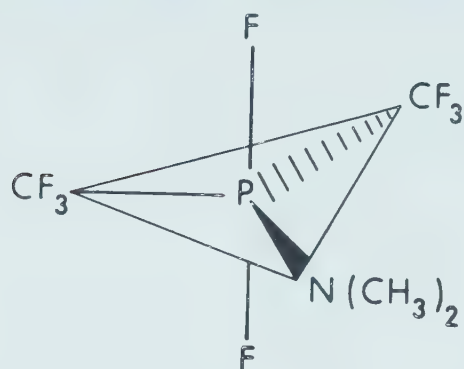
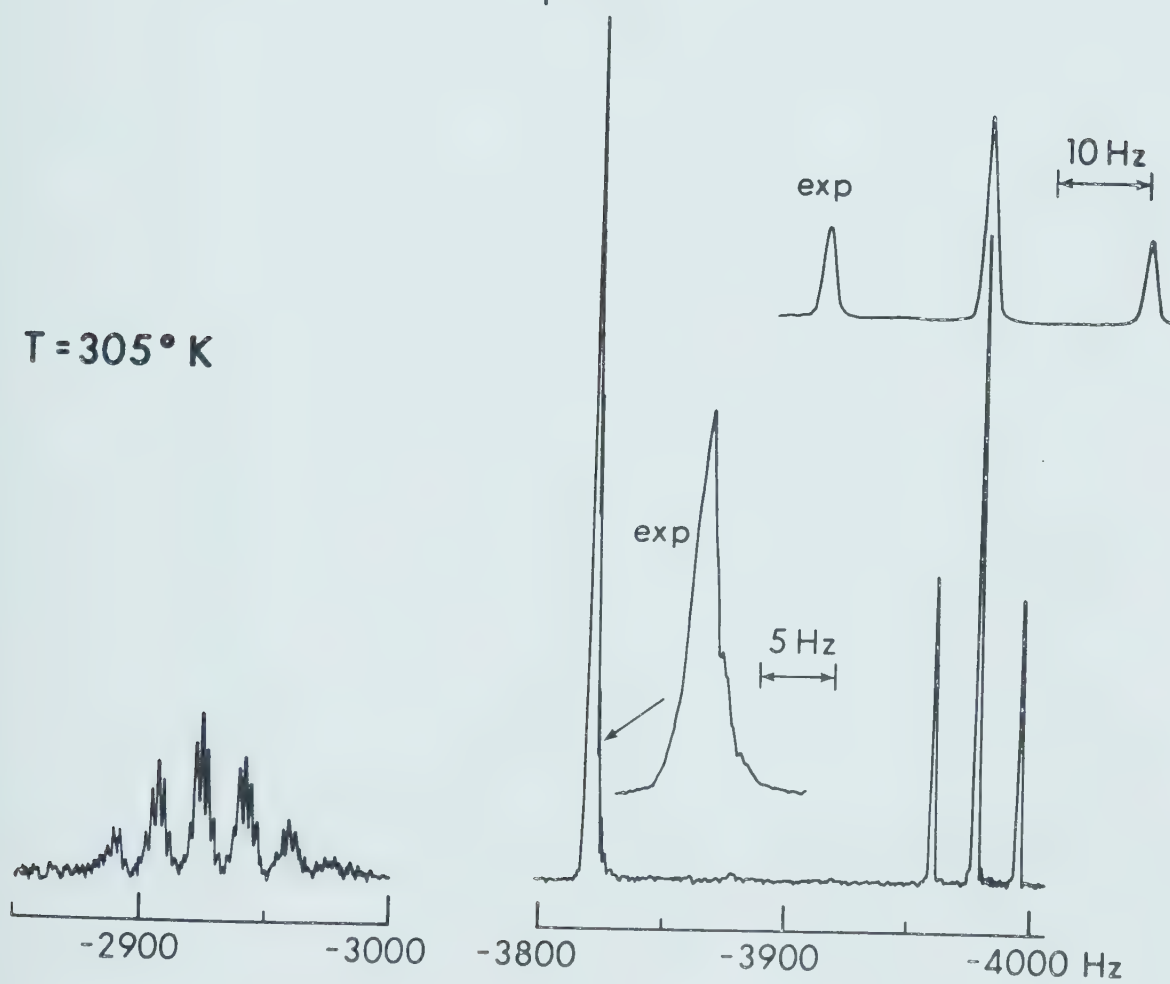
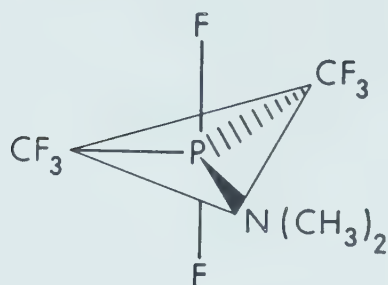
^{19}F (56.4 MHz) nmr Spectra of $T = 305^\circ \text{K}$ 

Figure V-24A

Figure V-24B Observed ^{19}F (94.1 MHz) nmr spectrum of $(\text{CF}_3)_2\text{PF}_2\text{N}(\text{CH}_3)_2$ at 303°K and obtained from a solution in CFCl_3 with about 5% TMS. The frequency scale is given in Hz relative to internal CFCl_3 .

^{19}F (94.1 MHz) nmr Spectra of



T = 303°K

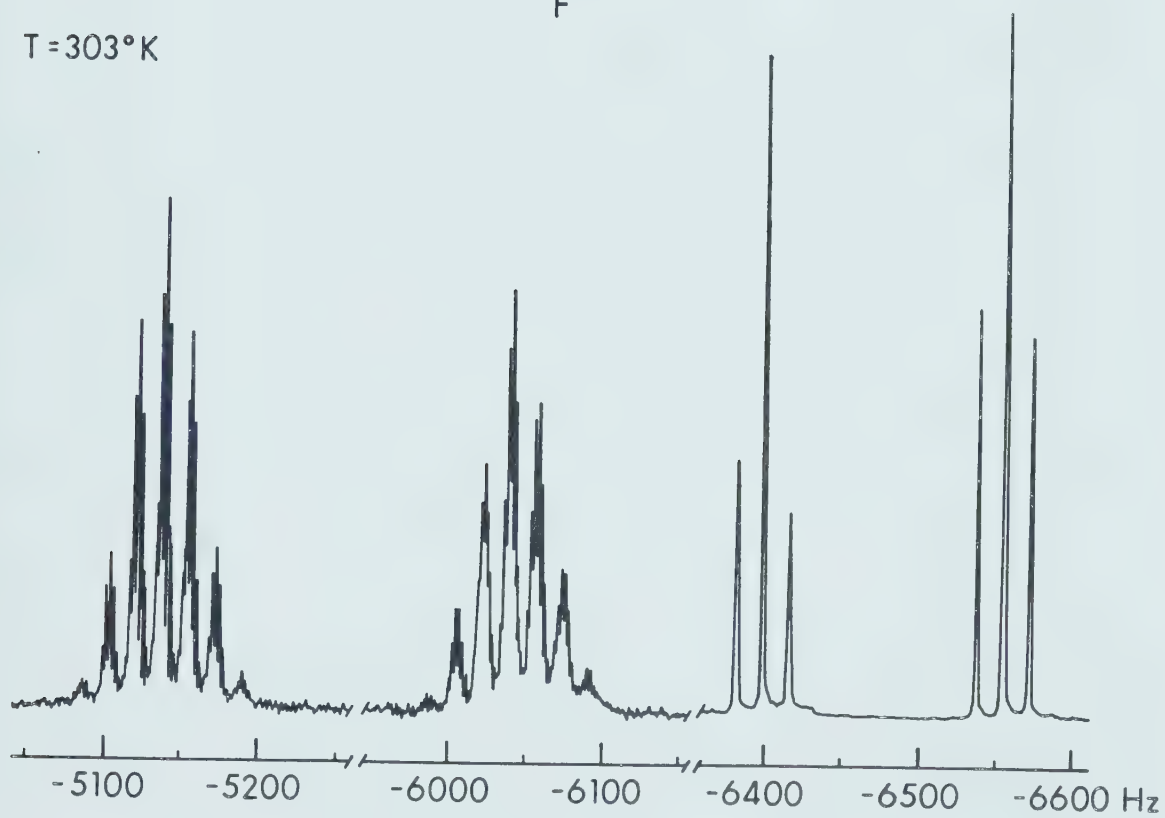


Figure V-24B

Figure V-24C

Calculated ^{19}F (56.4 MHz) spectra of $(\text{CF}_3)_2\text{PF}_2\text{N}(\text{CH}_3)_2$ for two possible sign combinations of $^1J_{\text{PF}}$ and $^2J_{\text{PF}}$. The spectra are insensitive to the relative sign of $^3J_{\text{FF}}$. Proton couplings have been omitted for clarity. Expansions are shown with arbitrary vertical scales.

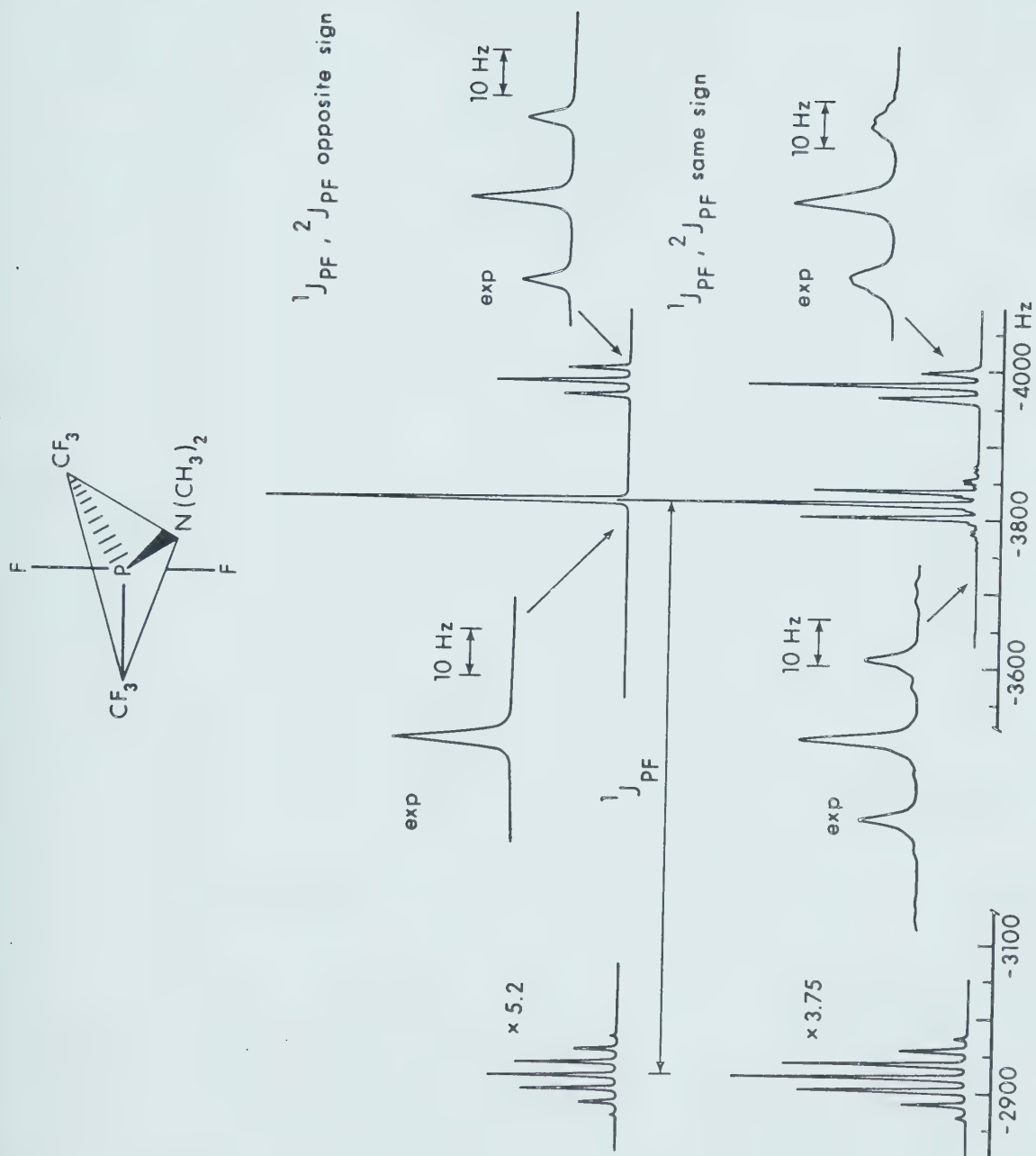
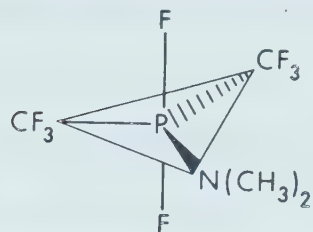


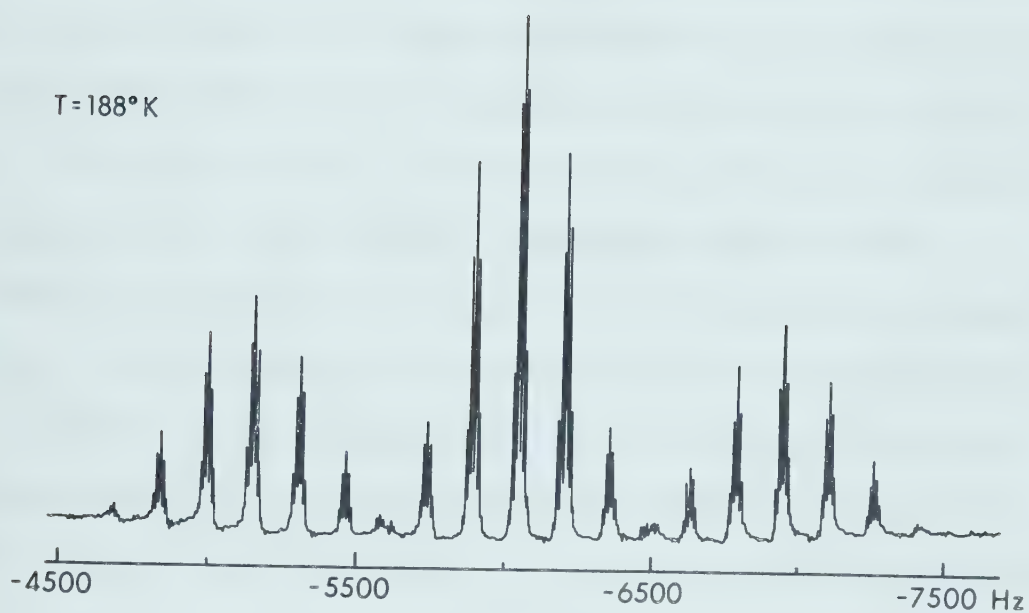
Figure V-24C

Figure V-25 Experimental ^{31}P (36.4 MHz) nmr spectrum of $(\text{CF}_3)_2\text{PF}_2\text{N}(\text{CH}_3)_2$ at 188°K obtained from a solution in approximately 50:50 $\text{CFCl}_3:\text{CF}_2\text{Cl}_2$ containing about 5% TMS. The chemical shift values which are given in Hz relative to P_4O_6 were measured relative to the ^{19}F (CFCl_3) heteronuclear lock and converted to appropriate values on the P_4O_6 scale.

^{31}P (36.4 MHz) nmr Spectrum of



T=188°K



CENTRAL PORTION

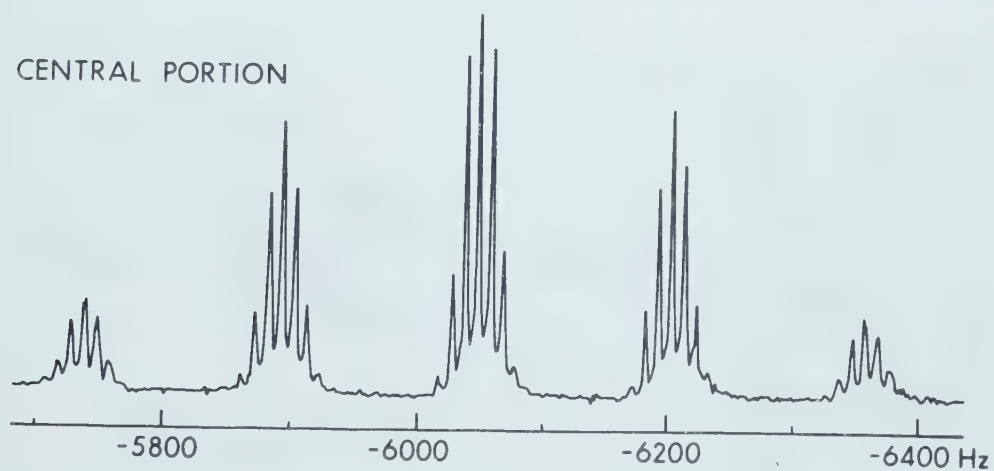


Figure V-25

directly-bound fluorines with the fluorines in the two CF_3 groups. With the exception of the outer lines in each septet, each line is visibly split into septets in the proton-coupled spectrum due to further coupling with the six dimethylamino protons.

The spectra of $(\text{CF}_3)_2\text{PF}_2\text{N}(\text{CH}_3)_2$ taken at 100 MHz (^1H); 94.1 MHz (^{19}F) and 36.4 MHz (^{31}P) (Fig V-25) are first-order and, on the basis of the number of P-F and CF_3 resonances, the number and magnitude of the coupling constants observed are compatible with structures (A) or (B) in Fig V-26. The electronegativity rule would suggest (A) as the ground state structure of the compound. The single $^1J_{\text{P-F}}$ value of 902 Hz and single $^2J_{\text{P-F}}$ value of 157 Hz are within the range of the magnitudes of axial F-P and equatorial CF_3 -P coupling parameters established by numerous previous investigations,²⁶⁻²⁸ and support the choice of (A) as the preferred structure.

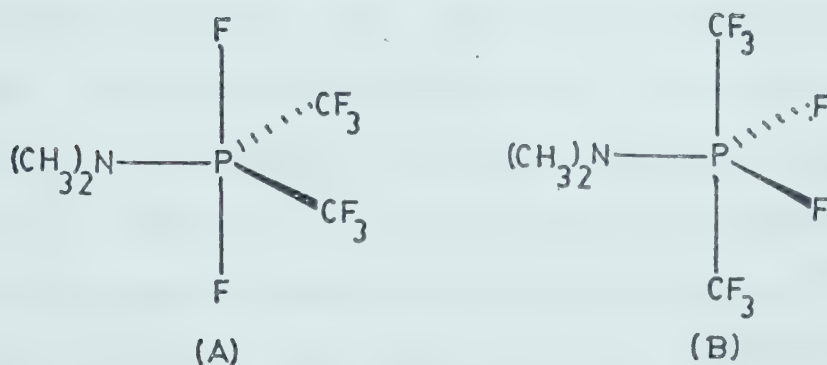


Figure V-26

G. Bis(trifluoromethyl)dimethylaminochlorofluorophosphorane.

The ^1H nmr spectrum of $(\text{CF}_3)_2\text{PFCln}(\text{CH}_3)_2$ consists of a broad doublet of doublets, the principal doublet arising from coupling with phosphorus and the secondary doublet from coupling with the single directly-bound fluorine. The proton coupling to the CF_3 fluorines is not resolved (Fig V-27).

The ^{19}F nmr spectrum consists of a doublet of doublets in the CF_3 region, and a doublet of septets of septets in the P-F region. The major doublet in each region is due to coupling with phosphorus. The doublet fine structure in the CF_3 region is due to coupling of the directly-bound fluorine with the CF_3 fluorine atoms. The multiplets in the P-F region arise from fluorine coupling with the six fluorines in the two equivalent CF_3 groups and then further coupling with the six dimethylamino protons (Fig V-28).

The proton-decoupled ^{31}P nmr spectrum is a doublet of apparent quintets. The ratio of the line intensities however, is in better agreement with the central 5 lines of a septet ($1:2\frac{1}{2}:3\frac{1}{3}:2\frac{1}{2}:1$) than with that of a quintet ($1:4:6:4:1$) hence it is assumed that the outermost unit intensity lines of each septet have been lost in the background noise. This proposed septet splitting of the P-F doublet is to be expected from phosphorus coupling

Figure V-27 Observed ^1H (60.0 MHz) nmr spectrum of $(\text{CF}_3)_2\text{PF}_2\text{N}(\text{CH}_3)_2$ at 303°K and obtained from a solution in approximately 50:50 $\text{CFCl}_3:\text{CFCl}_2$ containing about 5% TMS. The frequency scale is given in Hz relative to internal TMS.

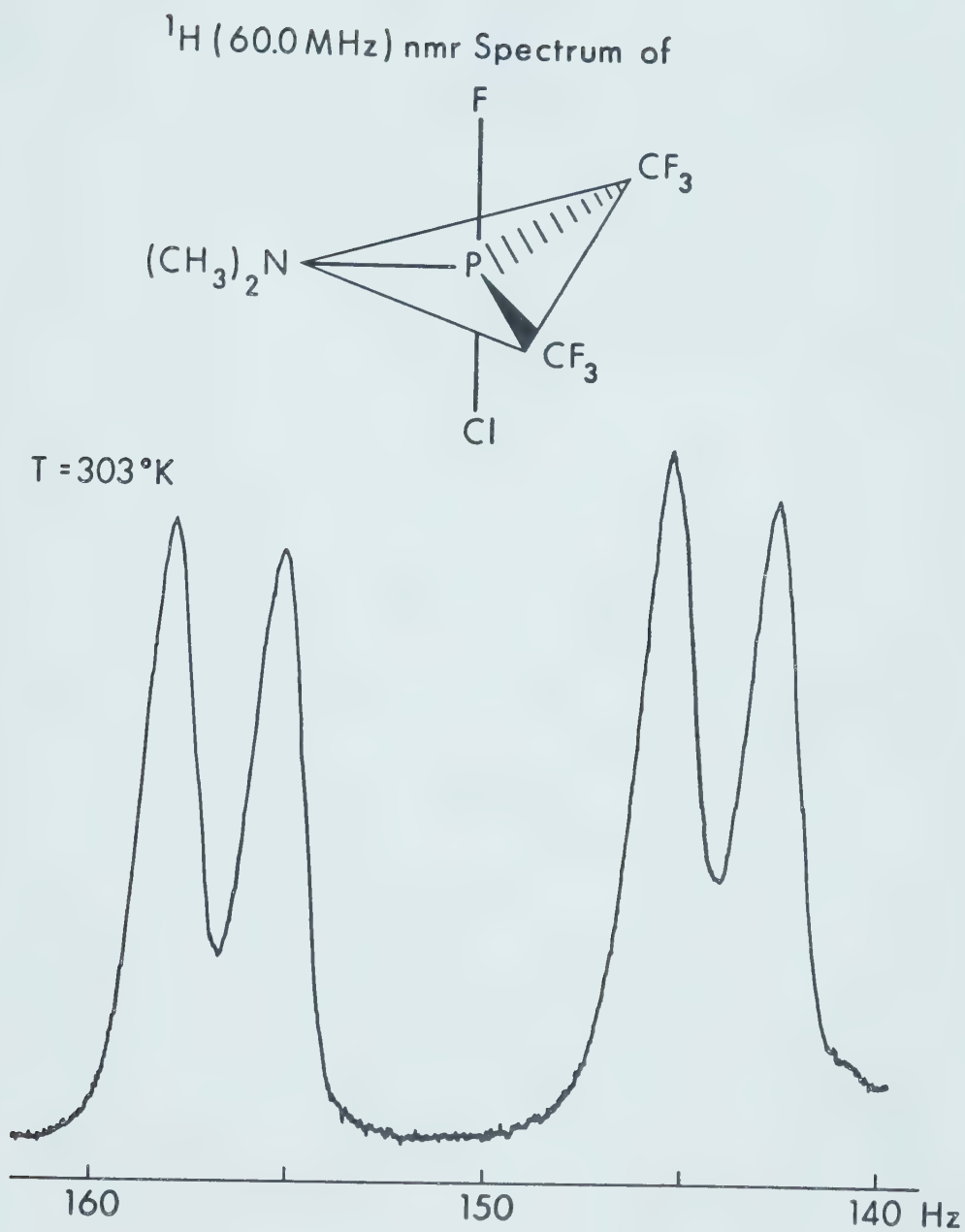
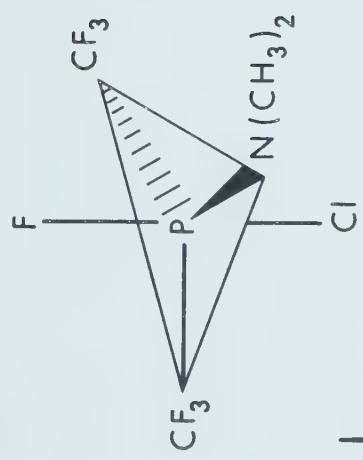


Figure V-27

Figure V-28

Experimental ^{19}F (94.1 MHz) nmr spectrum of $(\text{CF}_3)_2\text{PFClN}(\text{CH}_3)_2$ at 303°K, obtained from a solution in CFCl_3 with about 5% TMS. The frequency scale gives the chemical shift values in Hz relative to internal CFCl_3 . The small peaks marked (*) are due to an impurity in the sample.

^{19}F (94.1 MHz) nmr Spectrum of



$T = 303^\circ\text{K}$

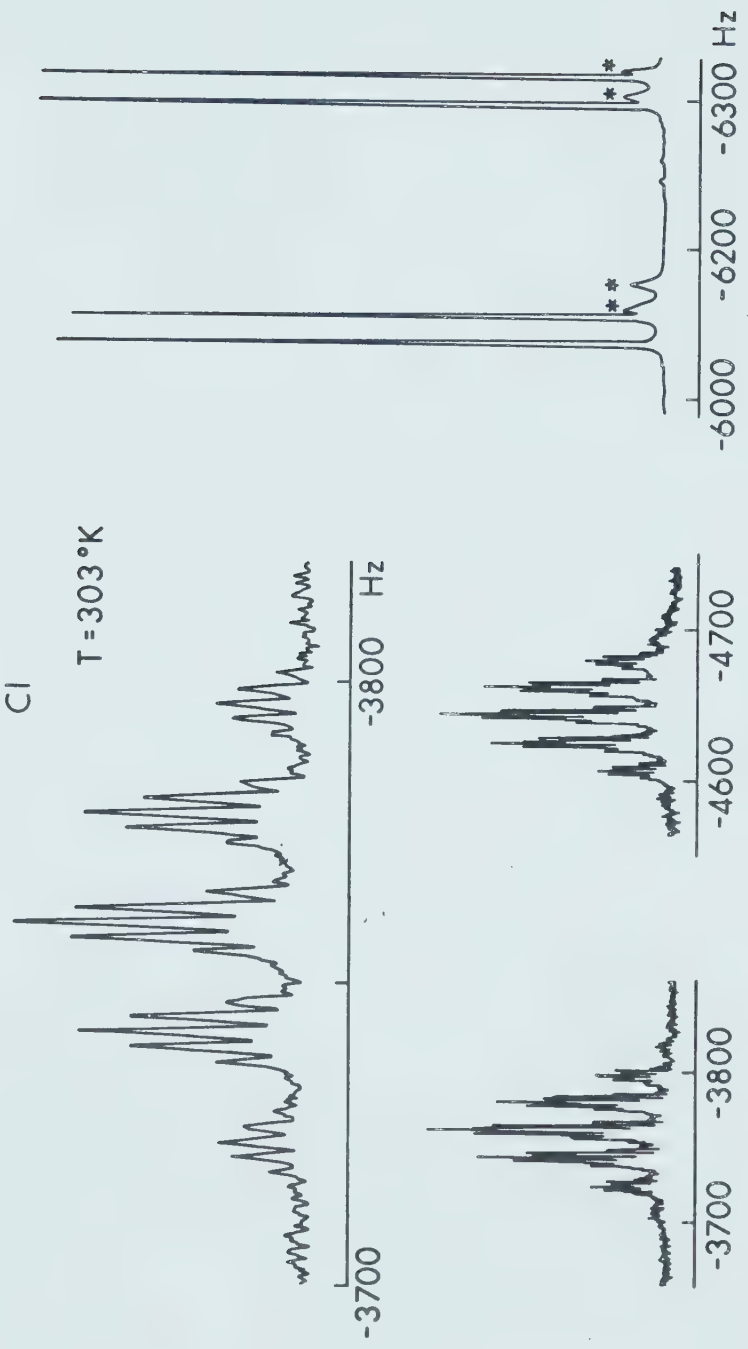


Figure V-28

Figure V-29 Observed $^{31}\text{P} \sim \{^1\text{H}\}$ (36.4 MHz) nmr spectrum of $(\text{CF}_3)_2\text{PFCIN}(\text{CH}_3)_2$ at 303°K obtained from a solution in CFCl_3 with about 5% TMS. The frequency scale which gives chemical shift values in Hz relative to P_4O_6 , was measured relative to the ^{19}F (CFCl_3) heteronuclear lock and converted to appropriate values of the ^{31}P reference.

^{31}P (36.4 MHz) $\sim \{^1\text{H}\}$ Spectrum of

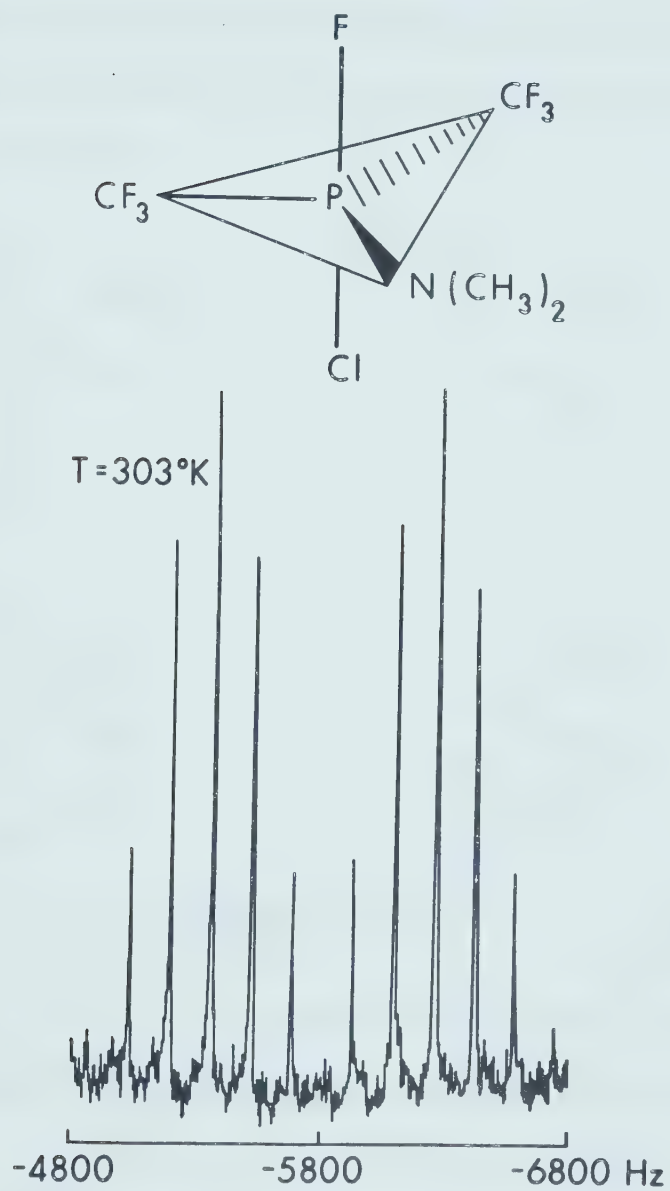


Figure V-29

with six fluorines in the two equivalent CF_3 groups (Fig V-29). The proton-coupled spectrum shows additional septet splitting of the original septets due to phosphorus coupling with the six dimethylamino protons.

The spectral patterns discussed above are consistent with any one of the four following trigonal bipyramidal structures (Fig V-30).

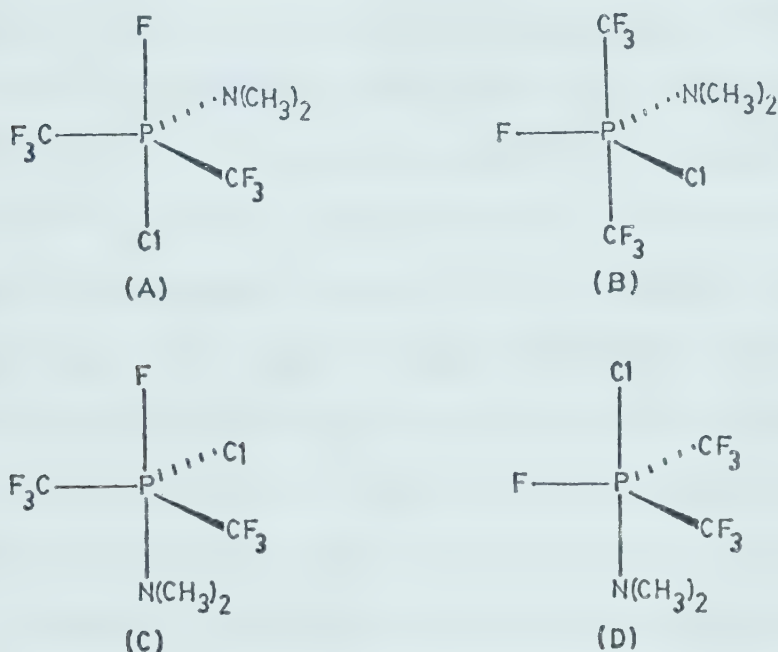


Figure V-30

From the ^1H , ^{19}F , ^{31}P spectral splitting pattern and line intensities of $(\text{CF}_3)_2\text{PFClN}(\text{CH}_3)_2$ it is clear that there is a single CF_3 environment and free rotation of the CF_3 and $\text{N}(\text{CH}_3)_2$ groups. Furthermore, the invariance of the ^{19}F nmr spectrum with temperature in contrast with that of $(\text{CF}_3)_2\text{PF}(\text{OCH}_3)\text{N}(\text{CH}_3)_2$ indicates that not only are the two CF_3 groups in $(\text{CF}_3)_2\text{PFClN}(\text{CH}_3)_2$

magnetically equivalent, there is also no observable ligand exchange occurring within the temperature range investigated (305°K to 203°K). Either the ligand exchange is fast at all temperatures, a situation which is unlikely in view of the ease with which different CF_3 environments were detected in the case of $(\text{CF}_3)_2\text{PF}(\text{OCH}_3)\text{N}(\text{CH}_3)_2$, or the CF_3 groups do not participate in a ligand positional averaging process. The magnitudes of $^1J_{\text{P-F}}$ (883 Hz) and $^2J_{\text{P-F}}$ (161 Hz) observed are within the range established²⁶⁻²⁸ for axial directly-bound fluorine atoms and equatorial CF_3 groups, respectively. Therefore, we propose that the axial positions are occupied by F and Cl and that both CF_3 groups occupy equivalent sites. The only other alternative providing equivalent CF_3 groups requires that Cl be placed in an equatorial position with two CF_3 groups requiring that the axial sites be occupied by F and $\text{N}(\text{CH}_3)_2$ groups, an unlikely situation since Cl is very much more electronegative than the $\text{N}(\text{CH}_3)_2$ group. From these considerations the most likely ground state structure for $(\text{CF}_3)_2\text{PFClN}(\text{CH}_3)_2$ is structure (A) in Fig V-30.

If the above arguments are correct, two of the phosphoranes investigated herein appear to provide exceptions to Muetterties' "electronegativity rule"⁷ namely, $\text{CH}_3(\text{CF}_3)\text{PCl}_3$ and $(\text{CF}_3)_2\text{PFClN}(\text{CH}_3)_2$. In both cases chlorine appears to exhibit a greater tendency to occupy the axial positions than the CF_3 group although the latter has a greater electronegativity than the former.

Similar observations have been reported by Cavell and co-workers²⁶⁻²⁸ in their studies on chlorophosphoranes containing the trifluoromethyl group. They have pointed out that the apicophilicity series evident from nmr spectroscopic investigation of a number of phosphoranes containing such substituents as F, Cl, CF₃, OSi(CH₃)₃, OCH₃, SCH₃, and N(CH₃)₂, is more in agreement with the order of the inductive parameters σ_I of the substituents than with their electronegativity values.²⁶⁻²⁸ The apparent effectiveness of the σ_I parameter, which is thought to give the pure inductive, i.e., electron-withdrawing character, of a specific group suggests that apicophilicity may be strongly influenced by σ bonding effects. In other words, axial site occupation may be strongly influenced by the ability of the substituent to stabilize the charged structures, e.g., X-P⁺-X⁻ in the axial bonding framework, and hence the bonding scheme proposed by Rundle⁷¹ may be appropriate. If such is the case, the contribution of π bonding to the equatorial preference of such groups as OCH₃, SCH₃, N(CH₃)₂ may be very small. It may well be that since such groups have low inductive character they will therefore not occupy the axial positions but rather will occupy the equatorial sites.

Conclusions

The interpretation of the nmr spectra of the phosphoranes studied in this work was based on the assumption of a trigonal bipyramidal ground state geometry in agreement with extensive data obtained from nmr,^{7,8,26-28} vibrational,¹⁸⁻⁷⁵ electron diffraction and X-ray crystallographic^{13,15-17} studies on closely related compounds. The interpretations appear substantiated by the agreement of the nuclear magnetic resonance parameters evaluated from the nmr spectra within the characteristic limits established for such parameters in such magnetic environments. It has been maintained²⁶⁻²⁸ that different fluorine environments can be distinguished through the magnitude of their one-bond and two-bond coupling with phosphorus which may be evaluated from their limiting low-temperature nmr spectra. Nuclear magnetic resonance parameters evaluated from room temperature spectra in the case of $\text{CH}_3(\text{CF}_3)\text{PF}_3$ and $\text{CH}_3(\text{CF}_3)\text{PF}_2(\text{SCH}_3)$ both show averaged values due to permutation of ligand environments in the first case and a P-S bond rotation process in the second case. At low temperatures, however, the distinctly different P-F environments were detectable. The nature and energetics of the averaging processes in these and related compounds will be discussed in Chapters VI and VII.

The nmr spectra of $(\text{CF}_3)_2\text{PF}(\text{OCH}_3)\text{N}(\text{CH}_3)_2$ at normal temperature showed two different CF_3 environments which

were assigned to one axial and one equatorial site based on the relative magnitude of the two-bond phosphorus-fluorine coupling constants (62 Hz and 130 Hz, respectively). The resolution of the two different CF_3 environments at such relatively high temperatures implies that the energy barrier to the ligand averaging process suggested by the nmr spectra obtained at elevated temperatures (e.g., 343°K) is high.

The nmr spectra of $(\text{CF}_3)_2\text{PF}_2\text{N}(\text{CH}_3)_2$ and $(\text{CF}_3)_2\text{PFCl-N}(\text{CH}_3)_2$ did not show positional averaging phenomena at low temperatures, and in keeping with the previous suggestion of a lower apical preference of the CF_3 group relative to Cl, which is contrary to that expected on the basis of the "electronegativity rule", the ground state structures with exclusive equatorial CF_3 substitution are proposed for these molecules.

CHAPTER SIX

THE EXCHANGE BARRIER OF $\text{CH}_3(\text{CF}_3)\text{PF}_3$ FROM DYNAMIC NMR SPECTROSCOPY

Introduction

One of the major developments in nmr spectroscopy has been the application of the technique to the study of molecular dynamics. With the general availability of the necessary pulse and computer hardware, studies of time- and/or field-dependent effects in simple spectra have become nearly routine even for non-specialists.

In the present work, bandshape analysis of dynamic nmr spectra was employed to determine the energetics of the averaging processes observed at normal temperatures and implied by the low-temperature spectra of some of the phosphoranes investigated and the results are discussed in terms of the rearrangement processes which occur in these fluxional molecules.

Stereochemical Non-rigidity in Phosphoranes

The fluxional character of pentacoordinate phosphorus compounds has long been recognized and has been extensively studied both because these compounds are believed to be intermediates in biological processes involving phosphate esters and because the ligand permutations in these compounds provide experimentally tractable examples of the fluxional behavior which is an important feature of

many pentacoordinate inorganic compounds.

Because the ligand rearrangement is observable experimentally, the mode (or modes) of the rearrangement, i.e., the different combinational possibilities for isomerization are, in principle, also observable. In practice, however, experiment can distinguish among the various rearrangement modes only if the permutation involves a one-step process or if there are unusual sets of constraints in the molecule to rule out the other possible modes of rearrangement. This arises because single-step rearrangements of some modes are equivalent to multi-step rearrangements of others.⁹³ Information regarding the mechanism of these rearrangements on the other hand, is usually only inferred on the basis of the expected energy barrier of the reaction path in the hypothesized mechanism.

A number of mechanisms have been proposed to account for the rearrangement processes in phosphoranes. Two suggested mechanisms which involve an equivalent cyclic permutation of ligands are the Berry Pseudorotation (BPR)⁷⁵ mechanism and the "turnstile rotation" (TR) mechanism.⁷⁶ The BPR, which was the first mechanism proposed, was invoked to explain the magnetic equivalence of the five fluorine ligands in the ¹⁹F nmr spectrum of PF₅⁷⁵ although ir and subsequently electron diffraction studies^{15a,b} confirmed the expected distinguishability

of the axial and equatorial P-F bonds. A one-step ligand rearrangement process is proposed operating *via* a synchronous pairwise exchange of two axial and two equatorial ligands. The pathway for this exchange may be imagined to result from a vibrational bending motion of both axial and equatorial ligands traversing a square pyramidal transition state (see Fig VI-1). Ligand 3 serves as a pivot and executes little or no motion during the exchange process.

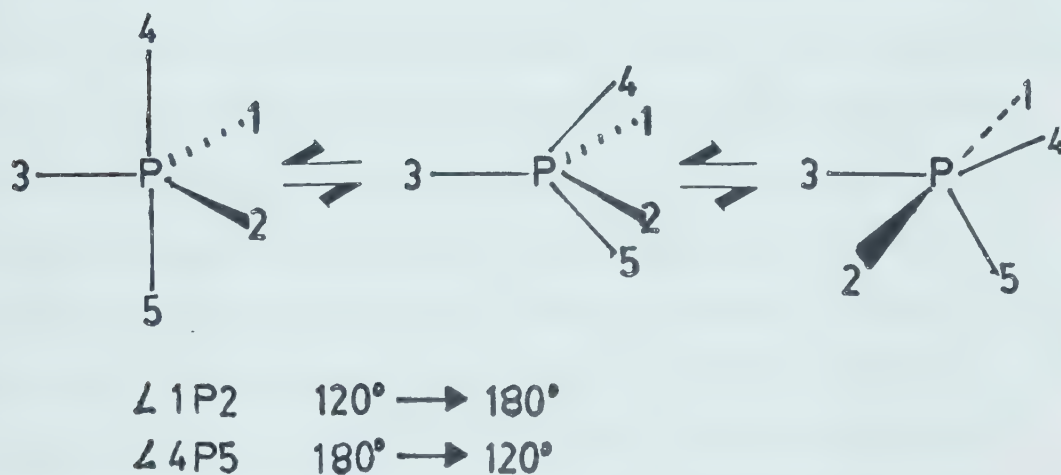


Figure VI-1

Normal coordinate vibrational analysis¹⁰ and semi-empirical MO calculations¹² have indicated that the

energy pathway for this exchange involves a greater contribution of the in-plane equatorial bending motion relative to the axial bend.

This model of exchange was initially accepted as the general mechanism for the ligand permutation processes in phosphoranes. Thus the classic work of Whitesides and Mitchell⁷⁷ on the fluorine ligand rearrangement in $\text{F}_4\text{PN}(\text{CH}_3)_2$ was initially interpreted to be consonant only with the BPR mechanism.^{11,78} This view has since been modified because the TR mechanism provides an alternative means of obtaining cyclic pairwise exchange of ligands.^{14,66} The TR mechanism, which may be visualized as a combination of the three motions (see Fig VI-2), involves an internal contrarotation of a pair consisting of one apical and one equatorial ligand *versus* the three remaining ligands acting as a trio from an initially deformed trigonal bipyramid. The components of the process may be described as follows: Two equatorial ligands, 2 and 3, undergo an initial relative bending motion reducing the normal 120° bond angle between them to approximately 90° . Ligands 1 and 4 tilt by about 9° (Fig. II-2a) while maintaining their mutually perpendicular relative positions. The third component is an internal rotation of the pair of ligands, 1 and 4, against the trio of ligands 2, 3, and 5 (Fig. II-2b). The barrier situation (Fig VI-2c) is reached after a

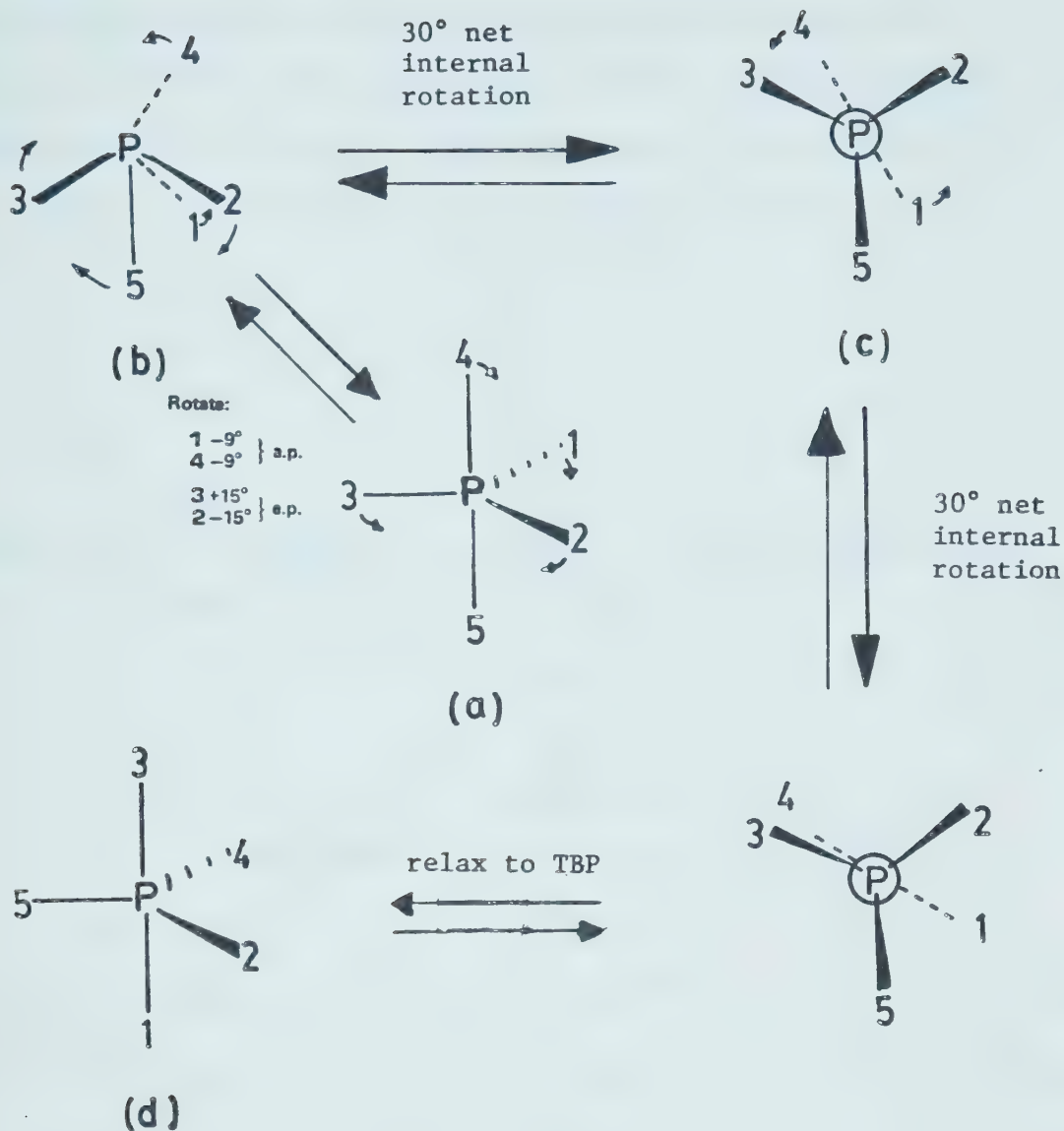


Figure VI-2

relative internal rotation of 30° . Further rotation by 30° , and relaxation of the bond angles gives the isomeric trigonal bipyramid (Fig. VI-2d).

The TR mechanism shares some common features with BPR, namely, (1) angular momentum is conserved in an idealized case, and (2) a cyclic permutation of two axial with two equatorial ligands occurs. Note that if

the BPR permutation cycle is represented by $(ae''a'e')$ with e as pivot, the same result can be achieved by any of the four TR processes represented by $(ee'a)(a'e'')$, $(ee'a')(ae'')$, $(ee''a)(a'e')$, and $(ee''a')(ae')$.

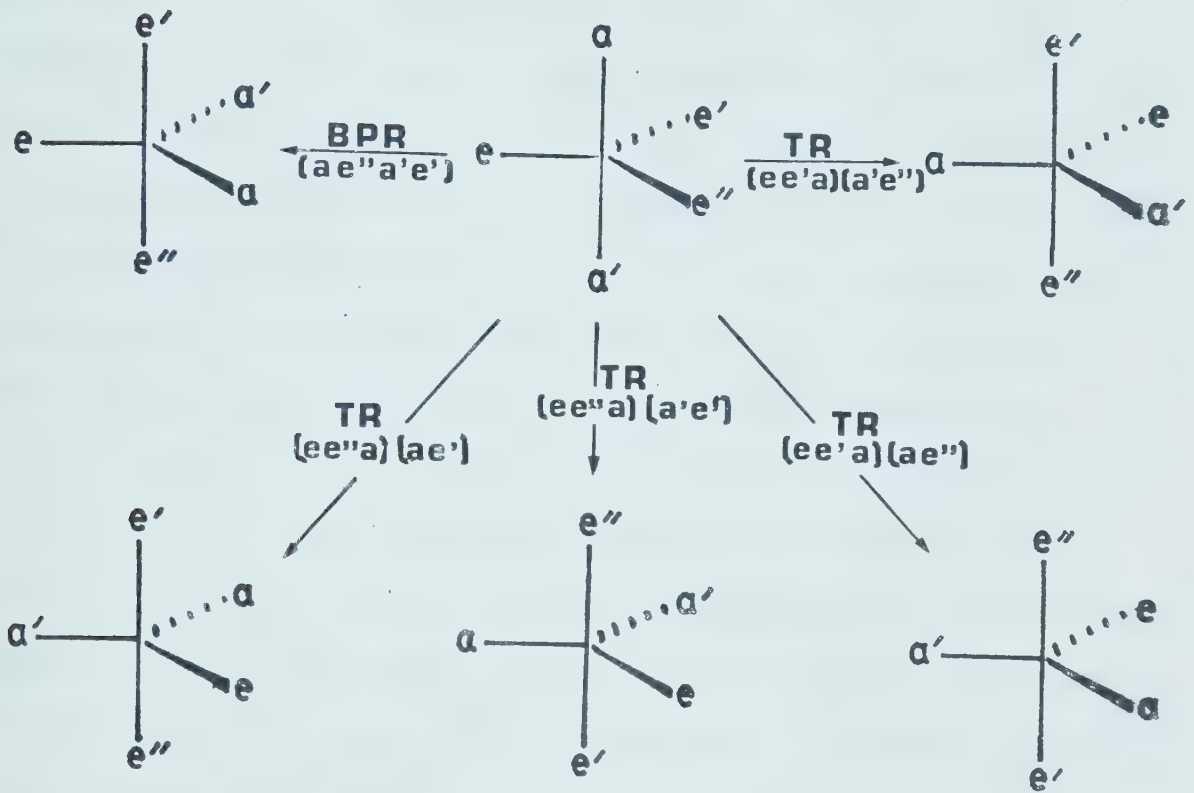


Figure VI-3

The four equivalent TR processes are united by the fact that the "trio" contains the pivot e of the corresponding BPR process, and the relative direction of

"trio" rotation is such that the ligand *e* moves to replace the other originally equatorial ligand, and this second equatorial ligand moves to the axial position.

The fundamental difference between the BPR and TR mechanisms is that the TR mechanism involves an internal rotation about an axis through the central atom whereas the BPR does not. Consequently, these two mechanistic pathways proceed through entirely different geometries, symmetry, and potential energies, and therefore the two mechanisms may provide very different barriers. Although, as indicated above, only the mode of a permutational process is observable by nmr spectroscopy, insight into the exchange mechanism can be provided by a knowledge of the energetics of the process coupled with *ab initio* calculations of the potential surfaces involved in the various proposed mechanisms. In addition, if intermediate species can be detected, a more detailed analysis of a multi-step mechanism would be possible. However, since short-lived intermediates are not readily detected by nmr spectroscopy, such expectations would be achieved only in fortunate circumstances.

High Resolution NMR Bandshape Analysis

There have been two main approaches to the theoretical description of high-resolution nmr spectra of fluids:

(1) the phenomenological description in terms of the

Bloch equations, and (2) the quantum - mechanical description in terms of a spin Hamiltonian. The Bloch equations are useful in describing complicated effects, e.g., time- or field-dependent effects, in simple spectra, i.e., spectra of molecules with a single magnetic nucleus. These equations incorporate two relaxation times, T_1 and T_2 , which govern the spectral line shape. The spin Hamiltonian on the other hand, is useful in describing complicated spectra, i.e., spectra of molecules with several magnetic nuclei. It contains two molecular parameters, the chemical shift and the coupling constant. Line positions and intensities, but not line shapes, can be obtained from the spin Hamiltonian. Line shapes in complicated spectra are most conveniently described by the density matrix treatment. The methods used herein have been extensively described in the literature.⁷⁹⁻⁸¹

The ligand-exchange-broadened spectra of $\text{CH}_3(\text{CF}_3)\text{-PF}_3$ discussed in this chapter and the methylthiophosphoranes $(\text{CH}_3)_n(\text{CF}_3)_m\text{PF}_{4-m-n}(\text{SCH}_3)$ ($n = 0, m = 0 \text{ to } 3; n = m = 1$) discussed in Chapter VII were computer-simulated using the program EXCHSYS.⁸² This requires the formulation of a kinetic exchange or a K matrix which is essentially an array of the probabilities of exchange of magnetization between the lines in the spectrum. The lines arise from allowed transitions between magnetic spin states of the observed nucleus. The multiplicity of the system is governed by the mutual interactions of the observed nucleus and the other magnetic nuclei in the molecule.

Results

The K matrix used to describe the exchange in $\text{CH}_3(\text{CF}_3)\text{PF}_3$ is given in Table 1 (Appendix) . Figure VI-4 shows the simulated and experimental ^{31}P nmr spectra in the intermediate exchange region where the most rapid change with temperature occurs. The limiting spectra for fast and slow exchange have been given earlier (Fig V-5). At all temperatures a reasonably good fit between the experimental spectrum and that calculated for an appropriate rate constant was readily achieved. The rate constant for the exchange process obtained at each particular temperature by this visual shape fitting and the temperature were used to evaluate the thermodynamic parameters in equations VI-3 and VI-5 by means of the program ACTEN.⁸³ The results are shown in Table 10.

The rates of exchange k (taken to be the pseudo first-order rate) at different temperatures (T , °K) are fitted numerically to the Arrhenius equation:

$$\ln k = \frac{-E_a}{RT} + \ln A \quad (\text{VI-1})$$

and the activation energy, E_a is calculated from the slope of the straight line. Plots of this equation for the various systems are given in Figure VII-1. The assumption that E_a and A are temperature independent appears to hold over the range of temperatures investigated in the present

TABLE 10

Activation Parameters for "Pseudorotation"^e in Some Phosphoranes^a

Compound	ΔG^\ddagger	E_a	Temperature Quoted	Solvent(s)	Reference
$\text{CH}_3(\text{CF}_3)\text{PF}_3$	9.4 ± 1.0	6.5 ± 0.2	298°K	$\text{CFCl}_3/\text{CF}_2\text{Cl}_2$	b
$(\text{CH}_3)_2\text{NPF}_4$	8.8 ± 0.2		188°K	CHCl_2F	c
ClPF_4	4.2 ± 0.3		96°K	CHCl_2F	c
$(\text{CH}_3)_2\text{PF}_3$	17.8		333°K	-	d
$(\text{CH}_3)_2\text{NPF}_3$	19.6		343°K	-	d
$(\text{C}_6\text{H}_5)_2\text{PF}_3$	18.7		379°K	-	d
H_2PF_3	10.2		218°K	-	d
$\text{CF}_3(\text{H})\text{PF}_3$	6.3		133°K	-	d
Cl_2PF_3		7.2 ± 0.5		-	d
Br_2PF_3		7.2 ± 0.5		-	d
$(\text{CF}_3)_2\text{PF}_3$		fluxional at 153°K		-	d
CH_3PF_4		fluxional at 96°K		-	d

FOOTNOTES FOR TABLE 10

a All activation parameters are in kcal/mole

b Present work

c Ref. 99

d Ref. 86 and references therein

e Ref. 102

Figure VI-4 Experimental and calculated $^{31}\text{P} \sim \{^1\text{H}\}$ (36.4 MHz) nmr spectra of $\text{CH}_3(\text{CF}_3)\text{PF}_3$ at particular temperatures and appropriate rates of exchange of magnetization. The experimental spectra were obtained from a solution in approximately 50:50 $\text{CFCl}_3:\text{CF}_2\text{Cl}_2$ containing about 5% TMS. The calculated spectra were obtained using a K matrix assuming an intramolecular axial-equatorial fluorine exchange mechanism (Table 1, Appendix). The frequency scale which gives chemical shift values in Hz relative to P_4O_6 was measured relative to the CFCl_3 heteronuclear lock and converted to appropriate values of the ^{31}P reference.

^{31}P (36.4 MHz) - $\{^1\text{H}\}$
SPECTRA OF

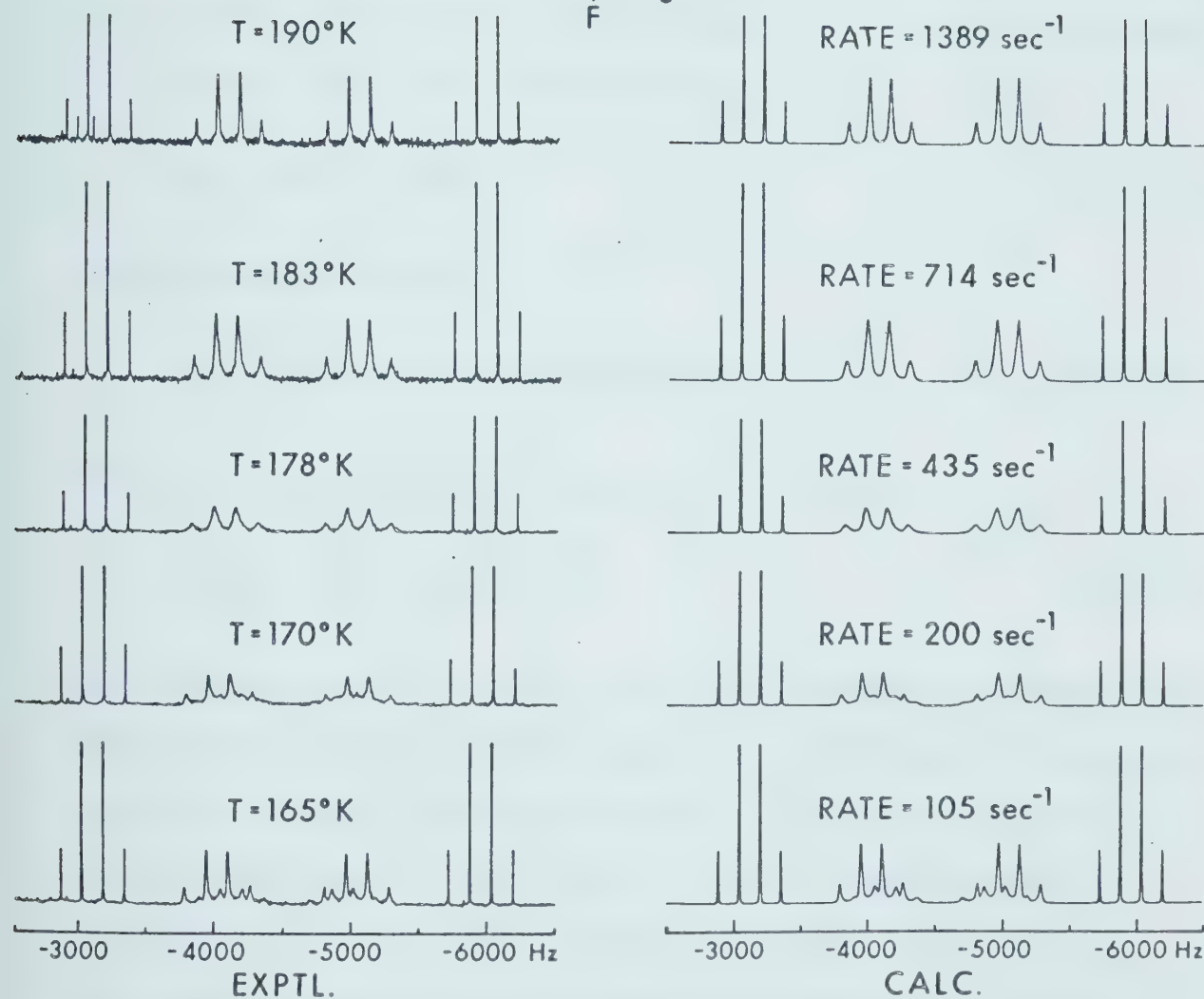


Figure VI-4

study.

In addition, the Eyring equation

$$k = \kappa \left(\frac{kT}{h} \right) \exp(-\Delta G^\ddagger / RT) \quad (\text{VI-2})$$

where k is the rate constant, κ the transmission coefficient (set equal to unity), k is the Boltzmann constant, R the gas constant, h is Planck's constant and ΔG^\ddagger the free energy of activation, rearranged by substitution of the equality given in equation VI-3 into equation VI-2.

$$\Delta G^\ddagger = \Delta H^\ddagger - T\Delta S^\ddagger \quad (\text{VI-3})$$

gives equation VI-4;

$$k = \left(\frac{kT}{h} \right) \exp(-\Delta H^\ddagger / RT) \exp(\Delta S^\ddagger / R) \quad (\text{VI-4})$$

which was then rearranged to equation VI-5;

$$\ln\left(\frac{k}{T}\right) = \ln\frac{k}{h} - \frac{\Delta H^\ddagger}{RT} + \frac{\Delta S^\ddagger}{R} \quad (\text{VI-5})$$

The linear plot of $\ln(k/T)$ versus $1/T$, obtained by numerical data fitting, gives a slope equal to $-\Delta H^\ddagger/R$ and an intercept equal to $\ln(k/h) + \Delta S^\ddagger/R$ from which ΔH^\ddagger and ΔS^\ddagger values can be calculated. As before, κ is set to unity and it is assumed that ΔH^\ddagger and ΔS^\ddagger are independent of temperature. The barrier obtained is expressed in terms of ΔG^\ddagger since this parameter is the least sensitive to the errors inherent in these analyses,⁸⁴ whereas ΔH^\ddagger and ΔS^\ddagger are more

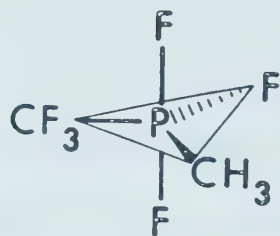
influenced by error albeit in a compensating fashion. The results for $\text{CH}_3(\text{CF}_3)\text{PF}_3$ and the other compounds studied are given in Table 13 (Chapter VII). For purposes of comparison all ΔG^\ddagger values are given at 298°K.

Discussion

A number of factors must be considered in the interpretation of exchange-broadened nmr spectra. First, the temperature dependence of the chemical shifts, and to a lesser extent, of the coupling constants. The latter, if pronounced, generally indicates the occurrence of some exchange process between two or more molecular states. Second, the possible occurrence of more than one broadening mechanism. Third, changes in solvent properties and instrumental magnetic field inhomogeneities with temperature, and finally, inaccuracies in temperature measurements.

The first factor did not significantly affect the present work because the averaging phenomena simulated were coupling constant-, not chemical shift - averaging effects, and the high- and low-temperature limiting spectra were obtained in all cases, all of which showed appropriate numerical relationships between high temperature averaged coupling constants and low temperature limiting values. In one instance magnetic field inhomogeneity broadening was suspected and confirmed. It was successfully overcome in a repeat determination of the spectrum. The temperature accuracy of $\pm 1^{\circ}\text{C}$, established by calibration, was the best that could be obtained with the existing controllers although the temperature

Figure VI-5 Calculated $^{31}\text{P} \sim \{^1\text{H}\}$ (36.4 MHz) nmr spectra of $\text{CH}_3(\text{CF}_3)\text{PF}_3$ at the fast-exchange limit, an intermediate rate and at the slow-exchange limit using a K matrix constructed for an intermolecular exchange mechanism.



(P-F BOND BREAKING)

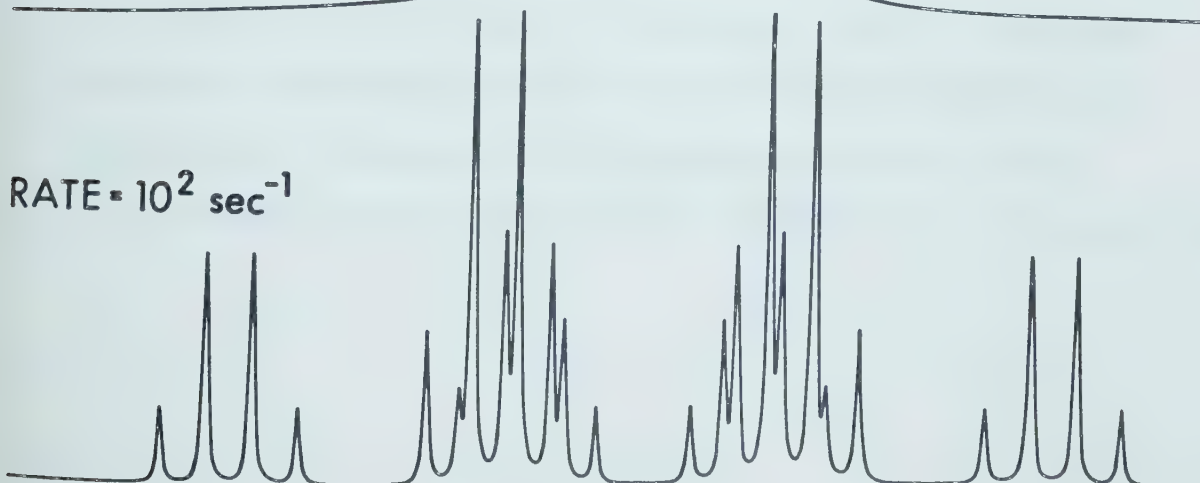
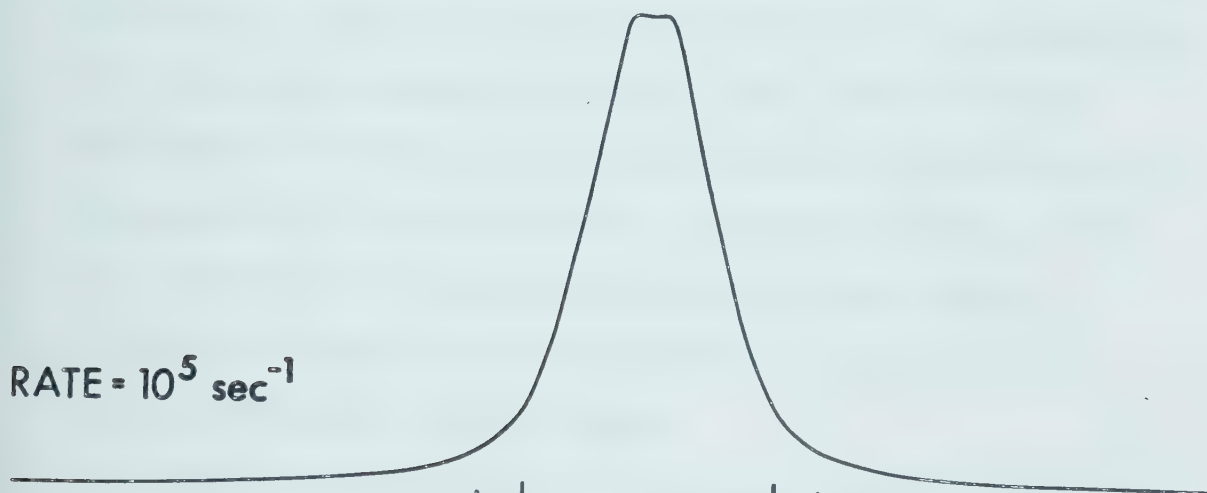
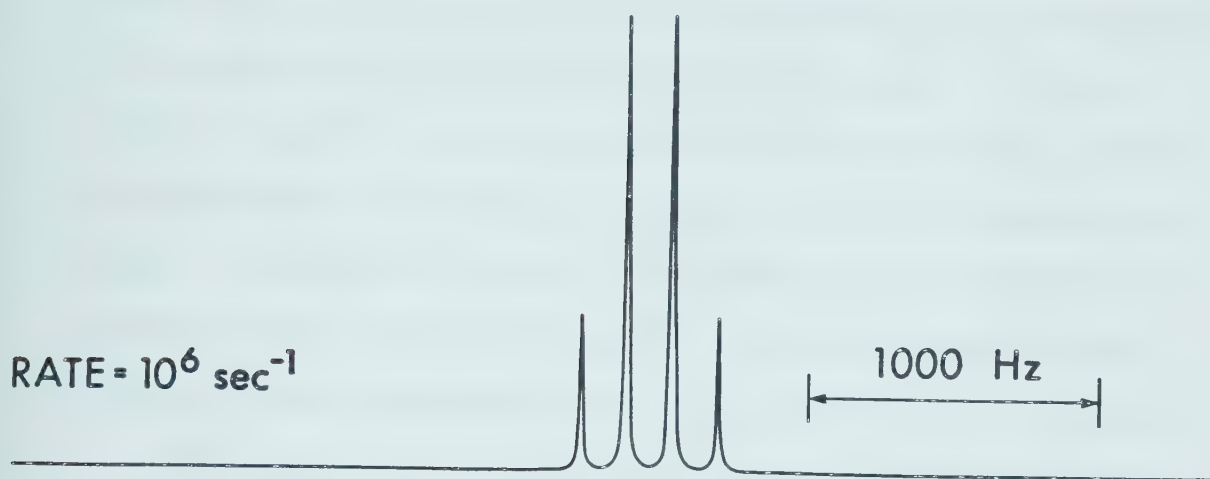


Figure VI-5

could be maintained to better than $\pm 0.5^\circ\text{C}$ at any particular value and no measurable temperature gradients existed over the length of the sample tube.⁸⁵

The possibility of an intermolecular exchange mechanism for $\text{CH}_3(\text{CF}_3)\text{PF}_3$ was ruled out by the invariance of the spectral patterns with concentration. Further confirmation of the intramolecular nature of the process was obtained in the case of $\text{CH}_3(\text{CF}_3)\text{PF}_3$, by demonstrating that a different K matrix incorporating an intermolecular process gave calculated spectra which did not fit the observed low-temperature limiting spectrum (see Fig VI-5).

Finally we considered some possible intramolecular pathways to see if a reasonable choice of a pathway for the averaging process in $\text{CH}_3(\text{CF}_3)\text{PF}_3$ could be made. Two possible routes, both intramolecular processes, are presented in Figures VI-6 and -7 for $\text{CH}_3(\text{CF}_3)\text{PF}_3$, with [] indicating the substituent acting as a pivot. Figure VI-6 includes an approximate energy profile expected for the BPR processes.

There are at least two possible ways of effecting magnetic equivalence of the three fluorine ligands in $\text{CH}_3(\text{CF}_3)\text{PF}_3$ through the BPR mechanism. One is by a single-step process depicted as (1) \rightleftharpoons (2) in Figure VI-6.

Figure VI-6 Berry Pseudorotation permutation pathway for the equilibration of the three directly-bound fluorine ligands in $\text{CH}_3(\text{CF}_3)\text{PF}_3$. The accompanying energy diagram was constructed assuming that the relative increment of activation energy required to place CH_3 in an axial position is considerably greater than that for CF_3 referred to fluorine in the axial position.

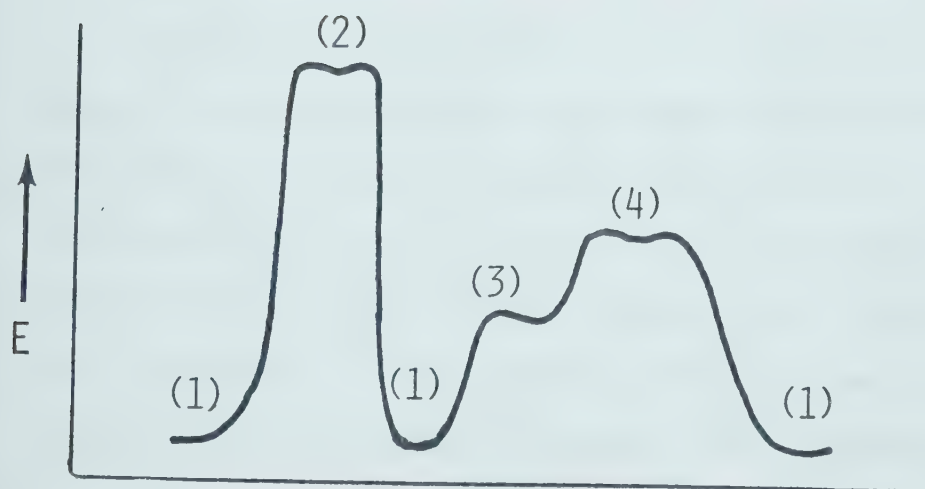
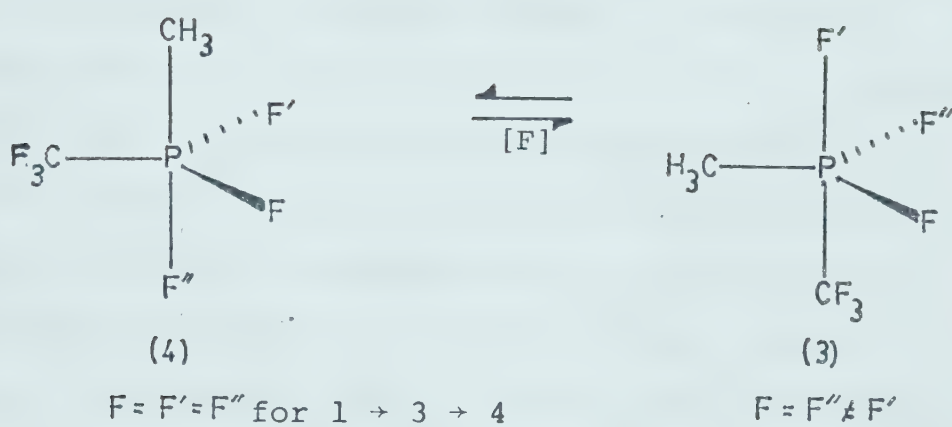
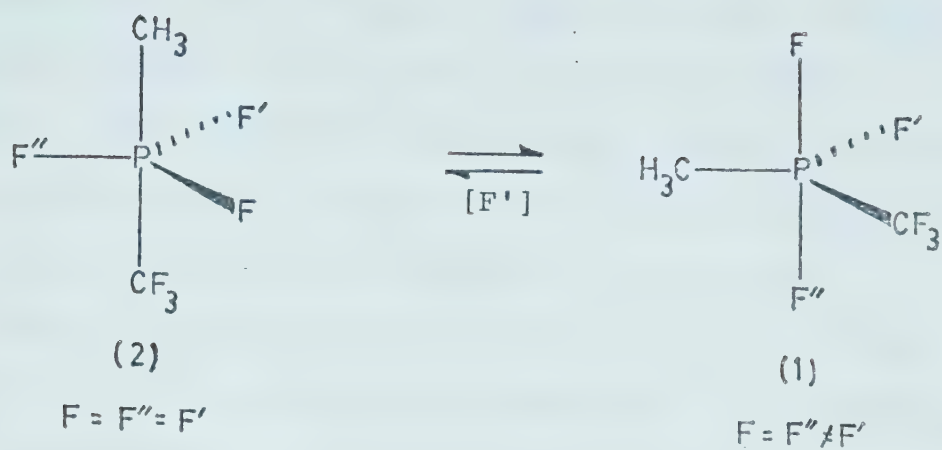


Figure VI-6

The intermediate (or transition state) species structure (2) however places both CH_3 and CF_3 groups in axial positions. Semi-empirical calculations indicate this to be a very high energy species and so this particular route may not be readily accessible to the system.⁷⁶ A second route is the multi-step process $(1) \rightleftharpoons (3) \rightleftharpoons (4)$ (Fig. VI-6). It traverses two intermediate (or transition state) structures (3) and (4), each of which is expected to be of lower energy than structure (2). Hence the multi-step BPR exchange may provide a more favorable route than the single-step rearrangement process. The "turnstile rotation" mechanism however, provides a possible alternative route to the BPR and has an apparent advantage over the latter in that the TR species (*cf.* Fig VI-7, structures (2), (3) and (4)) need not relax to trigonal bipyramidal intermediates and therefore can achieve magnetic equivalence of the directly-bound fluorine atoms without going through high-energy configurations.

It should be mentioned that *ab initio* MO calculations using a large basis set on the model compound PH_5 gave much smaller barriers for the BPR (2 kcal/mole) process as compared to the TR process (10.1 kcal/mole).⁶⁵ These results however, may not be indicative of the situation which prevails in more complex molecules such as $\text{CH}_3\text{-(CF}_3\text{)PF}_3$ since the model molecule was a symmetrically

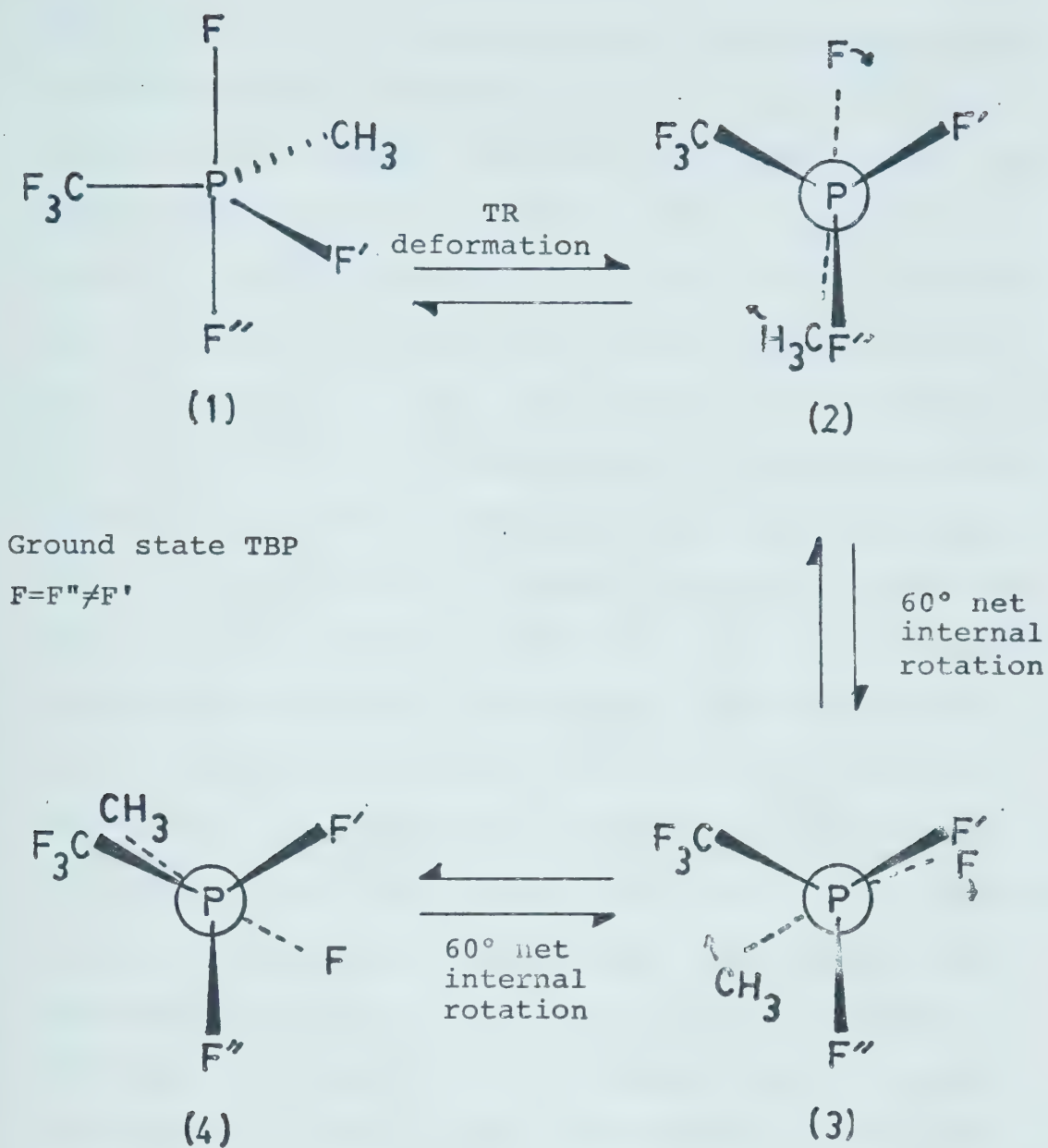


Figure VI-7

Turnstile Rotation of $\text{CF}_3(\text{CH}_3)\text{PF}_3$

substituted simple phosphorane, and hence neither ligand electronegativity difference nor steric effect was involved in the ligand rearrangement. Furthermore, the authors themselves imply that the very low activation energy for the BPR process arises from the high symmetry (C_{4v}) of the transition state/transient intermediate for PH_5 , in contrast to the C_s transition state involved in the TR process. Methyl(trifluoromethyl)trifluorophosphorane, $CH_3(CF_3)PF_3$, however, possesses only a plane of symmetry even in the ground state trigonal bipyramid. Therefore, symmetry considerations should not be of much consequence in the energy barrier to the ligand averaging process in this compound since the transition state/transient intermediate in the BPR is at best of C_s symmetry, and certainly not much more symmetrical than the C_1 transition state involved in the TR mechanism. Furthermore, the difference in ligand electronegativities introduces an additional contribution to the barrier because certain placements of ligands become prohibitively "expensive" in energy.

Table 16 gives relevant information on the activation energies for the ligand averaging processes in $CH_3(CF_3)PF_3$ and related X_2PF_3 ($X = H, CH_3, C_6H_5, N(CH_3)_2, Cl, Br, CF_3$) as well as on the XPF_4 ($X = CH_3, N(CH_3)_2, Cl, CF_3$) system. The ΔG_{298}^\ddagger value for the equilibration of the three directly-bound fluorine atoms in $CH_3(CF_3)PF_3$ is 9.4 ± 0.5 kcal/mole. It is interesting to note that

analogous resolution of the expected axial and equatorial fluorine environments in CF_3PF_4 has not been achieved even at 123°K . The higher barrier in $\text{CH}_3(\text{CF}_3)\text{PF}_3$ could be the result of the electronic effect of the CH_3 group since a consistent increase in the barrier appears to accompany the introduction of CH_3 into a phosphorane. For instance, the ΔG^\ddagger value for $(\text{CH}_3)_2\text{PF}_3$ ⁸⁶ is 17.8 kcal/mole while $(\text{CF}_3)_2\text{PF}_3$ remains fluxional even down to 148°K ^{7,63} in spite of numerous attempts at resolution. The difference in the barriers of $(\text{CF}_3)_2\text{PF}_3$, $\text{CH}_3(\text{CF}_3)\text{PF}_3$ and $(\text{CH}_3)_2\text{PF}_3$ is understandable if one assumes a BPR permutation. With two methyl groups in $(\text{CH}_3)_2\text{PF}_3$ the necessary exchange steps involve an axial position for at least one CH_3 (*cf.* Fig VI-6) with a concomitantly high barrier, whereas placement of CF_3 in an axial position in place of F would have a lower barrier because of the high electronegativity of the CF_3 group. Hence the barrier to ligand permutation is lowest in $(\text{CF}_3)_2\text{PF}_3$, intermediate in $\text{CH}_3(\text{CF}_3)\text{PF}_3$, and highest in $(\text{CH}_3)_2\text{PF}_3$.

However, anomalous cases do exist. The distinct axial-equatorial fluorine atom environments have been resolved in such trifluorophosphoranes as H_2PF_3 ,⁸⁷ $(\text{CH}_3)_2\text{PF}_3$,⁸⁶ $(\text{C}_6\text{H}_5)_2\text{PF}_3$,⁸⁸ $\text{CF}_3(\text{H})\text{PF}_3$,⁸⁷ Br_2PF_3 ,⁸⁹ and Cl_2PF_3 ,⁸⁹ yet as mentioned earlier, $(\text{CF}_3)_2\text{PF}_3$ remains fluxional down to 148°K .^{7,63} The behavior of $(\text{CF}_3)_2\text{PF}_3$ is not easy to understand since the CF_3 group appears to

be less apicophilic than $\text{Cl}^{26-28,63}$ and Br^{63} and therefore $(\text{CF}_3)_2\text{PF}_3$ should have a higher barrier to ligand positional exchange than either Cl_2PF_3 or Br_2PF_3 . Even more unexpected is the behavior of CH_3PF_4 , which shows a single (averaged) fluorine environment down to 96°K^{89} whereas resolution of the axial-equatorial fluorine atom environments has been achieved not only in $(\text{CH}_3)_2\text{NPF}_4^{89}$ but also in ClPF_4^{89} implying a higher barrier for the ligand permutational process in ClPF_4 relative to that for CH_3PF_4 . While it is clear that a BPR permutation mode is open to the XPF_4 (but not X_2PF_3) system which does not necessitate axial position for the X substituent (i.e., X acts as a pivot), and therefore a simple and direct relationship between electronegativity and permutational barriers may not be expected, it is obvious from the higher exchange barrier of $(\text{CH}_3)_2\text{NPF}_4$ ($\Delta G_{188}^\ddagger = 8.8 \text{ kcal/mole}^{89}$) relative to that of ClPF_4 ($\Delta G_{96}^\ddagger = 4.2 \text{ kcal/mole}^{89}$) that the electronic effect arising from the substituent is of considerable consequence to the ligand exchange barriers.

We cannot, of course, rule out the possibility that the lack of observable non-equivalence in $(\text{CF}_3)_2\text{PF}_3$ and CF_3PF_4 is due to fast intermolecular exchange or catalyzed dissociation processes but such possibilities do not appear likely, especially for $(\text{CF}_3)_2\text{PF}_3$.

Conclusions

Computer-simulation of the variable-temperature ^{31}P nmr spectra in the intermediate exchange region of $\text{CH}_3(\text{CF}_3)\text{PF}_3$ suggested that the exchange process is intramolecular and not intermolecular in nature.

Both BPR and TR mechanisms can account for the ligand averaging process in $\text{CH}_3(\text{CF}_3)\text{PF}_3$. The BPR requires adoption of axial positions for both the CH_3 and the CF_3 groups at different points in the multi-step exchange route. These are expected to require high energy on account of the lower electronegativities of the two groups relative to fluorine. A TR process need not traverse such high energy species and provides an acceptable alternative. No reliable figures are available on the energy required to place a CH_3 or CF_3 group in an axial position, in a trigonal bipyramid nor to achieve the TR intermediate, and hence no choice between these two mechanisms can be made. The involvement of "high energy" conformations is however compatible with the apparent trend of the barriers in the series $(\text{CF}_3)_2\text{PF}_3$, $\text{CH}_3(\text{CF}_3)\text{PF}_3$, and $(\text{CH}_3)_2\text{PF}_3$.

CHAPTER SEVEN

EXCHANGE PROCESSES IN SOME METHYLTHIOPHOSPHORANES REVEALED BY VARIABLE-TEMPERATURE DYNAMIC NMR SPECTROSCOPY

Introduction

The observation of magnetic non-equivalence of the two axial fluorines in $\text{CH}_3(\text{CF}_3)\text{PF}_2(\text{SCH}_3)$ (*cf.* Chapter V) and reports on similar observations in the ^{19}F and ^{31}P nmr spectra of alkyl- and arylthiophosphoranes of the type RSPF_4 and $\text{RS}(\text{R}')\text{PF}_3$ ($\text{R} = \text{CH}_3, \text{C}_2\text{H}_5, \text{or } \text{C}_6\text{H}_5$; $\text{R}' = \text{CH}_3 \text{ or } \text{C}_6\text{H}_5$)³⁹ prompted a dynamic nmr study of the series of compounds of the type $(\text{CF}_3)_n\text{PF}_{4-n}(\text{SCH}_3)$ with $n = 0$ to 3 to determine the energy barriers associated with the environmental averaging processes responsible for the high-temperature magnetic equivalence observed in the ^{19}F and ^{31}P nmr spectra with the hope of gaining further insight into the nature of these processes. The compounds investigated herein are F_4PSCH_3 , $\text{CF}_3\text{PF}_3(\text{SCH}_3)$, $(\text{CF}_3)_2\text{PF}_2\text{SCH}_3$ and $(\text{CF}_3)_3\text{PF}(\text{SCH}_3)$.

Experimental

Variable-temperature ^{31}P nmr spectra of $(\text{CF}_3)_2\text{PF}_2\text{SCH}_3$ and $(\text{CF}_3)_3\text{PF}(\text{SCH}_3)$ suitable for line-shape analysis were furnished by Dr. Kwat I. The of this laboratory.

F_4PSCH_3 was prepared by co-condensing³⁹ a 1:1 mole ratio of $(\text{CH}_3)_3\text{SiSCH}_3$ and PF_5 in a 10 ml reaction tube.

This was sealed under vacuum, maintained in an ice-water bath for 30 minutes and then vacuum fractionated through traps at -63°C , -78°C , -96°C and -196°C . The bulk of F_4PSCH_3 was trapped at -78°C . A second fractionation of the material trapped at -78°C removed traces of $(\text{CH}_3)_3\text{SiF}$, the other product of the reaction.

$\text{CF}_3\text{PF}_3(\text{SCH}_3)$ was synthesized in a similar manner using a 1:1 mole ratio of CF_3PF_4 and $(\text{CH}_3)_3\text{SiSCH}_3$. The reaction system was maintained at -23°C for 1 hour. Vacuum fractionation yielded $\text{CF}_3\text{PF}_3(\text{SCH}_3)$ at -78°C , $(\text{CH}_3)_3\text{SiF}$ at -96°C and unreacted CF_3PF_4 at -196°C .

$\text{CF}_3\text{PF}_3(\text{SCH}_3)$ was characterized by its hydrolysis reactions in both neutral and basic medium.

(i) Neutral hydrolysis

Treatment of $\text{CF}_3\text{PF}_3(\text{SCH}_3)$ (0.169 g, 0.828 mmole) with neutral water for three days at room temperature did not yield CF_3H . Nmr spectra of the hydrolysate indicated the presence of at least three phosphorus-fluorine containing compounds: a simple doublet ($\phi_{\text{F}} = 74.8$ ppm, $J = 112$ Hz) and two doublets of asymmetric multiplets. A peak at 150.4 ppm which showed a 1:1:1:1 quartet fine structure ($J = 15$ Hz) was assigned to BF_4^- ^{35}S ion. The nmr spectra of the -196°C fraction showed it to consist of CH_3SH and a phosphorus-fluorine containing compound ($\phi_{\text{F}} = 50.7$ ppm, $J = 84$ Hz).

(ii) Alkaline hydrolysis

Treatment of $\text{CF}_3\text{PF}_3(\text{SCH}_3)$ (0.107 g, 0.524 mmole) with about 0.5 ml of degassed saturated NaOH solution for three days did not liberate any CF_3H . ^1H and ^{19}F nmr spectra of the hydrolysate indicated the presence of $(\text{CH}_3)_2\text{S}_2$ ($\tau = 7.84$), $^{96}\text{CF}_3\text{PO}_3^-$ ions, and again two unidentified phosphorus-fluorine containing compounds (two sets of doublets of highly asymmetric multiplets). The nmr spectra of the -196°C fraction showed peaks which were assigned to CH_3SH ($\tau_{\text{CH}_3} = 8.19$ (doublet), $\tau_{\text{SH}} = 9.2$ (quartet), $J = 7.0$ Hz), and $(\text{CH}_3)_2\text{S}_2$ ($\tau = 7.80$).

The formation of unidentifiable phosphorus-fluorine containing compounds in both neutral and alkaline media might have arisen from a decomposition rather than hydrolytic reaction of $\text{CF}_3\text{PF}_3(\text{SCH}_3)$. Because of this ambiguity and also because the products could not be identified on the basis of their nmr parameters no further elaboration of the pathway of these reactions was undertaken.

Results and Discussion of Dynamic Nmr Spectra

Since F_4PSCH_3 has been reported to be unstable to decomposition³⁹ and $CF_3PF_3(SCH_3)$ was expected to behave similarly, all the nmr spectra were obtained at or below 273°K.

A. Tetrafluoro(methylthio)phosphorane.

The ^{19}F nmr spectrum of F_4PSCH_3 (Figs VII-1A & 1B) at 243°K showed two very broad peaks, each nearly 700 Hz wide. The peaks sharpened as the temperature was lowered. At 213°K two distinct fluorine resonances were apparent, one, a doublet of triplets of doublets, the other, at higher field, was a doublet of triplets with the center peaks showing signs of further doublet splitting. Lowering the temperature an additional 30° yielded what appeared to be the limiting spectrum with three sets of fluorine resonances, in agreement with the published ^{19}F nmr spectrum³⁹ of this compound. The first fluorine resonance, centered at 7.5 ppm, consisted of a doublet of triplets, the doublet separation being 918.0 Hz. Each triplet component ($J = 90.5$ Hz) was further split into a doublet with a separation of 19.0 Hz. The second set, with a chemical shift of 14.1 ppm also consisted of a doublet of triplets of doublets, with the outer set of doublets in each triplet component showing quartet fine structure and the center set, a quintet fine structure. Further

TABLE 11

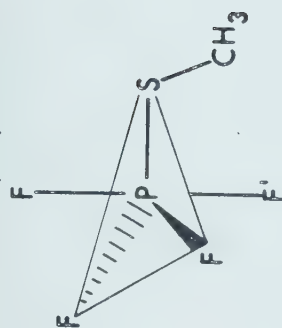
Nmr Data for Methylthiofluorophosphoranes

Compound	Temp.	τ^a	ϕ_F^b	$\phi_{CF_3}^b$	σ_{31}^c	$1d_{J_{P-F}eq}$	$1d_{J_{P-F}ax}$	$2d_{J_{P-F}}$	$3d_{J_{P-H}}$	$3d_{J_{F-H}}$	$4d_{J_{F-H}}$	$2d_{J_{F-F}}$	$3d_{J_{F-F}}$
F_4PSCH_3		8.07	45.5 ^e	-	146.2 ^e	1032 ^f	-	-	21.8	-	-	-	-
	-90°		14.1 ^g 7.5 ^h 58.2 ⁱ			1044 1055 ^j 917 ^k						90.5 ^l 105.0 ^m 19.0 ⁿ	
$CF_3PF_2(SCH_3)$	0°	7.65		69.2	140.0			168.0	23.2	1.8		86 ^l	12.0 ^f
	-90°		16.1 ^g 24.8 ^h 76.2 ⁱ			1082 927 ^j 1057 ^k						72 ^m 41 ⁿ	16.0 ^o 4.0 ^p 16.0 ^r
$(CF_3)_2PF_2(SCH_3)$	-70°						929 ^j	130.5					
	-100°					870	984 ^k						
$(CF_3)_3PF(SCH_3)$	-6°						975	102.5 ^f					
	-70°							33.8 ^q 134 ^q					13 ^q

FOOTNOTES For TABLE 11

- a τ ppm relative to internal tetramethylsilane, $\tau = 10.0$
- b ϕ ppm relative to internal CCl_3F with positive values indicating resonance to high field of the standard
- c ppm vs. P_4O_6 as external (capillary) reference, positive values indicating resonance to high field of the standard
- d in units of Hertz
- e ref. 38
- f average value
- g unique axial environment of one F (type A), designated F_{ax}
- h unique axial environment of one F (type B), designated F'_{ax}
- i equatorial fluorine atom environments
- j phosphorus coupling with type A axial fluorine
- k phosphorus coupling with type B axial fluorine
- l $F'_{\text{ax}} - F_{\text{eq}}$ coupling constant
- m $F_{\text{ax}} - F_{\text{eq}}$ coupling constant
- n trans $F_{\text{ax}} - F'_{\text{ax}}$ coupling constant
- o coupling between the CF_3 group and the type A axial fluorines
- p coupling between the CF_3 group and the equatorial fluorine
- q ref. 27
- r coupling between the CF_3 group and the type B axial fluorine

Figure VII-1A Observed and calculated ^{19}F (94.1 MHz) nmr spectra of F_4PSCH_3 in the intermediate exchange range and at the slow-exchange limit. Three fluorine environments are indicated in the low-temperature limiting spectrum namely, two non-equivalent axial fluorines: one giving rise to the groups of peaks at -200 and -1200 Hz ($^1\text{J}_{\text{P-Fa}} \sim 960$ Hz), and another giving rise to the group of peaks at -700 and -1750 Hz ($^1\text{J}_{\text{PFa}}$, ~ 1050), and two equivalent equatorial fluorines giving rise to the high field group of peaks at -5000 and -6000 Hz ($^1\text{J}_{\text{P-Feq}} \sim 1050$ Hz). The experimental spectra were obtained from a solution in approximately 50:50 $\text{CFCl}_3:\text{CF}_2\text{Cl}_2$ containing about 5% TMS and the frequency scale was measured relative to internal CFCl_3 .

^{19}F (94.1 MHz) Spectra of

Temp. = 213° K



Temp. = 183° K



CALC.

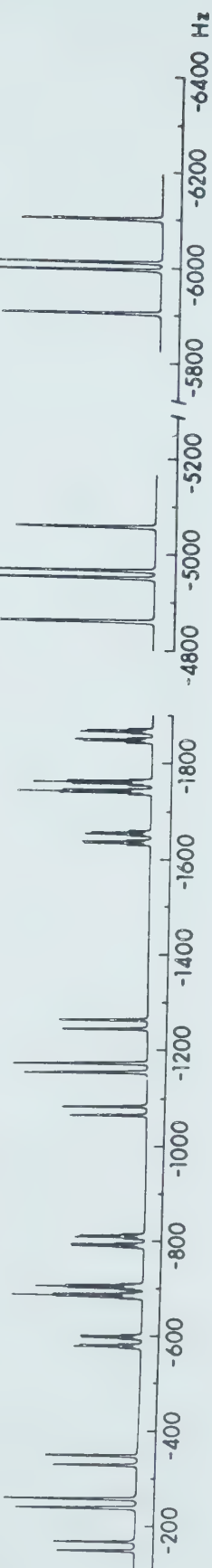


Figure VII-1A

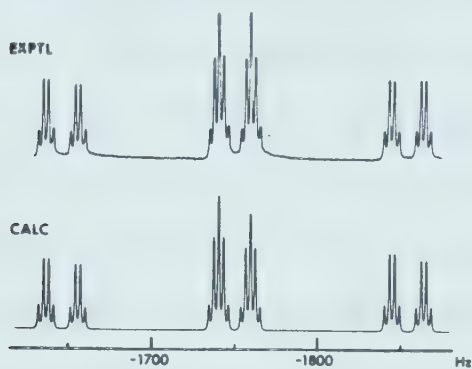
Figure VII-1B Observed and calculated ^{19}F (94.1 MHz)
half-spectra of F_4PSCH_3 at the low-temperature
limit. The frequency scale gives chemical
shift values relative to internal CFCl_3 .

^{19}F (94.1 MHz) nmr Half-Spectra of

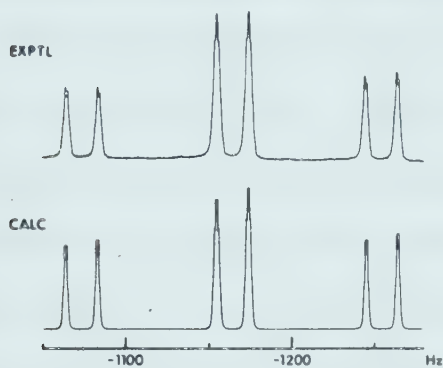


$T = 183^\circ\text{K}$

Half-Spectrum (High Field Portion) of Axial F (type A)



Half-Spectrum (High Field Portion) of Axial F (type B)



Half-Spectrum (Low Field Portion) of Equatorial F

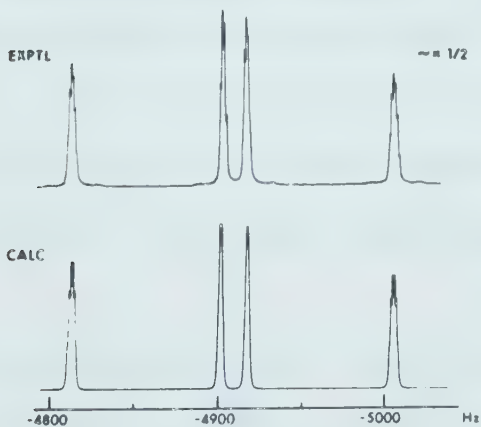


Figure VII-1B

upfield was a pair of four peaks with the central two peaks nearly twice as intense as the outer set. The three fluorine resonances had an approximate intensity ratio of 1:1:2 with the set at highest field being the most intense.

Based on the magnitude of the chemical shift and the P-F coupling, the two downfield sets of doublets were assigned to the two non-equivalent axial fluorines, and the highest field set to the two equivalent equatorial fluorines. The principal triplet splitting of the two sets of axial P-F doublets resulted from coupling with the two equatorial fluorines. Mutual coupling of the two axial fluorines caused the doublet splitting of each triplet component (Fig VII-1B). The fine structure of this twelve-line axial fluorine subspectrum was due to axial fluorines coupling with the methyl protons. The additional splitting of the central secondary doublets arose from a second-order effect rather than nonequivalent equatorial fluorine environments since the spectrum was reproduced in detail (Fig VII-1A) by NUMARIT⁹⁰ using only chemical shift and coupling constant parameters which were consistent with equivalent equatorial fluorine atoms.

The non-equivalence of the axial fluorines in the low-temperature limiting ^{19}F nmr spectrum of F_4PSCH_3 has been rationalized by Schmutzler *et. al.*³⁹ as arising

from a slowing down of the P-S bond rotation, causing the CH_3 group to be closer to one axial fluorine than to the other (Fig VII-2)

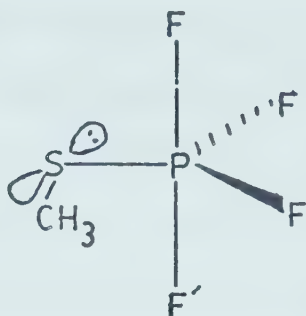


Figure VII-2

It was further suggested that the sulfur-carbon bond lay in a common plane with the axial F-P-F bonds. This interpretation was supported by several molecular orbital calculations^{66,67,70} which indicated that the most stable orientation of donor ligands in the equatorial positions of a trigonal bipyramid was the configuration in which the donor π orbitals lay in the equatorial plane. With the SCH_3 group, this would result in a coplanarity of the sulfur-carbon bond with the F-P-F axial framework.

Although free rotation of the SCH_3 group about the P-S bond rationalizes the magnetic equivalence of the two axial fluorines observed at temperatures of the order of 213°K (Fig VII-1A), it cannot account for the magnetic equivalence of the four fluorine atoms in F_4PSCH_3 observed at higher temperatures. If rotation

of the SCH_3 group about the P-S bond were the only averaging process occurring in F_4PSCH_3 , two distinct sets of fluorine resonances corresponding to axial and equatorial fluorine ligands should be consistently observed at higher temperatures. Obviously, some kind of ligand positional exchange also occurs but a ligand permutation process alone cannot effect magnetic equivalence of the four fluorine atoms either. This is shown in the following diagram (Fig VII-3) for the model compound X_4PSR and assuming a BPR mechanism of exchange purely for convenience.

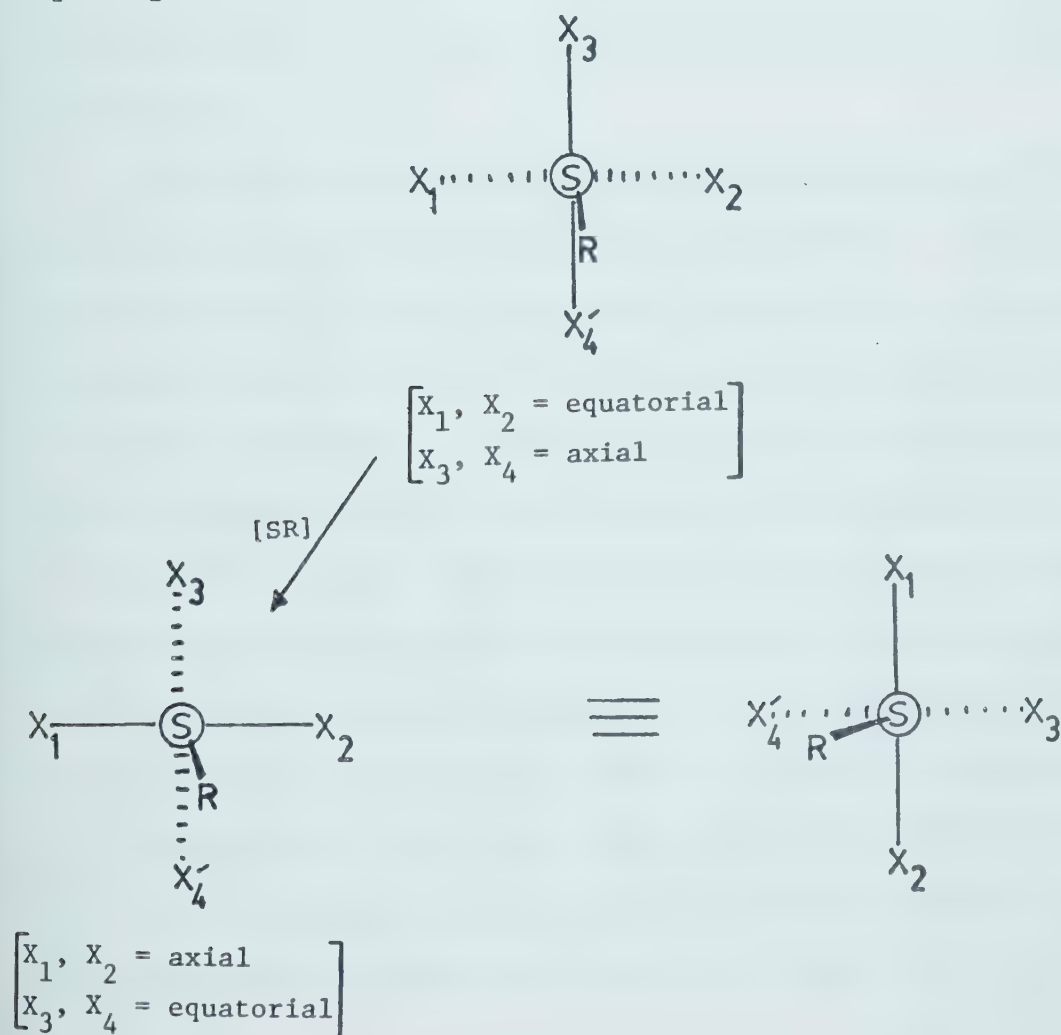


Figure VII-3

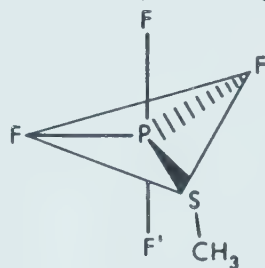
It is seen that the ligand X_4 would always be unique if a fixed orientation of the SR group is assumed. To equilibrate all of the four fluorine environments it is necessary to allow the SR group to simultaneously rotate freely about the P-S bond. Actually a full rotation of the SR group is not required; a quarter rotation suffices.

The proton-decoupled ^{31}P low-temperature limiting nmr spectrum of F_4PSCH_3 (Fig VII-4) supports the assignments based on the ^{19}F nmr spectrum. It consists of twelve lines, a triplet of doublets of doublets. The stick diagram in Figure VII-4 shows the origin of the splittings.

Computer-simulation of the proton-decoupled ^{31}P nmr spectrum was not straightforward (Fig VII-5). The P-S bond rotation process in F_4PSCH_3 appears to be closely coupled with the ligand rearrangement because only one K matrix (Appendix , Table 2) could be used to represent two processes which, being coupled, must necessarily have close ΔG^\ddagger values. Arbitrary rate factors were introduced into the K matrix elements apportioning the permutation and rotation component processes to the probability of magnetization transfer in order to achieve the best fit. Table 3 (Appendix) shows the different K matrices investigated and the corresponding calculated spectra obtained in the intermediate exchange region are shown in Figure VII-6.

Figure VII-4 $^{31}\text{P} \sim \{^1\text{H}\}$ (36.4 MHz) limiting spectrum of F_4PSCH_3 . The frequency scale gives chemical shift values relative to P_4O_6 actually measured relative to the ^{19}F heteronuclear lock and converted to the ^{31}P reference scale. The stick diagram illustrates the formation of the pattern of a triplet of doublets of doublets due to two equivalent equatorial fluorines and two non-equivalent axial fluorines at the low temperature limit.

$^{31}\text{P} \sim \{^1\text{H}\}$ (36.4 MHz) Limiting nmr Spectrum of



$T = 188^\circ\text{K}$

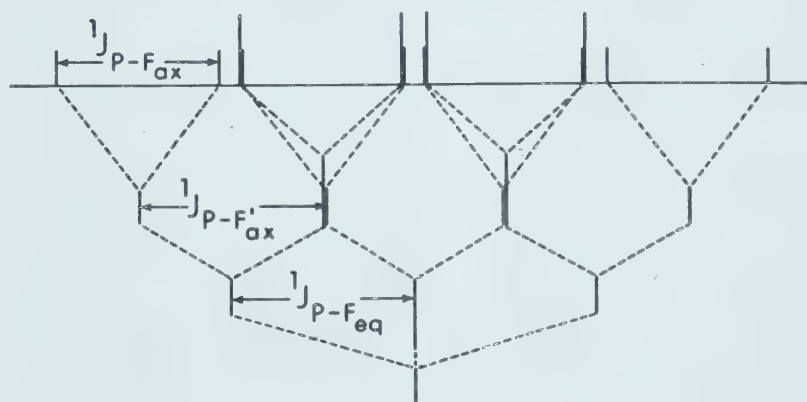
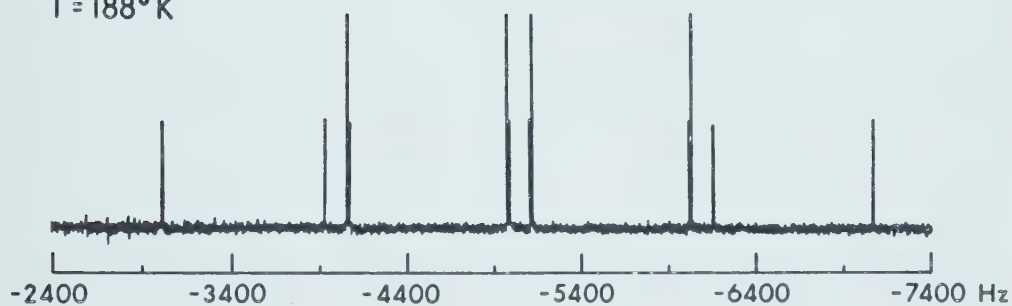


Figure VII-4

Figure VII-5 Experimental and calculated $^{31}\text{P} \sim \{^1\text{H}\}$ (36.4 MHz) nmr spectra of F_4PSCH_3 at particular temperatures and appropriate rates of exchange of magnetization. The experimental spectra were obtained from a solution in approximately 50:50, $\text{CF}_2\text{Cl}_2:\text{CFCl}_3$. The frequency scale which gives chemical shift values in Hz relative to P_4O_6 was measured with respect to the ^{19}F heteronuclear lock on CFCl_3 and subsequently converted to the P_4O_6 scale. The K matrix used was the one containing 80% "BPR" (cf. ref. 102) and 20% rotation (Table 2, Appendix).

^{31}P (36.4 MHz) $\sim \{^1\text{H}\}$ Spectra of

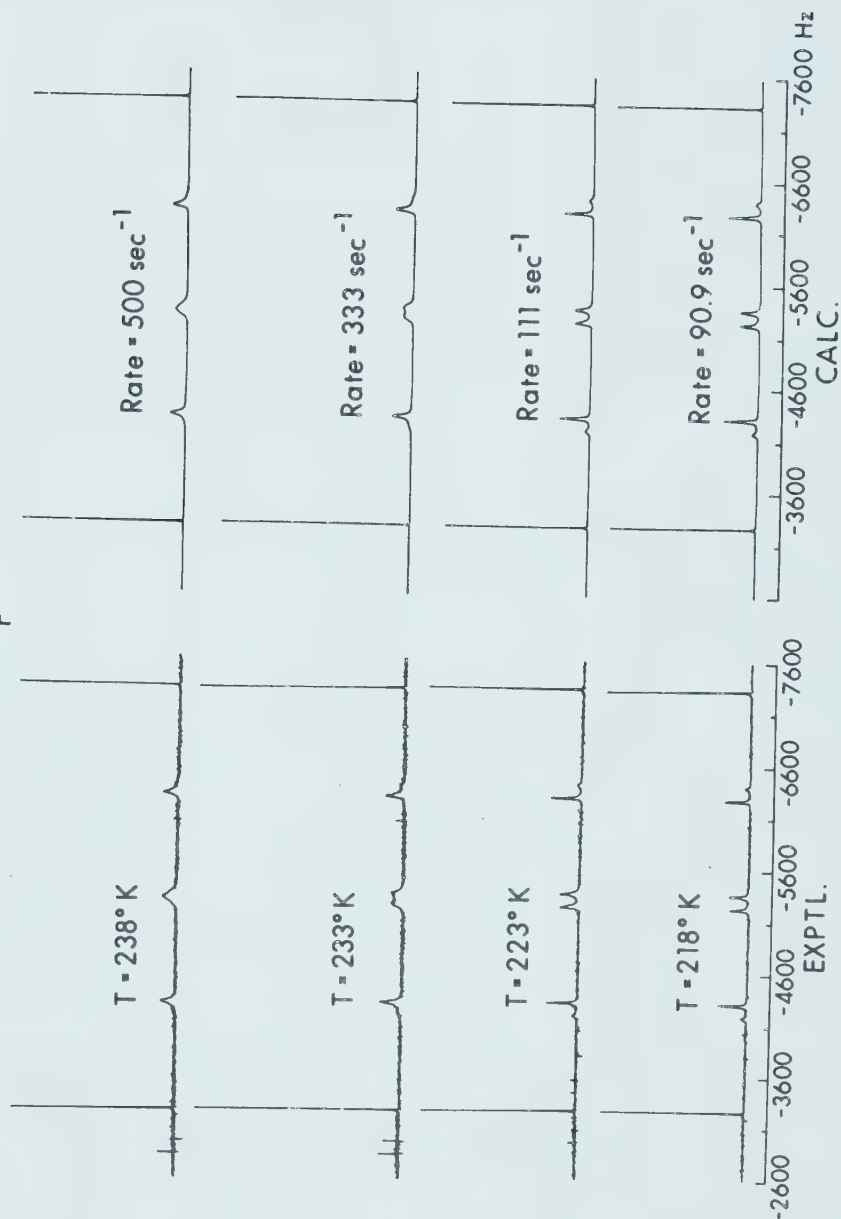
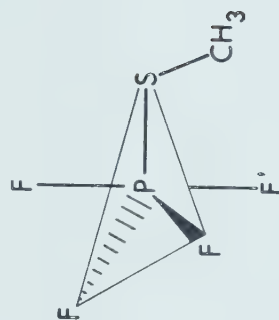


Figure VII-5

Computer-simulation of ${}^3\text{I}_\text{P} \sim \{{}^1\text{H}\}$ (36.4 MHz) nmr spectra of F_4PSCH_3 in the intermediate exchange region using different exchange matrices (cf. Table 3, Appendix). Scales are as described in Fig VII-5.

Figure VII-6

Various Exchange Matrices
for F_4PSCH_3

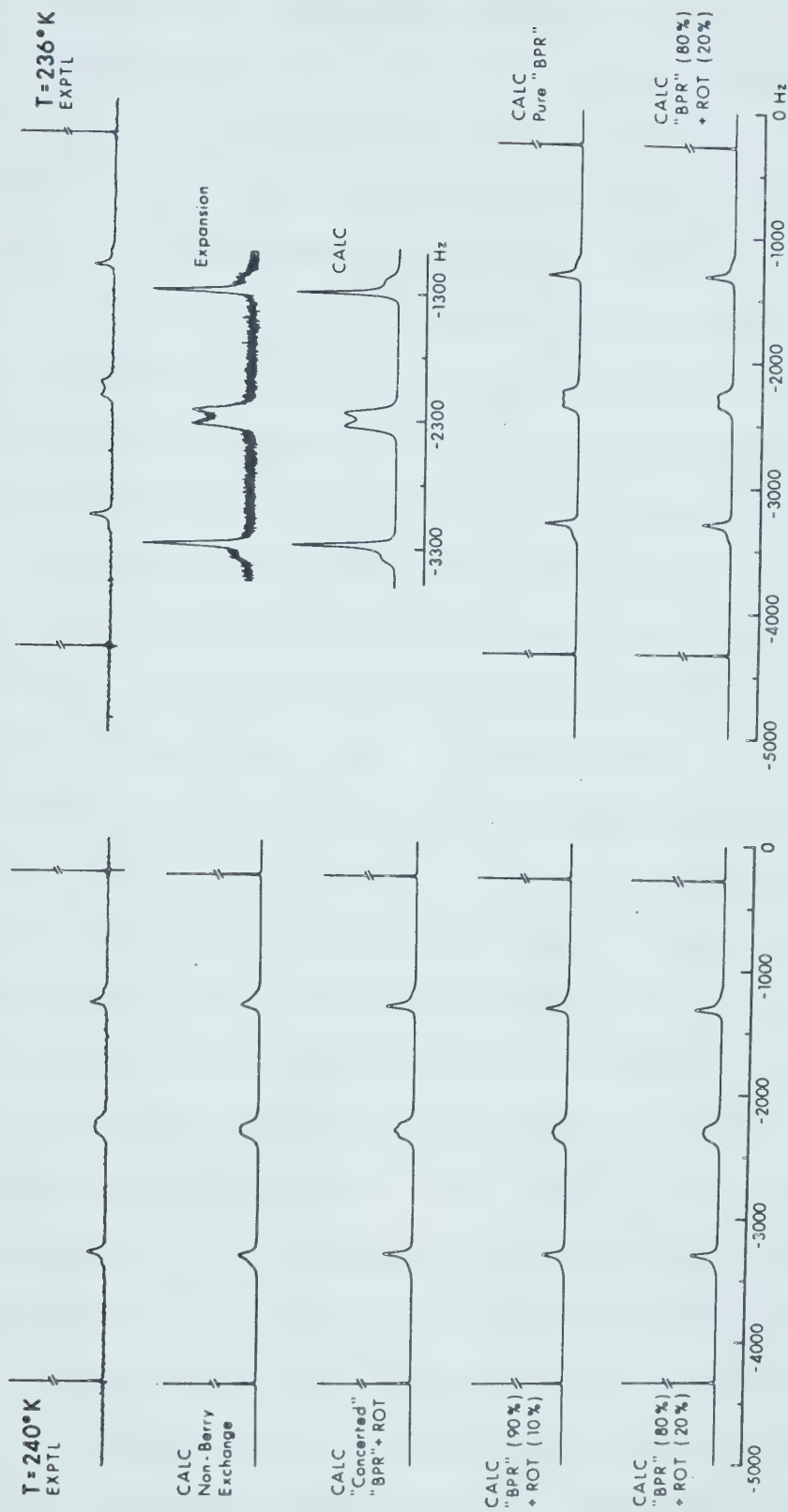


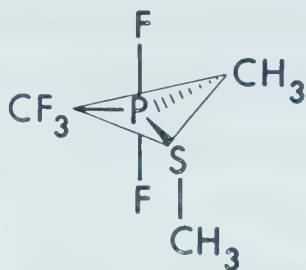
Figure VII-6

B. Methyl(trifluoromethyl)difluoro(methylthio)phosphorane.

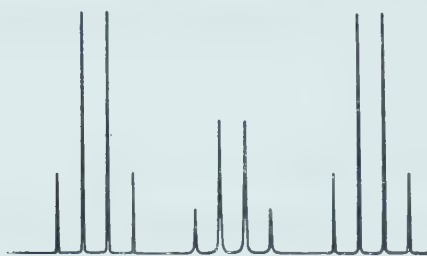
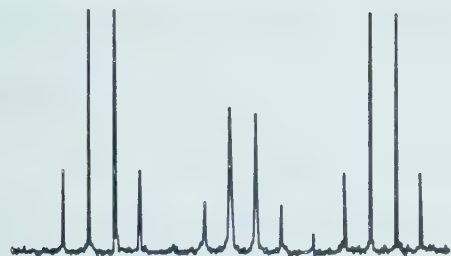
The temperature-dependent behavior of the ^{19}F and ^{31}P nmr spectra of $\text{CH}_3(\text{CF}_3)\text{PF}_2(\text{SCH}_3)$ has been described in Chapter 5. In this compound the magnetic non-equivalence of the two directly-bound fluorine atoms observed at low temperatures can arise from (a) a cessation of the free rotation of the SCH_3 group about the P-S bond, or, less likely, (b) a cessation of an intramolecular exchange process which interchanges the fluorine environments relative to the fixed SCH_3 group, the CH_3 group of which must not lie in the equatorial plane. Such an intramolecular exchange process cannot be of the BPR or TR type for neither of these two processes can exclusively effect the magnetic equivalence of the two directly-bound fluorine atoms with a rigid orientation of the SCH_3 group (*vide infra*). A third alternative (c), is a concerted mechanism, one with the P-S bond rotation closely coupled with a ligand positional exchange process.

Interpretations based on a ground state structure with two different directly-bound fluorine atoms, i.e., one axial and one equatorial, with the CF_3 group occupying the remaining axial position, are omitted in view of the considerable, although not overwhelming evidence in support of the diaxial-fluorine ground state structure. However, we cannot rule out the possibility that these alternative structures participate as intermediates in some

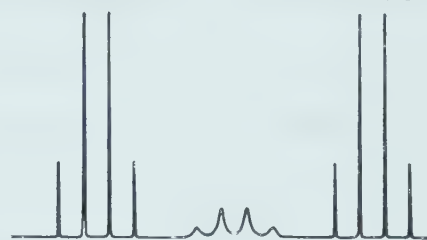
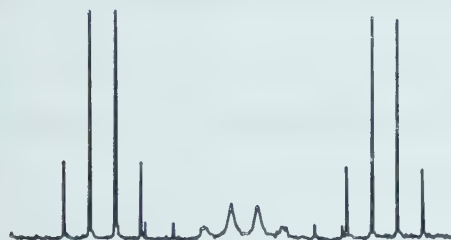
Figure VII-7 Experimental and calculated $^{31}\text{P} \sim \{^1\text{H}\}$ (36.4 MHz) nmr spectra of $\text{CH}_3(\text{CF}_3)\text{PF}_2(\text{SCH}_3)$ at particular temperatures and appropriate rates of exchange of magnetization. The experimental spectra were obtained from a solution in approximately 50:50 $\text{CFCl}_3:\text{CF}_2\text{Cl}_2$ containing 5% TMS. The K matrix used to obtain the calculated spectra is given in Table 4, Appendix A. The frequency scale which gives chemical shift values in Hz relative to P_4O_6 was measured with CFCl_3 as the ^{19}F heteronuclear lock and converted to appropriate ^{31}P scale values.

^{31}P (36.4 MHz) - $\{^1\text{H}\}$ SPECTRA OF

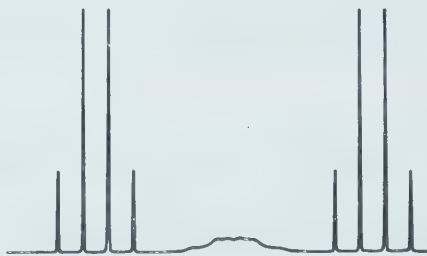
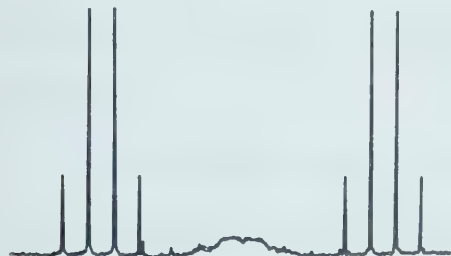
TEMP = 250°K

RATE = 4000 sec⁻¹

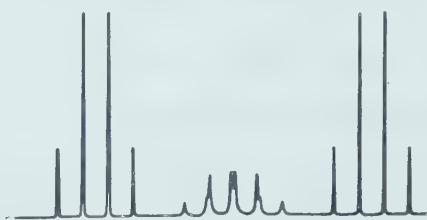
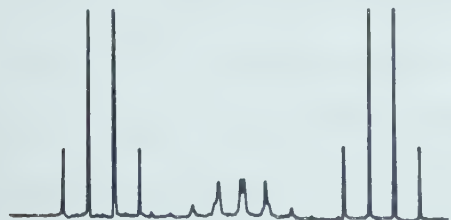
TEMP = 230°K

RATE = 714 sec⁻¹

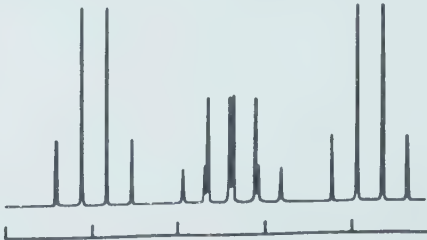
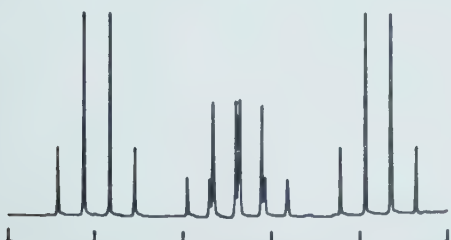
TEMP = 220°K

RATE = 250 sec⁻¹

TEMP = 203°K

RATE = 33 sec⁻¹

TEMP = 190°K

RATE = 7.1 sec⁻¹

-4000 -5000 -6000 Hz

-4000 -5000 -6000 Hz

EXPTL.

CALC.

Figure VII-7

intramolecular fluorine exchange mechanism.

The simplest interpretation which suffices to explain the observed behavior of the spectrum is the P-S bond rotation mechanism, (a), but because the K matrices for mechanisms (a) and (c) are identical (Appendix , Table 4) these two processes cannot be distinguished from each other.

The appropriate rates of (a) and (c) are however related by a factor of two and this has a small effect on the derived thermodynamic parameters. The barriers were evaluated for both the rotation, (a), and concerted rotation - "pseudorotation" process, (c). The $\Delta G_{298}^{\ddagger}$ value for the concerted mechanism is slightly lower than for the pure rotation mechanism (*cf.* Fig VII-7 for a comparison of the calculated and the experimental spectra).

Ligand positional exchange in $\text{CH}_3(\text{CF}_3)\text{PF}_2(\text{SCH}_3)$, if considered independently, would involve high energy species for a BPR mechanism, or a complicated interchange of pair and trio components for a TR process, which may provide a lower energy barrier. These two mechanistic routes are depicted in Figure VII-8, with [] to indicate the substituent acting as a pivot in the BPR route.

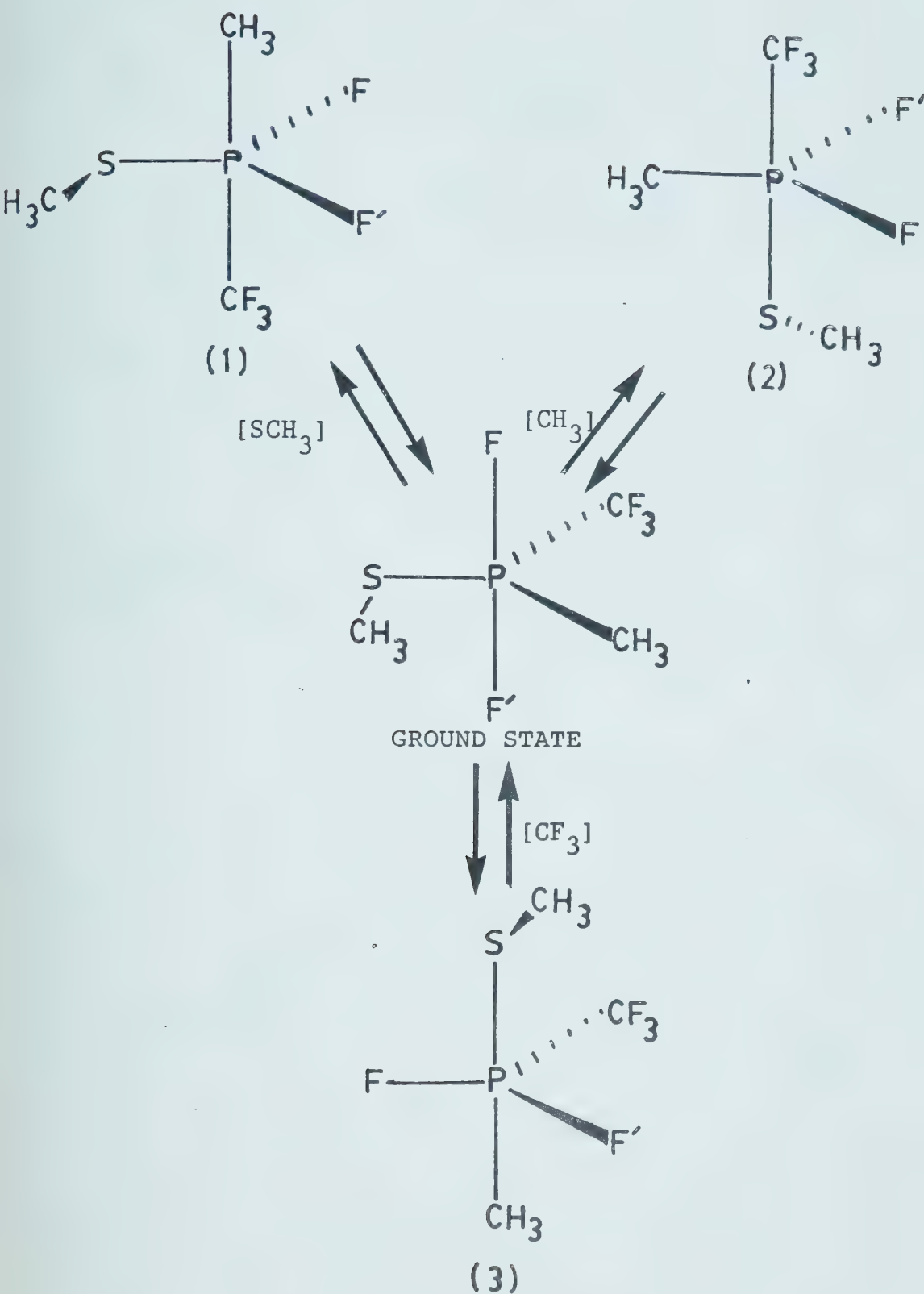


Figure VII-8A

Berry Pseudorotation in $\text{CF}_3(\text{CH}_3)\text{PF}_2(\text{SCH}_3)$

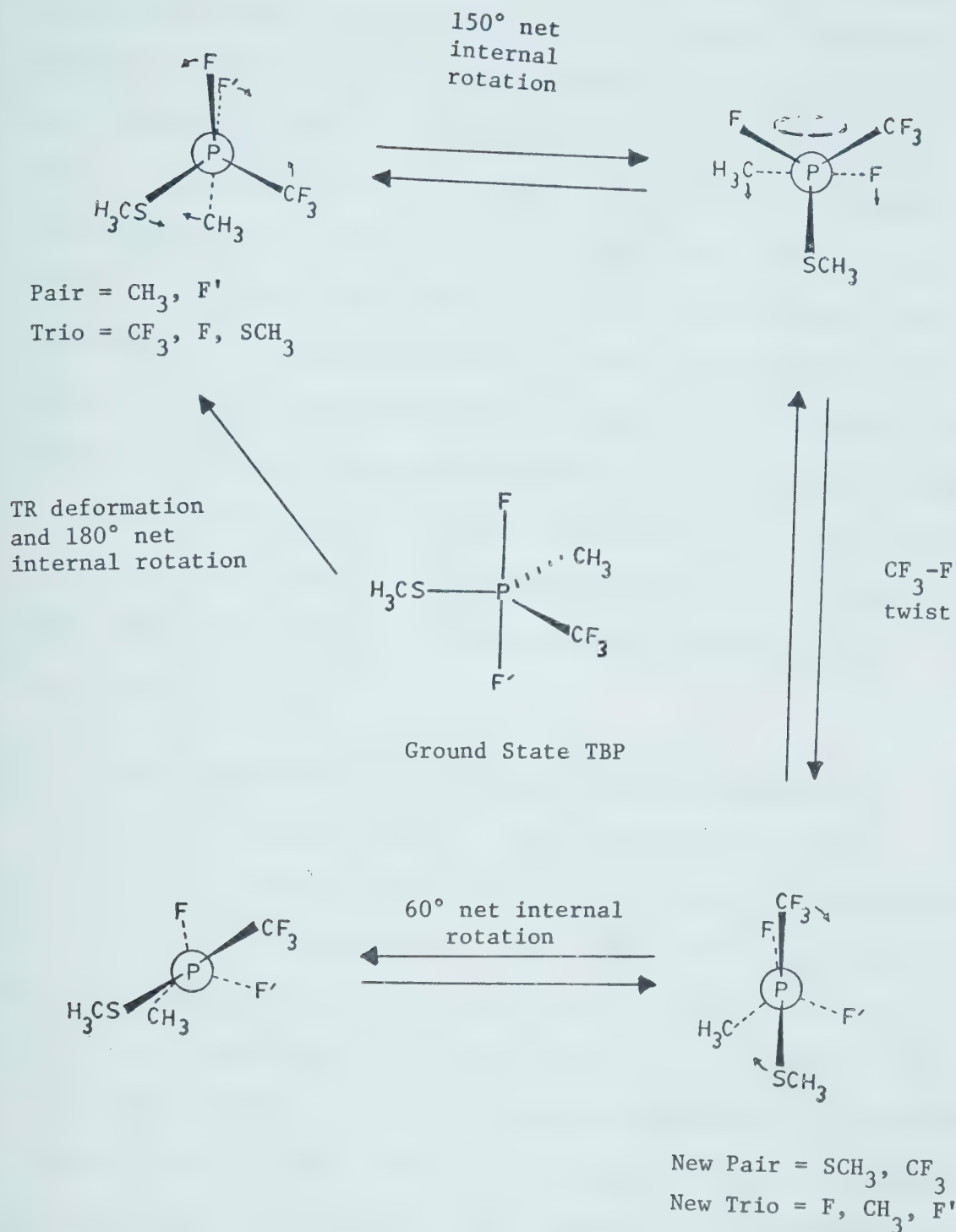


Figure VII-8B

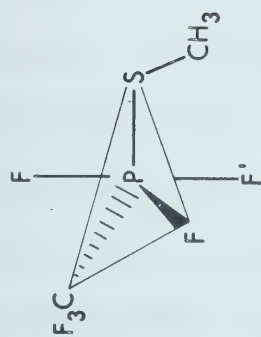
Turnstile Rotation

Figure VII-8A shows that all three possible single-step routes employing a BPR mechanism involve the placement of substituents of lower electronegativity compared to fluorine in axial positions, therefore intermediates of high energy would be required. An equivalent ligand permutation *via* TR mechanism can avoid such high energy intermediates but this mechanistic pathway involves an interchange between the pair and trio components of the TR species (1) in Figure VII-8B. Finally, it is obvious from Figure VII-8 that ligand permutation process alone, either *via* BPR or TR mechanism, cannot equilibrate the two directly-bound fluorine atoms in $\text{CH}_3(\text{CF}_3)\text{PF}_2(\text{SCH}_3)$ unless the SCH_3 group is assumed to simultaneously rotate freely about the P-S bond.

C. Trifluoromethyltrifluoro(methylthio)phosphorane.

The ^{19}F nmr spectrum of $\text{CF}_3\text{PF}_3(\text{SCH}_3)$ (Fig VII-9) at 273°K (the highest temperature investigated), consisted of (a) a very broad doublet, ($\phi_{\text{F}} = 23.2$ ppm, $^1\text{J}_{\text{PF}} = 1000$ Hz) due to fluorine atoms bound directly to phosphorus, (b) a doublet of quartets, ($\phi_{\text{F}} = 69.2$ ppm, $^2\text{J}_{\text{P-F}}$ of 168 Hz) due to the CF_3 groups, and (c) a single broad band (600 Hz wide) centered at 81.1 ppm which, considering the low temperature spectra, must be one-half of the second P-F resonance having an estimated chemical shift of 75.7 ppm and $^1\text{J}_{\text{P-F}}$ of approximately 1050 Hz. At 273°K axial and equatorial

Figure VII-9 Experimental ^{19}F (94.1 MHz) nmr spectra of $\text{CF}_3\text{PF}_3(\text{SCH}_3)$ at various temperatures in the intermediate exchange region and at the slow-exchange limit obtained from a solution in approximately 50:50 $\text{CFCl}_3:\text{CF}_2\text{Cl}_2$. The frequency scale gives chemical shift values in Hz relative to internal CFCl_3 . Four fluorine environments are indicated at the slow-exchange limit. Two non-equivalent axial fluorines are observed at low field; one with $^1J_{\text{P-Fa}} \sim 950$ Hz, assigned to the pair of peaks at -1400 and -2350 Hz and a second axial fluorine environment with $^1J_{\text{PF}} \sim 1060$ Hz due to the pair of peaks at -1800 and -2850 Hz. One CF_3 group (doublet of triplets of doublets) at -6400 to -6600 Hz and one equatorial fluorine ($^1J_{\text{P-Feq}} \sim 1080$ Hz) at -6600 (weak triplet) and -7700 Hz are also clearly seen in the 173°K spectrum.

^{19}F (94.1 MHz) Spectra of

Temp. = 273° K

Temp. = 243° K

Temp. = 193° K

Temp. = 173° K

(F & F' axial)

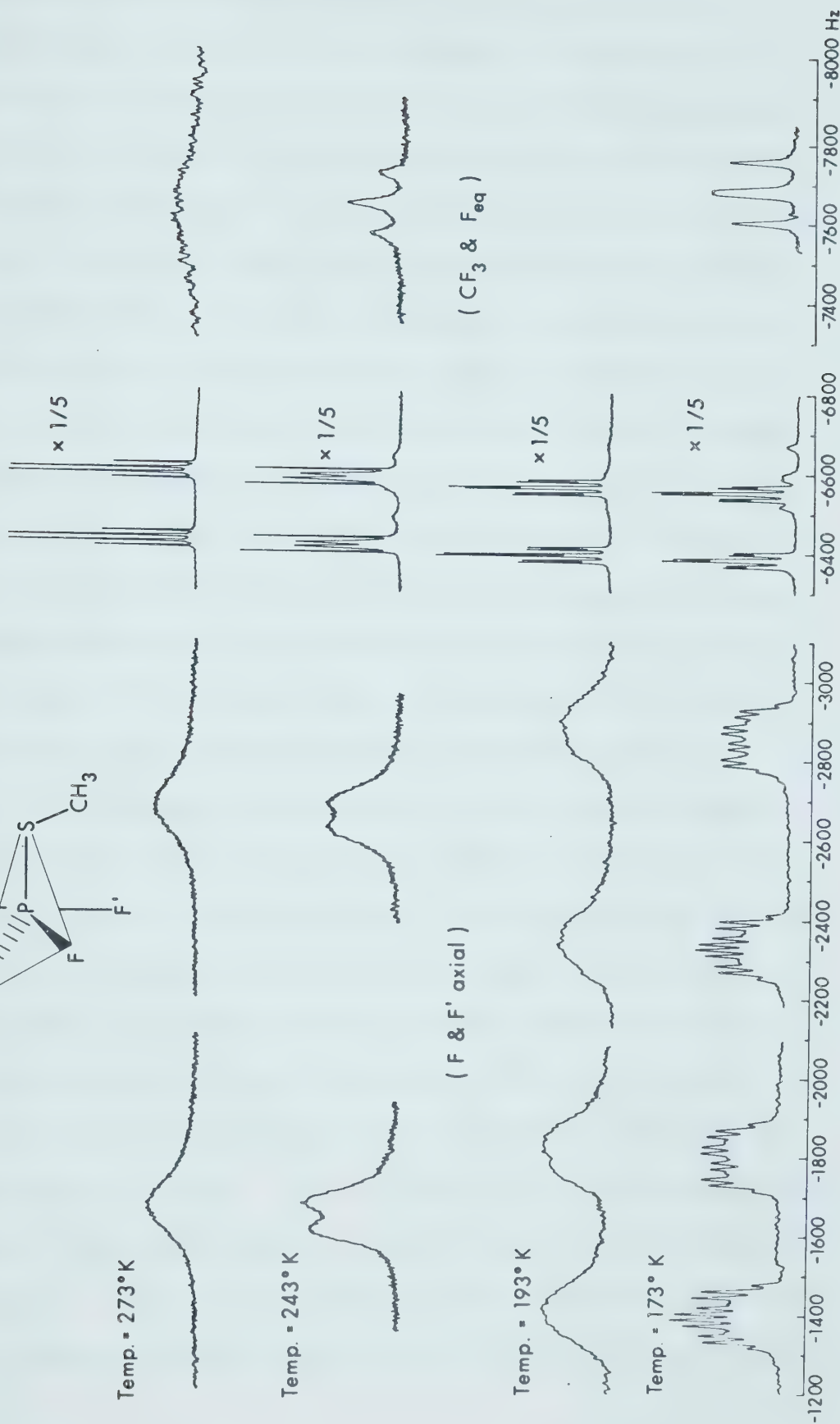
(CF_3 & F_{eq})

Figure VII-9

fluorine atoms are non-equivalent but the system is in an intermediate exchange condition and the lines are very broad. At 243°K distinct changes in the appearance and splitting pattern of the spectrum were observed; the broad doublet downfield became a doublet of broad doublets, the central peaks in the quartet component of the central field doublet (CF_3 resonance) broadened and were seen to be of lower height than the outer peaks. Furthermore, an incipient triplet appeared in this region, partly hidden under the higher field quartet component. The limiting spectrum was obtained at 173°K, the appearance of which is consonant with an assignment of four different fluorine environments arising from one equatorial fluorine, two different axial fluorines, and one equatorial CF_3 group. In the lower field region were two set of doublets of doublets of quartets, corresponding to the two different axial fluorines, with the primary doublet separation of 927 Hz and 1057 Hz, respectively. Centered around 68.7 ppm was a doublet of triplets of doublets and was assigned to the CF_3 group. At this temperature the "triplet" which lay underneath one of the components of the CF_3 signal became much more obvious and was assigned as one-half of the equatorial F signal. The other half of this equatorial F "triplet" lay about 1000 Hz upfield from these overlapping signals. In the high field portion of the equatorial fluorine resonance the central peak of the "triplet" showed

signs of doublet splitting. The pattern is best assigned as a doublet of doublets with two nearly coincident central peaks because the two coupling constants have similar magnitudes (86 Hz and 72 Hz, respectively). Although the axial fluorines are clearly non-equivalent in the low-temperature limiting spectrum, the CF_3 fluorine signal is an apparent triplet because the two couplings of the CF_3 group to the different axial fluorines happen to have the same magnitude. The temperature dependence of the CF_3 subspectrum was shown to be a rate, not a second-order effect.

Consideration of the low temperature spectra and the relative magnitudes of the spectral parameters, especially coupling constant values (Chapter V), lead to the conclusion that the ground state structure adopted by $\text{CF}_3\text{PF}_3(\text{SCH}_3)$ at the low-temperature limit is that shown in Figure VII-10 and is thus similar to that of F_4PSCH_3 .

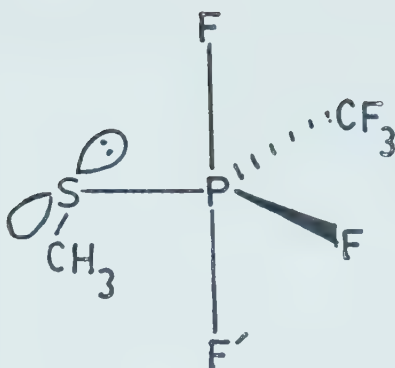


Figure VII-10

The axial-equatorial F ligand permutation is further substantiated by the temperature dependence of the CF_3 subspectrum in each of the ^{19}F nmr spectra (*cf.* Fig VII-9). Computer-simulation of these subspectra in the intermediate exchange region was attempted to see how the ΔG_{298}^\ddagger value obtained from this simulation would compare with that obtained from the variable-temperature ^{31}P nmr spectra. Table 5 (Appendix) gives the K matrix, and Figure VII-12 the comparison of the calculated and the experimental spectra.

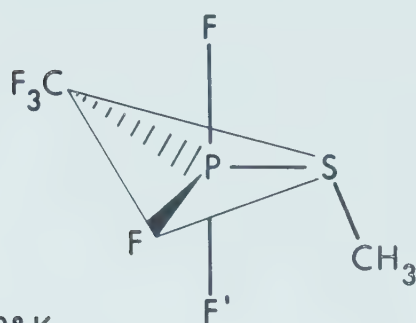
The proton-decoupled ^{31}P variable temperature nmr spectra (Fig VII-11) were even more interesting. At 293°K it consisted of a quartet of quartets. The intensity

Figure VII-11 Experimental $^{31}\text{P} \sim \{^1\text{H}\}$ (36.4 MHz) nmr spectra of $\text{CF}_3\text{PF}_3(\text{SCH}_3)$ at the high- and low-temperature exchange limits indicating the two distinct and separable exchange processes occurring in the compound. The spectra were obtained from an approximate 50:50 solution in $\text{CFCl}_3:\text{CF}_2\text{Cl}_2$. Chemical shift values in Hz were measured relative to the ^{19}F (CFCl_3) heteronuclear lock which were subsequently converted to the ^{31}P reference (P_4O_6) scale.

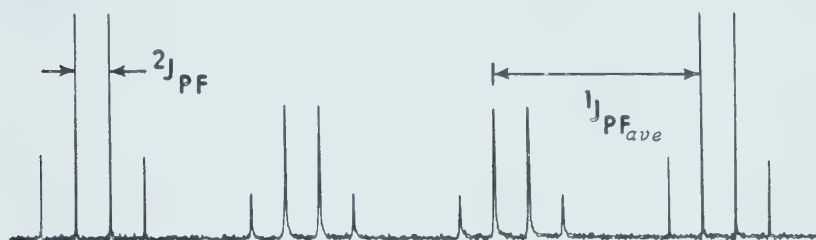
The spectral intensity ratios at 243° are not ideal because the two averaging processes are not completely separable, i.e., the rotation slows down simultaneously with the "pseudorotation"¹⁰² albeit at a much slower rate.

The term pseudorotation as used here refers to a general intramolecular ligand exchange without implying any particular mechanistic pathway. See reference 102.

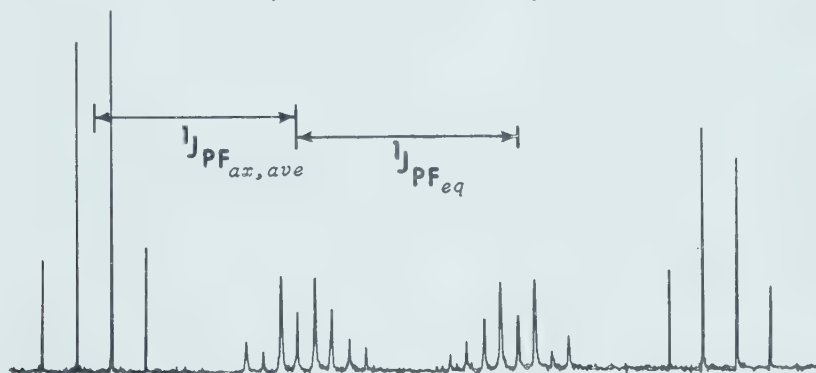
^{31}P (36.4 MHz) $\sim \{^1\text{H}\}$ Spectra of



TEMP. = 293° K



TEMP. = 243° K (Pseudorotation)



TEMP. = 173° K (Rotation)

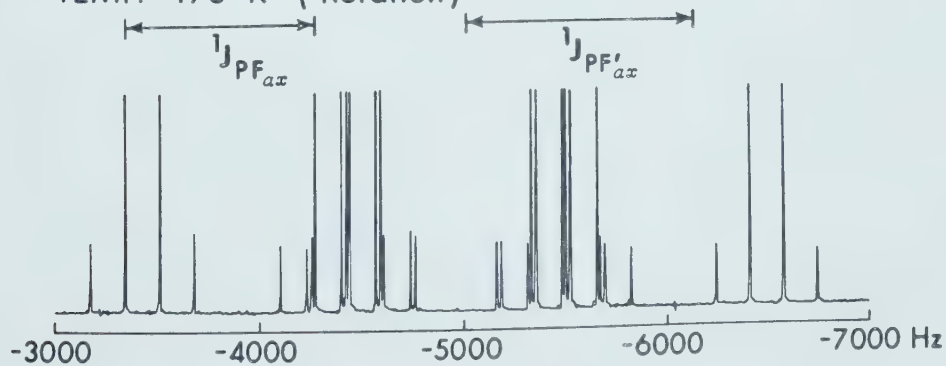


Figure VII-11

Figure VII-12 Observed and calculated $^{31}\text{P} \sim \{^1\text{H}\}$ (36.4 MHz) nmr spectra of $\text{CF}_3\text{PF}_3(\text{SCH}_3)$ at particular temperatures and appropriate rates of exchange of magnetization. The experimental spectra were obtained from a solution in $\text{CFCl}_3/\text{CF}_2\text{Cl}_2$. The calculated spectra were obtained using two different K matrices (Table 5, Appendix A) for the two distinct and separable exchange processes occurring in $\text{CF}_3\text{PF}_3(\text{SCH}_3)$. The frequency scale which gives chemical shift values in Hz relative to P_4O_6 was measured with reference to CFCl_3 as the heteronuclear ^{19}F lock and subsequently converted to the ^{31}P scale.

The term pseudorotation as used here refers to a general intramolecular ligand exchange without implying any particular mechanistic pathway. See reference 102.

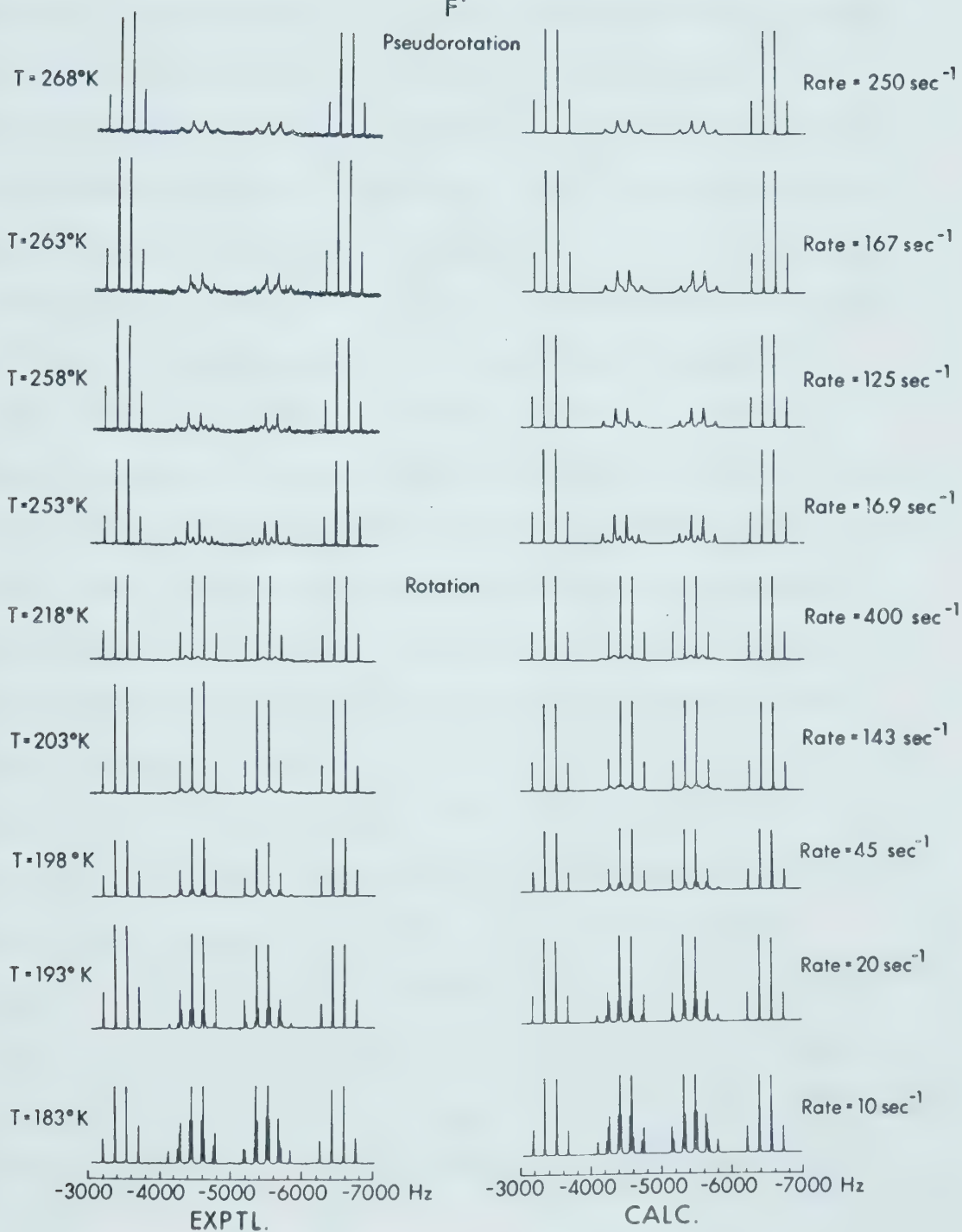
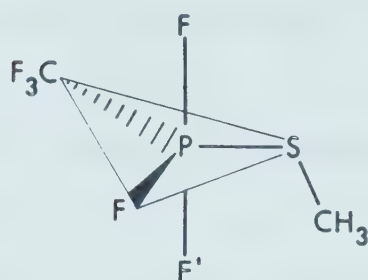
^{31}P (36.4 MHz) $\sim \{^1\text{H}\}$ Spectra of


Figure VII-12

ratios and widths of the central quartets suggested that the changes were due to a reduction of the rate of a molecular process, in particular the averaging of the three directly-bound fluorine environments. Further changes were observed as the temperature was lowered, and at 243°K, the spectral appearance and splitting pattern indicated two different fluorine environments "seen" by phosphorus, implying complete cessation of the ligand rearrangement process which was equilibrating the axial and equatorial fluorine environments. At the low rate (temperature) limit the spectrum consisted of a doublet of triplets of quartets consistent with phosphorus coupling to one equatorial fluorine atom, two axial fluorine atoms, and the three fluorines of the CF_3 group, respectively. The anomalous band widths and intensities arose from a concomitant slowing down of a second intramolecular averaging process, one which rendered the two axial fluorines equivalent, and which can be most reasonably ascribed to the free rotation of the SCH_3 group about the P-S bond. The limiting spectrum, obtained at 173°K, consisted of 32 lines and was interpreted as arising from a main, P-F axial doublet ($^1J_{\text{PF}} = 1057 \text{ Hz}$), each component of which was further split into a doublet due to phosphorus coupling with the other axial fluorine ($^1J_{\text{PF}} = 927 \text{ Hz}$). The components of this doublet of doublets suffered additional doublet

splitting due to coupling with the single equatorial fluorine ($^1J_{\text{PF}_{\text{eq}}} = 1027 \text{ Hz}$), and finally quartet splitting from coupling with the CF_3 group (Fig VII-12).

There are therefore two averaging processes in $\text{CF}_3\text{PF}_3(\text{SCH}_3)$ and the difference in the potential barriers between the two processes is sufficient to permit individual analysis. As in F_4PSCH_3 neither one of the processes alone can completely account for the splitting patterns and intensities observed in the ^{19}F and ^{31}P nmr spectra in the high and low temperature limits. If the ligand positional exchange in $\text{CF}_3\text{PF}_3(\text{SCH}_3)$ is considered only in terms of either the BPR or the TR mechanism, the latter would seem to be the more favorable route (*cf.* analogous discussion on $\text{CH}_3(\text{CF}_3)\text{PF}_3$, and the corresponding illustration in Figure VI-7) since it would preclude "high energy" species with CF_3 and SCH_3 in axial positions in a TBP.

Figure VII-12 shows a comparison of selected experimental and calculated ^{31}P nmr spectra in the intermediate exchange regions for each process and from which the barriers were determined.

D. Bis(trifluoromethyl)difluoro(methylthio)phosphorane.

The proton-decoupled ^{31}P nmr spectrum (Fig VII-13) of $(\text{CF}_3)_2\text{PF}_2(\text{SCH}_3)$ at 300°K comprised a triplet of septets consistent with phosphorus coupling with two types of

Figure VII-13

The high- and low-temperature $^{31}\text{P} \sim \{^1\text{H}\}$ (36.4 MHz) limiting nmr spectra were obtained from a solution in CF_2Cl_2 . The chemical shift scale in Hz is given relative to P_4O_6 but was measured relative to CF_2Cl_2 as the ^{19}F heteronuclear lock and subsequently converted to the ^{31}P scale.

^{31}P (36.4 MHz) $\sim \{^1\text{H}\}$ Spectra of

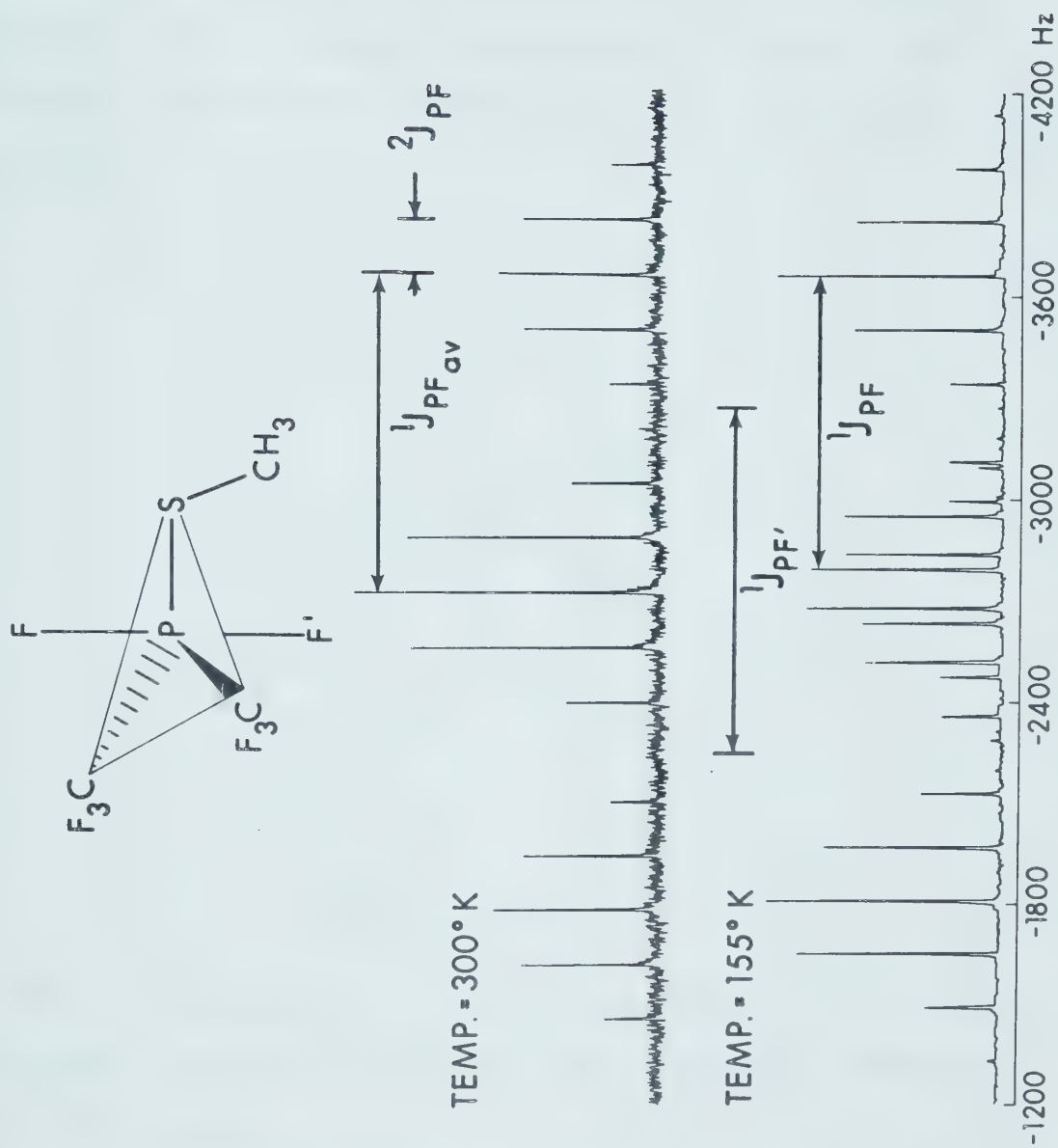


Figure VII-13

fluorine environments: axial directly-bound fluorine atoms and six fluorines on the two trifluoromethyl groups. The spectrum at the low temperature limit, which consisted of 28 lines, a doublet of doublets of septets, strongly suggesting loss of magnetic equivalence of the two axial fluorines, was assigned to the ground state structure Figure VII-14:

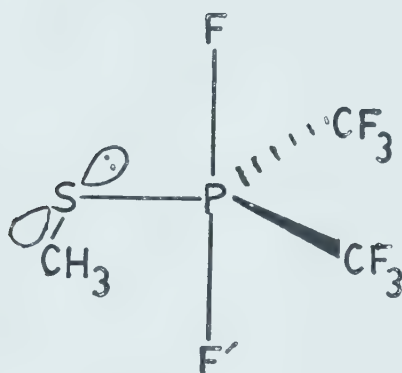


Figure VII-14

Again the invariance of the $^2J_{P-F}$ value with temperature suggested non-exchanging equatorial positions of the CF_3 groups.

Computer-simulation of the variable temperature proton-decoupled ^{31}P nmr spectra gave a reasonably good fit with the experimental spectra, as shown by a selected set of data spanning the intermediate exchange region

Figure VII-15

Experimental and observed $^{31}\text{P} \sim \{^1\text{H}\}$ (36.4 MHz) nmr spectra of $(\text{CF}_3)_2\text{PF}_2(\text{SCH}_3)$ at particular temperatures and appropriate rates of exchange of magnetization. The experimental spectra were obtained from a solution in CF_2Cl_2 . The K matrix constructed to obtain the calculated spectra does not distinguish between "pseudorotation" and rotation. The frequency scale which gives chemical shift values in Hz relative to P_4O_6 was measured relative to CF_2Cl_2 as the ^{19}F heteronuclear lock and subsequently converted to the ^{31}P scale.

^{31}P (36.4 MHz) $\sim \{^1\text{H}\}$ Spectra of

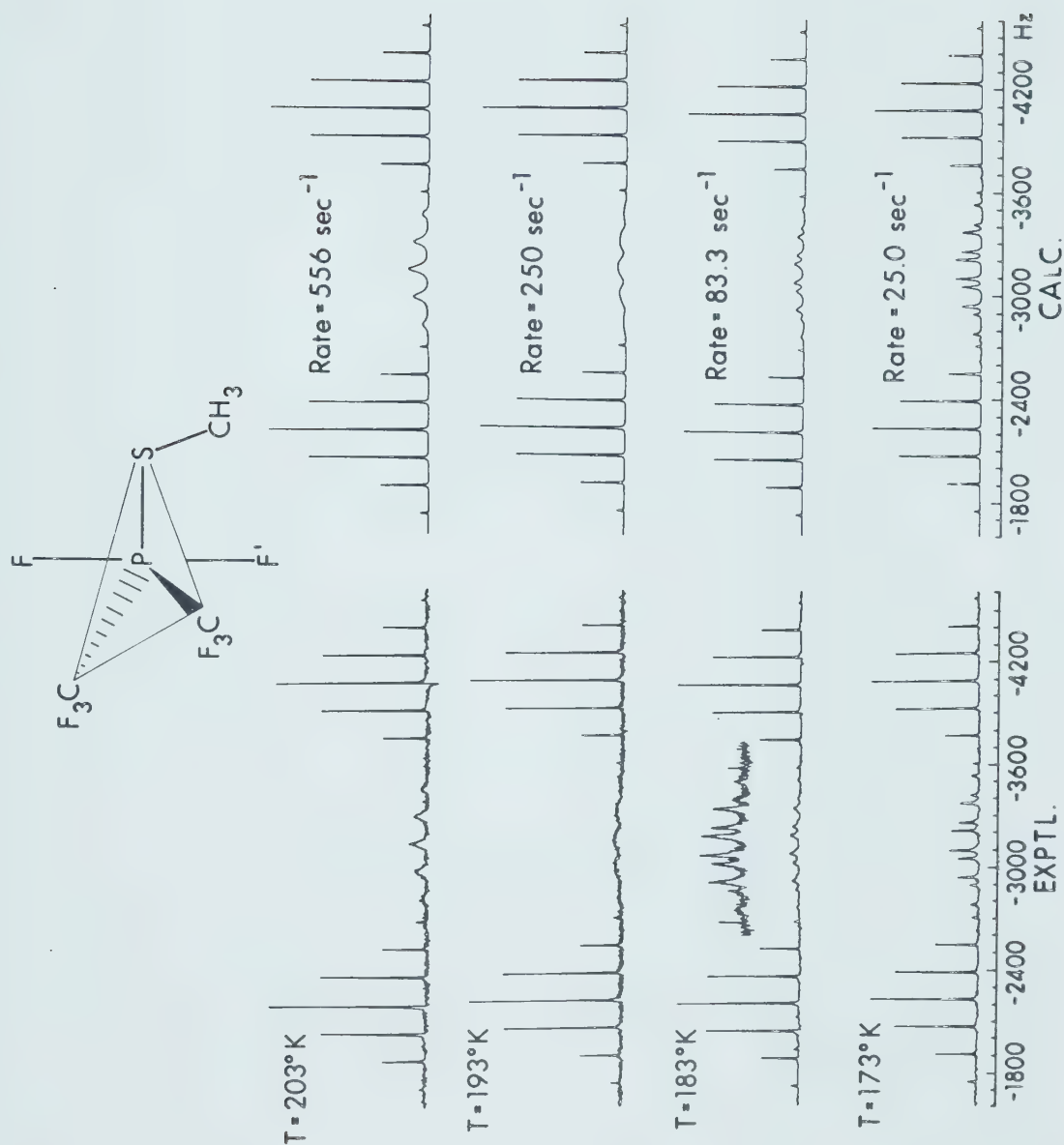
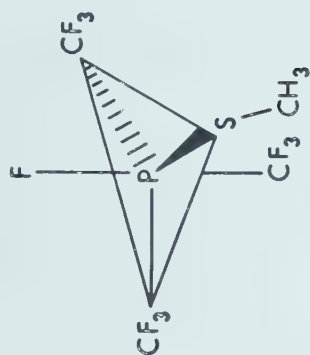


Figure VII-15

Figure VII-16 Experimental $^{31}\text{P} \sim \{^1\text{H}\}$ (36.4 MHz) nmr spectrum of $(\text{CF}_3)_3\text{PF}(\text{SCH}_3)$ in a fast-exchange region, obtained from a solution in CF_2Cl_2 . The frequency scale gives chemical shift values in Hz relative to P_4O_6 but was measured relative to CF_2Cl_2 as the ^{19}F heteronuclear lock and subsequently converted to the ^{31}P scale.

$^{31}\text{P} \sim \{^1\text{H}\}$ (36.4 MHz) nmr Spectrum of



T = 273°K

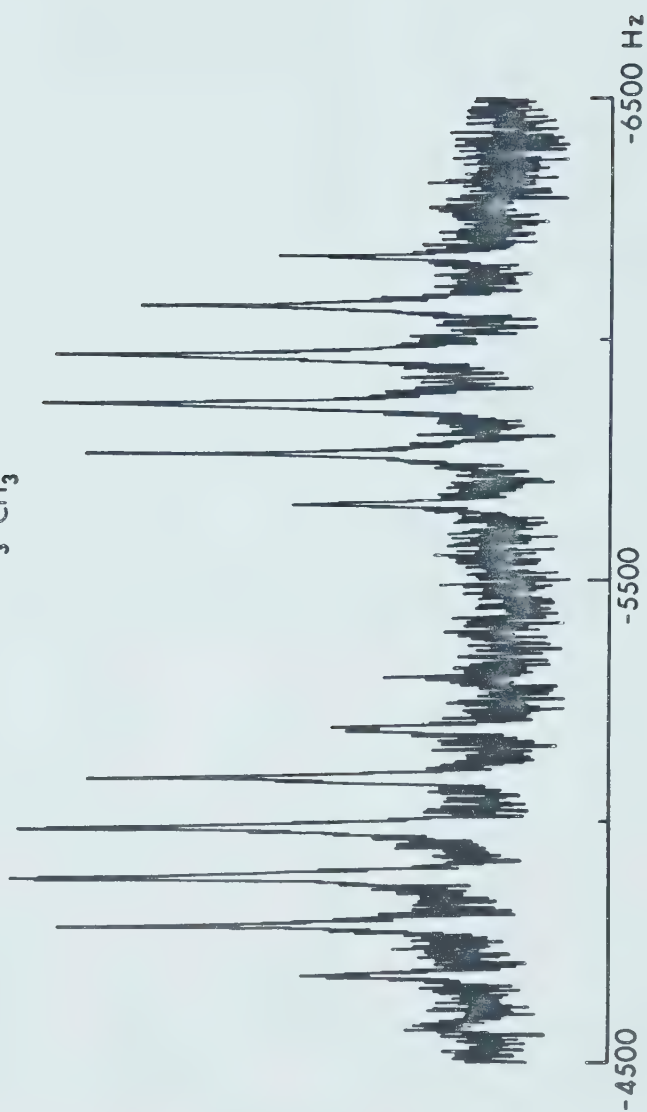


Figure VII-16

(Fig VII-15). From these and additional data, the energetics of the exchange process were derived.

E. Tris(trifluoromethyl)fluoro(methylthio)phosphorane.

The proton-decoupled ^{31}P nmr spectrum (Fig VII-16) of $(\text{CF}_3)_3\text{PF}(\text{SCH}_3)$ at 273°K consisted of a doublet of eight lines with the intensity ratio of roughly 1:4:9:10:10:9:4:1, approximating that of the central eight lines of a decet which would appear to obey the ratio $1:4:9\frac{1}{3}:14:14:9\frac{1}{3}:4:1$, suggesting the equivalence of the three CF_3 groups. The breadth of the peaks suggested, however, that a rate reduction of some intramolecular exchange process was responsible for the appearance of the spectrum. A limiting spectrum was obtained at 213°K which (Chapter 5) indicated the ground state structure illustrated in Figure VII-17.

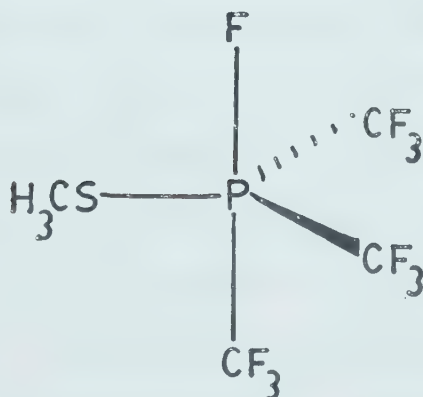


Figure VII-17

The spectrum at 213°K comprised a doublet of "quintet" of quartets. The ratio of the band intensities in the quintet grouping was closer to those of the central five lines of a septet (6:15:20:15:6) than those of a real quintet (1:4:6:4:1). The spectrum was interpreted as arising from a splitting of P-F axial doublet components into a septet due to coupling with the fluorines in the two equatorial CF_3 groups and further resolved into quartets from coupling with fluorines of the axial CF_3 group. The magnetic equivalence of the three sets of CF_3 groups observed at higher temperatures is therefore likely due to a ligand rearrangement which averaged the two CF_3 environments.

It must be emphasized that the observed spectra have been investigated only between 263° and 213°K and do not provide any evidence for a fixed orientation of the SCH_3 group relative to the molecular plane. We might expect SCH_3 rotation to cease at very low temperatures comparable to those required for $(\text{CF}_3)_2\text{PF}_2(\text{SCH}_3)$ and $\text{CH}_3(\text{CF}_3)\text{PF}_3(\text{SCH}_3)$. However, the very low temperature spectra which might reveal the effects of this additional process in $(\text{CF}_3)_3\text{PF}(\text{SCH}_3)$ were not investigated because the signal to noise ratio of the spectra was poor, and because the effects of magnetic non-equivalence on the axial CF_3 portion of the spectrum are probably small. Furthermore, by analogy with the analogous systems such as $(\text{CF}_3)_3\text{PFN}(\text{CH}_3)_2$, $(\text{CF}_3)_3\text{PF}(\text{OCH}_3)$, etc,⁹² the spectra are likely to be very complex and may not be interpretable. The only process revealed by the nmr spectra of

Figure VII-18 Observed and calculated $^{31}\text{P} \sim \{^1\text{H}\}$ (36.4 MHz) nmr spectra of $(\text{CF}_3)_3\text{PF}(\text{SCH}_3)$ at particular temperatures and appropriate rates of exchange of magnetization. The experimental spectra were obtained from a solution in CF_2Cl_2 and the calculated spectra were obtained using a K matrix constructed for a "pseudorotation" (cf. ref. 102) mechanism of exchange. The frequency scale gives the chemical shift values in Hz relative to P_4O_6 but was measured relative to CF_2Cl_2 as the ^{19}F heteronuclear lock and converted to the ^{31}P scale.

$^{31}\text{P} \sim \{^1\text{H}\}$ (36.4 MHz) half-Spectra of

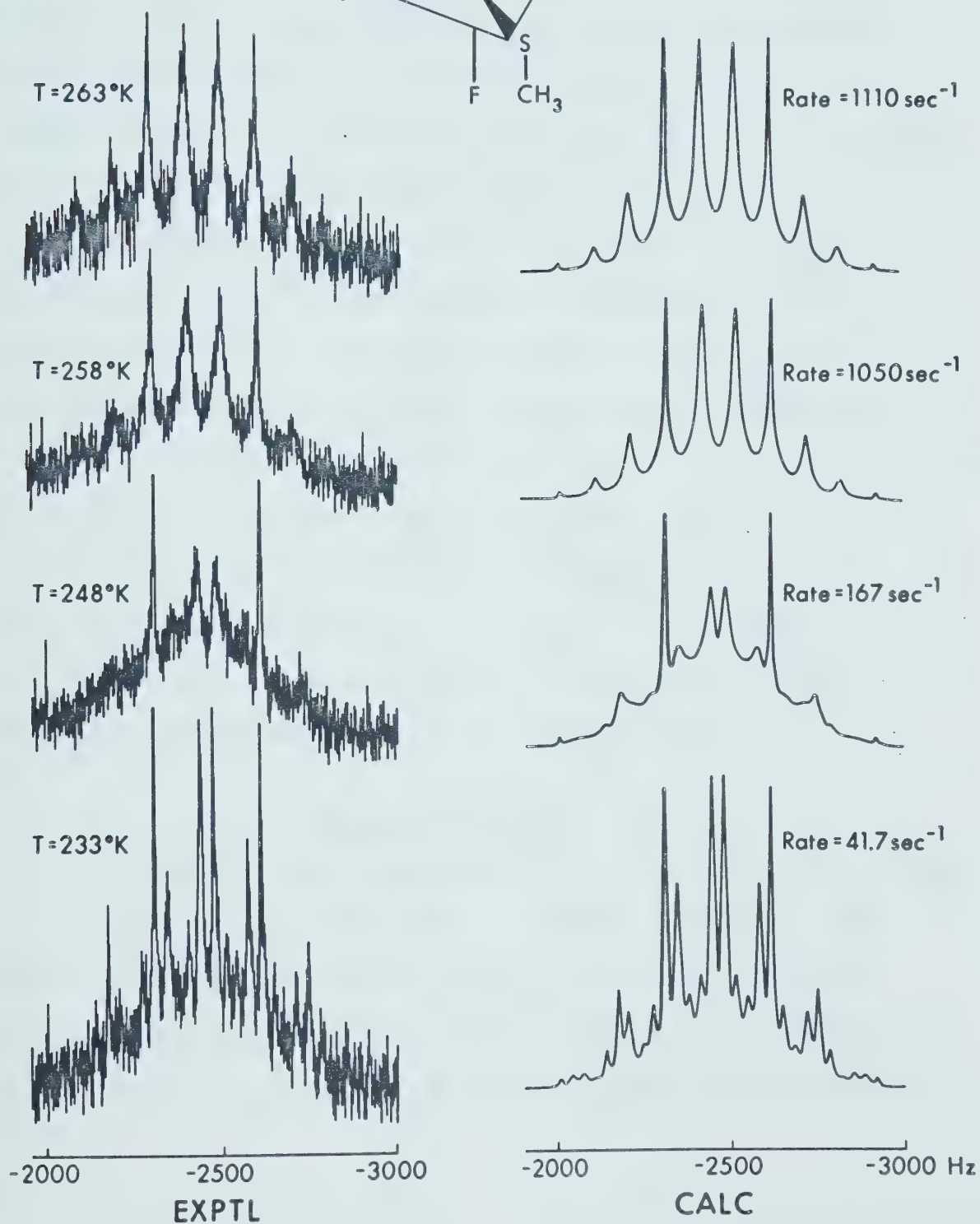
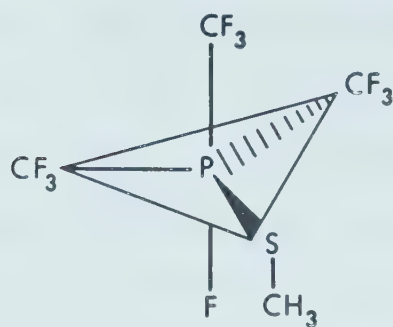


Figure VII-18

$(\text{CF}_3)_3\text{PF}(\text{SCH}_3)$ is therefore the permutational interchange of CF_3 groups between axial and equatorial sites.

It is worth noting that the $^2J_{\text{P-F}}$ values obtained at the high temperature limit are the average of the two different $^2J_{\text{P-F}}$ values obtained at the low temperature limit, in support of an exchange process involving interchange of CF_3 groups between axial and equatorial positions in a trigonal bipyramidal ground state structure.

Computer-simulation of the variable-temperature proton-decoupled ^{31}P nmr spectra at various rates gave spectra which could be fitted reasonably well to the experimental spectra, but the large amount of background noise in the experimental spectra (Fig VII-16,18) introduced a greater error in the fitting procedure and consequently, in the ΔG^\ddagger value. A selection of experimental and calculated spectra used to calculate the rates of exchange are illustrated in Figure VII-18. The K matrix used to generate the spectra is given in Table 6 (Appendix).

Energy Barriers

The thermodynamic parameters for the series of compounds investigated herein are given in Tables 12 and 13. The limits of error given are greater than those given by the numerical analysis in order to compensate for fitting errors and other factors. The last column describes the

Table 12

Free Energy of Activation for Exchange
in Some Phosphoranes^a

Compound	$\Delta G_{298}^{\ddagger}$ (kcal/mole)	Averaging Process
$\text{CH}_3(\text{CF}_3)\text{PF}_3$	9.4 ± 1.0	"Pseudorotation" ^b
$\text{CH}_3(\text{CF}_3)\text{PF}_2(\text{SCH}_3)$	10.6 ± 1.0	Concerted Mechanism
	11.0 ± 1.0	Rotation
F_4PSCH_3	11.0 ± 1.0	"Pseudorotation" ^b plus some rotation
$\text{CF}_3\text{PF}_3(\text{SCH}_3)$	12.8 ± 2.0	"Pseudorotation" ^b
	10.2 ± 1.0	Rotation
$(\text{CF}_3)_2\text{PF}_2(\text{SCH}_3)$	10.0 ± 1.0	Rotation
$(\text{CF}_3)_3\text{PF}(\text{SCH}_3)$	11.5 ± 3.0	"Pseudorotation" ^b (?)

^a Full thermodynamic parameters are given in Table 18.

^b See reference 102

TABLE 13

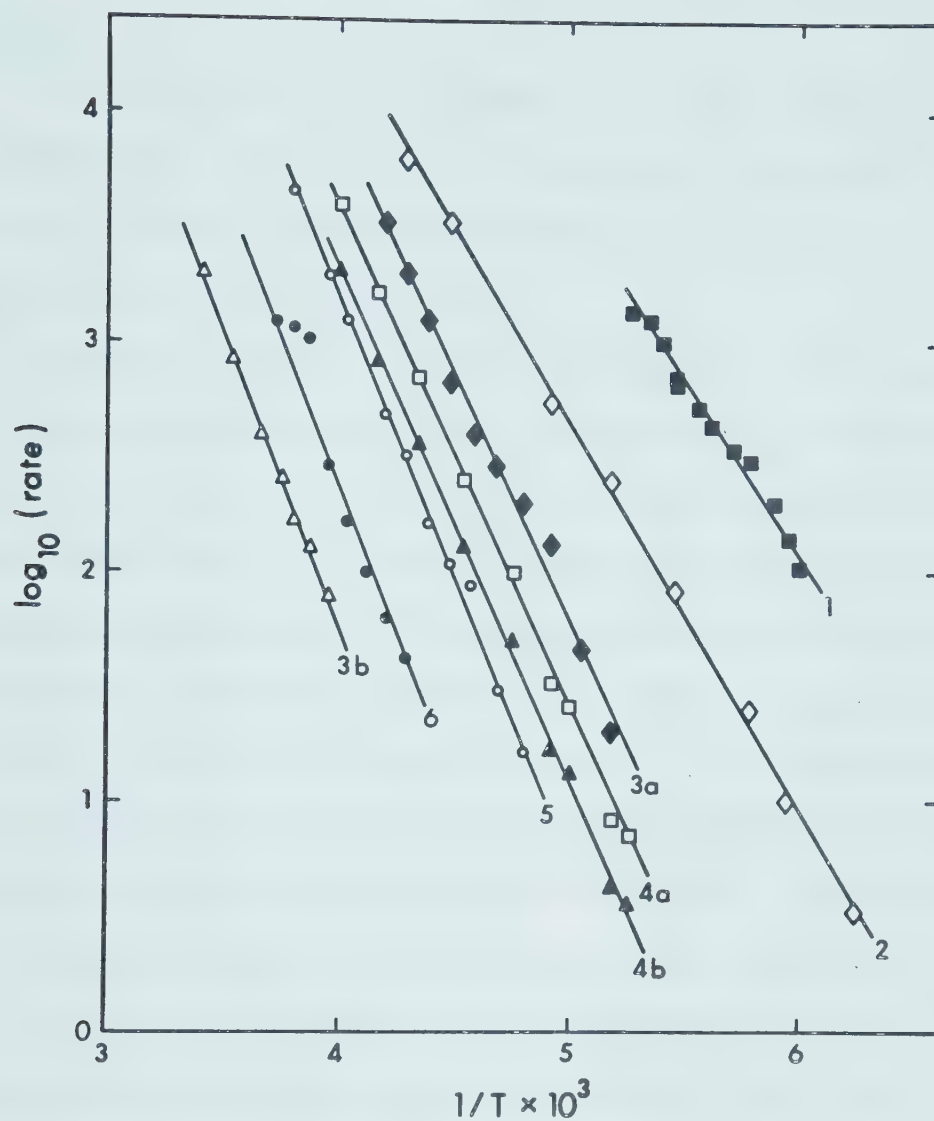
Activation Parameters of Some Trifluoromethylphosphoranes^a

Compound	E_A	ΔH^\ddagger	ΔS^\ddagger	ΔG_{298}^\ddagger	Remarks
$\text{CH}_3(\text{CF}_3)_2\text{PF}_3$	6.5 ± 0.2	6.2 ± 0.2	-10.7 ± 1.3	9.4 ± 1.0	
$\text{CH}_3(\text{CF}_3)_2\text{PF}_2(\text{SCH}_3)$	10.1 ± 0.2	9.7 ± 0.2	-4.2 ± 0.7	11.0 ± 1.0	d
F_4PSCH_3	10.8 ± 0.2	10.4 ± 0.2	-2.0 ± 0.9	11.0 ± 1.0	
$\text{CF}_3\text{PF}_3(\text{SCH}_3)$	11.8 ± 0.4	11.3 ± 0.4	-5.0 ± 1.6	12.8 ± 1.0	e
	9.8 ± 0.2	9.3 ± 0.2	-2.9 ± 0.9	10.2 ± 1.0	f
$(\text{CF}_3)_2\text{PF}_2(\text{SCH}_3)$	7.7 ± 0.1	7.3 ± 0.1	-9.2 ± 0.6	10.0 ± 1.0	
$(\text{CF}_3)_3\text{PF}(\text{SCH}_3)$	13.6 ± 0.4	13.1 ± 0.4	5.4 ± 1.5	11.5 ± 3.0	
$(\text{CF}_3)_2\text{PF}(\text{OCH}_3)\text{N}(\text{CH}_3)_2$	30.1 ± 0.8	29.4 ± 0.8	39.4 ± 2.3	17.7 ± 3.0	c
$(\text{CF}_3)_3\text{PFN}(\text{CH}_3)_2$	12.6 ± 0.2	12.1 ± 0.2	-0.4 ± 0.8	12.2 ± 1.0	g
$(\text{CF}_3)_3\text{PF}(\text{OCH}_3)$	9.1 ± 0.4	8.6 ± 0.4	-8.0 ± 1.5	11.0 ± 1.0	g

FOOTNOTES FOR TABLE 13

- a All parameters, except for ΔS^\ddagger , are in kcal/mole. ΔS^\ddagger values are in entropy units.
- b The limits of error given in this table are much higher than the values obtained from the numerical analysis to compensate for fitting error and other factors.
- c Only four tau values were fitted
- d Values given are for a SCH_3 rotation mechanism
- e For a "pseudorotation" mechanism
- f For a SCH_3 rotation mechanism
- g Ref. 91

Figure VII-19 Arrhenius plot of rate constant k (the pseudo first-order rate) versus $1/T$ for $\text{CH}_3(\text{CF}_3)\text{PF}_3$, $\text{CH}_3(\text{CF}_3)\text{PF}_2(\text{SCH}_3)$ and the series of compounds $(\text{CF}_3)_n\text{PF}_{4-n}(\text{SCH}_3)$ ($n = 0, 1, 2, 3$). The terms rotation and pseudorotation refer to the various processes upon which the magnetization transfer matrix construction was based.



Legend

- | | |
|---|--|
| 1 $\text{CH}_3(\text{CF}_3)\text{PF}_3$ | 5 F_4PSCH_3 |
| 2 $(\text{CF}_3)_2\text{PF}_2(\text{SCH}_3)$ | 6 $(\text{CF}_3)_3\text{PF}(\text{SCH}_3)$ |
| 3 $\text{CF}_3\text{PF}_3\text{SCH}_3$ | a rotation |
| | b pseudorotation |
| 4 $\text{CH}_3(\text{CF}_3)\text{PF}_2\text{SCH}_3$ | a pseudorotation & rotation |
| | b rotation alone |

Figure VII-19

possible nature of the averaging process. Figure VII-19 shows a plot of the pseudo first order rate k against temperature.

The $\Delta G_{298}^{\ddagger}$ values obtained for $\text{CF}_3\text{PF}_3(\text{SCH}_3)$ were taken as reference values for this series of compounds primarily because the two possible averaging processes were distinctly separable in this compound.

The ΔG^{\ddagger} value of 11.0 ± 1.0 kcal/mole obtained for F_4PSCH_3 is best ascribed to a coupled rotation-"pseudo-rotation" process. As was illustrated in Figure VII-3, simple rotation of the SCH_3 group alone cannot effect the magnetic equivalence of the four directly-bound fluorines observed in the high-temperature limiting spectrum of F_4PSCH_3 . A satisfactory fitting of the calculated with the experimental spectra in the intermediate exchange region was obtained only when a "coupled" effect was considered in the construction of the K matrix.

A barrier of 10.6 ± 1.0 kcal/mole was evaluated for a concerted averaging process in $\text{CH}_3(\text{CF}_3)\text{PF}_2(\text{SCH}_3)$, and 11.0 ± 1.0 kcal/mole for a pure rotation process. We suggest that the latter process alone is responsible for the averaging of the axial fluorine environments primarily on the basis of the observation that the CF_3 subspectra in the ^{19}F nmr spectra did not show any drastic change with temperature in contrast with the P-F region. It is not possible to conclusively select the process involved

on the basis of either ΔG^\ddagger values or the spectral behavior.

The ΔG_{298}^\ddagger value of 10.0 ± 1.0 kcal/mole evaluated for $(\text{CF}_3)_2\text{PF}_2(\text{SCH}_3)$ is closer to the rotation barrier of 10.2 ± 1.0 kcal/mole obtained for $\text{CF}_3\text{PF}_3(\text{SCH}_3)$ than to the "pseudorotation"¹⁰² barrier of 12.8 ± 0.2 kcal/mole for this same compound, and therefore the barrier in $(\text{CF}_3)_2\text{PF}_2(\text{SCH}_3)$ is assigned to P-S bond rotation process. This assignment is in accord with the observed invariance of the $^2J_{\text{P-F}}$ value with temperature which has previously been interpreted as indicating fixed positions for the CF_3 group.²⁶ In this case this should be the equatorial position since CF_3 has a lower electronegativity than F and therefore should have less preference for the axial positions. Furthermore, because of the lower electronegativity of the CF_3 group compared to F, the potential barrier for a "pseudorotation"¹⁰² averaging process would be expected to increase upon replacement of one of the fluorine atoms in $\text{CF}_3\text{PF}_3(\text{SCH}_3)$ with a CF_3 group to form $(\text{CF}_3)_2\text{PF}_2(\text{SCH}_3)$. Therefore a ΔG_{298}^\ddagger value at least equal to that for the "pseudorotation" value (12.8 ± 2.0 kcal/mole) in $\text{CF}_3\text{PF}_3(\text{SCH}_3)$ would be expected for $(\text{CF}_3)_2\text{PF}_2(\text{SCH}_3)$ assuming of course a similar "pseudorotation" mechanism for the two compounds.

A ΔG_{298}^\ddagger value of 11.5 ± 3.0 kcal/mole was obtained for the averaging process in $(\text{CF}_3)_3\text{PF}(\text{SCH}_3)$, which is assigned to a "pseudorotating" interchange of CF_3 groups

between axial and equatorial environments. In view of the relatively large limits of error in this case, this can be regarded as comparable to the "pseudorotation"¹⁰² barrier exhibited by $\text{CF}_3\text{PF}_3(\text{SCH}_3)$, which implies that the energy barriers are not greatly dependent on the mass of the pseudorotatory substituent. Whether the overall averaging process includes a rotational contribution is difficult to judge.

Conclusions

Line shape analyses of the proton-decoupled ^{31}P nmr spectra of F_4PSCH_3 , $\text{CF}_3\text{PF}_3(\text{SCH}_3)$, $(\text{CF}_3)_2\text{PF}_2(\text{SCH}_3)$ and $(\text{CF}_3)_3\text{PF}(\text{SCH}_3)$ suggest that: (a) two processes are clearly distinguished in $\text{CF}_3\text{PF}_3(\text{SCH}_3)$, the "pseudorotation"¹⁰² and the rotation of the SCH_3 group about the P-S bond, (b) the ΔG^\ddagger values of 10.0 ± 1.0 and 11.0 ± 1.0 kcal/mole obtained for $(\text{CF}_3)_2\text{PF}_2(\text{SCH}_3)$ and $\text{CH}_3(\text{CF}_3)\text{PF}_2(\text{SCH}_3)$ respectively, are considered indicative of a pure rotation process since there is no spectral evidence for a CF_3 -F positional interchange. These ΔG^\ddagger values are close to the lower of the two values obtained for $\text{CF}_3\text{PF}_3(\text{SCH}_3)$, which is ascribed to the P-S rotational barrier. The higher value of 12.8 ± 2.0 kcal/mole is attributed to a positional interchange process which averages the axial and equatorial fluorine atoms. Also (c) the process which equilibrates the four fluorine environments in F_4PSCH_3 is a coupled combination of both "pseudorotation"¹⁰² and P-S bond rotation from which only one barrier was obtained.

CHAPTER EIGHT

PROPERTIES OF SOME TETRACOORDINATE PHOSPHINE OXIDES AND SULFIDES .

Introduction

The compounds $\text{CH}_3(\text{CF}_3)\text{P}(\text{O})\text{F}$, $\text{CH}_3(\text{CF}_3)\text{P}(\text{O})\text{Cl}$, $\text{CH}_3(\text{CF}_3)\text{P}(\text{O})\text{OCH}_3$ and $\text{CH}_3(\text{CF}_3)\text{P}(\text{S})\text{Cl}$ were obtained as described in Chapter 3, as by-products in attempts to synthesize some phosphoranes. These tetracoordinate phosphorus compounds were characterized through hydrolysis reactions, nmr, ir spectroscopy, and mass spectroscopy.

One aspect of Letcher-van Wazer theory⁵⁸ of phosphorus chemical shifts, the additivity relationship, was applied to the present series of tetracoordinate phosphorus compounds. Letcher and van Wazer have demonstrated by examples that phosphorus chemical shifts are, to a first approximation, determined by the number and kind of atoms directly attached to phosphorus and that the chemical shifts are virtually independent of molecular charge.

The additivity concept of Letcher and van Wazer⁵⁸ says in effect that each directly-bound substituent in a phosphorus compound has a fixed contribution to the overall chemical shift. An empirical treatment was developed in 1962 to accommodate the large deviations from additivity which were known to exist. It was held that (a) the deviation from additivity is generally negative, and (b) the completely mixed tetracoordinate

phosphorus compounds, MPZTX (M = oxygen or sulfur) are covered by the same rationale as the MPZ_2T type of compounds. In other words, values of partial contributions of specific substituents can be used to predict the ^{31}P chemical shifts of phosphorus compounds. For a completely mixed compound MPZTX, the ^{31}P chemical shift is given by

$$\delta_{\text{MPZTX}} = \frac{1}{3} (\delta_{\text{MPZ}_3} + \delta_{\text{MPT}_3} + \delta_{\text{MPX}_3}) \quad (\text{VII-1})$$

and the deviation:

$$\Delta E = \delta_{\text{P}_{\text{observed}}} - \delta_{\text{P}_{\text{calculated}}} \quad (\text{VII-2})$$

Characterization of Methyl(trifluoromethyl)-
phosphine Oxides and Sulfides.

A. Hydrolytic Reactions.

(i) Methyl(trifluoromethyl)chlorophosphine oxide

Methyl(trifluoromethyl)chlorophosphine oxide (0.126 g, 0.759 mmole) was agitated with 0.5 ml of saturated NaOH solution for one week at room temperature. Vacuum fractionation yielded CF_3H (0.0525 g, 0.750 mmole), collected at -196°C , and CH_3PO_3^- which remained in the aqueous solution according to the ^1H nmr spectrum of the solution.

Neutral hydrolysis of $\text{CH}_3(\text{CF}_3)\text{P}(\text{O})\text{Cl}$ (0.050 g, 0.300 mmole) gave no CF_3H . Nmr spectroscopy (^1H , ^{19}F) of the aqueous solution showed the presence of the $\text{CH}_3(\text{CF}_3)\text{PO}_2^-$ ion.³⁴

(ii) Methyl(trifluoromethyl)fluorophosphine oxide

Treatment of $\text{CH}_3(\text{CF}_3)\text{P}(\text{O})\text{F}$ (0.040 g, 0.270 mmole) with 0.5 ml degassed saturated NaOH solution for one week at room temperature yielded CF_3H (0.0173 g, 0.25 mmole) collected at -196°C , and CH_3PO_3^- and F^- ions remained in the aqueous solution.

Treatment of $\text{CH}_3(\text{CF}_3)\text{P}(\text{O})\text{F}$ (0.096 g, 0.64 mmole) with water yielded no CF_3H . Nmr spectroscopy of the aqueous solution indicated the presence of $\text{CH}_3(\text{CF}_3)\text{PO}_2^-$ and HF_2^- ions.

(iii) Methyl(trifluoromethyl)(methoxy)phosphine oxide

Treatment of $\text{CH}_3(\text{CF}_3)\text{P}(\text{O})\text{OCH}_3$ (0.040 g, 0.244 mmole) with 0.8 ml degassed saturated NaOH solution for 10 days yielded, upon vacuum fractionation, CF_3H (0.028 g, 0.240 mmole) in the volatile fraction and CH_3PO_3^- ions and CH_3OH in the aqueous solution according to ^1H nmr.

Neutral hydrolysis of $\text{CH}_3(\text{CF}_3)\text{P}(\text{O})\text{OCH}_3$ (0.103 g, 0.496 mmole) yielded no CF_3H . ^{19}F and ^1H nmr spectra of the aqueous solution indicated the presence of CH_3OH and $\text{CH}_3(\text{CF}_3)\text{PO}_2^-$ ions in a 1:1 molar ratio.

(iv) Methyl(trifluoromethyl)chlorophosphine sulfide

No quantitative characterization was done on $\text{CH}_3\text{CF}_3\text{P}(\text{S})\text{Cl}$ because a pure sample could not be obtained. The compound was tentatively identified by means of infrared, nuclear magnetic resonance, and mass spectroscopy.

TABLE 14

Infrared Spectra of Tetracoordinated
Phosphorus Compounds^a

$\text{CH}_3\text{CF}_3\text{P(O)F}$	$\text{CH}_3\text{CF}_3\text{P(O)Cl}$	$\text{CH}_3\text{CF}_3\text{P(O)(OCH}_3\text{)}$	$\text{CH}_3\text{CF}_3\text{P(S)Cl}$	Assignment ^b
1420 w	1411 w	-	1410 m	$\sigma_{\text{as}} \text{CH}_3$
1340 s	1316 s	1320 m	-	$\nu_{\text{P=O}}$
1300 m	1291 m	1296 m	1295 m	$\sigma_{\text{sym}} \text{CH}_3$
1230 s	1211 m	1236 m	1204 s	} ν_{CF_3}
1160 s	1176 s	1151 s	1170 s	
-	1156 s	-	1150 s	
-	-	1050 s	-	P-OCH ₃
920 s	921 m	903 m	910 s	} P-CH ₃
883 s	893 m	884 m	885 s	
850 s	-	-	-	$\nu_{\text{P-F}}$
-	-	809 w	790 s	} $\sigma_{\text{as}} \text{CF}_3(?)$
765 m	766 m	757 w	745 vw	
730 m	739 m	727 w	-	
-	-	-	675 s	P = S
-	611 w	-	-	} $\nu_{\text{P-Cl}}$
540 w	561 s	-	540 w	
-	529 m	-	510 s	
480 s	471 w	499 m	400 s	} $\nu_{\text{P-CF}_3}$
420 m	444 m	464 w	405 s	
-	404 w	-	-	

^a Gas phase spectra, all values in cm^{-1} . s = strong, m = medium, w = weak, ν = stretching, σ = deformation, sym = symmetric, as = antisymmetric, ? = very tentative.

^b These assignments are tentative, and based mainly on available data on related compounds. See for instance, ref. 41, 103.

TABLE 15

NMR Data for Methyl(trifluoromethyl)phosphine Oxides

Compound	Temp	τ^a	ϕ_F^b	$\phi_{CF_3}^b$	σ_{31P}^c	$1^d J_{PF}$	$2^d J_{PF}$	$3^d J_{PH}$	$3^d J_{FH}$	$4^d J_{FH}$	$5^d J_{FH}$	$3^d J_{FF}$	$4^d J_{FF}$
$CH_3(CF_3)P(O)F$	30°	8.48	81.8	76.3	77.7	1076	117	16.7	=	8.3	0.7	-	7.5
$CH_3(CF_3)P(O)Cl$	30°	8.00	-	76.7	73.0	-	116	14.9	-	0.7	-	-	-
$CH_3(CF_3)P(O)OCH_3$	30°	8.33 ^e 6.13 ^f	-	76.3	79.3	-	98.5	15.9	10.8	0.7	0.6	-	-
$CH_3(CF_3)P(S)Cl$	30°	7.66	-	76.6	77.2	-	109.9	14.2	-	0.7 ^g	-	-	-

^a τ ppm relative to internal tetramethylsilane, $\tau = 10.0$ ^b ϕ ppm relative to internal CCl_3F standard with positive values indicating resonance to high field of the standard.^c ppm vs. P_4O_6 as external (capillary), positive values indicating resonance to high field of standard.
^d units in Hertz^e CH_3 region, doublet of quartets^f OCH_3 region, doublet of quartets^g from expansion of 1H nmr spectrum, a doublet of quartets

TABLE 16.

Mass Spectral Data for $\text{CH}_3(\text{CF}_3)\text{P}(\text{O})\text{F}$, $\text{CH}_3(\text{CF}_3)\text{P}(\text{O})\text{OCH}_3$
and $\text{CH}_3(\text{CF}_3)\text{P}(\text{S})\text{Cl}$

m/e	Intensity ^a		Assignment ^b
	$\text{CH}_3(\text{CF}_3)\text{P}(\text{O})\text{F}$	$\text{CH}_3(\text{CF}_3)\text{P}(\text{O})\text{OCH}_3$	
182		2.56	$\text{CH}_3(\text{CF}_3)\text{P}(\text{S})\text{Cl}$
150	9.89		$\text{CH}_3(\text{CF}_3)\text{P}(\text{O})\text{F}$
149		0.49	$\text{C}_2\text{H}_5\text{F}_3\text{O}_2\text{P}$, $\text{C}_2\text{H}_2\text{F}_3\text{ClP}$
148		0.89	$\text{C}_2\text{H}_4\text{F}_3\text{O}_2\text{P}$, $\text{C}_2\text{HF}_3\text{ClP}$
147		5.92	$\text{CF}_3\text{P}(\text{O})(\text{OCH}_3)$, $\text{CH}_3\text{CF}_3\text{PS}$
132		0.26	$\text{CF}_3\text{O}_2\text{P}$
131		0.36	$\text{CH}_3\text{CF}_3\text{P}(\text{O})$
117		0.51	$\text{C}_2\text{HF}_3\text{Cl}$
115		4.55	$\text{C}_2\text{H}_3\text{F}_3\text{P}$
114		0.28	$\text{C}_2\text{H}_2\text{F}_3\text{P}$
113		11.39	$\text{CH}_3\text{P}(\text{S})\text{Cl}$
109	0.99		$\text{C}_2\text{H}_3\text{FO}_2\text{P}$

TABLE 16 (continued)

103	4.30	0.33	1.14	$\text{CH}_3\text{F}_3\text{P}$
101	6.24			CHF_3P
100			0.28	CH_3PFCl
99			0.60	CH_2FClP
98			0.37	ClPS
97		0.36	10.82	$\text{C}_2\text{H}_3\text{F}_2\text{O}_2$, CFClP
96			0.34	CH_2FPS
95		0.43	0.43	$\text{C}_2\text{HF}_2\text{O}_2$, CHFPS
94		0.99	2.85	$\text{C}_2\text{F}_2\text{O}_2$, $\text{C}_2\text{H}_6\text{S}_2$
93		9.87	0.82	$\text{CH}_3\text{P}(\text{O})(\text{OCH}_3)$, $\text{C}_2\text{H}_5\text{S}_2$
92		6.58		$\text{C}_2\text{H}_5\text{O}_2\text{P}$
87			0.48	H_2FClP
85			1.39	FClP
84	6.02			$\text{C}_2\text{H}_3\text{F}_3$
83			0.91	$\text{C}_2\text{H}_2\text{F}_3$
82			0.28	C_2HF_3
81	17.20	2.96	3.13	CH_3FOP , C_2F_3

TABLE 16 (continued)

80			0.34	CH ₄ S ₂
79		0.99	1.99	CHFOP, CH ₃ S ₂
78		1.32	1.71	CFOP, CH ₂ S ₂
77		13.17	7.12	C ₂ H ₆ OP, CHS ₂
75		0.39	8.85	C ₂ H ₄ OP, CCLPS
74		1.65	0.48	C ₂ H ₃ OP, H ₃ F ₂ P
73		1.65	0.60	C ₂ H ₂ OP, H ₂ F ₂ P
69	17.63	2.63	2.85	CF ₃ , PF ₂
66			0.31	ClP
65	16.99	2.30	4.55	CH ₃ FP, CH ₆ OP
64			0.31	CH ₂ FP
63		13.17	8.26	CH ₄ OP, CHFP
62		1.32		CH ₃ OP, CFP
61			0.37	C ₂ H ₅ S
59		3.29		COP, C ₂ FO
50	4.52		0.40	CF ₂ , FP, CH ₃ Cl
49		1.65		CH ₂ OF

TABLE 16 (continued)

48			0.48	CHCl
47	17.20	8.89	1.00	CFO, CCl
46			1.22	CH ₃ P
45		4.61	5.69	CHO ₂ , CH ₂ P
44		0.39	1.42	CO ₂
43		0.76		CP
41		0.86		C ₃ H ₅
38			0.28	C ₃ H ₂
36			0.74	HCl
34		0.39		H ₂ O ₂
32		2.96	0.45	CHF, HP
31		6.75	0.31	CH ₃ O, CF
30		0.39		C ₂ H ₆

^a Intensity is expressed as % total ionization based on the sum of the intensities of ions with m/e greater than 30.

^b Assignments of some ions are given in terms of the structural formula for ease of recognition only.

TABLE 17

Mass Measurement Data for Tetracoordinated
Phosphorus Compounds

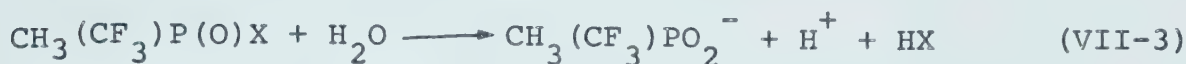
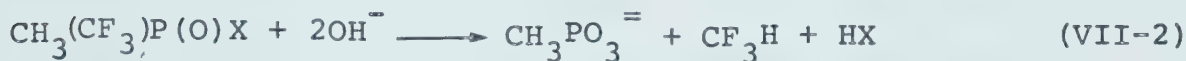
Compound	Ion ^a	m/e	
		Calculated	Measured
$\text{CH}_3(\text{CF}_3)\text{P}(\text{O})\text{F}$	$\text{CH}_3(\text{CF}_2)\text{P}(\text{O})\text{F}^+$	149.9858	149.9858
	CF_3^+	68.9952	68.9952
$\text{CH}_3(\text{CF}_3)\text{P}(\text{O})\text{CH}_3$	$\text{CH}_3(\text{CF}_3)\text{P}(\text{O})\text{OCH}_3^+$	162.0058	162.0066
	$\text{CH}_2(\text{CF}_3)\text{P}(\text{O})\text{OCH}_3^+$	160.9979	160.9970
	$\text{CF}_3\text{P}(\text{O})\text{OCH}_3^+$	149.9828	146.9819
	$\text{CH}_3(\text{CF}_3)\text{PO}^+$	130.9874	130.9868
	$\text{CH}_3\text{P}(\text{O})\text{OCH}_3^+$	93.0105	93.0110
$\text{CH}_3(\text{CF}_3)\text{P}(\text{S})\text{Cl}$	$\text{CH}_3(\text{CF}_3)\text{P}(\text{S})\text{Cl}^+$	181.9334	181.9341
	$\text{CH}_3(\text{CF}_3)\text{PCl}^+$	149.9613	149.9609
	$\text{CH}_3(\text{CF}_3)\text{PS}^+$	146.9645	146.9649
	$\text{CH}_3\text{P}(\text{S})\text{Cl}^+$	112.9381	112.9385
	CH_3PFCl^+	99.9645	99.9649
	$(\text{CH}_3)_2\text{S}^+$	62.0189	62.0192

^a A reasonable structural formula rather than the molecular formula is given for each fragment ion merely for convenience of recognition.

Discussion of Results

A. Hydrolytic Reaction.

The hydrolytic reactions of the phosphine oxides are summarized by the following equations:



In neutral media HCl is dissociated and HF forms HF_2^- . In alkaline media both HF and HCl give the halide ions F^- and Cl^- , respectively.

B. Infrared Spectra.

The infrared spectral bands of the phosphine oxides and chlorophosphine sulfide indicated by characteristic absorptions the presence of major structural units in each compound (Table 14). For instance the medium to strong intensity absorption bands between $1295\text{--}1300\text{ cm}^{-1}$ may be assigned to the symmetric C-H deformation. The P=O bond in $\text{CH}_3(\text{CF}_3)\text{P}(\text{O})\text{F}$, $\text{CH}_3(\text{CF}_3)\text{P}(\text{O})\text{Cl}$ and $\text{CH}_3(\text{CF}_3)\text{P}(\text{O})\text{OCH}_3$ was indicated by the absorption band lying between 1316 and 1340 cm^{-1} , and the P=S bond in $\text{CH}_3(\text{CF}_3)\text{P}(\text{S})\text{Cl}$ by the bands between 675 and 790 cm^{-1} . Characteristic P-X (X = halogen) absorptions are observed at $808\text{--}835\text{ cm}^{-1}$ in $\text{CH}_3(\text{CF}_3)\text{P}(\text{O})\text{F}$, at 522 in $\text{CH}_3(\text{CF}_3)\text{P}(\text{O})\text{Cl}$, and at $465\text{--}532\text{ cm}^{-1}$ in $\text{CH}_3(\text{CF}_3)\text{P}(\text{S})\text{Cl}$.

C. Mass Spectra.

The mass spectra of the tetracoordinate phosphorus compounds $\text{CH}_3(\text{CF}_3)\text{P}(\text{O})\text{F}$, $\text{CH}_3(\text{CF}_3)\text{P}(\text{O})(\text{OCH}_3)$ and $\text{CH}_3(\text{CF}_3)\text{P}(\text{S})\text{Cl}$ showed the parent ion peak in relatively good abundance and were confirmed by accurate mass measurement (Tables 16 and 17, respectively). All the compounds likewise showed CF_3^+ in their mass spectra (m/e calc., 68.9952; m/e meas., 68.9952).

D. Nmr Spectra.

(i) Methyl(trifluoromethyl)chlorophosphine oxide

The ^1H and ^{19}F nmr spectra of $\text{CH}_3(\text{CF}_3)\text{P}(\text{O})\text{Cl}$ each gave a first-order AX_3 splitting pattern from which the nmr parameters were readily evaluated (Figs VIII-1 and 2, respectively). The four-bond F-H coupling was not resolved in either spectrum and the lines were consequently broad. The ^{31}P nmr spectrum showed a sixteen line A_3MX_3 pattern; the major quartet due to P- CF_3 coupling and the minor quartet due to phosphorus coupling with the CH_3 protons (Fig VIII-3).

(ii) Methyl(trifluoromethyl)fluorophosphine oxide

The ^1H nmr spectrum of $\text{CH}_3(\text{CF}_3)\text{P}(\text{O})\text{F}$ consisted of four equally separated quartets of equal total intensities. This is analyzed as a doublet of doublets, the principal doublet splitting arising from the coupling of the CH_3 protons with phosphorus and the secondary doublet splitting

Figure VIII-1 Experimental ^1H (60.0 MHz) nmr spectrum of $\text{CH}_3(\text{CF}_3)\text{P}(\text{O})\text{Cl}$ at 303°K obtained from a solution in CFCl_3 containing 5% TMS. The frequency scale gives chemical shift values in Hz relative to TMS.

^1H (60.0 MHz) nmr Spectrum of

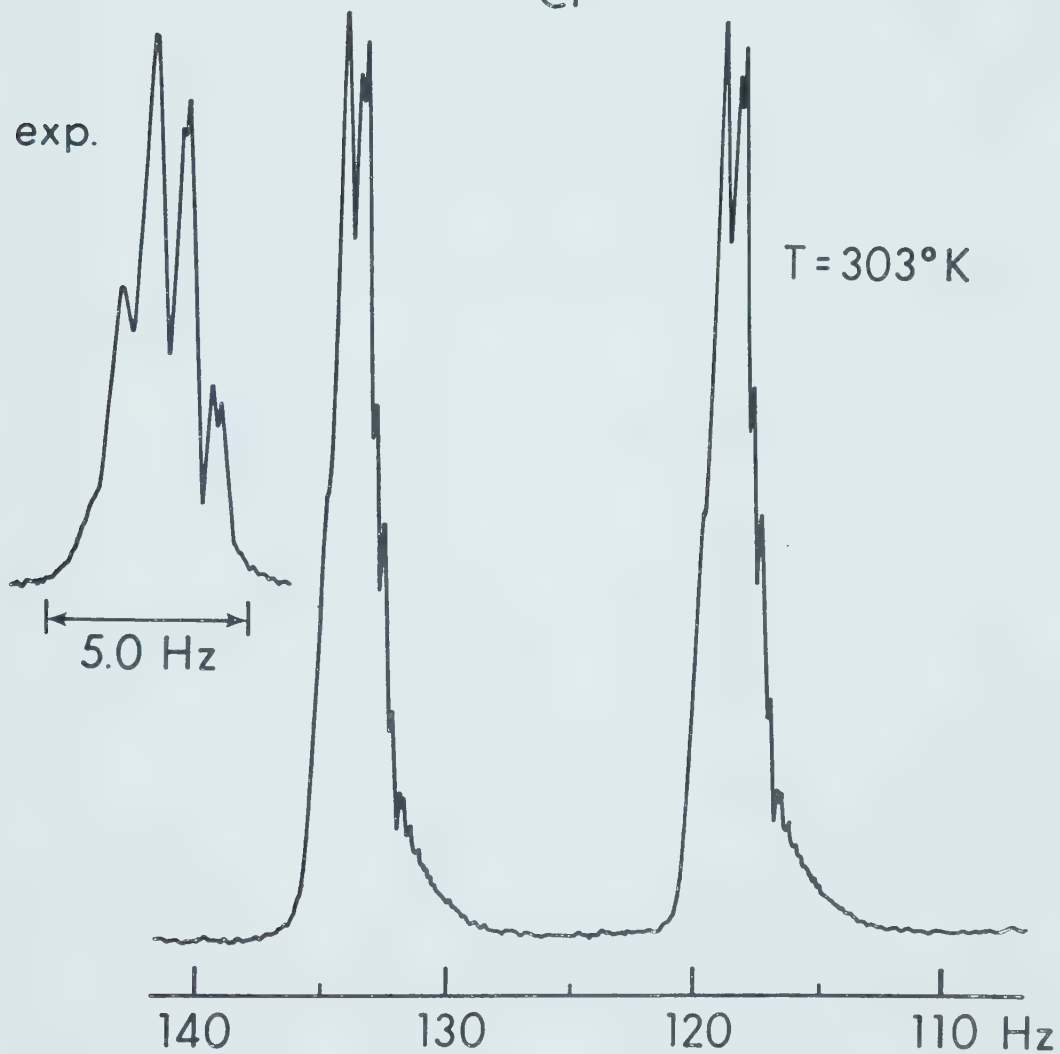
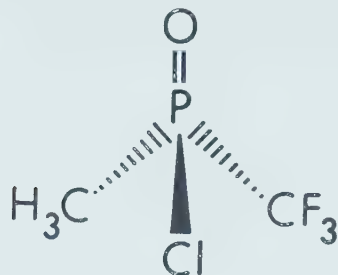


Figure VIII-1

Figure VIII-2 Observed ^{19}F (56.4 MHz) nmr spectrum of $\text{CH}_3(\text{CF}_3)\text{P}(\text{O})\text{Cl}$ at 303°K obtained from a solution in CFCl_3 containing 5% TMS. The frequency scale gives chemical shift values in Hz relative to CFCl_3 .

^{19}F (56.4 MHz) nmr Spectrum of

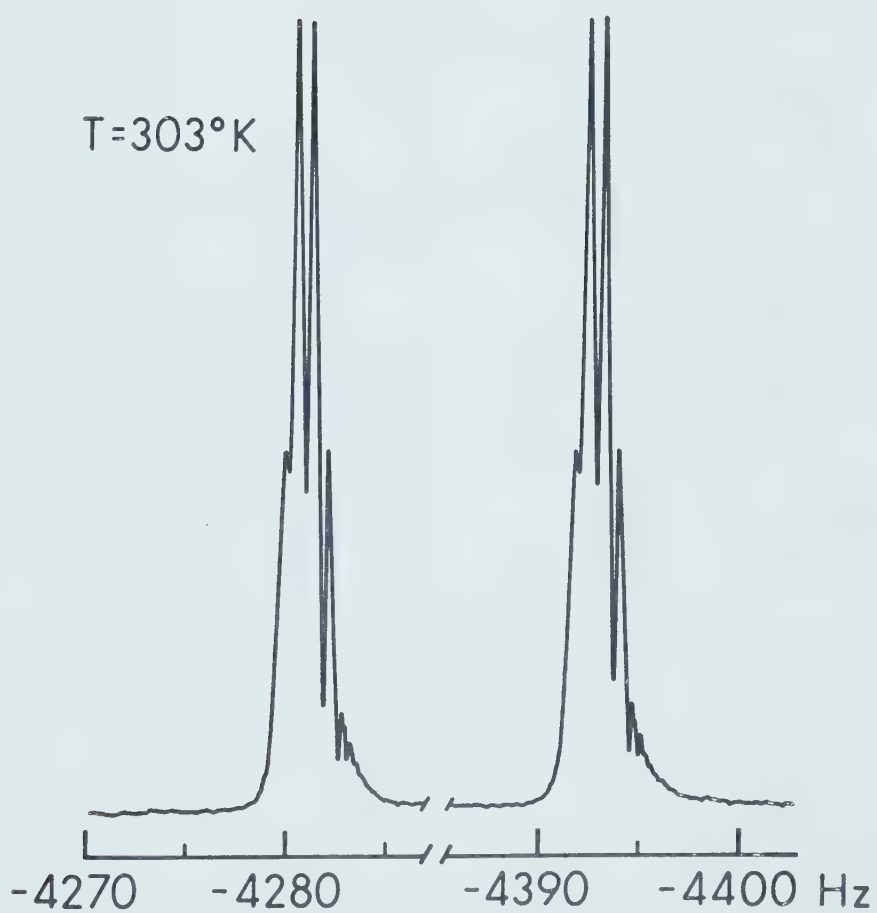


Figure VIII-2

Observed ^{31}P (36.4 MHz) nmr spectrum of $\text{CH}_3(\text{CF}_3)_2\text{P}(\text{O})\text{Cl}$ at 303°K obtained from a solution in CFCl_3 containing 5% TMS. The frequency scale which gives chemical shift values in Hz relative to P_4O_6 was measured relative to CFCl_3 as the ^{19}F heteronuclear lock and subsequently converted to the ^{31}P scale.

Figure VIII-3

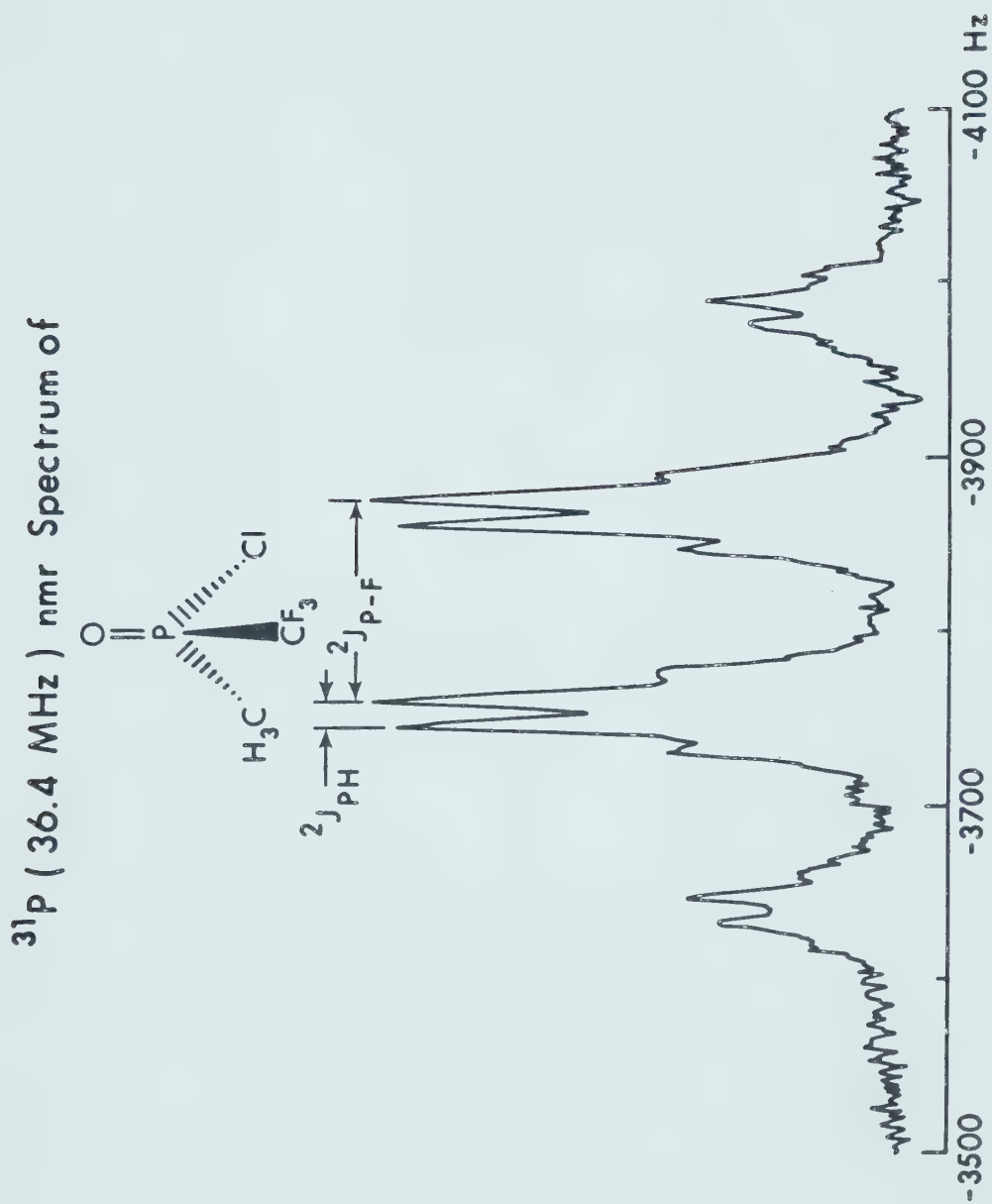
Figure VIII-3

Figure VIII-4 Observed ^1H (60.0 MHz) spectrum of $\text{CF}_3(\text{CH}_3)\text{P}(\text{O})\text{F}$ obtained from a solution in CCl_3F containing 5% TMS. The frequency scale gives chemical shift values in Hz relative to TMS.

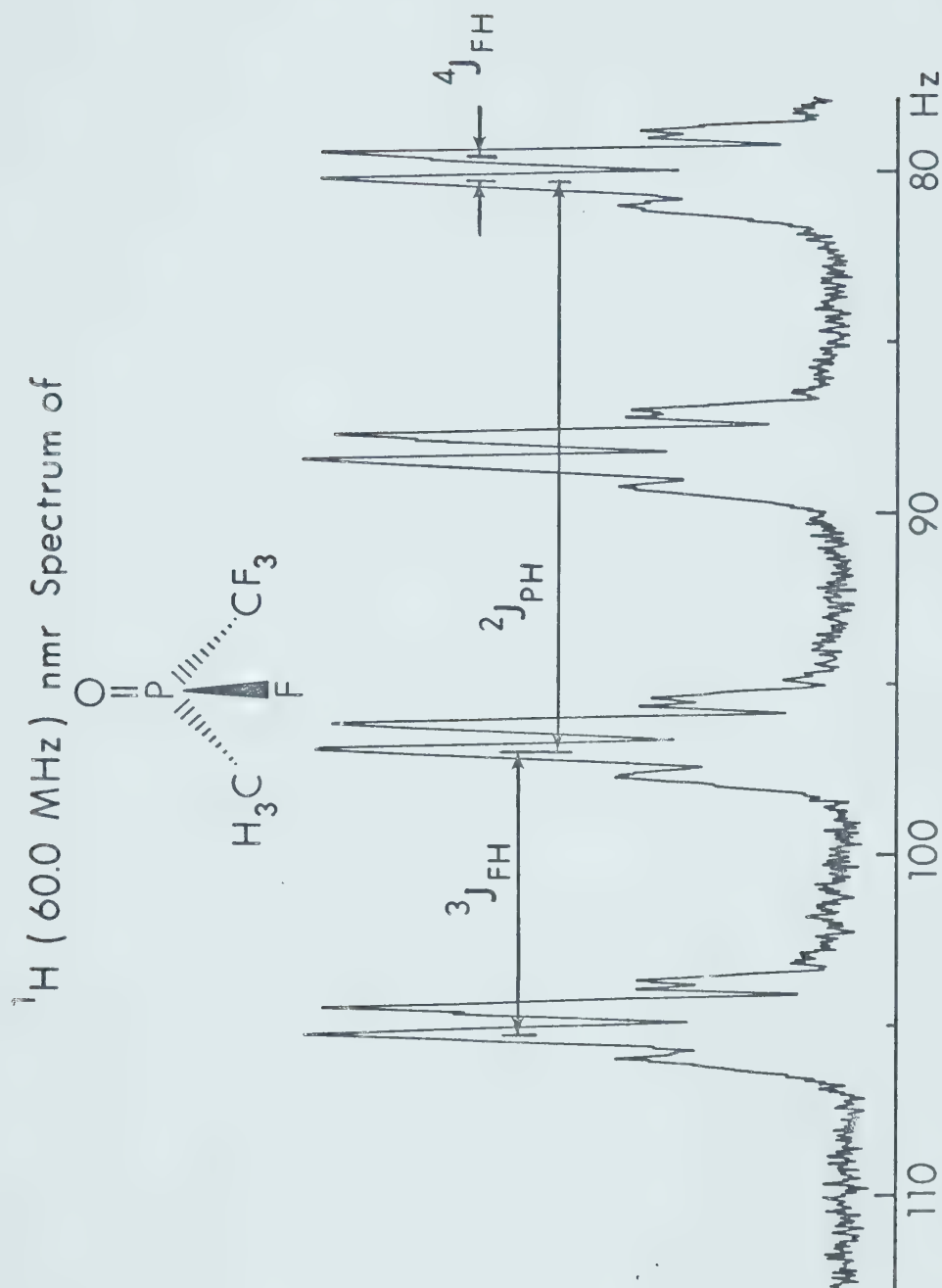


Figure VIII-4

Figure VIII-5 Experimental ^{31}P (36.4 MHz) nmr spectrum of $\text{CH}_3(\text{CF}_3)\text{P}(\text{O})\text{F}$ at 303°K obtained from a solution in CFCl_3 containing 5% TMS. The frequency scale which gives chemical shift values in Hz relative to P_4O_6 was measured relative to the ^{19}F (CFCl_3) heteronuclear lock and subsequently converted to the ^{31}P scale.

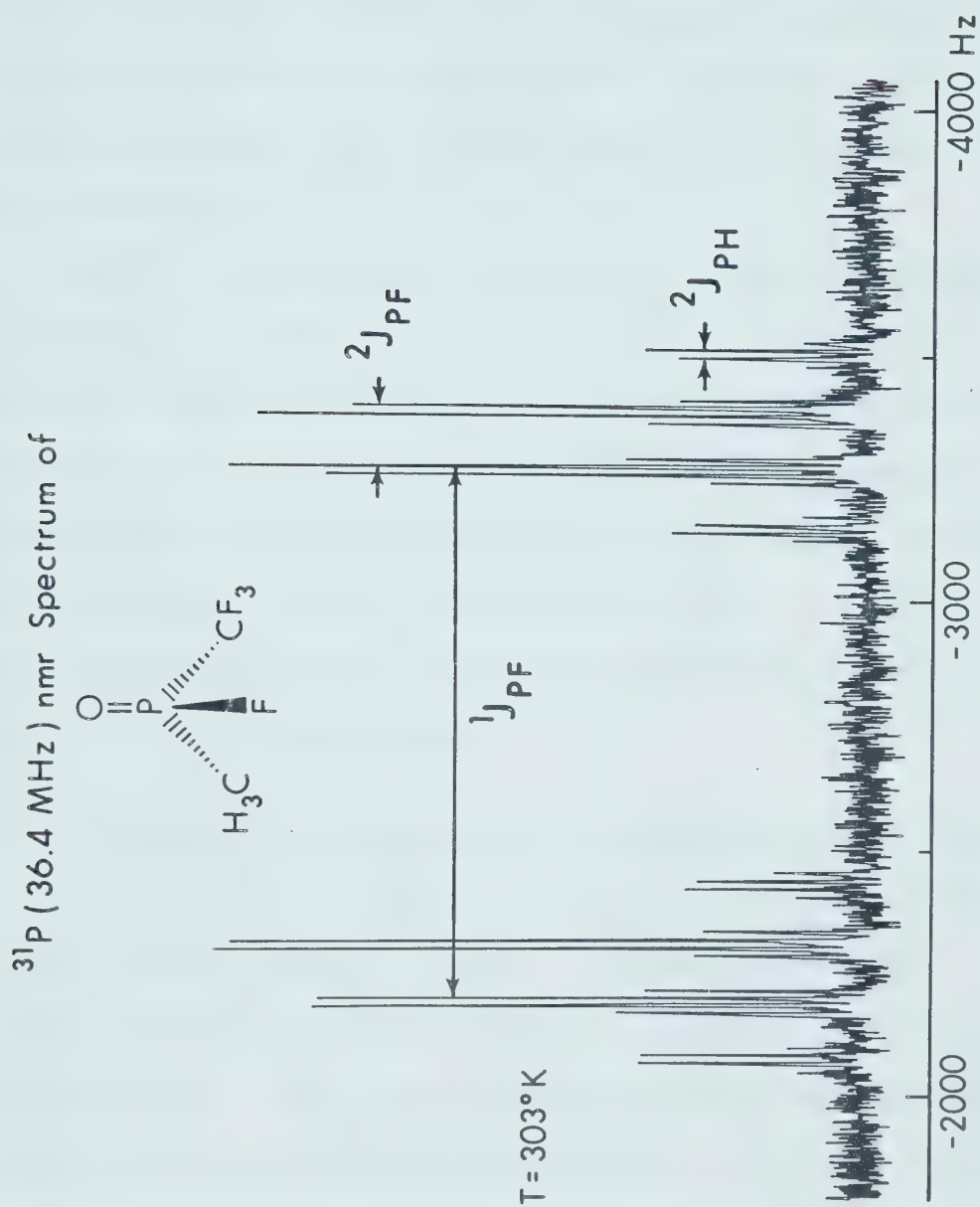


Figure VIII-5

from proton coupling with the directly-bound fluorine. The quartet fine structure is due to further coupling of the CH_3 protons with the three fluorines of the CF_3 group (Fig VIII-4). That the line separations are due to spin-spin coupling and not to chemical shift difference was demonstrated by the invariance of the splitting pattern and magnitudes of line separation with spectrometer frequency.

The ^{31}P nmr spectrum of $\text{CH}_3(\text{CF}_3)\text{P}(\text{O})\text{F}$ was a doublet of quartets of quartets, giving a total of 32 lines. The major quartet splitting of the P-F doublet components was due to phosphorus coupling with the CF_3 fluorines and the minor quartet splitting due to coupling of the phosphorus with the CH_3 protons (Fig VIII-5). The parameters evaluated from this supported the interpretation of the ^1H nmr spectrum.

(iii) Methyl(trifluoromethyl)methoxy phosphine oxide

The ^1H nmr spectrum of $\text{CH}_3(\text{CF}_3)\text{P}(\text{O})\text{OCH}_3$ consisted of two sets of doublets of equal intensities. The components of the doublets showed a quartet fine structure upon expansion. The two resonance regions corresponded to the two different groups of protons. The low field resonance was assigned to the OCH_3 group, the high field resonance to the CH_3 group. The doublet splitting in each resonance resulted from proton coupling with phosphorus and the quartet fine structure from proton coupling

with the CF_3 fluorines. The five-bond proton-proton coupling was not resolved and thus the lines are rather broad (Fig VIII-6).

The ^{19}F nmr spectrum was a broad doublet with each component showing a septet fine structure upon expansion with peak separation of about 0.72 Hz. Again, this "septet" resulted from near equality of $^3J_{\text{F-H}}$ and $^4J_{\text{F-H}}$ (0.78 Hz and 0.62 Hz, respectively) (Fig VIII-7).

The proton-coupled ^{31}P nmr spectrum consisted of a quartet of multiplets which, upon analysis of the line intensities, was shown to be a quartet of quartets of quartets. The main quartet splitting arose from phosphorus coupling with CF_3 , the secondary quartet splitting from phosphorus coupling with CH_3 protons and the final quartet fine structure is due to phosphorus coupling with the OCH_3 group. The stick diagram in Figure VIII-8 traces the origin of the splittings.

(iv) Methyl(trifluoromethyl)chlorophosphine sulfide

The ^1H nmr spectrum of $\text{CH}_3(\text{CF}_3)\text{P}(\text{S})\text{Cl}$ showed doublet splitting due to P-H coupling and a quartet fine structure on each doublet component upon expansion, arising from proton coupling with the CF_3 group.

Similarly, the ^{19}F nmr spectrum was a doublet of quartets, the doublet due to $^2J_{\text{P-F}}$ and the quartet due to $^4J_{\text{F-H}}$ (Fig VIII-9).

Figure VIII-6 Observed ^1H (100.1 MHz) nmr spectrum of $\text{CH}_3(\text{CF}_3)_2\text{P}(\text{O})\text{OCH}_3$ at 303°K obtained from a solution in CFCl_3 containing 5% TMS. Chemical shift values are given in Hz relative to internal TMS.

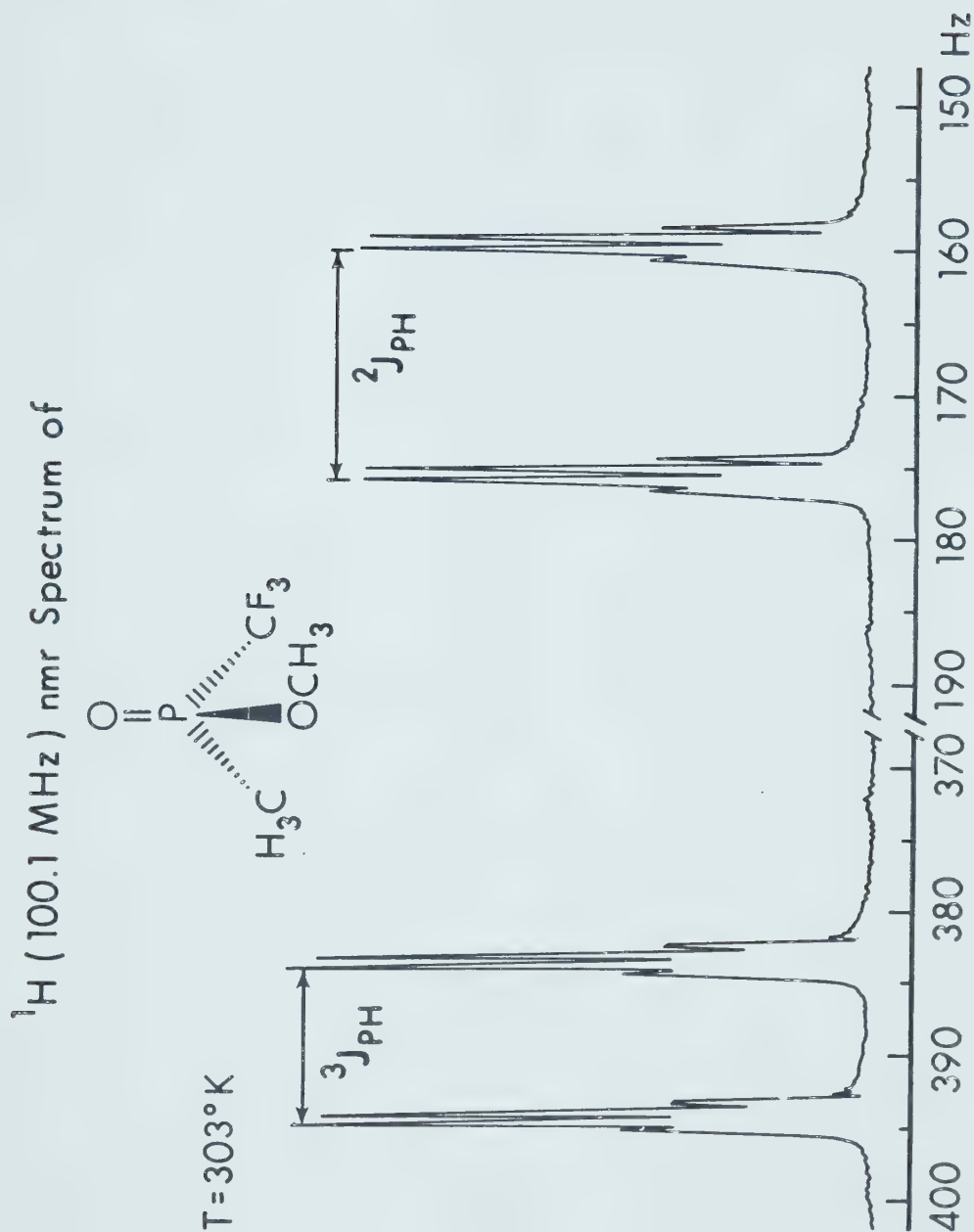


Figure VIII-6

Figure VIII-7 Observed ^{19}F (94.1 MHz) spectrum of $\text{CH}_3(\text{CF}_3)\text{P}(\text{O})\text{OCH}_3$ at 303°K obtained from a solution in CFCl_3 containing 5% TMS. The frequency scale gives chemical shift values in Hz relative to internal CFCl_3 . The expanded scale portion in the center shows the fine structure of one of the components of the major doublet.

^{19}F (94.1 MHz) nmr Spectrum of

$T = 303^\circ\text{K}$

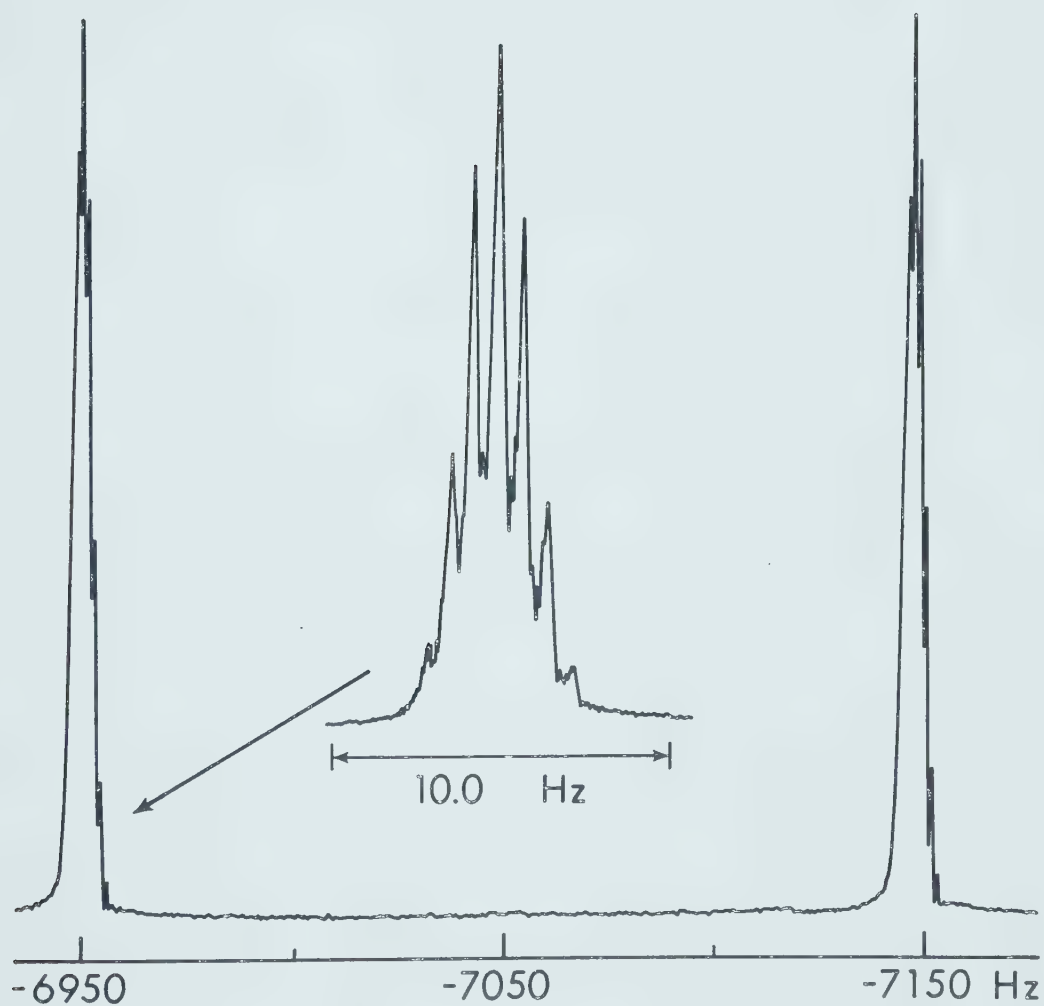
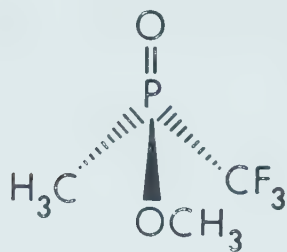
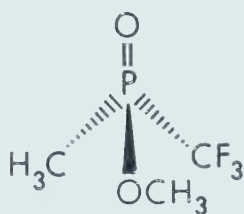


Figure VIII-7

Figure VIII-8 Observed $^{31}\text{P} \sim \{^1\text{H}\}$ (36.4 MHz) nmr spectrum of $\text{CH}_3(\text{CF}_3)\text{P}(\text{O})\text{OCH}_3$ at 300°K, obtained from a solution in CFCl_3 containing 5% TMS. The frequency scale which gives chemical shift values in Hz relative to P_4O_6 was measured relative to the ^{19}F (CFCl_3) heteronuclear lock and subsequently converted to the ^{31}P scale. The stick diagram traces the pattern of a quartet of quartets of quartets arising from splitting due to a CF_3 group, a CH_3 group and a OCH_3 group.

^{31}P (36.4 MHz) $\sim \{^1\text{H}\}$ nmr Spectrum of



$T=300^\circ\text{K}$

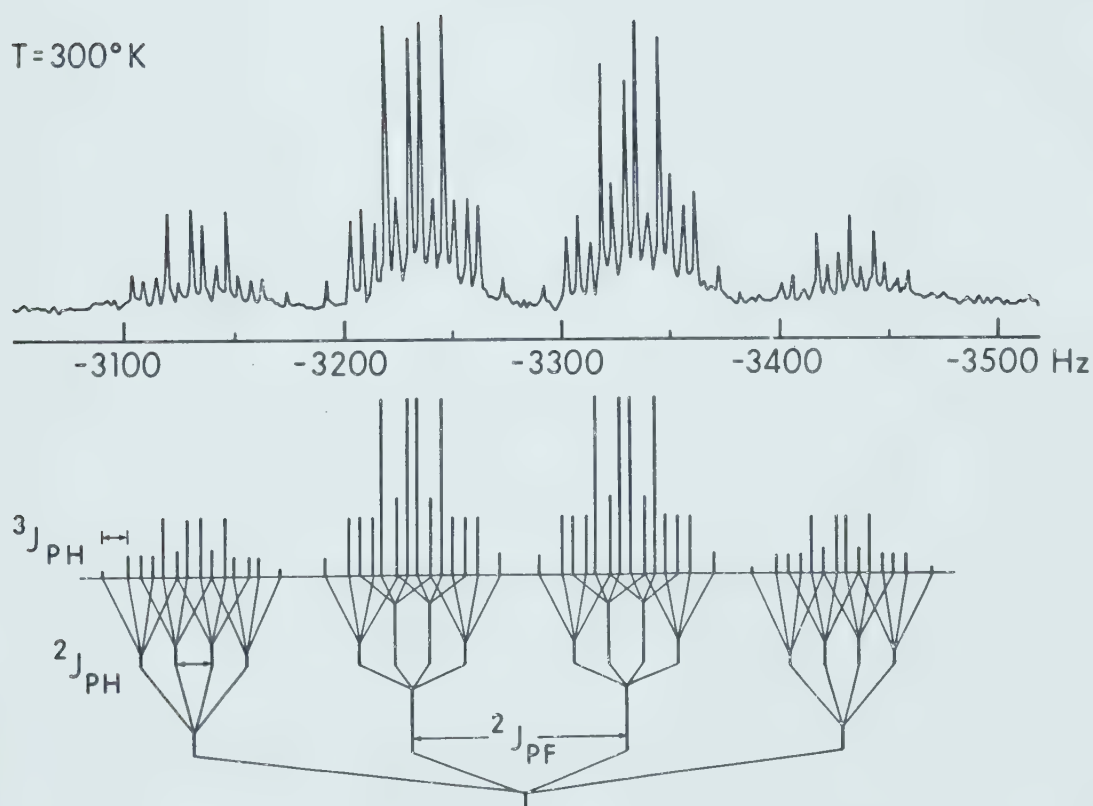


Figure VIII-8

Figure VIII-9 Observed ^{19}F (94.1 MHz) nmr spectrum of $\text{CH}_3(\text{CF}_3)\text{P}(\text{S})\text{Cl}$ at 303°K obtained from a solution in CFCl_3 containing 5% TMS. The frequency scale gives chemical shift values in Hz measured relative to internal CFCl_3 .

^{19}F (94.1 MHz) nmr Spectrum of

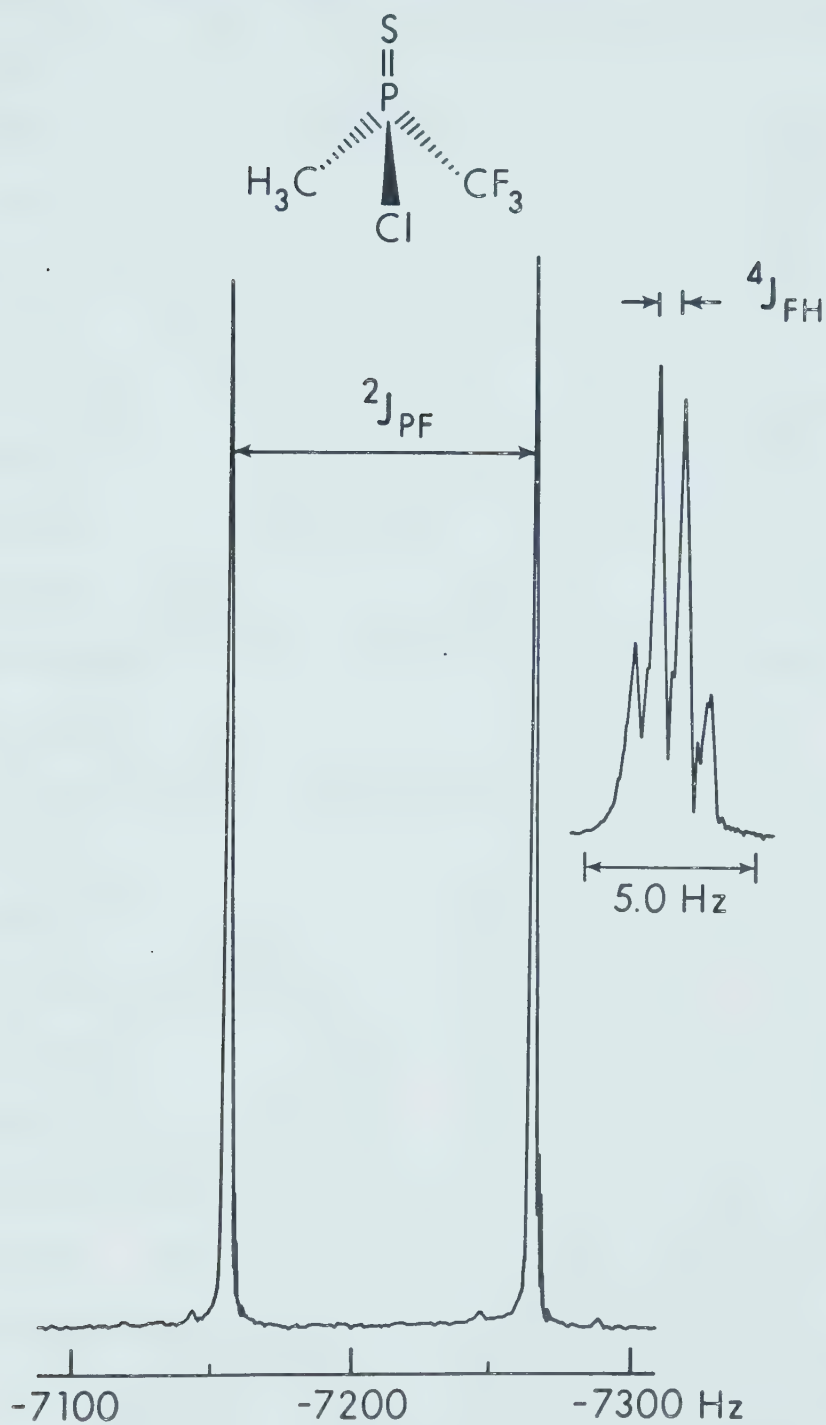


Figure VIII-9

The ^{31}P nmr spectrum was a quartet of quartets, the major quartet arising from coupling of phosphorus with the CF_3 fluorines, the minor quartet arising from coupling with the CH_3 protons.

The chemical shifts observed for the three phosphorus oxides $\text{CH}_3(\text{CF}_3)\text{P}(\text{O})\text{Cl}$ (+73.0 ppm (*vs.* P_4O_6)), $\text{CH}_3(\text{CF}_3)\text{P}(\text{O})\text{F}$ (+63.2 ppm), and $\text{CH}_3(\text{CF}_3)\text{P}(\text{O})(\text{OCH}_3)$ (+79.3 ppm) lie within the range reported for tetracoordinate phosphorus compounds.⁹² Attempts were made to see whether these chemical shift values conform to the additivity rule postulated by Letcher and van Wazer⁵⁸ discussed earlier in this chapter. The predicted ^{31}P chemical shifts were obtained from eq VIII-1, using the chemical shift values reported for $(\text{CH}_3)_3\text{PO}$, $(\text{CF}_3)_3\text{PO}$, Cl_3PO , F_3PO , and $(\text{CH}_3\text{O})_3\text{PO}$.³³ Upon making the necessary adjustment with respect to the reference compound and comparing the predicted ^{31}P chemical shift values with experimental values, the following deviations were obtained: -26.8 ppm for $\text{CH}_3(\text{CF}_3)\text{P}(\text{O})\text{Cl}$, -50.5 ppm for $\text{CH}_3(\text{CF}_3)\text{P}(\text{O})\text{F}$, and -21.0 ppm for $\text{CH}_3(\text{CF}_3)\text{P}(\text{O})\text{OCH}_3$. All the deviations are negative, in agreement with the postulate mentioned earlier in the chapter. However, these deviations are surprisingly large, suggesting that the approach leaves much to be desired. The empirical nature of the additivity concept precludes any analysis of the origin or the significance of these deviations. However, we might reasonably expect

an empirical approach to give reasonably good agreement with experiment even if the formal justification is not particularly rigorous.

Conclusions

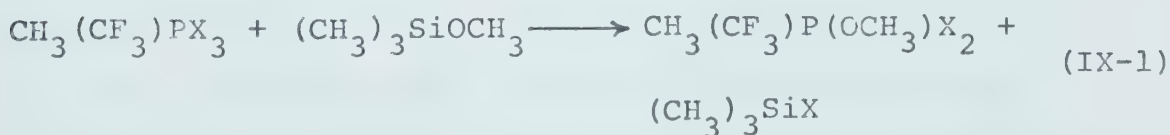
The greater stability of tetracoordinate phosphorus compounds compared to pentacoordinate phosphorus compounds is manifested by their hydrolytic reactions.

The additivity concept of Letcher and van Wazer⁵⁸ was applied to the three phosphine oxides. The deviations from additivity were negative as predicted in the formalism but the large deviations in all the three cases suggest that the approach is not particularly reliable.

CHAPTER NINE

SUMMARY AND CONCLUSIONS

As stated in the first chapter, the aims of this work were twofold: (1) to extend our knowledge of the chemistry of pentacoordinate phosphorus compounds and (2) to understand the factors that influence the positional preferences of the different substituents in pentacoordinate trigonal bipyramidal phosphoranes. The experimental results described and discussed in Chapters III and IV did illustrate some interesting substitutional chemistry of pentavalent pentacoordinate phosphorus compounds. The reactions of $\text{CH}_3(\text{CF}_3)\text{PX}_3$ ($\text{X} = \text{F}, \text{Cl}$) with either $(\text{CH}_3)_3\text{SiOCH}_3$ or $(\text{CH}_3)_3\text{SiSCH}_3$ sharply demonstrated the different chemical behavior of the chloro- and the fluorophosphoranes. It appears that the initial step in the reactions is a metathetical substitution of a halogen substituent in the halophosphorane with OCH_3 (or SCH_3 , eq IX-1).



In the case of $\text{CH}_3(\text{CF}_3)\text{PCl}_3$, the monomethoxydichlorophosphorane, $\text{CH}_3(\text{CF}_3)\text{P}(\text{OCH}_3)\text{Cl}_2$, appeared to immediately decompose into the phosphoryl halide and CH_3Cl (eq III-10), whereas further substitution occurred in $\text{CH}_3(\text{CF}_3)\text{P}(\text{OCH}_3)\text{F}_2$

producing $\text{CH}_3(\text{CF}_3)\text{P}(\text{OCH}_3)_2\text{F}$ which, although sufficiently stable to be detected in the nmr spectrum, nevertheless appeared to decompose into $\text{CH}_3(\text{CF}_3)\text{P}(\text{O})\text{F}$ and $(\text{CH}_3)_2\text{O}$ (eq III-14) with time. A metathetical substitution reaction between $\text{CH}_3(\text{CF}_3)\text{P}(\text{O})\text{F}$ and $(\text{CH}_3)_3\text{SiOCH}_3$ (eq III-15) was further postulated to account for the detection of $\text{CH}_3(\text{CF}_3)\text{P}(\text{O})\text{OCH}_3$ in the reaction system.

The reactions of $(\text{CF}_3)_2\text{PXN}(\text{CH}_3)_2$ ($\text{X} = \text{F}, \text{Y} = \text{Cl}; \text{X} = \text{Y} = \text{Cl}, \text{F}$) with $(\text{CH}_3)_3\text{SiOCH}_3$ similarly showed contrasting behavior of the fluoro- and the chlorophosphoranes. The greater lability of the P-Cl bond relative to the P-F bond was amply demonstrated in the greater resistance to or more rigorous conditions required for the reaction of the fluoro(dimethylamino)phosphoranes with $(\text{CH}_3)_3\text{SiOCH}_3$ compared to the chloroanalog. For instance, $(\text{CF}_3)_2\text{PF}(\text{OCH}_3)\text{N}(\text{CH}_3)_2$ was readily formed from the reaction between $(\text{CF}_3)_2\text{PFClN}(\text{CH}_3)_2$ and $(\text{CH}_3)_3\text{SiOCH}_3$ in sharp contrast to the high temperature required for its formation from and the incompleteness of the reaction between $(\text{CF}_3)_2\text{PF}_2\text{N}(\text{CH}_3)_2$ and $(\text{CH}_3)_3\text{SiOCH}_3$.

The stereochemistry of some of the phosphoranes investigated in this study also proved to be interesting. Variable-temperature ^{31}P and ^{19}F nmr spectroscopy was employed to follow the ligand averaging processes in the trihalophosphorane $\text{CH}_3(\text{CF}_3)\text{PF}_3$, and in a series of methylthiophosphoranes $(\text{CH}_3)_m(\text{CF}_3)_n\text{PF}_{4-m-n}(\text{SCH}_3)$ ($m = n = 1$;

$m = 0$, $n = 0$ to 3). Computer-simulation of the variable-temperature ^{31}P nmr spectra facilitated the calculation of the rearrangement rates at the different temperatures and consequently the potential barriers of these averaging processes. In addition to ligand positional exchange, a second mechanism for averaging the fluorine or tri-fluoromethyl ligand environments was evident from the nmr spectra of the various methylthiophosphoranes. This is by rotation of the SCH_3 group about the P-S bond. This was rigorously established in $\text{CF}_3\text{PF}_3(\text{SCH}_3)$ where the "pseudorotation" and the P-S bond rotation were distinct and clearly separable.

However, several questions remain unanswered regarding the chemistry and stereochemistry of the systems investigated in this work. A number of suggestions were made in the preceding chapters concerning some areas of further research. For instance, it would be interesting to establish the critical factors in the transformation of pentacoordinate aminofluorophosphoranes into the tetra- and hexacoordinate ions. Why, for example, does $(\text{CF}_3)_2\text{PF}_2\text{N}(\text{CH}_3)_2$ isomerize but not $\text{CH}_3(\text{CF}_3)\text{PF}_2\text{N}(\text{CH}_3)_2$, $\text{C}_6\text{H}_5\text{PF}_3\text{N}(\text{CH}_3)_2$ but not $\text{C}_6\text{H}_5\text{PF}_3\text{N}(\text{C}_2\text{H}_5)_2$? Why would $(\text{CF}_3)_2\text{PF}_2\text{N}(\text{CH}_3)_2$ require more rigorous conditions than $\text{C}_6\text{H}_5\text{PF}_3\text{N}(\text{CH}_3)_2$?

The assumption of a hindered P-S bond rotation to account for the appearance and splitting pattern in the

low temperature limiting spectra of the various methylthiophosphoranes implies a partial multiple character of the P-S bond. This appears to be tacitly assumed in the literature⁷⁴ but has not been confirmed by physical or chemical means. It would be interesting to investigate the character of the P-S bond by say, photoelectron spectroscopy. Perhaps the sulfur lone pair can be used as a probe in a comparative study of the methylthiophosphoranes and compounds where a $p\pi-d\pi$ interaction between sulfur and phosphorus has been established as well as compounds known to have only sigma bond between the two atoms.

The present state of pentacoordinate phosphorus chemistry is such that intensive, rather than extensive research is called for. A considerable number of compounds belonging to various series of phosphoranes have been prepared and studied to show certain trends in chemical and/or stereochemical behavior. There is a need to answer the questions about the existing phosphoranes before preparing new ones. It is hoped that the work reported in this thesis will have furthered the understanding of the chemistry and stereochemistry of trifluoromethylhalophosphoranes and will have provided a basis for future, more detailed studies.

REFERENCES

1. J. R. van Wazer (ed.), "Phosphorus and Its Compounds", p. 1281, Interscience Publishers, Inc., New York, (1961).
2. H. S. Gutowsky, D. W. McCall and C. P. Slichter, J. Chem. Phys., 21 279 (1953).
3. F. W. Bennett, H. J. Emeleus, and R. N. Haszeldine, J. Chem. Soc., 1565 (1953).
4. R. Schmutzler, Inorg. Chem., 3 410 (1964).
5. (a) J. F. Nixon, Chem. and Ind., 1555 (1963).
(b) A. B. Burg and G. Brendel, J. Amer. Chem. Soc., 80 3198 (1958).
6. T. J. Katz and E. W. Turnbloom, J. Amer. Chem. Soc., 95 4292 (1973).
7. E. L. Muettertides, W. Mahler, and R. Schmutzler, Inorg. Chem., 2 613 (1963).
8. E. L. Muettertides, W. Mahler, K. J. Packer, and R. Schmutzler, Inorg. Chem., 3 1298 (1964).
9. (a) R. J. Gillespie, J. Chem. Soc., 4672 (1963).
(b) *Ibid*, p. 4679.
10. R. R. Holmes, Accts. Chem. Res., 5 296 (1972).
11. E. L. Muettertides, Accts. Chem. Res., 3 266 (1970).
12. P. C. van der Voorn and R. S. Drago, J. Amer. Chem. Soc., 88 3256 (1965).
13. W. S. Sheldrick, J. Chem. Soc., Dalton, 2301 (1973).
14. F. Ramirez, Accts. Chem. Res., 1 168 (1968).

15. (a) K. W. Hansen and L. S. Bartell, *Inorg. Chem.*, 4 1775 (1965).
(b) *Ibid*, p. 1777.
16. W. J. Adams and L. S. Bartell, *J. Mol. Structure*, 8, 23 (1971).
17. H. Yow and L. B. Bartell, *J. Mol. Structure*, 15 209 (1973).
18. R. R. Holmes, R. P. Carter, and G. E. Peterson, *Inorg. Chem.*, 3 1748 (1964).
19. R. R. Holmes, *J. Chem. Phys.*, 46 3718 (1967).
20. R. R. Holmes, R. M. Dieter, and J. A. Galen, *Inorg. Chem.*, 2612 (1969).
21. R. R. Holmes and M. Fild, *J. Chem. Phys.*, 53 4161 (1970).
22. J. E. Griffiths, *J. Chem. Phys.*, 41 3510 (1964).
23. J. E. Griffiths, *J. Chem. Phys.*, 44 2686 (1966).
24. J. E. Griffiths, *J. Chem. Phys.*, 49 1307 (1968).
25. J. E. Griffiths, *In. Chim. Acta.*, 1 127 (1967).
26. (a) D. D. Poulin and R. G. Cavell, *Inorg. Chem.*, 13 2324 (1974).
(b) *Ibid*, p. 3012.
27. R. G. Cavell, D. D. Poulin, K. I. The, and A. J. Tomlinson, *Chem. Comm.*, 19 (1974).
28. (a) K. I. The and R. G. Cavell, *Chem. Comm.*, 279 (1975).
(b) *Ibid*, p. 716.

29. D. F. Shriver, in "The Manipulation of Air-Sensitive Compounds", p. 3, McGraw-Hill Book Company, New York (1969).
30. S. S. Sawin, Ph. D. thesis, University of Wisconsin, 1972.
31. K. I. The, Department of Chemistry, University of Alberta, personal communication.
32. (a) A. B. Burg, K. K. Joshi, and J. F. Nixon, J. Amer. Chem. Soc., 88 31 (1966).
(b) A. B. Burg and D. K. Kang, personal communication.
(c) R. G. Cavell, A. A. Pinkerton, D. D. Poulin, and A. J. Tomlinson, unpublished results.
33. V. Mark, C. H. Dungan, M. M. Crutchfield, and J. R. van Wazer, in "Topics in Phosphorus Chemistry", John Wiley and Sons, New York (1967).
34. R. G. Cavell and K. I. The, unpublished results.
35. C. H. Dungan, and J. R. van Wazer, in "Compilation of Reported F¹⁹ NMR Chemical Shifts", Wiley-Interscience, New York (1970).
36. R. G. Cavell, J. Chem. Soc., 1992 (1964).
37. K. I. The and R. G. Cavell, Inorg. Chem., 15 2518 (1976).
38. R. Schmutzler, J. Amer. Chem. Soc., 86 4500 (1964).
39. S. C. Peake and R. Schmutzler, J. Chem. Soc., (A), 1049 (1970).

40. T. A. Blazer and R. Schmutzler, *Z. Naturforsch.*, 24b 1081 (1969).
41. L. C. Thomas, in "Interpretation of Infrared Spectra of Organophosphorus Compounds", p. 276, Heyden, London, (1974).
42. R. G. Cavell, J. A. Gibson, and K. I. The, unpublished results.
43. J. F. Nixon, *J. Inorg. Nucl. Chem.*, 31 1615 (1969).
44. A. A. Pinkerton and R. G. Cavell, *Inorg. Chem.*, 10 2720 (1971).
45. S. C. Chan and C. J. Willis, *Can. J. Chem.*, 46 1237 (1968).
46. R. G. Cavell, A. A. Pinkerton, W. Sim and A. J. Tomlinson, unpublished results.
47. D. D. Poulin, A. J. Tomlinson, and R. G. Cavell, *Inorg. Chem.*, in press (1977).
48. A. B. Burg and J. E. Griffiths, *J. Amer. Chem. Soc.*, 82 3514 (1960).
49. H. S. Gutowsky and C. J. Hoffman, *J. Chem. Phys.*, 19 1259 (1951).
50. H. S. Gutowsky and D. W. McCall, *J. Chem. Phys.*, 22 162 (1954).
51. A. Saika and C. P. Slichter, *J. Chem. Phys.*, 22 26 (1956).
52. J. A. Pople, *Mol. Phys.*, 1 216 (1958).
53. L. Petrakis and C. H. Sederholm, *J. Chem. Phys.*, 35 1243 (1961).

54. J. A. Pople, W. G. Schneider, and H. J. Bernstein, in "High Resolution Nuclear Magnetic Resonance", p. 172, McGraw-Hill, New York (1959).
55. J. W. Emsley, J. Feeney, and L. H. Sutcliffe, in "High Resolution Nuclear Magnetic Resonance Spectroscopy", vol. 2, p. 871, Pergamon Press, Oxford (1966).
56. F. A. Bovey, in "Nuclear Magnetic Resonance Spectroscopy", p. 211, Academic Press, New York (1969).
57. J. R. van Wazer, C. F. Callis, J. N. Shoolery, and R. C. Jones, J. Amer. Chem. Soc., 78 5715 (1956).
58. J. R. van Wazer and J. H. Letcher, in "Topics in Phosphorus Chemistry", vol. 5, p. 75, John Wiley and Sons, New York (1967).
59. D. F. Evans, Mol. Phys., 5 183 (1962).
60. J. W. Emsley, J. Feeney, and L. H. Sutcliffe, in "High Resolution Nuclear Magnetic Resonance Spectroscopy", vol. 1, pp. 130-151, Pergamon Press, Oxford (1965).
61. J. A. Pople, Proc. Roy. Soc., A 239 541 (1957).
62. J. A. Howard, D. R. Russell, and S. Trippett, Chem. Comm., 856 (1973).
63. R. G. Cavell, J. A. Gibson, and K. I. The, unpublished results.
64. A. Rauk, L. C. Allen, and K. Mislow, J. Amer. Chem. Soc., 94 3035 (1972).
65. J. A. Altmann, K. Yates, and I. G. Csizmadia, J. Amer. Chem. Soc., 98 1451 (1976).

66. A. Strich and A. Veillard, J. Amer. Chem. Soc., 95 5574 (1973).
67. J. H. Howell, J. R. van Wazer, and A. R. Rossi, Inorg. Chem., 13 1747 (1974).
68. H. A. Bent, J. Inorg. Nucl. Chem., 19 43 (1961).
69. E. S. Gould, in "Mechanism and Structure in Organic Chemistry", pp. 250-296, Holt, Rinehart and Winston, New York (1959).
70. R. Hoffmann, J. M. Howell, and E. L. Muetterties, J. Amer. Chem. Soc., 94 3047 (1972).
71. R. E. Rundle, Rec. of Chem. Progr., 23 196 (1962).
72. J. B. Florey and L. C. Cusachs, J. Amer. Chem. Soc., 94 3040 (1972).
73. R. G. Cavell, R. D. Leary, and A. J. Tomlinson, Inorg. Chem., 11 2578 (1972).
74. J. Musher, J. Amer. Chem. Soc., 94 5662 (1972).
75. R. S. Berry, J. Chem. Phys., 32 933 (1968).
76. I. Ugi, D. Marquarding, H. Klusacek, and P. Gillespie, Accts. Chem. Res., 4 288 (1971).
77. G. M. Whitesides and H. L. Mitchell, J. Amer. Chem. Soc., 91 5384 (1969).
78. B. J. Dalton, J. Chem. Phys., 54 4745 (1971).
79. C. S. Johnson and C. G. Moreland, J. Chem. Educ., 50 477 (1973).
80. R. A. Sack, Mol. Phys., 1 163 (1958).

81. R. M. Lynden-Bell, in "Progress in Nuclear Magnetic Resonance Spectroscopy", vol. 2, p. 163 (1967).
82. The program EXCHSYS is a shortened version of the program of the same name obtained from the Mass. Inst. of Technology and established at the University of Alberta by R. G. Cavell. The theory and strategy of the calculations are described in ref. 94 and 95.
83. The program ACTEN is a shortened version of the program EXEN obtained from the Mass. Inst. of Technology and established at the University of Alberta by R. G. Cavell. For details, see ref. 95.
84. G. Binsch, in "Dynamic Magnetic Resonance Spectroscopy", p. 45, L. M. Jackman and F. A. Cotton (eds.) Academic Press, New York (1975).
85. Tom Nakashima, University of Alberta, personal communication.
86. C. G. Moreland, *et. al.*, J. Amer. Chem. Soc., 91 2161 (1976).
87. J. W. Gilje, R. W. Braun, and A. H. Cowley, Chem. Comm., 15 (1974).
88. C. G. Moreland, G. O. Doak, and L. B. Littlefield, J. Amer. Chem. Soc., 95 255 (1973).
89. W. Mahler and E. L. Muetterties, Inorg. Chem., 4 1520 (1965).
90. The program NUMARIT was written by J. S. Martin (University of Alberta) and K. Wervill (University of East Anglia) and was provided by J. S. Martin.

91. K. I. The, S. Pirakitigoon, and R. G. Cavell, unpublished results.
92. J. R. van Wazer and J. H. Letcher, in "Topics in Phosphorus Chemistry", vol. 5, p. 169, E. J. Griffiths and M. Grayson (eds.), John Wiley and Sons, New York, (1967).
93. W. Mahler, Inorg. Chem., 2 230 (1963).
94. J. K. Kreiger, J. M. Deutsch and G. M. Whitesides, Inorg. Chem., 12 1535 (1973).
95. J. K. Kreiger, thesis, Mass. Inst. of Technology, Boston, Mass., (1971).
96. By comparison with an authentic sample.
97. K. J. Packer, J. Chem. Soc. 960 (1963).
98. A. B. Burg and I. B. Mishra, Inorg. Chem., 8 1199 (1969).
99. M. Eisenhut, *et. al.*, J. Amer. Chem. Soc., 96 5385 (1974).
100. S. L. Manatt, D. D. Elleman, A. H. Cowley, and A. B. Burg, J. Amer. Chem. Soc., 89 4544 (1967).
101. D.E.C. Corbridge, in "Topics in Phosphorus Chemistry", M. Grayson and E. J. Griffiths (ed.), Interscience, New York, 3 57 (1966).
102. The term "pseudorotation" is used to mean a general intramolecular ligand exchange without necessarily implying any particular mechanistic pathway. It is distinct from the use of the word pseudorotation in

Berry Pseudorotation (BPR) where a particular pair-wise exchange mechanism is involved. The general usage of the term pseudorotation thereby includes BPR and the equivalent TR mechanisms or any other process which is permutationally equivalent.

103. H. A. Szymanski, in "Progress in Infrared Spectroscopy", vol. 2, pp. 127-151, Plenum Press, New York (1963).

APPENDIX

The following tables (1-6) give the K matrices used to calculate ^{31}P nmr spectra of the exchanging phosphoranes. Simple product functions were used to assign the lines in the spectrum rather than the correct symmetrized form functions because the former are more convenient to handle in big systems. This practice has a non-detectable effect, within our limits of error, on the behavior of the spectrum⁹⁵ in such complex systems.

TABLE 1

K Matrix for Axial-Equatorial F Exchange

in $\text{CH}_3(\text{CF}_3)\text{PF}_3^a$

	$\frac{e aa}{\alpha}$	$\frac{\alpha\alpha}{\alpha}$	$\frac{\alpha\beta}{\alpha}$	$\frac{\alpha\alpha}{\beta}$	$\frac{\beta\beta}{\alpha}$	$\frac{\alpha\beta}{\beta}$	$\frac{\beta\beta}{\beta}$
e aa							
$\alpha \alpha\alpha$	0	0	0	0	0	0	0
$\alpha \alpha\beta$	0	-0.5	0.5	0	0	0	0
$\beta \alpha\alpha$	0	1.0	-1.0	0	0	0	0
$\alpha \beta\beta$	0	0	0	-1.0	1.0	0	0
$\beta \alpha\beta$	0	0	0	0.5	-0.5	0	0
$\beta \beta\beta$	0	0	0	0	0	0	0

^a One of four 6 x 6 submatrices; for the ^{31}P spectrum. The spectrum consists of a quartet due to coupling of the CF_3 group with phosphorus. Complete reproduction of the $^{31}\text{P} \sim \{^1\text{H}\}$ spectrum with all couplings requires that the above matrix be repeated four times with line spacings given by $^2J_{\text{PF}}$.

TABLE 2

K Matrix for Axial-Equatorial F Exchange in
 F_4PSCH_3 (80% "Pseudorotation" and 20% Rotation)^a

	$\frac{ee a a}{\alpha\alpha \alpha \alpha}$	$\frac{\alpha\alpha \alpha \beta}{\alpha\alpha \alpha \beta}$	$\frac{\alpha\alpha \beta \alpha}{\alpha\alpha \beta \alpha}$	$\frac{\alpha\alpha \beta \beta}{\alpha\alpha \beta \beta}$	$\frac{\alpha\beta \alpha \alpha}{\alpha\beta \alpha \alpha}$	$\frac{\alpha\beta \alpha \beta}{\alpha\beta \alpha \beta}$	$\frac{\alpha\beta \beta \alpha}{\alpha\beta \beta \alpha}$	$\frac{\alpha\beta \beta \beta}{\alpha\beta \beta \beta}$	$\frac{\beta\beta \alpha \alpha}{\beta\beta \alpha \alpha}$	$\frac{\beta\beta \alpha \beta}{\beta\beta \alpha \beta}$	$\frac{\beta\beta \beta \alpha}{\beta\beta \beta \alpha}$	$\frac{\beta\beta \beta \beta}{\beta\beta \beta \beta}$
$ee a a'$												
$\alpha\alpha \alpha \alpha$	0	0	0	0	0	0	0	0	0	0	0	0
$\alpha\alpha \alpha \beta$	0	-1	0.2	0	0.8	0	0	0	0	0	0	0
$\alpha\alpha \beta \alpha$	0	0.2	-1.0	0	0.8	0	0	0	0	0	0	0
$\alpha\alpha \beta \beta$	0	0	0	-0.8	0	0	0	0	0.8	0	0	0
$\alpha\beta \alpha \alpha$	0	0.4	0.4	0	-0.8	0	0	0	0	0	0	0
$\alpha\beta \alpha \beta$	0	0	0	0	0	-0.6	0.6	0	0	0	0	0
$\alpha\beta \beta \alpha$	0	0	0	0	0	0.6	-0.6	0	0	0	0	0
$\alpha\beta \beta \beta$	0	0	0	0	0	0	0	-0.8	0	0.4	0.4	0
$\beta\beta \alpha \alpha$	0	0	0	0.8	0	0	0	0	-0.8	0	0	0
$\beta\beta \alpha \beta$	0	0	0	0	0	0	0	0.8	0	-1.0	0.2	0
$\beta\beta \beta \alpha$	0	0	0	0	0	0	0	0.8	0	0.2	-1.0	0
$\beta\beta \beta \beta$	0	0	0	0	0	0	0	0	0	0	0	0

^a For the $^{31}P \sim \{^1H\}$ spectrum.

TABLE 3

Different K Matrices Investigated for Axial-Equatorial F
Exchange in $F_4PSCH_3^a$

A. 90° "BPR" + 10° Rotation

$ee a a'$	$\alpha\alpha \alpha \alpha$	$\alpha\alpha \alpha \beta$	$\alpha\alpha \beta \alpha$	$\alpha\alpha \beta \beta$	$\alpha\beta \alpha \alpha$	$\alpha\beta \alpha \beta$	$\alpha\beta \beta \alpha$	$\alpha\beta \beta \beta$	$\beta\beta \alpha \alpha$	$\beta\beta \alpha \beta$	$\beta\beta \beta \alpha$	$\beta\beta \beta \beta$
$\alpha\alpha \alpha \alpha$	0	0	0	0	0	0	0	0	0	0	0	0
$\alpha\alpha \alpha \beta$	0	-1.0	0.1	0	0.9	0	0	0	0	0	0	0
$\alpha\alpha \beta \alpha$	0	0.1	-1.0	0	0.9	0	0	0	0	0	0	0
$\alpha\alpha \beta \beta$	0	0	0	-0.9	0	0	0	0	0.9	0	0	0
$\alpha\beta \alpha \alpha$	0	0.45	0.45	0	-0.9	0	0	0	0	0	0	0
$\alpha\beta \alpha \beta$	0	0	0	0	0	-0.55	0.55	0	0	0	0	0
$\alpha\beta \beta \alpha$	0	0	0	0	0	0.55	-0.55	0	0	0	0	0
$\alpha\beta \beta \beta$	0	0	0	0	0	0	0	-0.9	0	0.45	0.45	0
$\beta\beta \alpha \alpha$	0	0	0.9	0	0	0	0	0	-0.9	0	0	0
$\beta\beta \alpha \beta$	0	0	0	0	0	0	0	0.9	0	-1.0	0.1	0
$\beta\beta \beta \alpha$	0	0	0	0	0	0	0	0.9	0	0.1	-1.0	0
$\beta\beta \beta \beta$	0	0	0	0	0	0	0	0	0	0	0	0

^a To calculate $^3I_P \sim \{^1H\}$ spectrum.

TABLE 4K Matrix for Axial-Axial F Exchange in $\text{CH}_3(\text{CF}_3)\text{PF}_2(\text{SCH}_3)^a$

$a a'$	$\frac{a}{a'}$	$\frac{\alpha}{\alpha'}$	$\frac{\beta}{\alpha'}$	$\frac{\alpha}{\beta'}$	$\frac{\beta}{\beta'}$
$\alpha \alpha$		0	0	0	0
$\alpha \beta$		0	-1.0	1.0	0
$\beta \alpha$		0	1.0	-1.0	0
$\beta \beta$		0	0	0	0

^a One of four 4 x 4 submatrices; for calculation of the $^{31}\text{P} \sim \{^1\text{H}\}$ spectrum. The complete ^{31}P spectrum consists of a quartet due to coupling of the phosphorus with the CF_3 group. Complete reproduction of the $^{31}\text{P} \sim \{^1\text{H}\}$ spectrum with all couplings requires that this matrix be repeated four times with line spacings given by $^2J_{\text{PF}}$.

TABLE 5K Matrices for Axial-Equatorial F Exchange in $\text{CF}_3\text{PF}_3(\text{SCH}_3)^a$ "Pseudorotation"A. Reduced Matrix

$\begin{array}{c} a e \\ \hline aa e \end{array}$	$\begin{array}{c} \alpha \alpha \\ \hline \alpha\alpha \alpha \end{array}$	$\begin{array}{c} \beta \beta \\ \hline \alpha\alpha \beta \end{array}$	$\begin{array}{c} \alpha \beta \\ \hline \alpha\beta \alpha \end{array}$	$\begin{array}{c} \beta \beta \\ \hline \alpha\beta \beta \end{array}$	$\begin{array}{c} \alpha \alpha \\ \hline \beta\beta \alpha \end{array}$	$\begin{array}{c} \beta \beta \\ \hline \beta\beta \beta \end{array}$
$aa e$						
$\alpha\alpha \alpha$	0	0	0	0	0	0
$\alpha\alpha \beta$	0	-1.0	1.0	0	0	0
$\alpha\beta \alpha$	0	0.5	-0.5	0	0	0
$\alpha\beta \beta$	0	0	0	-0.5	0.5	0
$\beta\beta \alpha$	0	0	0	1.0	-1.0	0
$\beta\beta \beta$	0	0	0	0	0	0

B. Original 8 x 8 Matrix for SCH_3 rotation

$\begin{array}{c} a a' e \\ \hline a a' e \end{array}$	$\begin{array}{c} \alpha \alpha \\ \hline \alpha \alpha \alpha \end{array}$	$\begin{array}{c} \alpha \beta \\ \hline \alpha \alpha \beta \end{array}$	$\begin{array}{c} \alpha \beta \alpha \\ \hline \alpha \beta \alpha \end{array}$	$\begin{array}{c} \alpha \beta \beta \\ \hline \alpha \beta \beta \end{array}$	$\begin{array}{c} \beta \alpha \alpha \\ \hline \alpha \beta \alpha \end{array}$	$\begin{array}{c} \beta \alpha \beta \\ \hline \alpha \beta \beta \end{array}$	$\begin{array}{c} \beta \beta \alpha \\ \hline \beta \alpha \alpha \end{array}$	$\begin{array}{c} \beta \beta \beta \\ \hline \beta \alpha \beta \end{array}$
$a a' e$								
$\alpha \alpha \alpha$	0	0	0	0	0	0	0	0
$\alpha \alpha \beta$	0	0	0	0	0	0	0	0
$\alpha \beta \alpha$	0	0	-1.0	0	1.0	0	0	0
$\alpha \beta \beta$	0	0	0	-1.0	0	1.0	0	0
$\beta \alpha \alpha$	0	0	1.0	0	-1.0	0	0	0
$\beta \alpha \beta$	0	0	0	1.0	0	-1.0	0	0
$\beta \beta \alpha$	0	0	0	0	0	0	0	0
$\beta \beta \beta$	0	0	0	0	0	0	0	0

FOOTNOTE FOR TABLE 5

- ^a One of four submatrices. The quartet splitting of the spectrum arises from coupling of the phosphorus with the CF₃ group. Complete reproduction of the $^3\text{l}_\text{P} \sim \{^1\text{H}\}$ spectrum requires that this matrix be repeated four times with line spacing determined by $^2\text{J}_{\text{PF}}$.

TABLE 6

K Matrix for Axial-Equatorial CF_3 Exchange in
 $(\text{CF}_3)_3\text{PF}(\text{SCH}_3)^{91}$

A. The Full Matrix^a

64 x 64 matrix for $(\text{CF}_3)_3\text{P}$ system (2 equatorial, 1 axial)

* Unchanged by Exchange

^a To calculate $^{31}\text{P} \sim \{^1\text{H}\}$ spectrum

TABLE 6

B. The Contracted Matrix

[illegible]

TABLE 7

NMR Parameters of Miscellaneous Compounds/Ions

Encountered in this Investigation

Compound/Ion	$\phi_{\text{CF}_3}^a$	ϕ_{F}^a	τ_{H}^b	$1^{\text{C}}_{\text{J}_{\text{P-F}}}$	$2^{\text{C}}_{\text{J}_{\text{P-F}}}$	$2^{\text{C}}_{\text{J}_{\text{P-H}}}$	$2^{\text{C}}_{\text{J}_{\text{F-F}}}$	$3^{\text{C}}_{\text{J}_{\text{F-H}}}$	Reference
$\text{CF}_3\text{PF}_2[\text{N}(\text{CH}_3)_2]_2$	68.9	59.0	7.25	792	150.0	10.3	17.0	0.8	26b
$(\text{CF}_3)_2\text{P}(\text{O})\text{N}(\text{CH}_3)_2$	69.8	-	-	-	106.0	10.8	-	-	32c
$(\text{CF}_3)_2\text{P}(\text{O})\text{OCH}_3$	73.3	-	-	-	121.0	-	-	-	98
$(\text{CF}_3)_2\text{PCl}_3$	78.5	-	-	-	191	-	-	-	25, 97
$(\text{CF}_3)_2\text{PN}(\text{CH}_3)_2$	60.1	-	7.42	-	86	9.2	-	-	97
$(\text{CF}_3)_2\text{PCl}$	59.8	-	-	-	56	-	-	-	97
$(\text{CF}_3)_2\text{PF}_4^-$ d,e	70.3	77.3	-	965	82	-	14	-	45
$\text{CF}_3\text{P}[\text{N}(\text{CH}_3)_2]_3^+$ d,e	61.0	-	7.51	-	108	10.3	-	-	26a

FOOTNOTES For TABLE 7

- ^a Except for the ions (see note d) reported in this table, ϕ values are in ppm relative to internal CCl_3F standard with positive values indicating resonance to high field of the standard
- ^b τ ppm relative to internal tetramethylsilane, $\tau = 10.0$
- ^c units in Hertz
- ^d In CD_3CN solvent, ϕ values are in ppm relative to external CCl_3F standard with positive values indicating resonance to high field of the standard.
- ^e τ ppm relative to external tetramethylsilane, $\tau = 10.0$

B30179